# Etude de la région locomotrice mésencéphalique chez le primate : comportement et anatomie

Hayat Belaid

Université Pierre et Marie Curie

Ecole doctorale n° 158 ED3C

*ICM - UPMC-P6 UMR S 1127 - Inserm U 1127 - CNRS UMR 7225 /*

*Thérapeutique expérimentale*

# Etude de la région locomotrice mésencéphalique chez le primate: Comportement et Anatomie

Par

Hayat BELAID

Doctorat de Neurosciences

Soutenue le 11/12/2017 devant un jury composé de :

| | | |
|---|---|---|
| Pr | P. Cornu | Président |
| Dr | B. Piallat | Rapporteur |
| Pr | D. Guehl | Rapporteur |
| Pr | JJ. Lemaire | Examinateur |
| Dr | R. Carron | Invité |
| Dr | C. Karachi | Directeur |
| Dr | C. Francois | Co-Directeur |

# SOMMAIRE

# AVANT-PROPOS

La maladie de Parkinson (MP) est une maladie neurodégénérative secondaire à la mort des neurones dopaminergiques de la substance noire pars compacta (SNc). La cause de la mort de ces neurones est inconnue. Les signes cliniques cardinaux sont le tremblement de repos, l'akinésie et la rigidité. A ce jour aucun traitement curatif n'existe, cependant l'administration de L-dopa permet d'améliorer ces symptômes, conférant leur caractère dopa sensible. De même, la stimulation cérébrale profonde appliquée au noyau subthalamique (NST) est efficace pour traiter les signes cardinaux de la MP ainsi que les complications motrices liées au traitement dopaminergique (fluctuations et dyskinésies) (Limousin et al., 1995b). Avec l'évolution de la maladie, s'installent progressivement des troubles de la marche et de l'équilibre dopa-résistants responsables de chutes avec leurs complications sévères. Il s'agit d'un problème de santé publique important pour la population âgée, dépassant largement le cadre de la MP. La physiopathologie des troubles de la marche et de l'équilibre est mal connue, ce qui explique l'absence de thérapeutique efficace. Ils résistent au traitement substitutif dopaminergique et à la stimulation cérébrale profonde du NST, suggérant que leur origine provient d'un dysfonctionnement de circuits neuronaux non dopaminergiques.

De nombreux résultats expérimentaux et cliniques suggèrent qu'un dysfonctionnement de la région locomotrice mésencéphalique (MLR) du tronc cérébral serait une des régions clefs à l'origine de ces troubles de la marche et de l'équilibre. La MLR est formée du noyau pédonculopontin (PPN), caractérisé par la présence de neurones cholinergiques, et du noyau cunéiforme (CuN). Le rôle de la MLR dans le contrôle de la posture et de la locomotion a été initialement étudié chez le chat et le rongeur. La stimulation électrique de la MLR du chat et du rat décérébré est capable de provoquer une activité locomotrice (Garcia-Rill et al., 1990; Takakusaki et al., 2003). La marche s'accélère jusqu'à la course lorsque l'intensité du courant est augmentée (Grillner, 1981). En appliquant des trains de stimulation répétés au sein du PPN chez le chat éveillé (Mori et al., 1989), des comportements moteurs plus complexes apparaissent tels que la mise à l'affût et le saut. Des études récentes réalisées avec les techniques d'optogénétique chez la souris montrent qu'une activation de la MLR, ciblant

plutôt les neurones glutamatergiques, va induire une locomotion avec des temps de latence très courts (Lee et al., 2014). Chez l'homme sain, des études en IRM fonctionnelle utilisant l'imagination mentale de la marche suggèrent également une implication de la MLR dans le contrôle de la marche (Iseki et al., 2008; Jahn et al., 2008). Chez les patients parkinsoniens enfin, une perte partielle significative des neurones cholinergiques du PPN a été montrée à un stade avancé de la maladie (Hirsch et al., 1987; Zweig et al., 1989; Rinne et al., 2008), plus importante encore chez les patients parkinsoniens chuteurs (Karachi et al., 2010).

Compte tenu de l'ensemble de ces données, il a été proposé de stimuler à basse fréquence la MLR, en particulier la région du PPN, chez les patients parkinsoniens à un stade avancé de la maladie afin de stimuler les neurones restants pour améliorer les troubles de l'équilibre et de la marche. Après des premiers résultats prometteurs (Mazzone et al., 2005), les différentes études cliniques réalisées par la suite apportent des résultats hétérogènes, en dehors d'un effet objectif positif sur l'instabilité posturale, et globalement décevants pour la moitié des patients environ (Golestanirad et al., 2016). Les deux premières études contrôlées n'ont pas permis de démontrer une efficacité objective sur les échelles de marche en condition de stimulation « ON », cependant 30 % des patients ont tiré un bénéfice fonctionnel certain en terme de qualité de vie, soit par l'amélioration du freezing (Ferraye et al., 2010) soit par la diminution de la fréquence des chutes (Moro et al., 2010). Par la suite, des études plus récentes en double aveugle (Mestre et al., 2016; Thevathasan et al., 2011; Welter et al., 2015), ont montré un effet objectivable sur le freezing et la fréquence des chutes, mais dont le maintien à long terme reste incertain. La variabilité des résultats obtenus par les différentes équipes peut s'expliquer par plusieurs facteurs : 1) difficulté à évaluer les troubles de la marche et de l'équilibre du fait de leurs fluctuations dans le temps et dépendant de nombreux facteurs environnementaux imprévisibles; 2) conditions de stimulation et sélection des patients différents d'une étude à l'autre (stimulation uni ou bilatérale, patients déjà implantés dans le NST); 3) petit nombre de patients opérés; 4) absence de visualisation directe du PPN à l'IRM et de limites fermées des noyaux de la MLR rendant le ciblage neurochirurgical difficile avec une cible choisie au sein de la MLR qui n'est de ce fait pas identique selon les équipes.

Ces résultats témoignent en partie de la complexité anatomique et fonctionnelle de la MLR. C'est la raison pour laquelle une étude chez le primate a été menée au sein de notre équipe afin de déterminer le rôle du PPN, et plus précisément de sa partie cholinergique, dans la posture et la locomotion (Karachi et al., 2010). Il a ainsi été observé chez le singe normal qu'une lésion spécifique partielle des neurones cholinergiques du PPN est responsable de modifications importantes du tonus, et par conséquent de la posture et de la locomotion (Karachi et al., 2010). Chez le singe rendu parkinsonien, une lésion identique du PPN cholinergique entraîne des troubles de la posture et de la marche similaires, mais améliore les symptômes parkinsoniens dopa-sensibles, prouvant que MLR et ganglions de la base (GB) fonctionnent à la fois en synergie mais aussi de façon indépendante (Grabli et al., 2013).

Des études physiologiques récentes montrent que le PPN n'a pas seulement un rôle locomoteur, mais est impliqué aussi dans le contrôle de fonctions non motrices. Les troubles du sommeil sévères dont souffrent les patients parkinsoniens, qui résistent aux traitements par agoniste dopaminergique ou à la stimulation du NST, en sont un bon exemple avec un impact négatif sur la qualité de vie (Schrempf et al., 2014). Les neurones cholinergiques du PPN sont bien connus pour contrôler le cycle veille-sommeil, et plus particulièrement la phase de sommeil paradoxal (rapid eye movement (REM) sleep) ( Steriade et al., 1990; Rye, 1997; Datta, 2002). Des observations cliniques récentes effectuées chez les patients parkinsoniens avec des électrodes implantées dans le PPN ont d'ailleurs montré une efficacité de la stimulation à basse fréquence sur la qualité du sommeil. Ces patients présentent une amélioration de la qualité et de l'architecture du sommeil, suggérant fortement que ces symptômes sont étroitement corrélés à un dysfonctionnement des neurones cholinergiques du PPN (Arnulf et al., 2010; Peppe et al., 2012). Cependant, là encore, la variabilité de la localisation des électrodes ne permet pas de savoir quelle partie anatomique précise au sein de la MLR est impliquée, et il existe peu de modèles expérimentaux permettant d'explorer et de comprendre la physiopathologie des troubles du sommeil notamment chez le primate.

A travers l'ensemble de ces données expérimentales et cliniques, on perçoit la complexité de l'anatomie de la MLR, composée d'amas cellulaires sans limites nettes au sein de la formation réticulée, et la complexité fonctionnelle de cette structure dont le rôle spécifique du PPN et du CuN chez le primate reste encore méconnu. Aussi l'objectif principal de mon travail de thèse est de réaliser une étude fonctionnelle et anatomique de la MLR chez le primate. Le premier volet de ce travail a consisté à détailler le rôle des neurones cholinergiques du PPN dans le contrôle veille-sommeil chez le singe rendu parkinsonien. Le second volet a consisté à explorer les connections spécifiques du PPN et du CuN et leurs rapports avec les GB afin de déterminer si ces deux structures appartiennent ou non à des circuits différents. Cela permettrait d'apporter des éléments de réponse sur la physiopathologie des symptômes dopa-résistants visibles chez les patients parkinsoniens et à mieux définir la cible éventuelle au sein de la MLR pour la stimulation cérébrale profonde.

# ANATOMIE ET PHYSIOLOGIE DE LA REGION LOCOMOTRICE MESENCEPHALIQUE: Rappels

## A. ANATOMIE

Le PPN et le CuN sont deux noyaux faisant partie de la MLR (figure 1). Ils correspondent à des noyaux ouverts au sein de la formation réticulée mésencéphalique, sans limites précises quelles que soient les techniques d'immunohistologie utilisées. Ils sont tous les deux constitués de neurones glutamatergiques et GABAergiques, et seul le PPN contient des neurones cholinergiques. Il s'agit d'une structure hautement préservée chez l'ensemble des vertébrés.

### 1. Anatomie du PPN

Anatomiquement, le PPN est entouré latéralement par les fibres sensitives du lemnisque médian, médialement par la décussation des fibres des pédoncules cérébelleux supérieurs (ou brachium conjonctivum), ventralement par les noyaux du pont, dorsalement par le noyau cunéiforme, en avant par la substance noire (SN) et le noyau rouge, et en arrière par le locus coeruleus (Olszewski et Baxter, 1954; Edley et Graybiel, 1983; Geula et al., 1993; Lavoie et Parent, 1994a). Le PPN est caractérisé par la présence de neurones cholinergiques, associés au groupe cholinergique Ch5 de Mesulam (Mesulam et al., 1983; 1989). Deux sous-parties ont été identifiées en fonction de la densité cellulaire cholinergique calculée chez l'homme: la *pars compacta* (PPNc) et la *pars dissipata* (PPNd) (Olszewski et Baxter, 1954). Le PPNc est principalement composé de 80 à 90% de larges neurones cholinergiques (Mesulam et al., 1984; 1989) tandis que le PPNd est caractérisé par la présence d'environ 75% de neurones non cholinergiques. Ainsi des neurones glutamatergiques et GABAergiques ont été observés dans le PPN chez le rongeur et le chat (Clements et Grant, 1990; Clements et al., 1991; Ford et al., 1995; Jia et al., 2003; Martinez-Gonzalez et al., 2011; Mena-Segovia et al., 2009; Wang

et Morales, 2009). Cependant les données sont parcellaires et contradictoires chez le singe puisque des neurones glutamatergiques ont été détectés, mais pas de neurones GABAergiques (Lavoie et Parent, 1994a,c), alors que des terminaisons glutamatergiques et GABAergiques en provenance du PPN ont été décrites au niveau des neurones dopaminergiques de la SN (Charara et al., 1996). Chez l'homme, une seule équipe a mis en évidence la présence de neurones GABAergiques au sein du PPN (Pienaar et al., 2013). Enfin, il persiste une controverse quant à la co-expression ou non de différents médiateurs au sein des neurones du PPN. En effet les premières études anatomiques du PPN mettaient en évidence pour les neurones cholinergiques une co-expression avec soit le glutamate (40% chez le singe et le rongeur) (Clements et al., 1991; Lavoie et Parent, 1994c), soit le GABA (Charara et al., 1996), mais aussi l'oxyde nitrique ou la substance P (Vincent et al., 1983; 1986). Cependant une étude plus récente chez le rongeur, combinant l'hybridation in situ et l'immunohistochimie, a clairement montré qu'aucun neurone cholinergique ne co-exprimait le glutamate et/ou le GABA (Wang et Morales, 2009). Enfin, les différentes populations neuronales seraient distribuées de manière hétérogène dans le PPNd. Une topographie a été établie chez les rongeurs, avec un gradient positif rostro-caudal pour les neurones cholinergiques et glutamatergiques. Inversement, les neurones GABAergiques sont plus concentrés dans la partie rostrale du noyau (Martinez-Gonzalez et al., 2012; Mena-Segovia et al., 2009). Ces données n'ont pas encore été étudiées chez le primate.

**En conclusion**, la présence des neurones cholinergiques permet de délimiter le PPN (Lavoie et Parent, 1994a; Rolland et al., 2009). Mais il reste encore à déterminer la présence de différentes populations cellulaires et leur organisation topographique au sein du PPN chez le primate.

## 2. Anatomie du CuN

Le CuN est délimité ventralement par le PPN, dorsalement par les colliculi (supérieur et inférieur), médialement par la substance grise périaqueducale et latéralement par le lemnisque latéral. De même que le PPN, il est constitué de neurones GABAergiques (chez le singe écureuil (Lavoie et Parent, 1994a,c), chez le chat (Appell et Behan, 1990; Pose et al., 2000), et peut-être glutamatergiques (Pose et al., 2000). La présence de neurones substance P et enképhalinergiques a également été rapportée (Beitz, 1982; Sakanaka et al., 1987).

Certains atlas cyto- et myéloarchitectonique chez l'homme ont distingué les noyaux cunéiforme et sub-cunéiforme (Olszewski et Baxter, 1954) en se basant sur une différence de densité et de taille de corps cellulaires, sans préciser la limite exacte entre ces 2 parties. Ce serait dans cette dernière que la locomotion aurait été induite par une stimulation chez l'animal (Takakusaki et al., 2003) et qu'une modification de l'activité électrophysiologique a été mise en évidence chez l'homme lors d'une marche simulée (Piallat et al., 2009) (Ferraye et al., 2010). Cependant le CuN faisant partie de la formation réticulée, qui se caractérise par une hétérogénéité cyto-architecturale et neurochimique, la délimitation précise de ce noyau ouvert reste une source de controverses.

Figure 1: MLR chez le macaque
coupe transverse identifiant le CuN et le PPN
(par marquage immunohistochimique ChAT)

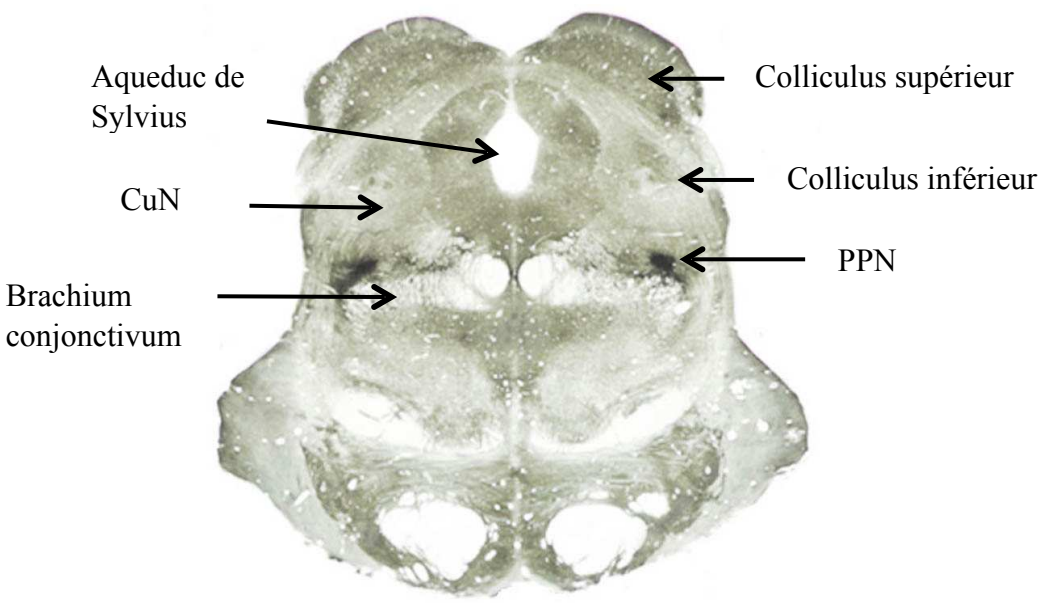

## B. PHYSIOLOGIE: RÔLES DU PPN ET DU CUN

### 1. Fonctions motrices: posture et locomotion

#### *a) Données expérimentales*

*Stimulation de la MLR*

Les fonctions motrices sont connues depuis les années 60, suite à des travaux sur le chat montrant que la stimulation électrique d'une région précise située à la jonction entre le mésencéphale et le tronc cérébral entraînait une réponse locomotrice (marche et course) (Shik et al., 1966). La région mésencéphalique locomotrice a été ainsi nommée sur des critères physiologiques, et de nombreuses études chez différents vertébrés ont confirmé la possibilité d'induire une locomotion lors de la stimulation électrique de cette région spécifique chez l'animal décérébré (transection au niveau pré-colliculaire et pré-mamillaire), aussi bien le chat (Garcia-Rill et Skinner, 1987a,b), le rat (Garcia-Rill et al., 1990), et le primate (Eidelberg et al., 1981).

Chez le chat, si une stimulation à fréquence moyenne (20-60 Hz) induit une locomotion, plusieurs trains de stimulations répétés sont nécessaires avant d'entraîner le premier pas (Garcia-Rill et Skinner, 1991). Les paramètres de stimulation du PPN sont déterminant pour le déclenchement de la locomotion, les fréquences moyennes étant les plus efficaces, tandis que les fréquences élevées induisent plutôt un blocage de la locomotion. De plus, une stimulation du PPN entraîne une modification du tonus musculaire chez le rat (Kelland et Asdourian, 1989) et le chat (Lai et Siegel, 1990), soit une augmentation ou une diminution en fonction des protocoles de stimulation (Garcia-Rill et al., 1990), la stimulation à haute fréquence chez le chat entraînant systématiquement une abolition du tonus musculaire (Lai et Siegel, 1990). Enfin, de nombreuses études ont également été effectuées chez la lamproie, sur des préparations semi-intactes (Sirota et al., 2000). La stimulation électrique de la MLR induit ainsi des mouvements de nage, dont la rapidité et la puissance sont corrélées à l'intensité. Cette même équipe a mis en évidence un rôle direct des neurones cholinergiques dans l'induction de la locomotion, via les neurones réticulo-spinaux ( Le Ray et al., 2003; Dubuc et al., 2008).

En se basant sur les effets de la stimulation chez le chat décérébré avec conservation de la SNr, une distinction fonctionnelle entre PPN et CuN a été suggérée: le PPN contrôlerait plutôt le tonus musculaire, et le CuN la locomotion (Takakusaki et al., 2003) (figure 2). A noter cependant une distinction entre la stimulation de la partie ventrale du PPN, qui induit une inhibition de la locomotion et une abolition du tonus musculaire, et la partie dorsale qui va d'abord faciliter la locomotion, avant de réduire celle-ci parallèlement à une diminution du tonus (Takakusaki et al., 2003). Ce modèle a été critiqué, notamment par l'équipe de Garcia-Rill, considérant le site principal induisant la locomotion comme étant la pars compacta du PPN, et plus précisément les neurones cholinergiques (Garcia-Rill, 1986; Garcia-Rill et al., 1987).

Figure 2: Organisation de la MLR chez le chat décérébré
*d'après Takakusaki et al (2003)*

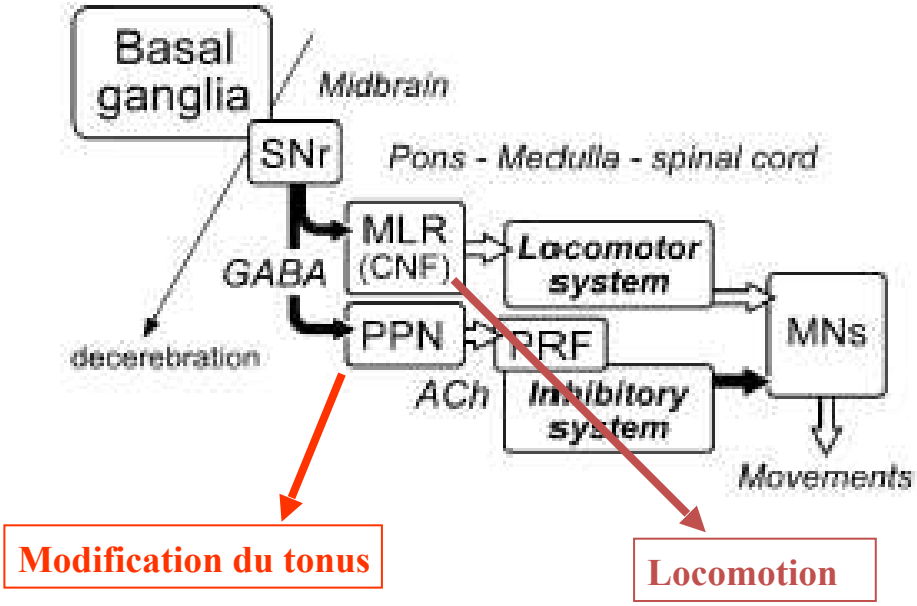

Bien qu'il perdure une controverse quant aux fonctions propres du PPN et du CuN dans le contrôle de la locomotion, des données plus récentes utilisant les techniques d'optogénétique chez la souris ont permis de mettre en évidence le rôle spécifique de chaque population neuronale du PPN dans l'induction de la locomotion (Roseberry et al., 2016) (figure 3). Dans cette étude il a été montré que l'activation spécifique des neurones cholinergiques va induire une augmentation de la vitesse lorsque la souris est déjà en condition de marche ou course, mais n'induit pas de locomotion si elle est à l'arrêt. Les neurones cholinergiques auraient ainsi, chez le rongeur, plutôt un rôle modulateur. Au contraire, l'activation spécifique des neurones glutamatergiques va systématiquement induire une locomotion, dont la vitesse est directement corrélée à la fréquence de stimulation. L'activation des neurones GABAergiques va quant à elle entraîner une décélération et un arrêt systématique de la locomotion.

Figure 3: Fonctions des différentes populations neuronales de la MLR dans la locomotion (cholinergique, GABAergique et glutamatergique) *d'après Roseberry et al (2016)*

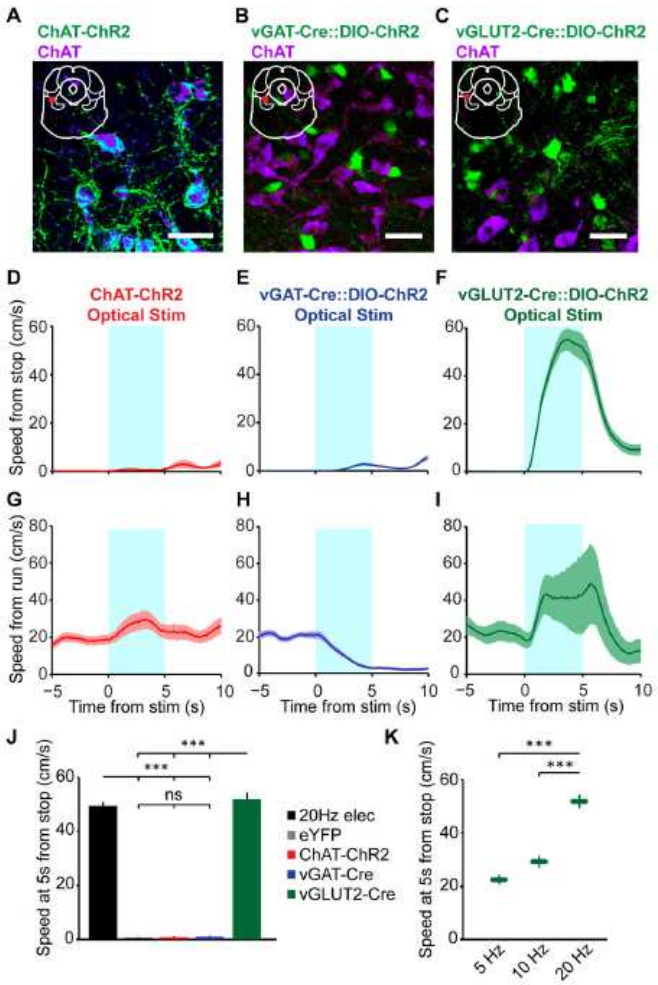

*Modulation pharmacologique et lésions*

Diverses autres études expérimentales utilisant des agents pharmacologiques ont montré des effets variés sur la locomotion. Chez le rat, des injections d'antagonistes GABA dans le PPN induisent une locomotion sur de courtes périodes, alors que l'injection d'agoniste GABA va bloquer la locomotion induite (Garcia-Rill et al., 1990). Toujours chez le rat, d'autres études ont montré une abolition du comportement de catalepsie induit par l'haloperidol après injection d'antagonistes GABA dans le PPN (Miwa et al., 1996). Les lésions excitotoxiques du PPN quant à elles vont avoir des effets différents en fonction du site. En effet, seules les lésions restreintes à la partie antérieure du PPN induisent des effets moteurs avec une réduction de la locomotion (Alderson et al., 2008), contrairement aux lésions du PPN postérieur qui n'ont pas d'impact sur la locomotion spontanée. Par contre, des lésions excitotoxiques restreintes au CuN n'induiraient pas d'altération de la locomotion (Allen et al., 1996).

Chez le primate, une lésion par radiofréquence unilatérale du PPN entraînerait une akinésie transitoire (Aziz et al., 1998), et une lésion bilatérale une akinésie prolongée (MunroDavies et al., 1999). Des lésions excitotoxiques unilatérales non spécifiques à l'acide kaïnique entraînent un hémiparkinsonisme avec une posture voutée et une hypokinésie controlatérale à la lésion (Kojima et al., 1997; Matsumura et Kojima, 2001). Des lésions bilatérales par injection de toxine spécifique des neurones cholinergiques du PPN effectuées chez le primate par notre équipe ont induit une altération de la marche associée à des troubles du tonus, qui n'étaient pas améliorés après traitement dopaminergique (Karachi et al., 2010).

*Electrophysiologie*

Les caractéristiques électrophysiologiques des neurones du PPN ont été étudiés d'abord chez le rat *in vitro* (Kang et Kitai, 1990; Takakusaki et al., 1997), montrant la présence de 2 types de neurones cholinergiques en fonction de leurs propriétés membranaires. Cette distribution bi-modale n'a pas été retrouvée chez le primate *in vivo* (Matsumura et al., 1997), où les enregistrements ont été réalisés au cours d'une tâche motrice de préhension volontaire. Les résultats montraient une modification de l'activité de plus de la moitié des neurones du PPN en réponse à la tâche motrice, à la fois controlatérale et ipsilatérale. Afin d'obtenir des données physiologiques au cours de la locomotion, un modèle expérimental de locomotion

bipède chez le macaque a récemment été développé (Goetz et al., 2012; 2016). Un enregistrement électrophysiologique était effectué dans la MLR chez les macaques restreints dans une chaise à primate, et entraînés à réaliser une marche bipède sur un tapis roulant. Trois groupes distincts de neurones ont été mis en évidence en fonction du type d'activité induite par la locomotion: les neurones répondeurs phasiques, les neurones répondeurs toniques, et les neurones non répondeurs. Si la localisation de ces neurones était généralement éparse dans l'ensemble de la MLR, les neurones répondeurs phasiques étaient majoritairement situés dans la partie la plus antérieure du PPN, contrairement aux neurones répondeurs toniques prédominant à la partie postérieure (PPNc et CuN). Par ailleurs aucune différence n'a été notée sur les propriétés électrophysiologiques des neurones du PPN et du CuN. Cette étude a été ainsi la première à confirmer l'implication directe de la MLR chez le primate au cours de la locomotion.

### b) Imagerie chez l'homme

Des études d'imagerie chez les volontaires sains ont permis d'avoir des données sur le rôle de la MLR lors de tâches de marche réelle en PET ou imaginaire en IRM fonctionnelle (IRMf). Une première étude a identifié les régions cérébrales activées chez des volontaires sains, lors de la réalisation de plusieurs tâches locomotrices imaginaires après entrainement: station debout, saut, marche et course. L'analyse des résultats a permis de mettre en évidence une activation de la MLR pendant les conditions de marche et de course (Jahn et al., 2008). Une autre étude a comparé les données obtenues en IRMf sur une tâche de marche imaginaire, aux données en PET au cours d'une marche réelle à vitesse constante chez les mêmes sujets (la Fougere et al., 2010). Les résultats ont montré à nouveau une activation de la MLR au cours des 2 tâches de marche réelle et imaginaire, validant ainsi les résultats obtenus en IRMf. Enfin une étude réalisée par notre équipe en IRMf a repris une version modifiée d'un paradigme précédemment décrit (Bakker et al., 2008), associant une tâche de marche imaginaire avec une tâche imaginant un disque mobile (Karachi et al., 2012), celles-ci étant effectuées à 2 vitesses différentes. Une ségrégation fonctionnelle a été montrée (figure 4), avec un réseau associant le PPN dorsal et le CuN impliqué dans les fonctions motrices, et le PPN ventral plutôt impliqué dans l'intégration sensorielle au cours de la locomotion.

Figure 4: Illustration des activations neuronales au sein du PPN
*d'après Karachi et al (2012)*
*(IG = marche imaginaire; IOM = imagination d'un disque mobile)*

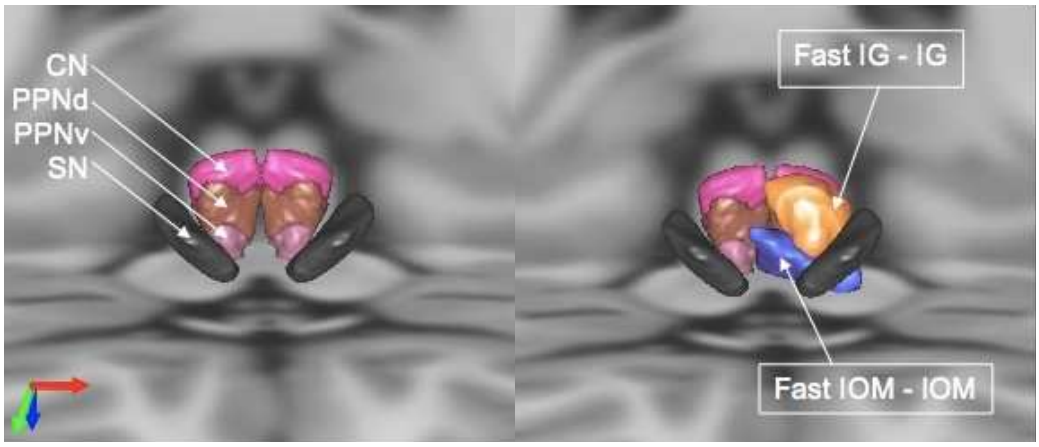


Le PPN et le CuN font ainsi vraisemblablement partie des nombreuses régions du tronc cérébral impliquées dans l'initiation de la locomotion, en activant les réseaux neuronaux d'un pattern locomoteur spécifique, et hautement préservés chez les vertébrés. Le retour sensoriel et visuo-spatial est un élément primordial de la locomotion, permettant l'adaptation au contexte. Cette intégration étant indispensable à l'initiation de la locomotion et à son maintien, le PPN et le CuN ont aussi d'autres fonctions permettant probablement cette intégration en tenant compte d'informations cognitives mais aussi émotionnelles permettant l'activation de programme tel que la fuite, et constituant une interface moteur/limbique au sein du mésencéphale latéral (Allen et al., 1996; Walker et Winn, 2007).

## 2. Fonctions non motrices

### a) *Fonctions cognitives*

L'implication du PPN dans les fonctions non motrices, c'est à dire cognitives, émotionnelles et motivationnelles, a été largement étudiée ces dernières années. Nous détaillerons ici principalement le rôle du PPN dans les fonctions d'apprentissage et de préférence contextuelle, et dans les processus motivationnels liés à la recherche de récompense.

*Rôle dans l'apprentissage*

Chez le rat, des injections locales unilatérales d'acide iboténique dans le PPN entraînent des perturbations de la mémoire de travail (Koch et al., 1993; Steiniger et Kretschmer, 2004), et des lésions bilatérales électrolytiques vont induire une détérioration des performances cognitives et de l'apprentissage (Homs-Ormo et al., 2003). De même, après une lésion excitotoxique du PPN, les rats étaient incapables de réaliser une nouvelle tâche s'ils n'avaient pas été préalablement entraînés (Alderson et al., 2004), montrant le rôle fondamental du PPN dans l'apprentissage de nouvelles tâches. Enfin, après injection locale de muscimol (agoniste GABAergique) dans le PPN postérieur, les rats perdaient la capacité de modifier et adapter leur action lorsqu'il se produisait un changement dans la conséquence de cette action, par rapport aux animaux contrôles (Maclaren et al., 2013).

On sait par ailleurs que la voie ascendante thalamo-corticale est impliquée dans le maintien d'un état attentionnel requis pour augmenter la performance lors de la réalisation de tâches comportementales (Garcia-Rill, 1991; Reese et al., 1995; Kinomura et al., 1996). Aussi, des travaux réalisés par l'équipe de Kobayashi ont montré le rôle des neurones du PPN dans la régulation de l'attention au cours de la réalisation de tâches complexes (Kobayashi et al., 2002; Okada et Kobayashi, 2015). Renforçant ces données expérimentales, des études réalisées chez les patients parkinsoniens implantés dans le PPN, ont confirmé l'implication du PPN dans ces fonctions avec un effet de la stimulation à basse fréquence sur les performances cognitives. Il a été ainsi mis en évidence une amélioration significative sur les tâches impliquant la mémoire de travail, avec une diminution du temps de réponse (Costa et al.,

2010). Des effets sur les fonctions exécutives et attentionnelles ont aussi été démontrés, ainsi que sur la fluence verbale et la mémoire à long terme (Ceravolo et al., 2011). Ces effets cliniques sont associés à une augmentation du métabolisme de certaines aires corticales, avec une augmentation de la consommation de glucose dans les aires pré-frontales bilatérales (dont le cortex dorso-latéral et orbito-frontal) mais aussi le striatum ventral et l'insula (Stefani et al., 2010).

*Implication dans les processus motivationnels et de récompense*

Le rôle du PPN dans la motivation et la prédiction de la récompense à obtenir au décours d'une action a été étudié chez les rongeurs (Thompson et Felsen, 2013) et le primate (Okada et al., 2009; Okada et Kobayashi, 2013). Cette dernière équipe a étudié l'activité unitaire des neurones du PPN lors d'une tâche comportementale, dont la récompense prévisible était indiquée par la forme de la cible de fixation (figure 5). Elle a ainsi mis en évidence la présence de 2 groupes de neurones distincts dans le PPN, impliqués dans la transmission de l'information liée à la récompense: un premier groupe de neurones FT (Fixation Target) est activé lors de la fixation jusqu'à la réception de la récompense, et l'autre groupe RD (Reward Delivery) est activé au moment de la réception de la récompense avec un degré d'activation proportionnel à l'amplitude de cette récompense. De plus, une modification de l'activité tonique des neurones du PPN a été montrée comme étant secondaire à l'anticipation de la récompense et à son amplitude lors de cette même tâche comportementale. Le PPN apparait ainsi comme ayant un rôle important dans le renforcement positif et l'association entre l'action et ses conséquences, indispensables pour permettre l'apprentissage.

Figure 5: Diagramme représentant la tâche comportementale
et l'activation des neurones FT et RD au cours de la tâche
*d'après Okada et al (2009 ) et Okada et Kobayashi (2013)*

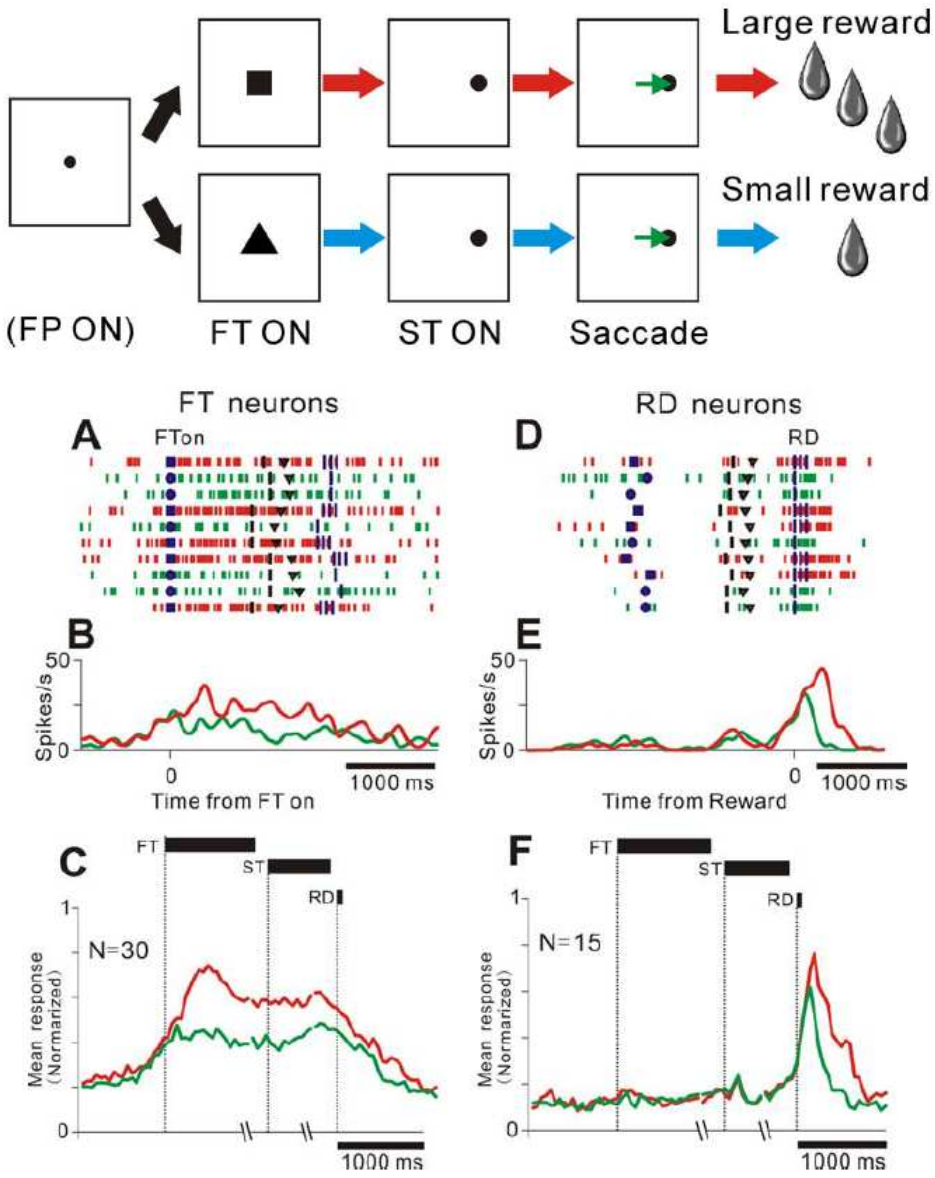

D'autres travaux chez le rongeur ont montré un effet impliquant les circuits liés à la récompense et à l'addiction. En effet, chez le rat après injection bilatérale de muscimol dans le PPN, il a été observé une diminution significative de l'auto-administration d'éthanol. Cette modification était similaire à celle observée après micro-injections bilatérales d'agonistes dopaminergiques dans le noyau accumbens (Samson et Chappell, 2001). En parallèle, des lésions excitotoxiques bilatérales du PPN vont entraîner une augmentation de la consommation en sucrose sélectivement dans les conditions d'excitation motivationnelle (Alderson et al., 2001). De même, l'auto-administration de nicotine va être elle aussi modifiée par une lésion du PPN postérieur (Alderson et al., 2006). Cette même lésion va aussi entraîner une altération de la réponse locomotrice induite par la nicotine, par atteinte de l'innervation du PPN vers la VTA, dont le rôle dans la réponse comportementale liée à la nicotine est essentielle (Alderson et al., 2008). Une lésion du PPN antérieur ne va quant à elle pas avoir d'effet sur la locomotion induite par la nicotine, suggérant à nouveau une ségrégation fonctionnelle au sein du PPN.

### *b) Contrôle des états de veille et sommeil*

Les premières expériences montrant l'implication de la formation réticulée du tronc cérébral dans le contrôle des cycles veilles-sommeil datent de 1949 (Moruzzi et Magoun, 1949). Chez le chat anesthésié, le système réticulé activateur ascendant (SRAA) fut identifié par la stimulation électrique du tegmentum mésencephalique induisant un éveil cortical, et la lésion induisant un coma. Les principaux systèmes impliqués dans le SRAA ont ensuite été définis sur le plan anatomique, comprenant les neurones adrénergiques du locus coeruleus, sérotoninergiques des noyaux du raphé et cholinergiques du noyau latéro-dorsal du tegmentum et du PPN (Shute et Lewis, 1967). On sait depuis qu'il existe plusieurs structures organisées en réseau du tronc cérébral vers le cortex, l'excitation pharmacologique de l'une d'elle étant systématiquement suivie par l'activation de l'ensemble des autres structures. Dans ce réseau, les neurones du PPN et du noyau latéro-dorsal du tegmentum (LDT) sont connectés avec le cortex via des projections principalement cholinergiques sur les noyaux intralaminaires postérieurs du thalamus (noyaux parafasciculaire et centro-médian) et sur le noyau périthalamique (Steriade et al., 1991; Oakman et al., 1995).

Les neurones cholinergiques du PPN font ainsi partie de la voie ascendante thalamo-corticale régulant les états de veille et sommeil, et le passage de l'un à l'autre. Une diminution de l'activité des neurones du PPN a été mise en évidence chez le chat et le rat durant le sommeil profond (à ondes lentes) ( Steriade et al., 1990; Rye, 1997; Datta, 2002). Par ailleurs, les neurones cholinergiques du PPN sont actifs pendant l'éveil et le sommeil paradoxal, et leur activité diminue durant les phases de sommeil (Steriade et al., 1990; Vincent, 2000; Garcia-Rill et al., 2007). Des lésions stéréotaxiques dans la région du PPN chez le chat (Webster et Jones, 1988; Shouse et Siegel, 1992) ou des traitements pharmacologiques d'antagonistes de l'acétylcholine dans des régions de projections du PPN diminuent ou abolissent le sommeil paradoxal et réduisent l'éveil (Velazquez-Moctezuma et al., 1989). La modulation des états de veille se ferait en activant la voie ascendante thalamo-corticale (Steriade et al., 1991) et le tonus musculaire grâce aux projections descendantes via le faisceau réticulo-spinal (Pare et al., 1988; Jones, 1993), le PPN étant ainsi impliqué dans l'atonie musculaire pendant le sommeil paradoxal (Takakusaki et al., 2003; Garcia-Rill et al., 2004). Ces données convergent donc vers un rôle clé des neurones cholinergiques du PPN dans la régulation du sommeil paradoxal et de l'éveil. Cependant, les études expérimentales plus récentes ne retrouvent pas de rôle spécifique « déclencheur » des transitions veilles-sommeil. Des études lésionnelles plus restreintes du PPN chez le rat (Deurveilher et Hennevin, 2001) montrent de profondes modifications du sommeil, avec notamment une diminution des phases de sommeil paradoxal, mais ces perturbations ne sont que transitoires. Parallèlement, une stimulation électrique ou pharmacologique du PPN chez le chat et le rat peut induire un état de sommeil paradoxal avec une atonie musculaire (Jones, 1993; Takakusaki et al., 2004). Plus récemment chez le rat, il a été montré que les neurones cholinergiques du PPN ont une activité maximale pendant les stades d'éveil et de sommeil paradoxal (Boucetta et al., 2014). Ces données ont été confirmées en optogénétique chez la souris, où la stimulation spécifique des neurones cholinergiques du PPN induit une augmentation de la fréquence des épisodes de sommeil paradoxal (Van Dort et al., 2015) (Figure 6). Enfin, des études en chémogénomique chez la souris montrent un rôle différent dans l'éveil et le sommeil en fonction des populations neuronales activées (Kroeger et al., 2017). En effet l'activation des neurones glutamatergiques va augmenter l'éveil et les comportements locomoteurs associés. L'activation des neurones cholinergiques va supprimer

les ondes lentes durant le sommeil profond, mais ne va pas avoir d'effet direct sur la durée ou la survenue des stades de sommeil paradoxal. Ces résultats suggèrent ainsi que le PPN va avoir un rôle dans l'initiation des états de veille et de sommeil paradoxal, plutôt qu'un rôle déclencheur.

Figure 6: Modulation et induction du sommeil paradoxal après activation optogénétique des neurones cholinergiques
*d'après Van Dort et al (2015)*

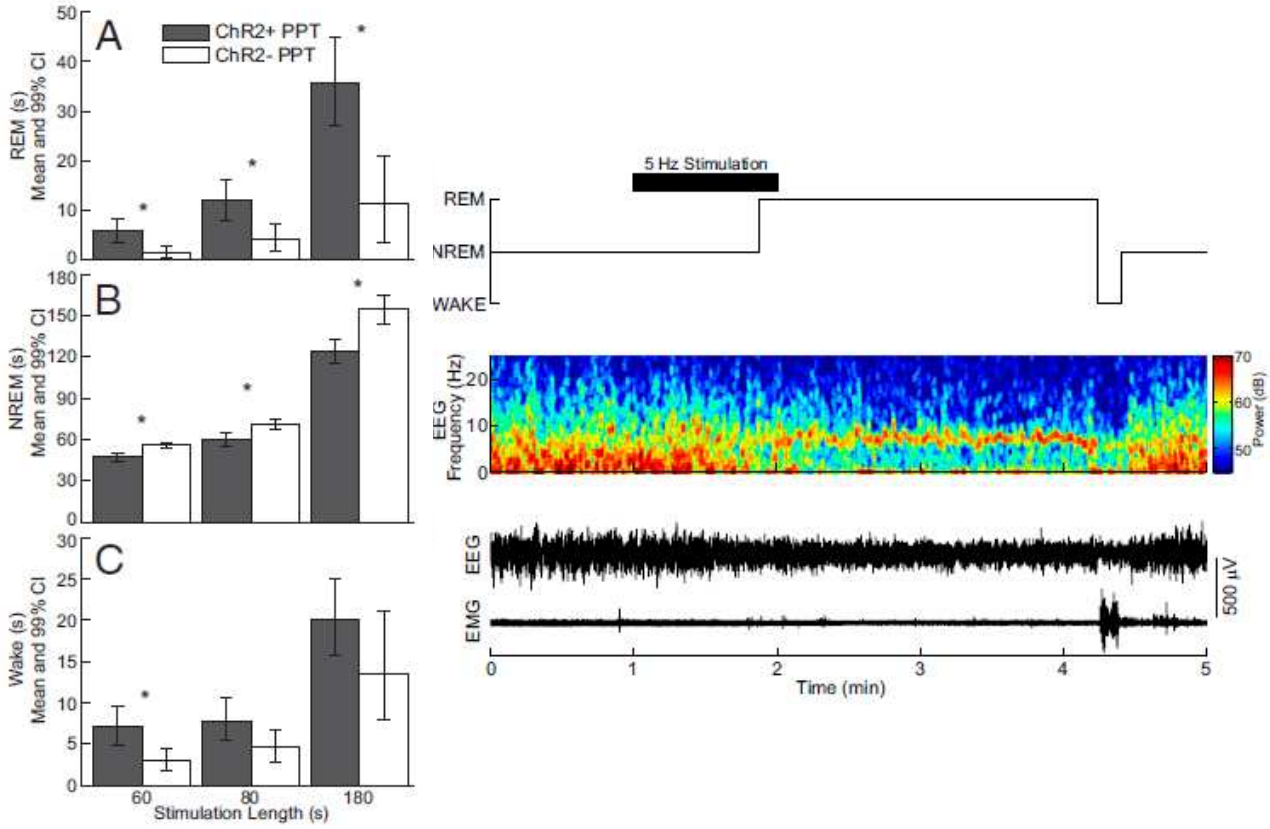


Ainsi, on peut considérer le PPN comme un des composants clefs du réseau de structures cérébrales contrôlant le sommeil, sans être l'unique régulateur ou déclencheur du sommeil paradoxal.

# Cholinergic mesencephalic neurons are involved in gait and postural disorders in Parkinson disease

Carine Karachi,[1,2,3,4] David Grabli,[1,2,3,4] Frédéric A. Bernard,[1,2,3,5] Dominique Tandé,[1,2,3] Nicolas Wattiez,[1,2,3] Hayat Belaid,[1,2,3,4] Eric Bardinet,[1,2,3] Annick Prigent,[1,2,3] Hans-Peter Nothacker,[6] Stéphane Hunot,[1,2,3] Andreas Hartmann,[1,2,3,4] Stéphane Lehéricy,[1,2,3] Etienne C. Hirsch,[1,2,3] and Chantal François[1,2,3]

[1]Université Pierre et Marie Curie — Paris 6, CR-ICM, UMR-S975, Paris, France. [2]INSERM, U975, Paris, France. [3]CNRS, UMR 7225, Paris, France. [4]Assistance Publique-Hôpitaux de Paris, Groupe Pitié-Salpêtrière, Paris, France. [5]Laboratoire d'Imagerie et de Neurosciences Cognitives, FRE 3289, CNRS/Université de Strasbourg, Strasbourg, France. [6]Department of Pharmacology, School of Medicine, University of California, Irvine, California, USA.

**Gait disorders and postural instability, which are commonly observed in elderly patients with Parkinson disease (PD), respond poorly to dopaminergic agents used to treat other parkinsonian symptoms. The brain structures underlying gait disorders and falls in PD and aging remain to be characterized. Using functional MRI in healthy human subjects, we have shown here that activity of the mesencephalic locomotor region (MLR), which is composed of the pedunculopontine nucleus (PPN) and the adjacent cuneiform nucleus, was modulated by the speed of imagined gait, with faster imagined gait activating a discrete cluster within the MLR. Furthermore, the presence of gait disorders in patients with PD and in aged monkeys rendered parkinsonian by MPTP intoxication correlated with loss of PPN cholinergic neurons. Bilateral lesioning of the cholinergic part of the PPN induced gait and postural deficits in nondopaminergic lesioned monkeys. Our data therefore reveal that the cholinergic neurons of the PPN play a central role in controlling gait and posture and represent a possible target for pharmacological treatment of gait disorders in PD.**

## Introduction

Gait disorders and postural instability represent a major burden in the elderly population and are commonly observed in severe and advanced forms of Parkinson disease (PD; ref. 1). While most parkinsonian symptoms can be alleviated by L-dopa replacement therapy, gait disorders respond poorly to dopaminergic drugs, which suggests that they are caused by nondopaminergic lesions.

Despite our current knowledge of the basic physiology of gait, the alterations in the central nervous system that cause gait disorders have yet to be identified. Experimental studies have revealed that the optimal site for the induction of rhythmic stepping behavior in decerebrate animals lies in a functionally defined mesencephalic locomotor region (MLR). Anatomically, the MLR encompasses the cuneiform nucleus (2) and the pedunculopontine nucleus (PPN), which is heterogeneously composed of cholinergic and noncholinergic neurons (3). Whether these structures are involved in human gait is still under debate, given the inconsistent results of functional MRI (fMRI) studies using mental imagery of gait to model real gait (4–6). In PD, among the different nondopaminergic neuronal systems affected (7), cholinergic cell loss was found in the PPN of patients with the most severe dopaminergic degeneration (8). Based on the assumption that gait failure is induced by PPN lesion or dysfunction (9), recent therapeutic trials tested the efficacy of electrical modulation of the PPN in reducing these symptoms in selected parkinsonian patients (10–14). However, the variability of the results raised doubts about the initial hypothesis and emphasized the need to determine the role of the PPN, in particular its cholinergic part, in gait and posture.

In the present study, using a broad range of approaches in humans and monkeys in either the normal or the parkinsonian state, we demonstrated that the PPN, and more particularly its cholinergic part, is essential in controlling the performance of gait and posture.

## Results

*The PPN region is activated during fast imagined walking in healthy humans*. Since PPN neurons are reported to increase their firing rate in response to step frequency in human parkinsonian patients (15), we hypothesized that the activity of the PPN region could be modulated by the speed of imagined gait. To address this issue, we performed an fMRI study in healthy subjects using a modified version of a previously validated paradigm (5). The subjects were instructed to perform an imagery of gait (IG) task at either normal or faster speed, based on the assumption that imaginary movement and actual movement execution activate overlapping areas (15). Imagery of object movement (IOM) was used as a control task; subjects were asked to imagine a disk moving in the same environment at either normal or faster speed (at around 30% faster). To ensure that the subjects had performed the tasks properly, we first measured imagery times required to perform the task, and verified that the faster the speed, the shorter the imagery time (Supplemental Figure 1; supplemental material available online with this article; doi:10.1172/JCI42642DS1). The comparison between the IG and IOM conditions yielded significant activations in a network of brain regions that include the superior frontal gyri and the cingulate cortex (Figure 1A and Table 1), as previously described (5). As expected, the comparison between the faster IG and normal IG conditions revealed substantial activation of a single cluster in the MLR in the left midbrain (Figure 1B). Superimposed anatomical structures revealed

**Authorship note:** Carine Karachi and David Grabli contributed equally to this work.
**Conflict of interest:** The authors have declared that no conflict of interest exists.
**Citation for this article:** *J Clin Invest.* 2010;120(8):2745–2754. doi:10.1172/JCI42642.

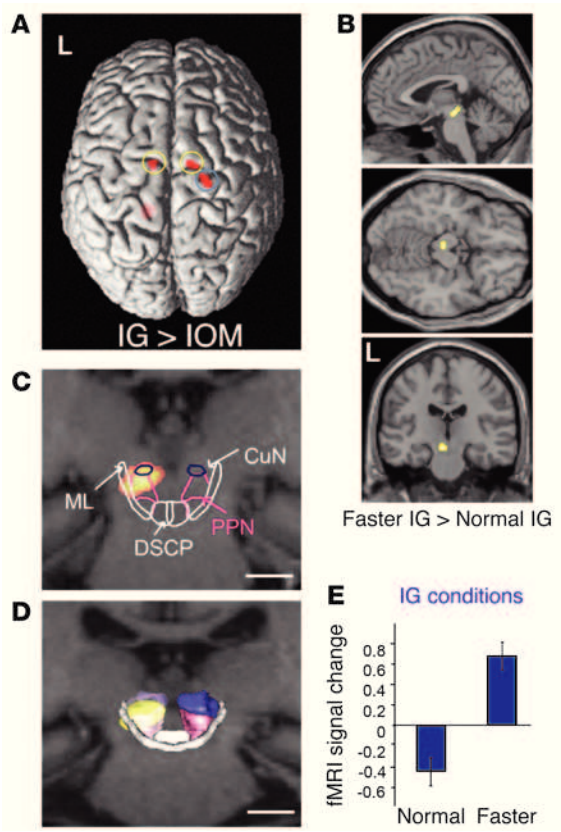


**Figure 1**
Cerebral activity during IG and IOM in 15 healthy volunteers. (**A**) Regions of significant activation superimposed on a rendered brain viewed from above, showing increased activity in the superior frontal gyrus bilaterally (yellow circles) and the right precentral gyrus (blue circle) for the comparison of IG versus IOM ($P < 0.001$, uncorrected for multiple comparisons; cluster size, >30 voxels). (**B**) Regions of significant activation superimposed on T1-weighted images (top, sagittal; middle, transverse; bottom, coronal), showing increased activity in the left PPN and cuneiform nucleus for the comparison of faster versus normal IG ($P < 0.001$, uncorrected for multiple comparisons; cluster size, >30 voxels). Activity in this region survived a small volume correction (10-mm radius) for multiple comparisons (family-wise error, $P < 0.05$). (**C**) Regions of significant activation, superimposed on the tracing of cerebral contours in the PPN region, in a coronal MRI section. (**D**) Posterior view of the PPN and cuneiform nucleus. (**E**) Plots of activity in left PPN and cuneiform nucleus ($x$, –3; $y$, –22; $z$, –13) for normal and faster IG conditions. For $t$ values of each contrast, see Table 1. CuN, cuneiform nucleus; DSCP, decussation of superior cerebellar peduncle; L, left; ML, medial lemniscus. Scale bars: 10 mm.

that this cluster included the PPN and the adjacent cuneiform nucleus (Figure 1, C and D). Therefore, the PPN and cuneiform nucleus were activated during fast IG.

*Cholinergic neurons in the PPN degenerate in faller PD patients*. Freezing of gait and postural instability are often encountered in severe and advanced forms of PD. Because several lines of evidence suggest that these symptoms may be related to the degeneration of cholinergic neurons within the PPN, we determined whether neuronal loss in this structure was more severe in PD patients with balance deficits and falls than in PD patients without them. Using stereology, we quantified the number of cholinergic neurons labeled for acetylcholinesterase (AChE) histochemistry on 5 anteroposterior, regularly interspaced PPN sections (Figure 2, A and B) in 3 groups of human brains: healthy controls ($n = 8$), PD patients without balance deficits or falls (nonfaller PD; $n = 6$), and PD patients with balance deficits and falls (faller PD; $n = 6$). The number of $AChE^+$ neurons in faller PD patients was significantly lower than in nonfaller PD patients (609 ± 61 vs. 934 ± 63 neurons; $P < 0.01$, Kruskall-Wallis test followed by Mann-Whitney $U$ test) and in controls (1,058 ± 52 neurons; $P < 0.01$; Figure 2C). The number of Nissl-stained neurons in the adjacent cuneiform nucleus, as measured by stereology, was not significantly different ($P = 0.59$, Mann-Whitney $U$ test) between faller PD patients (3,502 ± 567 neurons/$mm^3$; 31% loss compared with controls) and nonfaller PD patients (3,152 ± 241 neurons/$mm^3$; 38% loss compared with controls). As expected, the number of tyrosine hydroxylase–positive ($TH^+$) neurons in the substantia nigra, as quantified by stereology, was severely reduced in both PD groups compared with controls (faller PD, 32,495 ± 4,799 neurons; nonfaller PD, 80,478 ± 30,968 neurons; control, 260,955 ± 19,482 neurons; $P < 0.01$, Mann-Whitney $U$ test; Figure 2D). Interestingly, the loss of dopamine neurons was also significantly more severe in faller than in nonfaller PD patients ($P < 0.01$, Kruskall-Wallis test followed by Mann-Whitney $U$ test).

*A loss of cholinergic neurons is detected in the PPN of aged parkinsonian monkeys displaying balance deficits*. The current monkey models of PD are developed using 1-methyl-4-phenyl-1,2,3,6-tetrahydropyridine (MPTP), a selective neurotoxin that produces dopamine depletion but no loss of PPN cholinergic neurons in young adult monkeys (16, 17). Yet, because aged but not young monkeys develop balance and postural deficits after intoxication with MPTP (18), we tested the possibility that these symptoms are associated with a loss of cholinergic neurons in the PPN. Young and aged MPTP-treated monkeys (total $n = 8$) developed motor symptoms (akinesia, rigidity, and episodes of tremor). Young MPTP-treated monkeys ($n = 4$) scored 10–12 on a disability scale of 0–25 (18), with no balance or posture deficits. In contrast, aged MPTP-treated monkeys ($n = 4$) developed a more severe parkinsonism, with scores ranging between 14 and 19 on the disability scale, and displayed major balance deficits and abnormal postures, as previously reported (19). To identify neuronal correlates of these differences, we analyzed nigral dopaminergic neurons and cholinergic neurons in PPN following sacrifice of the animals. Both groups of MPTP-treated animals displayed a dramatic loss of dopaminergic neurons in the substantia nigra and of dopaminergic fibers in the striatum (Supplemental Figure 2). In the aged MPTP-treated monkeys, the density of $TH^+$ fibers, as quantified by optical density measurements, showed a significant decrease of 90% in the caudate nucleus and 95% in the sensorimotor putamen compared with the controls. In the young animals, the decreases were 93% and 96%, respectively. PPN cholinergic neurons were then identified by NADPH diaphorase histochemistry (Figure 3A), which selectively labels these neurons in the PPN (18). They were quantified by stereology on 5 anteroposterior, regularly spaced sections throughout the PPN. The total number of $NADPH^+$ neurons did not differ between young and aged monkeys (young, 1,038 ± 18 neurons; aged, 885 ± 55 neurons; Figure 3B). In contrast, whereas MPTP did not affect the number of $NADPH^+$ neurons in young animals (949 ± 33 neurons), it induced a 30% loss of cholinergic neurons in aged monkeys (600 ± 19 neurons; $P < 0.01$, Mann-Whitney $U$ test).

**Table 1**
Group analysis of the network activated during IG relative to IOM and faster versus normal gait

| Brain region | Side | BA | Stereotactic coordinate | | | *t* value |
|---|---|---|---|---|---|---|
| | | | *x* | *y* | *z* | |
| **IG versus IOM** | | | | | | |
| Superior frontal gyrus | L | 6 | –11 | –6 | 67 | 4.17 |
| Superior frontal gyrus | R | 6 | 13 | –8 | 78 | 4.12 |
| Precentral gyrus | R | 6 | 21 | –18 | 69 | 4.16 |
| Median cingulate and paracingulate gyri | L | 23 | –16 | –38 | 32 | 5.49 |
| Cerebellum | R | | 5 | –46 | –42 | 5.12 |
| **Faster IG versus normal IG** | | | | | | |
| Pedunculopontine and cuneiform nuclei | L | | –3 | –22 | –13 | 6.11 |

Shown are significant signal increases in various brain regions ($P < 0.001$, uncorrected, cluster size >30) for IG versus IOM and faster IG versus normal IG. Stereotactic coordinates are reported in MNI space. BA, Brodmann area; L, left; R, right.

Because microglia may contribute to changes in normal aging, we analyzed the microglial reaction in the PPN of our young and aged normal monkeys. An increased number of microglial cells stained for HLA-DR antigen was detected in aged compared with young monkeys (2.4 ± 0.3 versus 1.5 ± 0.2 cells/mm$^3$; $P < 0.01$, Mann-Whitney *U* test).

*Cholinergic lesion within the PPN induces gait and postural disorders*. Since the PPN was activated in the IG task in healthy humans, and since PPN cholinergic lesion was associated with gait disorders in both human disease and the monkey model of PD, we sought to demonstrate experimentally that PPN cholinergic lesion without dopaminergic injury is sufficient to induce a gait deficit. Bilateral injections of urotensin II–conjugated diphtheria toxin (3–10 μl, 20%–30%) in the PPN of 5 animals resulted in significant and reproducible changes in gait and posture during the 7–8 weeks of survival. These symptoms included a decrease in the angle of the knee and in step length and speed, an increase in the back curve, deviation of the hindquarters and of the head, modification of the tail position (axial rigidity), and arm and leg rigidity (Figure 4 and Table 2). Importantly, no modification of global motor activity in the home cage was detectable, except for animal M2. None of these gait and postural parameters improved after injection of 120 μg/kg apomorphine (Figure 4), which confirmed that they were unrelated to dopamine depletion.

Cholinergic neurons of the PPN were then studied postmortem by NADPH diaphorase histochemistry (Figure 5B). Mapping of the injection sites (Figure 5C) revealed that even though the loss of cholinergic neurons was variable from one monkey to another, all injection sites were located within the cholinergic part of the PPN in all animals (Figure 5D). The number of NADPH$^+$ neurons was reduced by a mean of 39% in the lesioned animals compared with controls (PPN-lesioned, 4,951 ± 621 neurons, $n = 5$; control, 8,178 ± 236 neurons, $n = 5$; $P < 0.01$, Mann-Whitney *U* test; Figure 5E). Moreover, we also determined that myelinated fibers were preserved after the toxin injections (Figure 5F).

*Comparison of gait and posture disorders between MPTP-induced dopaminergic injury and PPN lesion*. We then compared bilateral PPN lesion–induced gait and walking disorders with those induced by the dopaminergic depletion caused by MPTP injection. The most prevalent symptom observed in the 4 MPTP-treated macaques was akinesia, assessed on the basis of a dramatic and significant decrease in global activity in the home cage, in arm speed during a food retrieval task, and in step speed during locomotion (Figure 4). The animals also displayed a cog-wheel rigidity of the extremities, characteristic of the parkinsonian state and unlike the rigidity observed in monkeys with PPN lesion. Gait and posture deficits observed in the MPTP-treated macaques included a decrease in step length and speed and an increase in the back curve, as in monkeys after PPN lesion. However, the major difference between the 2 groups was that in MPTP-treated animals, these symptoms were significantly reversed by apomorphine treatment (Figure 4).

## Discussion

Identifying the brain structures involved in gait and balance and elucidating their dysfunction are prerequisites for the development of new treatments designed to reduce the occurrence of falls in the elderly, a major public health and community problem. Our study is the first to our knowledge to demonstrate that gait and posture in primates are under the control of cholinergic neurons of the PPN. This statement is based on converging evidence from (a) an fMRI study that showed increased activation of the MLR, and more particularly the PPN, during fast compared with normal IG in healthy human subjects and (b) an experimental study showing that lesion of the cholinergic neurons of the PPN was sufficient to produce gait and posture deficits in normal monkeys. In addition, we found a correlation between the loss of PPN cholinergic neurons and balance deficits in the parkinsonian state and in aged MPTP-treated monkeys. This result helps to clarify the pathophysiology of L-dopa–resistant deficits of gait and posture in advanced forms of PD and highlights the key role of a PPN cholinergic lesion in these symptoms.

One of the main findings of our study was that PPN lesion induced gait deficits. This is in line with previous experimental studies showing that electrical or pharmacological manipulations of the PPN region can modulate gait on a treadmill in decerebrate cats and rodents (2, 20, 21). In these experiments, increasingly higher levels of electrical stimulation of the PPN region drove the frequency of stepping from a walk to a gallop (22), which suggests that the activation level of the PPN area is critical for the cadence of gait. This is consistent with our fMRI results obtained in healthy humans during IG, in which the PPN region was activated after an increase in the speed of gait. Likewise, extracellular recordings of the PPN region obtained in human parkinsonian patients showed that neurons increase their firing rate according to step frequency (15). Conversely, PPN activation could be related to higher-order functions, such as the visuospatial or attentional processes needed to maintain a certain level of motor performance in faster gait. Experimental data in rodents suggest that the PPN establishes high-order function rather than basic motor control (23). In line with this concept, the axial deficits observed in the present study after specific cholinergic lesion of the PPN were surprising, since they contrast with previous results obtained after experimental lesion of the PPN without discrimination of targeted neuronal subtypes as performed with ibotenic lesions in rats. These ibo-

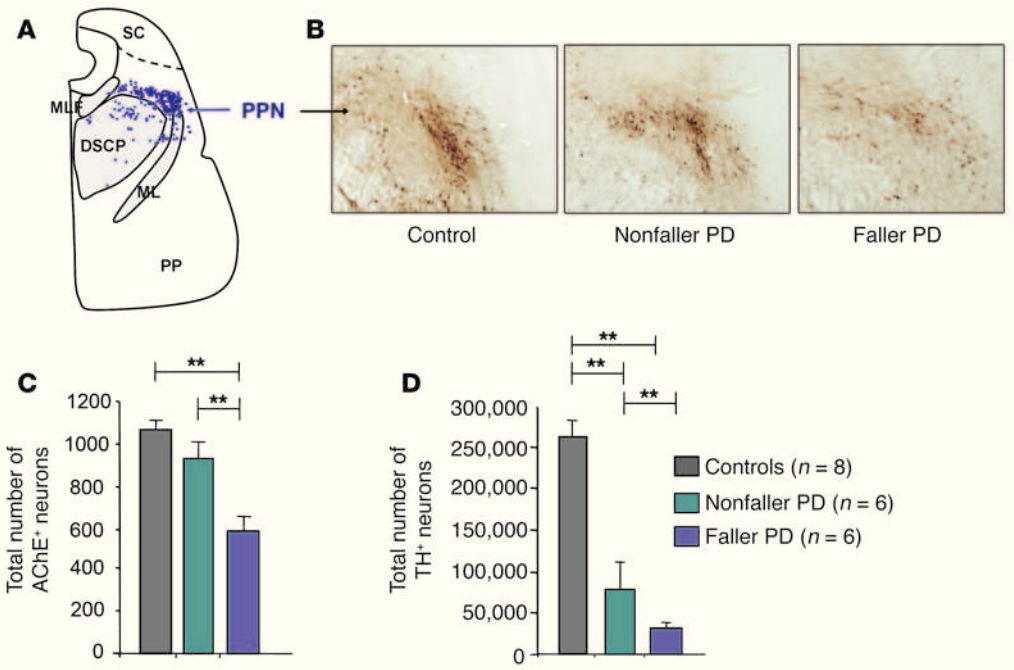


**Figure 2**

Relationship between loss of PPN cholinergic neurons and balance deficits in human PD patients. (**A**) Computer-generated map of AChE+ neurons in the PPN of a control brain. Blue dots represent individual neurons. (**B**) Transverse sections at PPN level illustrating that the loss of AChE+ neurons of a faller PD patient was more severe than in a nonfaller PD patient. (**C**) Total number of AChE+ neurons in the PPN of controls ($n = 8$), nonfaller PD patients ($n = 6$), and faller PD patients ($n = 6$). The mean value for the faller PD patients was significantly different from the mean for the control group and from the mean for the nonfaller PD patients. (**D**) Total number of TH+ neurons in the substantia nigra pars compacta of the same groups of control and PD patients. The mean values for the 2 PD groups were significantly different from the mean for the control group. MLF, medial longitudinal fasciculus; PP, pes pedunculi; SC, superior colliculus. $^{**}P < 0.01$, Mann-Whitney *U* test. Scale bar: 1 mm.

tenic PPN lesions resulted in subtle cognitive deficits, but failed to induce impairment in spontaneous locomotion (24, 25), except for a deficit in baseline activity when the lesion involved the anterior PPN (26). In monkeys, PPN lesion induced typical parkinsonism with akinesia and hypertonia, but the behavioral analysis in the previous studies did not focus on gait and posture (27–29). In this context, it is intriguing that the PPN lesions we performed in monkeys failed to produce akinesia. These discrepancies could be related to the subtype of injured neurons or to the size of the lesions. Indeed, in previous studies in primates, the lesions were made using kainate, an excitotoxin not specific to a particular neuronal population that produces strong seizures and very large lesions. Therefore, it is quite possible that some structures adjacent to the PPN also participated in the development of akinesia and hypertonia. Moreover, in the previous studies, primate behaviors were tested during the first 7 postoperative days, when excitotoxin had seizure-promoting activity (30), but not later. In contrast, the PPN lesions made in our macaques selectively targeted a small population of neurons and were not sufficient to produce akinesia, but were large enough to induce clear postural and gait deficits that persisted until 7 weeks after surgery.

The large cluster of activation that we detected in the left PPN region of right-handed healthy subjects during fast imagined walking suggests the dominance of this left brainstem region for the locomotor system. In support of this view, a further comparison between the faster and normal IG conditions with a more lenient threshold ($P < 0.005$, uncorrected) highlighted an additional activation located in the left supplementary motor area ($x$, –8; $y$, –2; $z$, 54), which is the repository of the dominant right leg representation and is connected to the left PPN. This left dominance is in line with previous studies demonstrating that certain higher motor functions, such as execution of movement sequences, might be controlled more by the left hemisphere than by the right for both left- and right-limb movements (31, 32).

The postural and gait deficits that we observed after PPN lesions may partially resemble those obtained after dopaminergic denervation, since they share common features, such as rigidity, reduction of step length, or stooped posture during walking. However, a cog-wheel rigidity of the limbs was a characteristic that macaques displayed only after MPTP treatment, not after PPN lesion. Moreover, results of more detailed analysis supported the conclusion that the deficits actually differed, since no improvement of the symptoms with dopamine agonist treatment were observed after PPN lesion. In summary, our data demonstrated that while the dopaminergic system participates in the control of gait and posture, the PPN cholinergic system plays a complementary role with a specific contribution for each of these 2 systems. Additional fMRI experiments comparing PPN activation in faller and nonfaller PD patients and in healthy subjects would provide further clues to the role of the PPN in axial symptoms.

A prominent finding of our study was that cholinergic neurons of the PPN were involved in gait and balance disorders. The toxin that we used preferentially targeted the cholinergic neurons of the PPN, yet because some noncholinergic neurons were also affected (Supplemental Figure 4, B and C), we cannot

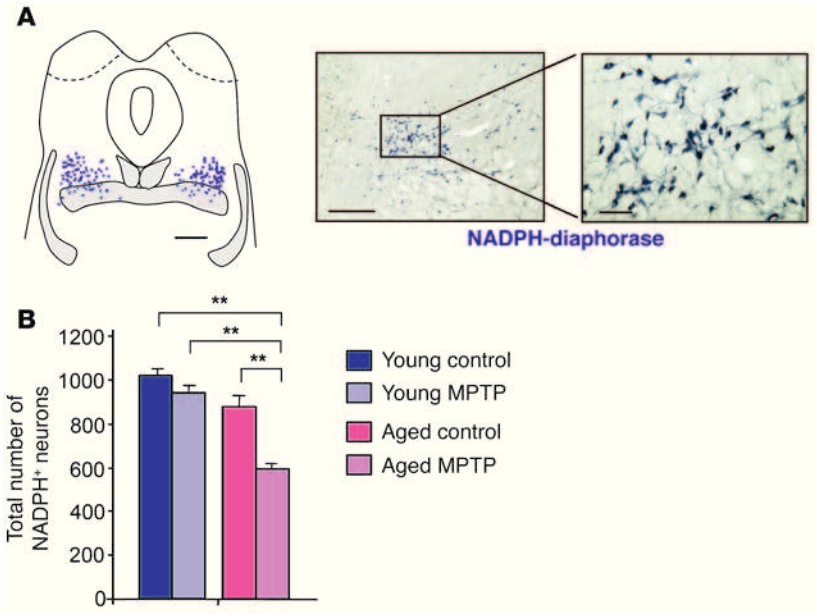


**Figure 3**
Loss of PPN cholinergic neurons in MPTP-treated macaques. (**A**) NADPH+ neurons mapped in the PPN of a control brain of a young macaque; hatched areas denote myelinated nerve fibers in the brainstem and blue dots represent individual neurons. Low- and high-magnification images are shown at right. (**B**) Total number of NADPH+ neurons quantified in young and aged MPTP-intoxicated macaques compared with their respective controls ($n = 4$ per group). MPTP did not affect NADPH+ neurons in young animals, but induced a 30% loss of cholinergic neurons in aged monkeys. $^{**}P < 0.01$, Mann-Whitney $U$ test. Scale bars: 2 mm (map); 500 μm (low magnification); 100 μm (high magnification).

entirely rule out the possibility that some symptoms may arise from a noncholinergic lesion. However, several lines of evidence from the postmortem data suggest that cholinergic lesions play a role in gait and balance disorders. Indeed, we observed a correlation between gait disorders and cholinergic neuronal loss within the PPN of PD patients. Previous studies already showed that cholinergic neuronal loss within the PPN was correlated with the level of dopaminergic degeneration (8) and with the clinical severity of the disease (33). However, to our knowledge, this is the first postmortem study in PD patients establishing a correlation between the occurrence of falls and freezing and the loss of cholinergic neurons in the PPN. We are aware that this correlation could be explained by confounding factors, such as a higher level of dopaminergic cell loss in patients with severe PPN cholinergic lesion. However, this possibility is unlikely, since the axial symptoms that we observed in the PD patients with prominent PPN cholinergic loss were not improved by dopaminergic treatment. Alternatively, the involvement of lesions in other brain structures (7) in the control of gait and posture might explain these symptoms. Nevertheless, the fact that the degree of neuronal loss in the cuneiform nucleus was not significantly different in the 2 groups of PD patients argues against the likelihood that whole-brain degeneration is more severe in faller than in nonfaller PD patients.

It is also interesting to note that PPN cholinergic neurons also degenerated in aged MPTP-treated monkeys, which develop postural and balance deficits after MPTP treatment (19). At first sight, this finding is puzzling since MPP+, the active metabolite of MPTP, is selectively taken up by dopaminergic terminals and thus does not act directly on cholinergic neurons. One possible explanation for this finding could be related to the profound atrophic changes that occur in cholinergic neurons of the PPN during aging (34, 35). An age-related increase in activated microglial cells in the PPN of aged normal monkeys, as observed in the present study, could also account for MPTP toxicity on cholinergic cells in aged MPTP-treated monkeys (36). Since PPN neurons project to nigral dopaminergic neurons (37), which, conversely, project back to PPN neurons (38), it is also possible that loss of target neurons or lack of proper dopaminergic inputs induced by MPTP treatment is added to age-related alteration of cholinergic neurons.

Finally, our findings provide a rationale for specifically targeting the cholinergic entity of the PPN as a strategy for the treatment of falls. Indeed, the direct involvement of PPN neurons in the control of gait and posture is in line with recent clinical data in PD patients showing that low-frequency electrical stimulation of the PPN area improved axial symptoms (10–14). The contribution of PPN cholinergic neurons could not have been determined previously from studies that used electrical stimulation or pharmacological manipulations. Thus, the identification of a specific subset of neurons crucially involved in postural control is of clinical significance, since better functional mapping of the PPN area may lead to the improvement of surgical targeting. Indeed, given the close proximity of the cholinergic and noncholinergic compartments within the PPN, the effects of electrical stimulation would vary according to current intensity and electrode location. Alternatively, pharmacologic manipulation of the surviving cholinergic neurons, or a strategy aimed at their protection, might represent an alternative therapeutic approach for falls in parkinsonian patients or for elderly people suffering from falls. Our results suggest that enhancing the cholinergic signal at the level of PPN targets could be a symptomatic treatment for gait failure in advanced PD. The administration of cholinesterase inhibitor would increase the efficiency of the acetylcholine released by the surviving cholinergic neurons. Yet, as observed for cognitive functions in patients with Alzheimer disease, the benefit of such manipulation would appear to be rather limited. Administration of nicotine or nicotinic agonists to act postsynaptically on cholinergic receptors might prove a more effective form of pharmacological manipulation. One of the main limitations of all these approaches is the lack of specificity of cholinergic manipulation for the PPN cholinergic system. Identification of cholinergic agonists specific to receptors expressed in the targets of cholinergic PPN neurons could also be a promising approach.

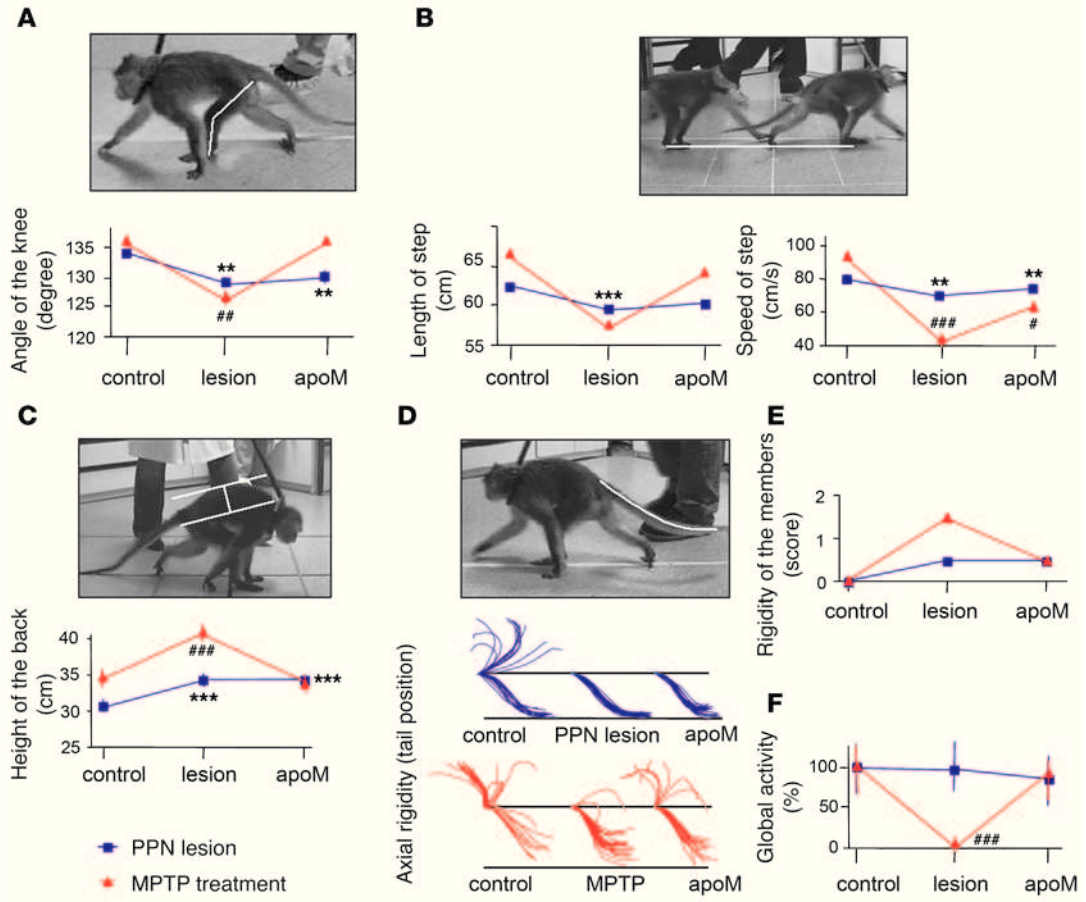


**Figure 4**

Comparison of MPTP-induced gait and postural disorders with those induced by bilateral cholinergic lesion. Gait and postural parameters were evaluated in macaques ($n$ = 9) in 3 conditions: under control conditions, after bilateral destruction of PPN cholinergic neurons ($n$ = 5) or MPTP intoxication ($n$ = 4), and after apomorphine treatment (apoM). Only results obtained in animal M4, with PPN lesion, and M6, treated by MPTP, are illustrated on the graphs. Symptoms included a decrease in the angle of the knee (**A**) and in step length and speed (**B**), an increase in the height of the back (**C**), modification of the tail position (axial rigidity; **D**), and arm and leg rigidity (**E**). The most prevalent symptom observed after MPTP intoxication was akinesia, as assessed by a dramatic and significant decrease in global activity (**F**). All these symptoms were significantly reversed by apomorphine treatment in MPTP-treated animals, but not in animals with PPN lesion. $^{*}P < 0.05$, $^{**}P < 0.01$, $^{***}P < 0.001$, PPN lesion versus control; $^{\#}P < 0.05$, $^{\#\#}P < 0.01$, $^{\#\#\#}P < 0.001$, MPTP intoxication versus control, Friedman test followed by Wilcoxon test.

## Methods

### *fMRI study*

*Subjects.* We scanned 15 healthy volunteers (7 females and 8 males) with a mean age of 24.7 ± 1.3 years. The study was approved by the local ethics committee, and written informed consent was obtained from all subjects in accordance with the Declaration of Helsinki. All participants were consistent right-handers (Edinburgh Handedness Inventory score, 89.88% ± 2.91%; ref. 39).

*Experimental task.* For the experimental task, subjects were first familiarized with a corridor with a path in the middle (length, 8 m; width, 2.30 m) and were asked to walk along the path 3 times at a normal speed (1.14 ± 0.10 m/s) and 3 times at around 30% faster (1.49 ± 0.12 m/s). Then, the subjects were shown video recordings of a disc moving in a straight line, at a uniform speed (either normal or faster speed) through the corridor. Subjects then performed a training session. There were 4 conditions: normal IG, faster IG, normal IOM, and faster IOM. For the IG conditions, subjects were asked to imagine walking along the path in a first-person perspective, as if their legs were moving, but without making any actual movements. For the IOM conditions, subjects were asked to vividly evoke a black disc moving along the path, starting from the beginning of the corridor and stopping at the end. During each trial, subjects first saw a photograph of the corridor, with a specific instruction written on it (normal IG, faster IG, normal IOM, faster IOM), projected onto a screen. Once the subjects were ready to start the imagery trial, they were instructed to close their eyes and press a button to signal that they had started imagining walking or seeing the disc moving. Subjects pressed the button again when they imagined that they or the disc had reached the end of the trajectory. A fixation cross was then presented on the screen (intertrial interval, 6–12 s), and the subjects could open their eyes. The training session was performed first outside the scanner (40 trials, 10 per condition), and then inside the MRI scanner (28 trials, 7 per condition). Functional imaging was done immediately after the training session, using an event-related design. Each stimulus presentation was controlled through a PC running Cogent software (Wellcome Department of Imaging Neuroscience). Motor responses (button presses with right thumb) were recorded via an MRI-compatible 1-button stick (Current Designs). The IG and IOM trials (80 trials, 20 per condition) were performed in 2 runs of around 15 minutes each. For each run, the trial order was pseudorandomized across the experimental factors (i.e., IG or IOM and normal or faster speed).

**Table 2**
Variations in posture and gait parameters after PPN lesion or MPTP intoxication and after apomorphine treatment in macaques

| Treatment | Angle of knee | Length of step | Speed of step | Global activity | Back curve | Arm speed | Limb rigidity | Pelvis deviation |
|---|---|---|---|---|---|---|---|---|
| **PPN lesion ($n$ = 5)** | | | | | | | | |
| Lesion | –7%[A] | –7%[A] | –11%[A] | NS | 10%[A] | NS | 0.7% | 0.5% |
| Apomorphine | –8%[A] | –9%[A] | –17%[A] | NS | 15%[A] | X | 0.7% | 0.5% |
| **MPTP intoxication ($n$ = 4)** | | | | | | | | |
| MPTP | NS | –16%[A] | –46%[A] | –87%[A] | 27%[A] | 138%[A] | 1.2% | 0% |
| Apomorphine | NS | NS | –23%[A,B] | –53%[A,B] | NS[B] | NS | 0.2% | X |

Mean values of parameters of posture and gait were calculated in monkeys with PPN lesion or intoxicated by MPTP, and after subsequent apomorphine treatment in both groups. Effects obtained are expressed as a percentage of the corresponding mean value in controls. Quantity of movement was calculated as described in Methods. The effect of lesion and apomorphine treatment on limb rigidity and pelvis deviation was evaluated on a 0–3 scale and was not statistically compared with the control condition. X, not measured. [A]$P < 0.01$ versus control; [B]$P < 0.01$ versus respective treatment prior to apomorphine, Kruskall-Wallis test followed by Mann-Whitney $U$ test in the event of statistically significant differences.

*MRI data collection*. Imaging data were collected at the Centre for NeuroImaging Research (CENIR) of Pitié-Salpêtrière Hospital using a Siemens Trio scanner operating at 3 Tesla. T2*-weighted echo-planar images depicting blood oxygenation level–dependent (BOLD) contrast were acquired in a single session (echo time, 30 ms; repetition time, 2.8 s; 40 coronal slices, interleaved acquisition; voxel size, 1.6 × 1.6 × 1.6 $mm^3$; field of view, 204.8 $mm^2$). High-resolution anatomical images were acquired using an MPRAGE sequence (echo time, 4.18 ms; repetition time, 2.3 s; 176 sagittal slices; voxel size, 1.0 × 1.0 × 1.0 $mm^3$; field of view, 256 $mm^2$).

*Data preprocessing*. Imaging data were preprocessed with SPM5 statistical parametric mapping software (http://www.fil.ion.ucl.ac.uk/spm) implemented on MATLAB (MathWorks Inc.). Images were corrected for differences in timing of slice acquisition, followed by rigid body motion correction. The motion parameters for translation ($x$, $y$, and $z$) and rotation (yaw, pitch, and roll) were included as covariates of noninterest in the general linear model. Following the coregistration of functional and structural images, the anatomical images were segmented and normalized to stereotactic Montreal Neurological Institute (MNI) space. Functional images were then normalized using the same normalization parameters and smoothed with a 10-mm full width at half-maximum isotropic Gaussian kernel. The time series were high-pass filtered (to a maximum of 1/128 Hz) to remove low-frequency noise. 4 event types were modeled: normal IG, faster IG, normal IOM, and faster IOM. The average hemodynamic response to each event type was modeled using a canonical, synthetic hemodynamic response function (40, 41). Onsets of the events were time-locked to the button press marking the onset of imagery, and duration was set at 0. Regions of significant activation were superimposed on the tracing of cerebral contours in the PPN region, drawn from a 3D histological atlas of the basal ganglia (40, 41) that had been deformed to the MRI template used for the fMRI analyses.

### *Human postmortem study in PD*

The study was performed on brain tissue sections from 8 control individuals, who died without known neurological or psychiatric deficit, and from 12 PD patients. Mean age at death was 85 ± 3 years for controls and 81 ± 3 years for PD patients. Clinical data were retrospectively extracted from patients' charts by 2 raters blinded to the results of stereological quantification of neurons. All PD patients had been treated with L-dopa or dopamine agonists. The diagnosis of PD was made on clinical grounds according to the UKPD Brain Bank Criteria (42) and confirmed postmortem on the basis of neuropathological examination. PD patients were distributed between 2 groups according to the scores for items 29 (balance) and 30 (gait) of the Unified PD Rating Scale (UPDRS; ref. 43) obtained while patients were in the "on" medication state. The range was 0–4, with a higher score indicating a more severe impairment. Patients scoring 2 or higher on one of these items were classified in the group characterized by balance deficits or falls ($n$ = 6). The other patients had no balance deficits or falls ($n$ = 6).

### *Macaque study*

*Animals*. All experiments were carried out in accordance with the recommendations contained in the European Community Council Directives of 1986 (86/609/EEC) and the NIH Guide for the Care and Use of Laboratory Animals and were approved by the French Animal Ethics Committee of INSERM. The animals were housed under conditions of constant temperature (21°C ± 1°C), humidity (55% ± 5%), and air replacement (16 times/h), on a 12-hour light/12-hour dark cycle with access ad libitum to food and water. In order to quantify the loss of PPN neurons after MPTP treatment, we used brain sections obtained from macaques previously analyzed for another study (35). There were 7 aged macaques (*Macaca arctoides*), estimated to be about 30 years old according to their dentition and the appearance of their hair, and 8 young macaques (*Macaca fascicularis*), aged 3–5 years. The present study also included 5 *M. fascicularis* used for testing the effect of bilateral PPN lesion on gait and posture and 4 *M. fascicularis* intoxicated by MPTP to test the effect of dopaminergic lesions on gait and posture; they were 5–6 years old and their weights ranged from 3 to 5 kg.

*Behavioral analysis*. We initially habituated 9 macaques to walk guided with a pole in a corridor; this learning period lasted about 2–3 months per animal. The animals were videotaped with orthogonally positioned cameras (face and profile). The animals' right and left sides were both considered. The video recordings were analyzed offline in order to quantify various parameters of gait and posture. For this purpose, images were extracted from the face and profile videos, each image being selected on the basis of the body axis of the animal during the walk sequence, which had to be parallel to a line drawn on the floor, and of the position of its arms and legs, which had to be identical from one image to another. The parameters were the angle of the knee and the elbow; the height of the pelvis (length of the perpendicular straight line between the tail insertion and the line between the 2 feet) and of the back (distance between the line extending from the tail insertion and the top of the neck and the parallel line tangent to the top of the back); the step length (distance between 2 consecutive contacts of the same foot) and speed (step length divided by its duration, estimated from the number of consecutive images between 2 consecutive ground contacts of the same foot); and the tail position. These different parameters were quantified using ImageJ software (http://rsb.info.nih.gov/ij/links.html). Animals were also trained to sit quietly in a primate chair and be manipulated by the examiner to clinically assess rigidity and tremor

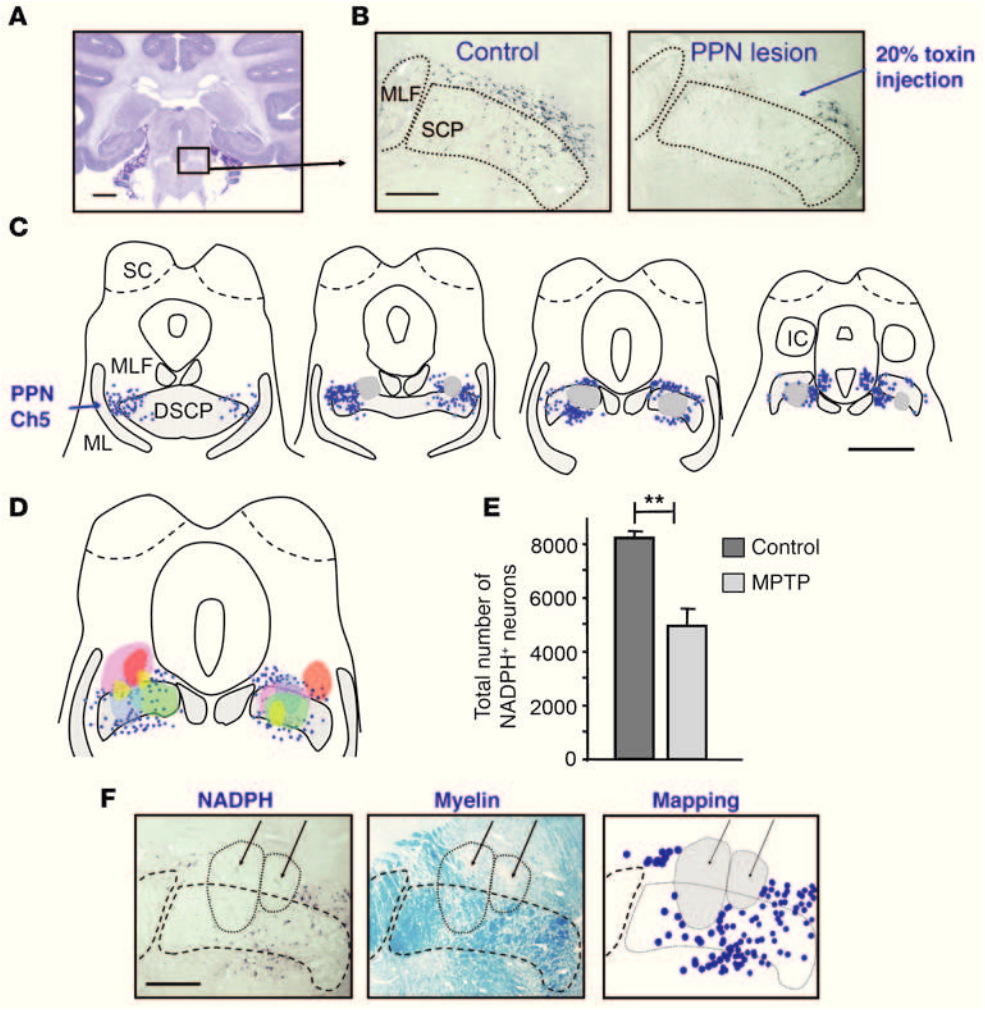


**Figure 5**

Loss of NADPH+ neurons after bilateral PPN lesion. (**A**) Nissl-stained section showing the anatomical localization of the PPN (boxed region) in a control macaque brainstem. (**B**) Photomicrographs of PPN sections labeled for NADPH diaphorase histochemistry, showing a 20% toxin injection site into the PPN compared with a control. (**C**) Computer-generated maps of NADPH+ neurons (blue) in 4 regularly spaced sections covering the anteroposterior extent of the structure in lesioned animal M4. Each dot represents an NADPH+ neuron; gray areas represent the extent of the injection site; hatched areas denote myelinated nerve fibers. (**D**) All injection sites of the 5 macaques were transferred onto the corresponding brainstem map of macaque M4. Each individual is represented by a different color. Note that the cholinergic part of the PPN was lesioned in all animals. (**E**) Quantification of the total number of NADPH+ neurons in the PPN, showing that neuronal loss reached 39% in lesioned animals ($n = 5$) compared with controls ($n = 5$). $^{**}P < 0.01$, Mann-Whitney *U* test. (**F**) Adjacent PPN sections, labeled for NADPH diaphorase histochemistry and for myelin staining with luxol fast blue, and mapping of NADPH+ neurons showed that myelinated fibers were preserved after toxin injections at 20%. Arrows indicate the center of 2 lesions. IC, inferior colliculus; SCP, superior cerebellar peduncle. Scale bars: 5 mm (**A** and **C**); 1 mm (**B** and **F**).

(rated between 0 and 3). They also learned a simple food retrieval task to study the execution of voluntary movements of the upper arms, during which speed of arm movement was quantified. The task consisted of picking up food pieces placed in wells on a 24-well board. The animals were taught to retrieve the food on the right and left part of the board with their right and left hands, respectively. The motor activity of the macaques was assessed when they were free to move in their home cage and was performed using a video image analyzer system (Vigie Primates ViewPoint). Using this system, the quantity of movement was expressed in arbitrary units and calculated as changes in gray level in pixels from one image to the next, counted every 80 ms for 20 minutes.

*MPTP treatment*. We used brain sections obtained from 3 aged and 4 young macaques that received MPTP treatment (0.25–0.60 mg/kg) as previously described, and 4 young and 4 aged macaques were used as controls (38). For the present study, we also intoxicated 4 young macaques (*M. fascicularis*) using the same protocol. Parkinsonian symptoms (akinesia, rigidity, postural instability, and intermittent episodes of tremor) were scored on a disability scale of 0–25 (18).

*Injection of urotensin II–conjugated diphtheria toxin*. PPN lesions were performed on 5 macaques. Animals were tranquilized with ketamine (10 mg/kg) and atropine (0.1 mg/kg) and placed in a stereotactic apparatus, where they were maintained on isoflurane anesthesia (1%–2%). A solution of isotonic saline was given i.v. to maintain fluid levels, and solumedrol (0.2 ml/kg) was administered to preclude brain edema. All surgical procedures were performed aseptically, and recordings of heart rate, respiration patterns, blood pressure, and body temperature were monitored throughout the surgery. Lesion was performed by injecting a urotensin II–conjugated diphtheria toxin locally into the PPN region. This toxin has been developed to specifically kill PPN cholinergic neurons, which have previously been shown to express specifically the urotensin II receptor in rodents (44). The stereotactic injections were guided by radiological visualization of ventricular landmarks (anterior and posterior commissures; ref. 45 and Supplemental Figure 3). A fine needle attached to a 10-μl Hamilton syringe beveled at a 30° angle was used for toxin infusion. Lesions were made by giving 4 infusions per hemisphere (2 depths at 2 anteroposterior locations). Each injection was slowly infused (0.2 μl/min), and the needle was maintained in position for an additional 10-minute period before infusing the next location. Once the injections had been performed, the skin was sutured, and Carprofene (0.1 ml/kg; Vericore Limited) was given for analgesia. The neurotoxin was first stereotaxically injected unilaterally; then, 3–4 weeks later, a contralateral injection was performed using the same procedure. To exclude nonspecific behavioral effects, a sham injection was performed in the right PPN of animal M2 at 2 weeks before the toxin was injected. No behavioral changes were observed under such conditions.

*Volume, concentration, and specificity of the toxin*. The effective range of toxin was explored in monkey M1. It was found that 10 μl of 3% and 5% doses

(diluted in sterile water and injected at 2 different anteroposterior levels of the same hemisphere) did not produce any postural deficits and resulted in very small lesions of the cholinergic neurons (17% maximum; Supplemental Figure 4A). The 10% dose injected 3 weeks later in the other hemisphere of the same animal induced very slight deficits and small lesions (21% maximum). We thus decided to inject a 30% dose in monkeys M2 and M3 (3 and 10 μl, respectively) and a 20% dose in monkeys M4 and M5 (10 μl). All these injections produced significant behavioral changes and cholinergic neuronal loss. We then tested the specificity of the toxin and estimated the loss of noncholinergic neurons on adjacent sections labeled for NADPH diaphorase and a marker of neuronal cell bodies (NeuN; Supplemental Figure 4B). Whatever the concentration used, some $NeuN^+$ neurons remained at the periphery of the injection site, where 100% of cholinergic neurons were lost. The higher the concentration, the greater the loss of noncholinergic neurons observed (Supplemental Figure 4C). In conclusion, the toxin preferentially, but not exclusively, destroyed cholinergic neurons.

*Apomorphine treatment in young macaques*. Apomorphine (120 μg/kg; Aguettent) was given i.m. after PPN lesion or MPTP intoxication (2–3 weeks after the surgery or the last MPTP injection when symptoms reached a maximum level of severity) in order to test whether the behavioral changes induced by the lesion are dopamine-resistant symptoms.

### *Histochemistry*

All macaques were deeply anesthetized and intracardially perfused with 4% paraformaldehyde in PBS. Brains were removed, immersed in 30% sucrose in PBS, and frozen. Transverse sections 50 μm thick were cut on a freezing microtome and stored at 4°C in PBS containing sodium azide until immunohistochemical analysis.

Series of regularly interspaced (500 μm apart) sections of macaque brains were processed for NADPH diaphorase histochemistry as previously described (46). Some sections were counterstained with neural red or Cresyl violet. Other series of free-floating sections used for immunohistochemistry were incubated in the antibodies mouse anti-TH (1:5,000; Immunostar) or mouse anti-NeuN (1:500; Chemicon) at 4°C for 2 days. They were then incubated in peroxidase-conjugated anti-mouse secondary antibody. The antibodies were visualized by peroxidase histochemistry with diaminobenzidine as substrate (Vector Labs). Some sections were also stained with luxol fast blue to label myelinated fibers. In order to analyze the microglial activation, series of sections were also stained for HLA-DR (α chain, 1:50 monoclonal antibody; Dako) as previously described (47).

After autopsy, the human brains were halved sagittally, and one half was dissected into smaller blocks of tissue and fixed in 4% paraformaldehyde and 15% picric acid as previously described (43). Regularly interspaced free-floating 40-μm frozen transverse sections of the PPN (every 720 μm) were then processed for histochemical detection of AChE (48) and counterstained with cresyl violet.

### *Data analysis*

The criteria used to delineate the boundaries of the PPN have been described previously (46). The number of $AChE^+$ neurons in humans and the number of $NADPH^+$ neurons in macaques were counted on 5 regularly interspaced PPN sections covering the anteroposterior extent of the structure. The sections were matched anatomically in each of the brains, while verifying that the cross-sections of the PPN were similar in all individuals. The extent of dopaminergic denervation in PD patients was assessed by counting $TH^+$ neurons on 8 regularly interspaced nigral sections (every 1,440 μm) using the same method. Estimation of the total number of cholinergic and dopaminergic neurons was performed using a semiautomatic stereology system with a computer-based system (Mercator; ExploraNova). The number of Nissl-stained noncholinergic neurons in the cuneiform nucleus, and of $HLA\text{-}DR^+$ cells in the PPN, was counted using the same stereological method and expressed as the number of cells per cubic millimeter. In MPTP-treated macaques, the density of $TH^+$ immunoreactivity was quantified in the striatum by measuring the optical density under brightfield illumination, as previously described (49).

### *Statistics*

For fMRI analysis, a paired *t* test was used to determine whether means from the healthy subject group varied over 2 test conditions: IG versus IOM and normal versus fast walking speed. Parameter estimates for IG and IOM at normal and faster speed were determined using planned contrasts. The linear combinations of parameter estimates for each contrast were stored as separate images for each subject. These contrast images were entered into a 1-sample *t* test, to permit inferences about condition effects across subjects that generalize to the population (i.e., a random-effects analysis). These contrasts produced statistical parametric maps (SPMs) of the *t* statistics at each voxel. Considering our a priori hypothesis regarding the involvement of the PPN region in IG versus IOM comparisons (including both normal and faster speed) and in faster versus normal IG, and given the small size of the structure, contrasts were thresholded with a *P* value of 0.001, uncorrected for multiple comparisons, unless stated otherwise. Only activations involving contiguous clusters of at least 30 voxels were interpreted.

A Kruskall-Wallis test followed by a Mann-Whitney *U* test was used to compare neuronal loss in 3 groups (faller PD, nonfaller PD, and control), and a Mann-Whitney *U* test alone was used to determine whether a difference existed between 2 groups of individuals.

The walk of each macaque was analyzed from 3–5 video sequences taken in 3 conditions: control, after PPN or dopaminergic lesion, and after apomorphine injection. For each animal, 25 images were extracted from frontal video, and 25 other images from profile video, each image being selected on the basis of the body axis of the animal during the walk sequence as described above. The mean values of each parameter were then calculated for a given individual, and a Friedman test was then used to analyze the differences among the 3 conditions, followed by a Wilcoxon paired-sample test in the event of statistically significant differences. The mean values of parameters calculated for a given animal were also expressed as a percentage in 5 monkeys with PPN lesion and after apomorphine treatment, and in 4 monkeys intoxicated by MPTP and after apomorphine treatment. A Kruskall-Wallis test was then used to analyze variance among the 3 conditions, followed by a Mann-Whitney *U* test in the event of statistically significant differences. The effect of lesion and apomorphine treatment on the limb rigidity and pelvis deviation parameters was evaluated on a scale of 0–3 and was not statistically compared with the control condition. All data are presented as mean ± SEM. A value of $P < 0.05$ was considered to be statistically significant, except for fMRI data ($P < 0.001$).

## Acknowledgments

This study was supported by INSERM, the Fondation de l'Avenir, and the Michael J. Fox Foundation. We would like to thank Eric Bertasi and Romain Valabregue for performing fMRI in healthy humans and Nick Barton for language editing.

Received for publication February 11, 2010, and accepted in revised form May 26, 2010.

Address correspondence to: Chantal François or Etienne C. Hirsch, GH Pitié Salpêtrière, 4ème étage, 47 Boulevard de l'Hôpital, 75651 Paris Cedex 13, France. Phone: 33.1.42.16.00.68; Fax: 33.1.45.82.88.93; E-mail: chantal.francois@upmc.fr (C. François). Phone: 33.1.42.16.22.02; Fax: 33.1.44.24.36.58; E-mail: Etienne.hirsch@upmc.fr (E.C. Hirsch).

1. Bloem BR, Hausdorff JM, Visser JE, Giladi N. Falls and freezing of gait in Parkinson's disease: a review of two interconnected, episodic phenomena. *Mov Disord*. 2004;19(8):871–884.
2. Garcia–Rill E. The pedunculopontine nucleus. *Prog Neurobiol*. 1991;36(5):363–389.
3. Mesulam MM, Mufson EJ, Levey AI, Wainer BH. Atlas of cholinergic neurons in the forebrain and upper brainstem of the macaque based on monoclonal choline acetyltransferase immunohistochemistry and acetylcholinesterase histochemistry. *Neuroscience*. 1984;12(3):669–686.
4. Jahn K, et al. Imaging human supraspinal locomotor centers in brainstem and cerebellum. *NeuroImage*. 2008;39(2):786–792.
5. Bakker M, et al. Motor imagery of foot dorsiflexion and gait: effects on corticospinal excitability. *Clin Neurophysiol*. 2008;119(11):2519–2527.
6. Iseki K, Hanakawa T, Shinozaki J, Nankaku M, Fukuyama H. Neural mechanisms involved in mental imagery and observation of gait. *NeuroImage*. 2008;41(3):1021–1031.
7. Hirsch EC, Orieux G, Muriel MP, Francois C, Feger J. Nondopaminergic neurons in Parkinson's disease. *Adv Neurol*. 2003;91:29–37.
8. Zweig RM, Jankel WR, Hedreen JC, Mayeux R, Price DL. The pedunculopontine nucleus in Parkinson's disease. *Ann Neurol*. 1989;26(1):41–46.
9. Pahapill PA, Lozano AM. The pedunculopontine nucleus and Parkinson's disease. *Brain*. 2000; 123(pt 9):1767–1783.
10. Plaha P, Gill SS. Bilateral deep brain stimulation of the pedunculopontine nucleus for Parkinson's disease. *NeuroReport*. 2005;16(17):1883–1887.
11. Stefani A, et al. Bilateral deep brain stimulation of the pedunculopontine and subthalamic nuclei in severe Parkinson's disease. *Brain*. 2007; 130(pt 6):1596–1607.
12. Zrinzo L, et al. Stereotactic localization of the human pedunculopontine nucleus: atlas-based coordinates and validation of a magnetic resonance imaging protocol for direct localization. *Brain*. 2008;131(pt 6):1588–1598.
13. Ferraye MU, et al. Effects of pedunculopontine nucleus area stimulation on gait disorders in Parkinson's disease. *Brain*. 2010;133(pt 1):205–214.
14. Moro E, et al. Unilateral pedunculopontine stimulation improves falls in Parkinson's disease. *Brain*. 2010;133(pt 1):215–224.
15. Piallat B, et al. Gait is associated with an increase in tonic firing of the sub-cuneiform nucleus neurons. *Neuroscience*. 2009;158(4):1201–1205.
16. Herrero MT, Hirsch EC, Javoy–Agid F, Obeso JA, Agid Y. Differential vulnerability to 1–methyl–4–phenyl–1,2,3,6–tetrahydropyridine of dopaminergic and cholinergic neurons in the monkey mesopontine tegmentum. *Brain Res*. 1993; 624(1–2):281–285.
17. Heise CE, Teo ZC, Wallace BA, Ashkan K, Benabid AL, Mitrofanis J. Cell survival patterns in the pedunculopontine tegmental nucleus of methyl-4-phenyl-1,2,3,6-tetrahydropyridine-treated monkeys and 6OHDA-lesioned rats: evidence for differences to idiopathic Parkinson disease patients? *Anat Embryol (Berl)*. 2005;210(4):287–302.
18. Luquin MR, et al. Recovery of chronic parkinsonian monkeys by autotransplants of carotid body cell aggregates into putamen. *Neuron*. 1999;22(4):743–750.
19. Ovadia A, Zhang Z, Gash DM. Increased susceptibility to MPTP toxicity in middle-aged rhesus monkeys. *Neurobiol Aging*. 1995;16(6):931–937.
20. Shik ML, Severin FV, Orlovskii GN. Control of walking and running by means of electric stimulation of the midbrain. *Biofizika*. 1966;11(4):659–666.
21. Takakusaki K, Habaguchi T, Ohtinata-Sugimoto J, Saitoh K, Sakamoto T. Basal ganglia efferents to the brainstem centers controlling postural muscle tone and locomotion: a new concept for understanding motor disorders in basal ganglia dysfunction. *Neuroscience*. 2003;119(1):293–308.
22. Grillner S. Control of locomotion in bipeds, tetrapods and fish. In: Brooks VB, ed. *Handbook of Physiology - the nervous system II*. Baltimore, Maryland, USA: American Physiological Society; 1981:1199–1236.
23. Winn P. Experimental studies of pedunculopontine functions: are they motor, sensory or integrative? *Parkinsonism Relat Disord*. 2008;14 suppl 2:S194–S198.
24. Inglis WL, Winn P. The pedunculopontine tegmental nucleus: Where the striatum meets the reticular formation. *Prog Neurobiol*. 1995;47(1):1–29.
25. Inglis WL, Olmstead MC, Robbins TW. Selective deficits in attentional performance on the 5-choice serial reaction time task following pedunculopontine tegmental nucleus lesions. *Behav Brain Res*. 2001;123(2):117–131.
26. Alderson HL, Latimer MP, Winn P. A functional dissociation of the anterior and posterior pedunculopontine tegmental nucleus: excitotoxic lesions have differential effects on locomotion and the response to nicotine. *Brain Struct Funct*. 2008;213(1–2):247–253.
27. Munro-Davies LE, Winter J, Aziz TZ, Stein JF. The role of the pedunculopontine region in basal-ganglia mechanisms of akinesia. *Exp Brain Res*. 1999;129(4):511–517.
28. Kojima J, et al. Excitotoxic lesions of the pedunculopontine tegmental nucleus produce contralateral hemiparkinsonism in the monkey. *Neurosci Lett*. 1997;226(2):111–114.
29. Matsumura M, Yamaji Y. The role of the pedunculopontine tegmental nucleus in experimental parkinsonism in primates. *Stereotact Funct Neurosurg*. 2001;77(1–4):108–115.
30. Winn P, Stone TW, Latimer M, Hastings MH, Clark AJ. A comparison of excitotoxic lesions of the basal forebrain by kainate, quinolinate, ibotenate, N-methyl-D-aspartate or quisqualate, and the effects on toxicity of 2-amino-5-phosphonovaleric acid and kynurenic acid in the rat. *Br J Pharmacol*. 1991;102(4):904–908.
31. Haaland KY, Harrington DL. Hemispheric asymmetry of movement. *Curr Opin Neurobiol*. 1996; 6(6):796–800.
32. Sacco K, Cauda F, Cerliani L, Mate D, Duca S, Geminiani GC. Motor imagery of walking following training in locomotor attention. The effect of 'the tango lesson'. *NeuroImage*. 2006;32(3):1441–1449.
33. Rinne JO, Ma SY, Lee MS, Collan Y, Roytta M. Loss of cholinergic neurons in the pedunculopontine nucleus in Parkinson's disease is related to disability of the patients. *Parkinsonism Relat Disord*. 2008;14(7):553–557.
34. Zhang JH, Sampogna S, Morales FR, Chase MH. Age-related changes in cholinergic neurons in the laterodorsal and the pedunculo-pontine tegmental nuclei of cats: a combined light and electron microscopic study. *Brain Res*. 2005;1052(1):47–55.
35. George O, et al. Smad-dependent alterations of PPT cholinergic neurons as a pathophysiological mechanism of age-related sleep-dependent memory impairments. *Neurobiol Aging*. 2006;27(12):1848–1858.
36. Sheffield L, Berman NE. Microglial expression of MHC class II increases in normal aging of nonhuman primates. *Neurobiol Aging*. 1998;19(1):47–55.
37. Lavoie B, Parent A. Pedunculopontine nucleus in the squirrel monkey: cholinergic and glutamatergic projections to the substantia nigra. *J Comp Neurol*. 1994;344(2):232–241.
38. Rolland AS, et al. Evidence for a dopaminergic innervation of the pedunculopontine nucleus in monkeys, and its drastic reduction after MPTP intoxication. *J Neurochem*. 2009;110(4):1321–1329.
39. Oldfield RC. The assessment and analysis of handedness: the Edinburgh inventory. *Neuropsychologia*. 1971;9(1):97–113.
40. Friston KJ, et al. Event-related fMRI: characterizing differential responses. *NeuroImage*. 1998;7(1):30–40.
41. Friston KJ, Josephs O, Rees G, Turner R. Nonlinear event-related responses in fMRI. *Magn Reson Med*. 1998;39(1):41–52.
42. Hughes AJ, Daniel SE, Kilford L, Lees AJ. Accuracy of clinical diagnosis of idiopathic Parkinson's disease: a clinico-pathological study of 100 cases. *J Neurol Neurosurg Psychiatry*. 1992;55(3):181–184.
43. Fahn S. Concept and classification of dystonia. *Adv Neurol*. 1998;50:1–8.
44. Clark SD, et al. Fusion of diphtheria toxin and urotensin II produces a neurotoxin selective for cholinergic neurons in the rat mesopontine tegmentum. *J Neurochem*. 2007;102(1):112–120.
45. Percheron G, Yelnik J, François C. Systems of coordinates for stereotactic surgery and cerebral cartography: advantages of ventricular systems in monkeys. *J Neurosci Methods*. 1986;17(2–3):69–88.
46. Hirsch EC, Graybiel AM, Duyckaerts C, Javoy–Agid F. Neuronal loss in the pedunculopontine tegmental nucleus in Parkinson disease and in progressive supranuclear palsy. *Proc Natl Acad Sci U S A*. 1987;84(16):5976–5980.
47. Barcia C, et al. Evidence of active microglia in substantia nigra pars compacta of parkinsonian monkeys 1 year after MPTP exposure. *Glia*. 2004;46(4):402–409.
48. Graybiel AM, Hirsch EC, Agid YA. Differences in tyrosine hydroxylase-like immunoreactivity characterize the mesostriatal innervation of striosomes and extrastriosomal matrix at maturity. *Proc Natl Acad Sci U S A*. 1987;84(1):303–307.
49. Jan C, et al. Quantitative analysis of dopaminergic loss in relation to functional territories in MPTP-treated monkeys. *Eur J Neurosci*. 2003;18(7):2082–2086.

doi:10.1093/brain/awv047 BRAIN 2015: 138; 1284–1296 | 1284

BRAIN
A JOURNAL OF NEUROLOGY

# The integrative role of the pedunculopontine nucleus in human gait

**Brian Lau,[1] Marie-Laure Welter,[1,2] Hayat Belaid,[2] Sara Fernandez Vidal,[1,3] Eric Bardinet,[1,3] David Grabli[1,2] and Carine Karachi[1,2]**

See Windels *et al.* for a scientific commentary on this article (doi:10.1093/brain/awv059).

The brainstem pedunculopontine nucleus has a likely, although unclear, role in gait control, and is a potential deep brain stimulation target for treating resistant gait disorders. These disorders are a major therapeutic challenge for the ageing population, especially in Parkinson's disease where gait and balance disorders can become resistant to both dopaminergic medication and subthalamic nucleus stimulation. Here, we present electrophysiological evidence that the pedunculopontine and subthalamic nuclei are involved in distinct aspects of gait using a locomotor imagery task in 14 patients with Parkinson's disease undergoing surgery for the implantation of pedunculopontine or subthalamic nuclei deep brain stimulation electrodes. We performed electrophysiological recordings in two phases, once during surgery, and again several days after surgery in a subset of patients. The majority of pedunculopontine nucleus neurons (57%) recorded intrasurgically exhibited changes in activity related to different task components, with 29% modulated during visual stimulation, 41% modulated during voluntary hand movement, and 49% modulated during imaginary gait. Pedunculopontine nucleus local field potentials recorded post-surgically were modulated in the beta and gamma bands during visual and motor events, and we observed alpha and beta band synchronization that was sustained for the duration of imaginary gait and spatially localized within the pedunculopontine nucleus. In contrast, significantly fewer subthalamic nucleus neurons (27%) recorded intrasurgically were modulated during the locomotor imagery, with most increasing or decreasing activity phasically during the hand movement that initiated or terminated imaginary gait. Our data support the hypothesis that the pedunculopontine nucleus influences gait control in manners extending beyond simply driving pattern generation. In contrast, the subthalamic nucleus seems to control movement execution that is not likely to be gait-specific. These data highlight the crucial role of these two nuclei in motor control and shed light on the complex functions of the lateral mesencephalus in humans.

1 Sorbonne Universités, UPMC Univ Paris 06, UMR S 1127, CNRS UMR 7225, ICM, F-75013, Paris, France
2 Assistance Publique-Hôpitaux de Paris, Groupe Hospitalier Pitié-Salpêtrière, 47 boulevard de l'Hôpital, 75013 Paris, France
3 Centre de Neuroimagerie de Recherche, Institut du Cerveau et de la Moelle épinière, F-75013, Paris, France

Correspondence to: Brian Lau,
Institut du Cerveau et de la Moelle épinière
UMR S 1127, CNRS UMR 7225
Hôpital de la Pitié Salpêtrière
47 Bd de l'Hôpital
75013, Paris, France
E-mail: brian.lau@upmc.fr

**Keywords:** pedunculopontine nucleus; subthalamic nucleus; Parkinson's disease; deep brain stimulation; gait

**Abbreviations:** DBS = deep brain stimulation; PPN = pedunculopontine nucleus; STN = subthalamic nucleus

Received October 12, 2014. Revised December 11, 2014. Accepted January 6, 2015. Advance Access publication March 12, 2015

# Introduction

Moving through the environment is a crucial and highly evolved ability in vertebrates, which humans primarily accomplish using the unique capacity to walk on two legs. This ability is controlled by neural networks linking automatic pattern generators in the spinal cord with supraspinal brainstem and forebrain structures responsible for selecting, initiating and regulating locomotor behaviour (Orlovsky *et al.*, 1999). The brainstem lateral mesencephalus is a highly conserved supraspinal locomotor centre that has been identified in vertebrates ranging from lampreys to primates (Le Ray *et al.*, 2011), and includes the pedunculopontine (PPN) and cuneiform nuclei. The PPN is a complex structure divided into a pars compacta containing mainly cholinergic neurons and a pars dissipata containing glutamatergic and GABAergic neurons (Olszewski and Baxter, 1954). The pedunculopontine and cuneiform nuclei receive direct cortical inputs, and are well positioned to influence locomotor behaviour via ascending outputs to the basal ganglia and thalamus (Pahapill and Lozano, 2000), as well as via descending outputs to the spinal cord (Rolland *et al.*, 2011).

The brainstem region containing the pedunculopontine and cuneiform nuclei is commonly referred to as the mesencephalic locomotor region based on observations that electrical stimulation of this region can initiate and modulate locomotion in animals (Shik *et al.*, 1966; Eidelberg *et al.*, 1981; Skinner and Garcia-Rill, 1984; Mori *et al.*, 1989), and that chemical modulation (Takakusaki *et al.*, 2003) as well as lesioning cholinergic PPN neurons in monkeys (Karachi *et al.*, 2010) impairs gait. The mesencephalic locomotor region is modulated by changes in imagined locomotion in healthy humans (Jahn *et al.*, 2008; Karachi *et al.*, 2012), which also modulates cortical networks similar to those involved during real gait (La Fougère *et al.*, 2010). Further evidence implicating the mesencephalic locomotor region in locomotor control comes from pathophysiological studies of gait and balance disorders, which are major causes of chronic disability and mortality in the elderly (Snijders *et al.*, 2007), suggesting that PPN dysfunction may be key to understanding the pathophysiology of gait disorders resistant to dopaminergic treatment (Pahapill and Lozano, 2000; Snijders *et al.*, 2007; Demain *et al.*, 2014).

In Parkinson's disease, dopamine replacement therapy and deep brain stimulation (DBS) of the subthalamic nucleus (STN) effectively treat tremor, rigidity and akinesia caused by dopamine cell death (Limousin *et al.*, 1998). These interventions can also effectively treat DOPA-sensitive gait and balance disorders, but as Parkinson's disease advances gait disorders can become resistant to dopamine medication and STN-DBS (Grabli *et al.*, 2012), which may be related to degeneration of cholinergic neurons in the PPN (Hirsch *et al.*, 1987; Jellinger, 1988; Zweig *et al.*, 1989). This is associated with decreased thalamic cholinergic activity, and both brainstem cholinergic loss and decreases in thalamic cholinergic activity correlate with the history of falls in patients with advanced Parkinson's disease (Bohnen *et al.*, 2009; Karachi *et al.*, 2010). Functional imaging in patients with Parkinson's disease indicates that PPN area activity depends on the severity of gait disorders, where blood oxygenation level-dependent enhancement during imaginary gait may reflect compensation for brainstem atrophy observed in patients with gait disorders (Snijders *et al.*, 2011; Demain *et al.*, 2014; Maillet *et al.*, 2015).

Deep brain stimulation of the PPN has recently been tested for treating severe dopamine-resistant gait disorders in patients with Parkinson's disease, using stimulation parameters thought to stimulate the remaining neurons (Mazzone *et al.*, 2005; Plaha and Gill, 2005; Stefani *et al.*, 2007; Ferraye *et al.*, 2010; Moro *et al.*, 2010). Electrophysiological recordings performed in these patients during DBS surgery have revealed that some PPN neurons respond to behavioural manipulations intended to elicit locomotor contexts, including alternating leg movements (Piallat *et al.*, 2009) and imaginary gait (Tattersall *et al.*, 2014). While these results are consistent with a role for the mesencephalic locomotor region in controlling locomotion, it remains unclear how neural activity in the human mesencephalic locomotor region relates to sensory perception and the selection, initiation and modulation of motor programs supporting locomotion.

We sought to improve understanding of the role of the PPN in gait control by recording neural activity in this nucleus in patients with Parkinson's disease undergoing DBS surgery for intractable gait disorders. We used a validated imaginary gait task (Bakker *et al.*, 2007; Karachi *et al.*, 2012) and compared PPN neural activity to STN recordings made in a second group of patients with Parkinson's disease performing this same task. We provide the first comparative analysis of the neural activity of these two nuclei in a locomotor context, and our results suggest distinct roles for the PPN and STN in locomotor control.

# Materials and methods

## Patients

Fourteen patients with idiopathic Parkinson's disease were recruited at the Pitié-Salpêtrière Hospital. We included eight patients using standard criteria for STN-DBS (Welter *et al.*, 2002). For PPN-DBS, we included six patients using the same criteria except that gait and balance disorders measured by freezing of gait and/or falling subscores were $\geqslant 2$ ON DOPA (Tables 1 and 2). Thus, patients in the PPN-DBS group exhibited significantly more DOPA-resistant gait disorders compared to the STN-DBS group. Patients in each group participated in separate clinical trials that were approved by the local ethical committee of the Salpêtrière Hospital and the INSERM-DGOS (PPN trial #NCT02055261, STN trial #NCT01682668). Randomization

**Table 1 Demographic and clinical features of patients**

| | Gender, Age | Disease duration | Activities of daily living (UPDRS II) | | Motor disability (UPDRS III) | | Levodopa motor complications | Levodopa-equivalent dosage | Cognitive status | | | |
|---|---|---|---|---|---|---|---|---|---|---|---|---|
| | | | OFF | ON | OFF | ON | | | MMS | MDRS | Frontal score | WCST |
| **PPN-DBS** | | | | | | | | | | | | |
| S01 | M, 69 | 19 | 21 | 19 | 44 | 18 | 4 | 1700 | 28 | 132 | 47 | 12 |
| S02 | F, 70 | 18 | 26 | 9 | 45 | 16 | 9 | 570 | 25 | 140 | 52 | 15 |
| S03 | F, 68 | 23 | 28 | 19 | 61 | 30 | 9 | 700 | 29 | 130 | 51 | 12 |
| S04 | F, 64 | 10 | 22 | 6 | 38 | 19 | 4 | 1050 | 25 | 141 | 52 | 12 |
| S05 | M, 63 | 14 | 11 | 11 | 38 | 16 | 5 | 585 | 29 | 139 | 54 | 20 |
| S06 | M, 46 | 12 | 22 | 5 | 50 | 19 | 10 | 1300 | 27 | 139 | 58 | 20 |
| Mean (SD) | 63 (8.9) | 16 (4.9) | 22 (5.9) | 12 (6.2) | 46 (8.6) | 20 (5.2) | 7 (2.8) | 984 (453) | 27 (1.9) | 137 (4.6) | 52 (3.6) | 15 (3.9) |
| **STN-DBS** | | | | | | | | | | | | |
| S07 | M, 55 | 9 | 17 | 14 | 18 | 3 | 5 | 1000 | 30 | 143 | 59.5 | 20 |
| S08 | F, 53 | 7 | 33 | 7 | 46 | 11 | 8 | 1130 | 27 | 143 | 60 | 20 |
| S09 | F, 51 | 13 | 15 | 1 | 32 | 1 | 6 | 450 | 30 | 144 | 60 | 20 |
| S10 | M, 55 | 11 | 24 | 16 | 53 | 11 | 7 | 625 | 25 | 122 | 46 | 12 |
| S11 | F, 57 | 10 | 24 | 2 | 26 | 4 | 9 | 875 | 29 | 143 | 54 | 15 |
| S12 | M, 60 | 10 | 25 | 11 | 53 | 27 | 8 | 1080 | 28 | 144 | 58 | 20 |
| S13 | F, 58 | 11 | 35 | 11 | 58 | 17 | 7 | 400 | 30 | 144 | 58 | 20 |
| S14 | F, 67 | 10 | 18 | 2 | 37 | 15 | 5 | 1125 | 28 | 129 | 44 | 9 |
| Mean (SD) | 57 (4.9) | 10 (1.7)* | 24 (7.3) | 8 (5.9) | 40 (14.3) | 11 (8.6)* | 7 (1.5) | 836 (303) | 28 (1.8) | 139 (8.6) | 55 (6.4) | 17 (4.4) |

*$P < 0.05$ unpaired *t*-test comparing STN-DBS patients with PPN-DBS; MMS = Mini-Mental Status (range 0–30, higher score indicates better cognitive function); MDRS = Mattis Dementia Rating Scale (range 0–144, higher score indicates better cognitive function); UPDRS = Unified Parkinson's Disease Rating Scale (part II: range 0–52; part III: range 0–108; part IV: range 0–44; higher scores indicate worse parkinsonian status); WCST = Wisconsin Card Sorting Test (range 0–20; higher scores indicate better cognitive status). OFF and ON refer to dopaminergic medication.

was not used to assign patients, and the authors were not blinded to the group allocations. All patients agreed to participate and signed a written consent.

## Imagery tasks

### Imaginary gait task

Patients performed an imaginary gait task previously described (Karachi *et al.*, 2012). Prior to surgery, patients were trained to walk along an 8-m long segment of a corridor. On separate trials they were instructed to walk at normal speed and then 30% faster. After practicing walking at each speed, patients were seated in front of a computer screen and trained to perform the imaginary gait task. Each trial began with the presentation of a white cross at the centre of the screen. After a delay, an image showing the corridor that the patient had walked along was displayed, along with instructions indicating the speed at which to imagine gait (normal or rapid, pseudo-randomized). When the patient was ready, he closed his eyes and initiated imaginary gait by pressing a button. Finally, the patient terminated imagery with a second button press, and then opened his eyes.

### Imaginary object movement task

Patients in the PPN-DBS group were also trained on an imaginary object movement task where they imagined an object moving at two different speeds along the same 8-m corridor segment. These conditions were indicated by 'normal object' and 'rapid object'. The trials were otherwise identical in terms of stimulus presentation, times and the sequence of button pressing and eye closing the subject was instructed to perform to initialize and terminate imagery.

During surgery, patients only performed the imaginary gait task due to time limitations. In postsurgical sessions, four PPN patients performed both imaginary gait and object movement tasks (conditions pseudo-randomly interleaved).

## Surgical procedure and localization of neurons and definitive DBS electrodes

We targeted the PPN and STN using a combination of direct MRI targeting (Bejjani *et al.*, 2000; Zrinzo *et al.*, 2008) and a 3D histological atlas of the basal ganglia that were deformed to the preoperative $T_1$ MRI of each patient's brain obtained the day before surgery (Yelnik *et al.*, 2007). We obtained a set of coordinates with each method, aiming for the lowest contact to be just outside the lower limit of the nucleus, and defined a target for each side by averaging these coordinates. We chose trajectories that avoided ventricles, the caudate nuclei, and blood vessels, and accounted for the size of the brainstem (for PPN surgeries). During surgery, we used a Leksell frame (Elekta Instruments, Inc.) with X-ray imaging to control the position of the electrodes. For PPN recordings, we used only two microelectrodes (instead of three to five) per side to reduce haemorrhagic risk. For STN recordings, we used three microelectrodes for both sides. Individual neurons were localized within the structures using preoperative MRI and perioperative X-rays to validate microelectrode

**Table 2 Gait and balance disorders of patients**

| | Falling (item 13-UPDRS II) | | FOG (item 14-UPDRS II) | | Axial motor score (UPDRS III) | | Postural stability (item 29-UPDRS III) | | Gait (item 30-UPDRS III) | |
|---|---|---|---|---|---|---|---|---|---|---|
| | OFF | ON | OFF | ON | OFF | ON | OFF | ON | OFF | ON |
| **PPN-DBS** | | | | | | | | | | |
| S01 | 4 | 4 | 4 | 4 | 8 | 2 | 2 | 1 | 3 | 1 |
| S02 | 2 | 2 | 3 | 2 | 12 | 6 | 3 | 2 | 3 | 2 |
| S03 | 2 | 2 | 3 | 3 | 11 | 8 | 3 | 1 | 3 | 3 |
| S04 | 2 | 2 | 3 | 1 | 8 | 3 | 2 | 1 | 3 | 1 |
| S05 | 2 | 2 | 3 | 3 | 4 | 4 | 2 | 1 | 2 | 2 |
| S06 | 2 | 2 | 3 | 2 | 9 | 1 | 2 | 2 | 3 | 0 |
| Mean (SD) | 2 (0.8) | 2 (1.2) | 3 (0.4) | 2 (1.0) | 9 (2.8) | 4 (2.6) | 2 (0.5) | 1 (0.5) | 3 (0.4) | 2 (1.0) |
| **STN-DBS** | | | | | | | | | | |
| S07 | 0 | 0 | 0 | 0 | 0 | 0 | 0 | 0 | 0 | 0 |
| S08 | 0 | 0 | 3 | 0 | 14 | 2 | 2 | 0 | 4 | 0 |
| S09 | 0 | 0 | 0 | 0 | 3 | 0 | 1 | 0 | 1 | 0 |
| S10 | 0 | 0 | 0 | 0 | 3 | 0 | 1 | 0 | 1 | 0 |
| S11 | 0 | 0 | 3 | 0 | 3 | 0 | 0 | 0 | 1 | 0 |
| S12 | 2 | 0 | 3 | 1 | 11 | 5 | 2 | 0 | 4 | 1 |
| S13 | 1 | 0 | 4 | 1 | 11 | 3 | 1 | 0 | 3 | 1 |
| S14 | 0 | 0 | 0 | 0 | 10 | 4 | 0 | 0 | 2 | 0 |
| Mean (SD) | 0 (0.7)* | 0 (0)* | 2 (1.8)* | 0 (0.5)* | 7 (5.2) | 2 (0.1) | 1 (0.8)* | 0 (0)* | 2 (1.5) | 0 (0.5)* |

*$P < 0.05$ unpaired *t*-test comparing STN-DBS patients with PPN-DBS; UPDRS = Unified Parkinson's Disease Rating Scale [part II: Falling and freezing of gait (FOG) scores: range 0–4; part III: axial score: range 0–20; gait and postural instability scores: range 0–4; higher scores indicate worse parkinsonian status]. OFF and ON refer to dopaminergic medication.

trajectories and depths. We localized the definitive DBS electrodes for each patient using a postoperative helicoidal CT scan registered to the preoperative $T_1$-weighted MRI (Bardinet *et al.*, 2009).

## Data collection

The patient was brought out of anaesthesia, and tungsten microelectrodes (1 MΩ impedance; FHC Inc.) were lowered together using a microdrive. We started physiological recordings 5 mm above the target. We reminded patients of the imaginary gait task, which was presented on a mounted LCD screen. When neural activity could be stably recorded, the patients performed the task for ~15 min, using the hand contralateral to the recorded PPN or STN to press the button. Patients were free to discontinue the experiment at any time. After finishing the task and the clinical assessments, the patient was re-anaesthetized and the definitive DBS electrode was implanted. This entire procedure was repeated for the other hemisphere.

Neuronal activity was amplified, filtered and written to disk for offline analysis (Guideline 4000, FHC Inc. or Leadpoint, Medtronic). Action potentials were isolated using manual clustering on the basis of several waveform parameters including principal components, peak and trough amplitudes, as well as the presence of a refractory period (Offline Sorter, Plexon Instruments). We characterized over half of the unit activities as single-unit, with signal-to-noise ratios >4 (Tattersall *et al.*, 2014) (PPN, $n = 27$, mean signal-to-noise ratio = 6.01, min signal-to-noise ratio = 4.14; STN, $n = 36$, mean signal-to-noise ratio = 6.34, min signal-to-noise ratio = 4.30). When multiple action potentials could not be separated into well-defined clusters, we thresholded the raw voltage signal at ~3 standard deviations (SD) from the mean and labelled this multi-unit activity (PPN, $n = 22$, mean signal-to-noise ratio = 3.43, min signal-to-noise ratio = 3.01; STN, $n = 31$, mean signal-to-noise ratio = 3.39, min signal-to-noise ratio = 2.81). There was no difference in the proportion of single-units isolated in each area ($P > 0.5$), nor in the signal-to-noise ratios between areas ($P$-values > 0.4).

Postsurgical recordings were made 4 days after surgery for PPN patients. Local field potentials were recorded bilaterally from the definitive DBS electrodes (model 3389, Medtronic Neurological Division), which had four cylindrical platinum-iridium cylindrical contacts (1.27 mm in diameter and 1.5 mm in length) separated by 0.5 mm. Signals were amplified, low pass filtered at 250 Hz and digitized at 512 Hz (Basis BE System, EB Neuro S.p.A.). Bipolar recordings were made between adjacent contacts of each electrode, yielding six recording channels per patient (three per side). Patients were on their dopaminergic medication, and were comfortably seated in front of a screen to perform the imagery tasks for ~30 min. Five patients participated in the postsurgical local field potential recordings. We excluded data from two of these patients; one due to excessive signal artefacts, and the second patient could not perform the task due to postsurgical fatigue. Local field potentials were processed to remove power line noise by fitting a parametric function to the power spectral density of the raw voltage signal in the vicinity of 50 Hz (±2 Hz). The raw voltage signal was then filtered using the inverse of the fitted function so that the resulting spectrum at 50 Hz was similar to that of surrounding frequencies (Zanos *et al.*, 2011). We excluded data from individual trials when the amplitude of the raw voltage signal exceeded 500 μV or 6 SD of the amplitude distribution across the session.

## Data analysis

We performed all analyses using MATLAB (version 2013a, Mathworks Inc.) and R (version 3.10, R Core Development Team). We fit the linear mixed models described below using the R package lme4 (version 1.1), and assessed significance with mixed-effects ANOVAs using the R package lmerTest (version 2.0) with Satterthwaite's approximation for the denominator degrees of freedom of the F-statistic.

## Behavioural analyses

We analysed the durations between button presses initiating and terminating imagery. Trials where this duration was $<2$ or $>30$ s were excluded, leaving 1463 (97.5%) trials of intrasurgical data and 577 (96.7%) trials of postsurgical data for analysis. We modelled imagination duration using a linear mixed model, including fixed effects of target location (PPN or STN), speed (rapid or normal) and imagery type (gait or object movement), with an additive random effect for each patient. Imagination time distributions were positively skewed, and we log-transformed the data to symmetrize and stabilize residuals. Resulting model residuals were symmetrically distributed, but had heavier than Gaussian tails. We checked that this did not affect our conclusions by fitting robust versions of the models (robustlmm version 1.6), and confirmed that our conclusions were unchanged.

## Analysis of spiking activity

We compared activity within a trial to baseline using a Wilcoxon rank sum test. The activity for every trial of each neuron was first smoothed using a Gaussian kernel density estimator with optimal bandwidth (Shimazaki and Shinomoto, 2010). We estimated baseline rate by averaging activity from $-2.5$ to $-0.1$ s before visual instruction onset for each trial, and compared activity at every millisecond to this baseline distribution. We adjusted for multiple comparisons using the procedure of Benjamini and Hochberg (1995) to control the false discovery rate (FDR).

We quantified modulation strength in three time windows (Visual, 0 to 0.5 s after visual instruction onset; Motor, $-0.5$ to 0.5 s relative to button presses; Imaginary gait, 2 to 4 s after imagery was initiated), $z$-scoring absolute responses by subtracting mean baseline activity and dividing by its standard deviation (baseline from $-2.5$ to $-0.1$ s before visual instruction onset). We modelled modulation strength using a linear mixed model, including fixed effects of target location (PPN or STN), recording side (right or left) and recording depth, with an additive random effect for each patient. Distributions of the resulting model residuals were positively skewed, and we checked that this did not affect our conclusions by power transforming modulation strength to symmetrize and stabilize residuals. This yielded residuals that were Gaussian (Lilliefors test) with homogeneous variance across patients (Levene's test). The results from these fits agreed with those presented in the 'Results' section; PPN modulation strength was significantly greater than STN modulation strength in the Visual ($P = 0.031$) and Imaginary gait ($P = 0.037$) epochs, but not the Motor epoch ($P = 0.367$).

## Comparing recording locations

We compared the anatomical localization of neurons with different response properties by treating the location of each neuron ($x$, $y$, $z$ position) as a sample, and testing for differences between sample distributions non-parametrically using a test based on statistical energy (Székely and Rizzo, 2013). $P$-values were calculated by bootstrap.

## Time-frequency analysis

We estimated spectral power as a function of time and frequency using a multi-taper estimation algorithm (Mitra and Bokil, 2007) implemented in the Chronux library (version 2.10, http://chronux.org). For each bipolar local field potential recording, power was calculated in 500 ms windows stepped by 30 ms, using five orthogonal tapers with a time-bandwidth product equal to 3. Spectrograms were normalized to the average baseline spectrum measured $-3$ to $-1$ s before visual instruction onset, and transformed to decibels. We quantified changes in the same three time windows we used to analyse spiking data, modelling spectral modulations with a linear mixed model that included fixed effects of recording depth (dorsal, intermediate or ventral), imagination speed (rapid or normal), imagination type (gait or object movement) and recording side (right or left), with an additive random effect for each patient. Resulting model residuals were symmetrically distributed, but had heavier than Gaussian tails. We checked that this did not affect our conclusions by fitting robust versions of the models, and confirmed that our conclusions were unchanged.

# Results

## Behavioural performance

We trained 14 patients with Parkinson's disease to perform an imaginary gait task 1 month before and again the day prior to DBS surgery. Each trial consisted of viewing an instruction on a screen and pressing a button to initiate and terminate an epoch of gait imagination with the eyes closed. Patients were instructed to imagine walking down a corridor they were familiar with, and they practiced both real and imaginary gait until they reliably produced shorter imagination times when instructed to imagine walking faster compared to walking at a normal speed. They performed this task when brought out of anaesthesia during DBS surgery while we recorded the spiking activity of neurons in the PPN or STN using microelectrodes (intrasurgical), and in a subset of PPN patients 4 days later while we recorded local field potentials from the implanted DBS macroelectrodes (postsurgical). Patients successfully performed the imagery tasks, producing shorter imagination times when instructed to imagine walking faster compared to normal walking speed, both intrasurgically (7.26 s versus 8.75 s, $P < 0.001$) and postsurgically (7.55 s versus 8.88 s, $P < 0.001$). Imagination times did not depend on patient group (PPN versus STN, $P > 0.4$), and all patients except

one in the STN group produced shorter imagination times during rapid compared to normal speed trials. For the post-surgical recordings, patients also imagined object motion at two different speeds, and their performance in these trials was not different from imaginary gait trials ($P > 0.8$). Thus, both patient groups performed imagery gait similarly, despite differences between patient groups during real gait (Table 2).

## PPN and STN neurons respond differently during imaginary gait

We recorded 49 single- or multi-units in the PPN of five patients and 67 single- or multi-units in the STN of eight patients. Figure 1A illustrates a range of task-related activity that we observed in individual neurons in the PPN and STN, including modulations during imaginary gait, visual instruction, and the physical movements (button presses) initiating and terminating imaginary gait. We summarized the prevalence of task-related changes by comparing activity at each point in time throughout the trial to baseline activity before visual stimulus presentation, pooling significance across neurons within each nucleus (Fig. 1B). There were substantially more modulated neurons in the PPN compared to the STN, which was evident beginning with visual instruction presentation and was maintained until patients terminated imaginary gait. In contrast, there were relatively few modulated neurons in the STN; significant changes from baseline occurred primarily around the time of button presses, and significant changes during imaginary gait were less coherent across the population. For both PPN and STN neurons, we occasionally observed small differences between the rapid and normal speed conditions, but we found fewer than 5% significant differences at any point in time when comparing these conditions, and we therefore pooled the data for all analyses.

Individual neural responses within both the PPN and the STN could exhibit positive or negative modulations relative to baseline (Fig. 1C). There was no significant difference between the proportions of neurons with each sign of response defined by the peak response over the entire trial ($P > 0.30$ for both PPN and STN). We quantified modulation strength using the absolute response change $z$-scored relative to baseline (Fig. 1D), and found that across all neurons PPN modulation magnitudes were significantly greater during the visual stimulus (PPN-STN = 0.541, SE = 0.264, $P < 0.05$) and imaginary gait (PPN-STN = 0.190, SE = 0.080, $P < 0.05$) epochs. PPN and STN modulation magnitudes did not differ during the button presses initiating and terminating imaginary gait (PPN-STN = 0.085, SE = 0.106, $P > 0.4$).

Individual neurons could exhibit modulation during one or more epochs of the imaginary gait task. We observed that the proportion of neurons modulated during at least one of three epochs (Fig. 1E; Visual, Motor, Imaginary gait) was significantly greater in the PPN compared to STN [57.1% versus 26.9%, 95% confidence interval (CI) for difference = 11.1–49.5, $P < 0.01$]. In addition, significantly task-related neurons more frequently exhibited joint modulation in two or three of task epochs in the PPN compared to the STN (62.5% versus 30.2%, 95% CI for difference = 2.12–58.9, $P < 0.05$).

The location of each single- or multi-unit activity is illustrated in Fig. 2. We did not find any difference between the spatial distributions of task-related neurons compared to those without significant modulations (Fig. 2A) in either the PPN or the STN ($P$-values $> 0.10$). Nor did we find evidence of spatial clustering when comparing spatial distributions of neurons modulated in the visual, motor or imaginary gait epochs (Fig. 2B) in either the PPN ($P$-values $> 0.09$) or the STN ($P$-values $> 0.5$). This lack of difference is perhaps unsurprising in the PPN, where many individual neurons were modulated by more than one task event.

## PPN local field potentials exhibit distinct temporally and spatially localized frequency modulations

We further explored PPN activity during imaginary gait by recording local field potentials from the definitive DBS macroelectrodes in a postsurgical session (Fig. 3A). Patients performed the same imaginary gait task as they did intrasurgically, with two additional conditions where they imagined an object moving down the corridor at the two different speeds (normal and rapid). We estimated spectrograms grouping bipolar pairs across patients by relative recording depth (Fig. 3B). PPN local field potentials exhibited robust changes in spectral power that depended on both task events and depth within the nucleus. Following visual instruction onset, we observed transient increases in theta (4–8 Hz), alpha (8–13 Hz), beta (13–30 Hz) and gamma (30–100 Hz) power. These increases were spatially localized, with those in the theta, beta and gamma bands largest at the intermediate dipole, and those in the alpha band equally strong at the dorsal and intermediate dipoles but diminishing significantly at the ventral dipole ($P$-values $< 0.001$, see also Supplementary Table 1).

Aligning to the button presses that initiated and terminated imagery revealed that power modulations in all frequency bands were also greatest at the intermediate dipole ($P$-values $< 0.001$). During imagination, sustained changes in theta, alpha and beta power were also significantly spatially localized; theta power decreased at all dipoles with the smallest decrease at the intermediate dipole, alpha power increased maximally at the intermediate dipole, while beta power increased maximally at the dorsal and intermediate dipoles ($P$-values $< 0.001$). Gamma band power increased at the initiation of imagination, but then decreased below baseline in a non-spatially localized manner until imagery ended, although this

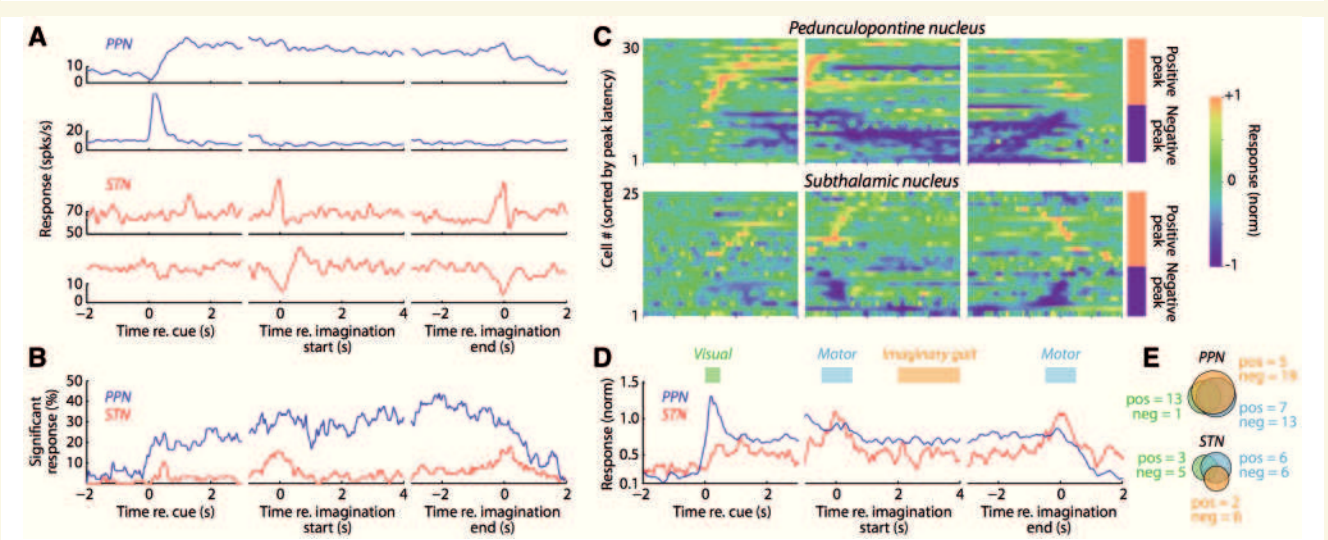


**Figure 1 Neural responses in the human PPN and STN during imaginary gait.** (**A**) Example PPN and STN activity. Each row represents a different neuron, with each column illustrating activity aligned to one of three different trial events. Activity was smoothed with an optimal Gaussian kernel and averaged over trials. We pooled data from normal and rapid gait imagination since we did not observe any differences between these conditions. (**B**) The PPN is more responsive than the STN during the imaginary gait task. For each neuron, we compared activity at each point in time with the baseline activity of that neuron taken before the presentation of the instruction cue. Significance was pooled across all neural responses after FDR correction, and smoothed with a 50 ms moving average. (**C**) Individual activity profiles for significantly modulated neural responses. All neurons that were significantly modulated relative to baseline are plotted, aligning to the same events as **A** and **B**. The activity for each neural response is smoothed with an optimal Gaussian kernel and normalized to the peak absolute response across the entire trial. In each panel, the neural responses are sorted according to the time of the peak absolute response (separately for positive and negative peak responses). The sign of the peak absolute response is indicated to the right of the last column. (**D**) The PPN and STN respond differently during imaginary gait. Population activity profile including all neurons that were significantly modulated relative to baseline. Neural activity was z-scored relative to baseline before averaging the absolute response. (**E**) Neural responses in the PPN more frequently occur to different task epochs than those in the STN. Individual neural responses were tested for significant differences during three different epochs (indicated in **D**): (i) Visual, corresponding to the presentation of the instruction cue (green); (ii) Motor, corresponding to the overt button presses that indicated the beginning and end of imaginary gait (blue); and (iii) Imaginary gait, when patients had their eyes closed and were imagining walking (orange). 'Pos' and 'neg' indicate the number of neurons exhibiting positive or negative modulations of activity for each epoch.

decrease did not reach significance ($P = 0.0674$). Thus, while visual instruction and physical movement were associated with spatially and temporally localized broadband increases in power, mental imagery was associated with spatially localized sustained increases in power specifically in the alpha and beta bands, with suppression elsewhere. Local field potential power changes were similar during both imaginary gait and imaginary object movement, and none of the changes in theta, alpha, beta or gamma band power depended on the type of imagination (gait or object) or speed (normal or rapid) in any of the visual, motor or imagination epochs ($P$-values $> 0.10$).

# Discussion

We used locomotor imagery to explore the different contributions of the PPN and STN in human gait. Our study has two important strengths. First, we recruited homogeneous populations of patients with idiopathic Parkinson's disease, with the only notable difference between the two surgical groups being the severity of dopamine-resistant gait and balance disorders. All patients were cognitively normal and extensively trained, ensuring reliable performance of the motor imagery tasks, which required focus, particularly in the operating room. Second, we used an imaginary gait task that has been validated in imaging studies of healthy subjects (Jahn *et al.*, 2008; Karachi *et al.*, 2012) and patients with Parkinson's disease (Snijders *et al.*, 2011; Crémers *et al.*, 2012). This task has separable phases allowing us to correlate neural activity with distinct events. We found that both the PPN and STN were modulated during motor imagery, but the prevalence of PPN modulations spanning multiple events supports the hypothesis that the PPN, but not the STN, likely integrates multiple sources of information to influence locomotor behaviour in humans.

It is important to consider the limitations of comparing the brain activity of two different patient groups. At our centre, STN-DBS is contraindicated by severe DOPA-resistant gait disorders. We note that patients in both the PPN-DBS and STN-DBS groups exhibit gait and balance disorders. These disorders are alleviated by DOPA-

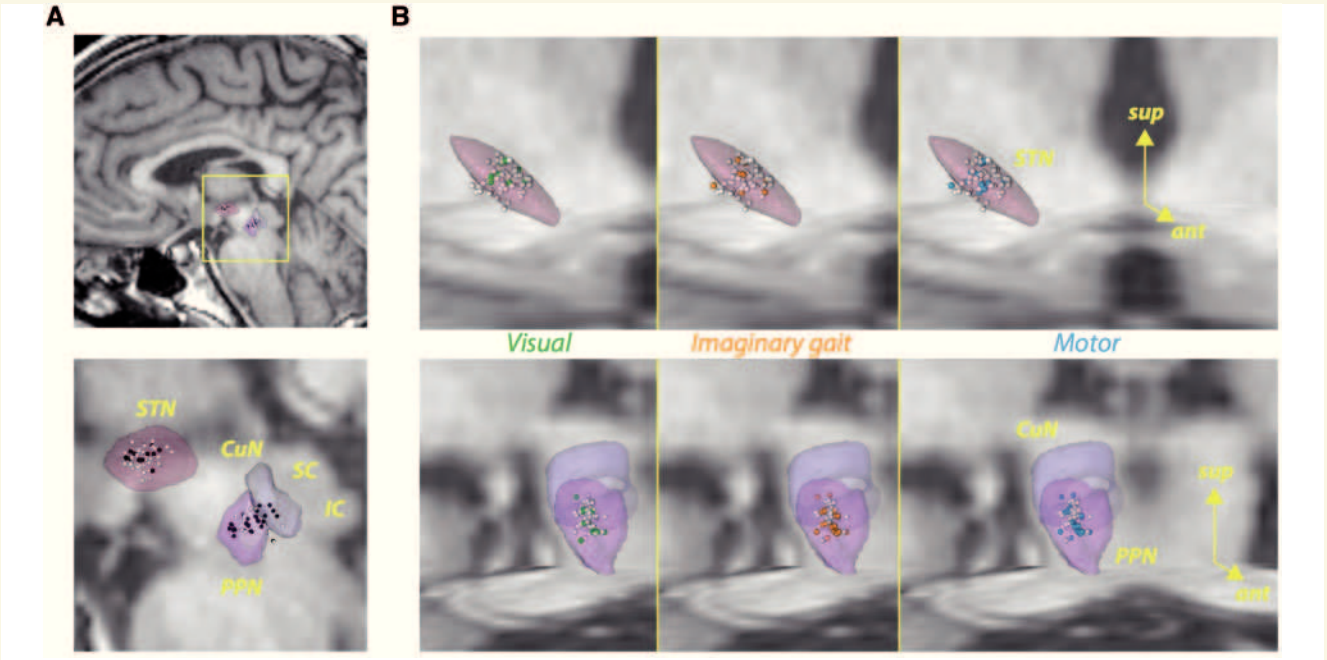


**Figure 2 Localization of neurons in the STN and PPN.** (**A**) Sagittal views of task-related (black) and non-task-related (white) neurons. (**B**) Localization within the STN (*top row*) or cuneiform nucleus (CuN)/PPN (*bottom row*) of neurons with significant modulations in activity during visual instruction (first column, green spheres), imaginary gait (second column, orange spheres), and button press (third column, blue spheres). White spheres represent the remaining neurons. The STN and CuN/PPN figures include axial and coronal $T_1$-weighted MRI sections of the histological atlas of Yelnik *et al.* (2007). IC = inferior colliculus; SC = superior colliculus.

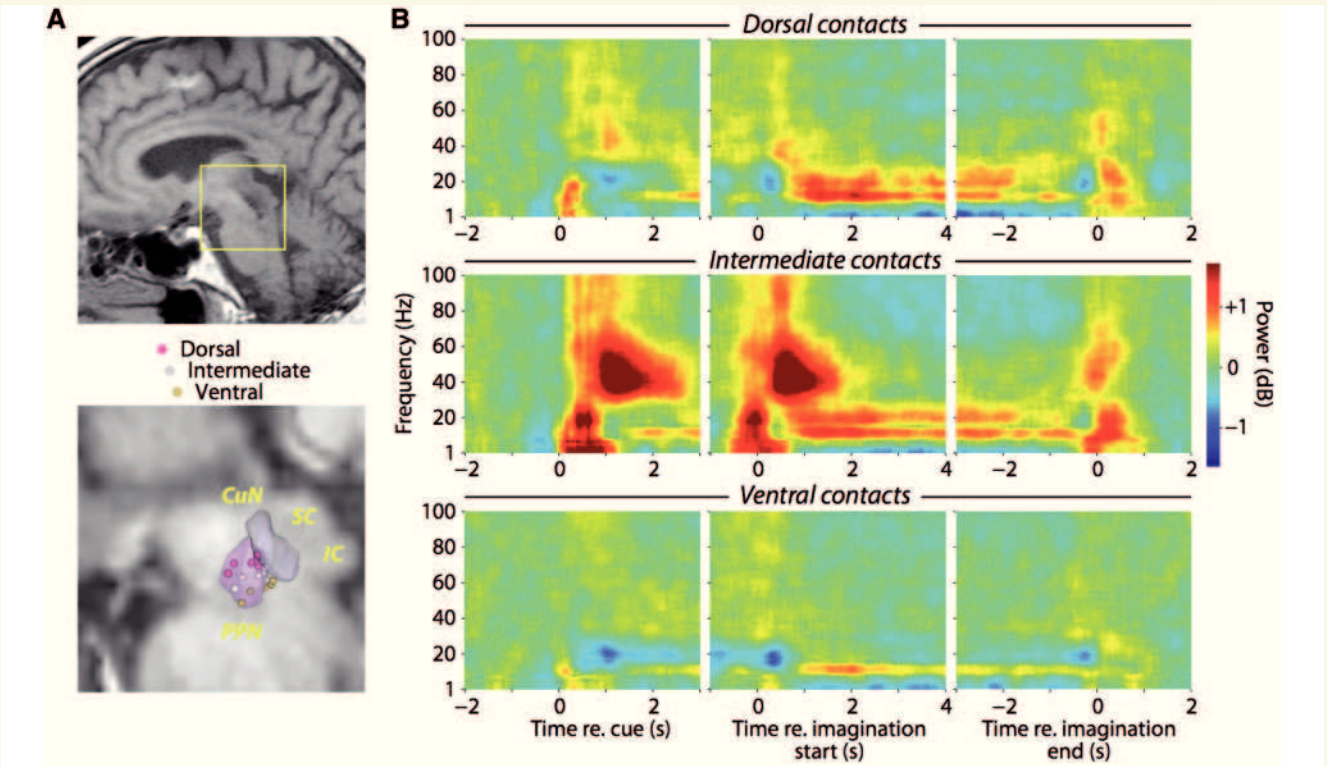


**Figure 3 Task-related local field potential activity is spatially localized within the PPN.** (**A**) Sagittal view of post-surgical localization of PPN electrodes in $T_1$-weighted MRI image from one patient (*top*). Illustration of dipole centres for all patients in the histological atlas of Yelnik *et al.* (2007) (*bottom*). Each sphere represents the midway point between adjacent contacts contributing to each bipolar recording. (**B**) Spectrograms of local field potentials recorded from definitive DBS contacts. Recordings from each patient were averaged by dorsal-ventral arrangement along the electrode shaft (*rows*). The panels within each row are aligned to presentation of the visual instruction cue, initiation and termination of imaginary gait. Spectral power is normalized relative to prestimulus power (−3 to −1 s before instruction onset). IC = inferior colliculus; SC = superior colliculus.

therapy in both groups, although the PPN group exhibited significantly more severe DOPA-resistant gait symptoms. It is ours and others experience that most patients with Parkinson's disease eventually develop DOPA-resistant gait and balance disorders, with these disorders signifying the evolution of the same disease (Grabli *et al.*, 2012). This suggests that the STN-DBS group is a reasonable comparison group for the PPN-DBS patients. The differences in real gait led us to use a locomotor imagery task, a useful paradigm in part because patients with Parkinson's disease have preserved locomotor imagery (Snijders *et al.*, 2011; Crémers *et al.*, 2012), despite being impaired during actual movements. Thus we are not comparing activity related to abnormal movements, but rather to processes related to locomotor imagery that are preserved in both patient groups. Indeed, despite differences in real gait between the PPN and STN cohorts, there was no difference in the duration of imaginary gait between PPN and STN groups, nor was there any correlation between step length during real gait and the duration of imaginary gait. This suggests that while the cohorts differed in terms of real gait, they performed locomotor imagery similarly, suggesting our conclusions are reasonable in the context of previous work in healthy humans and animal models discussed in detail below.

We found that the majority of PPN neurons were modulated during imaginary gait. Our post-surgical recordings further revealed that changes in spiking activity were paralleled by sustained increases in alpha- and beta-band power in the PPN during imaginary gait. These changes in spiking and local field potential activity may be relevant for real gait, strengthening observations that mimicking stepping with alternating movements of the legs (passive or active) during DBS surgery (Piallat *et al.*, 2009; Tattersall *et al.*, 2014) and locomotion in animals (Garcia-Rill *et al.*, 1983; Lee *et al.*, 2014) can elicit activity changes in PPN neurons. Furthermore, in patients with Parkinson's disease, prominent alpha-band oscillations within the PPN (Androulidakis *et al.*, 2008) are enhanced during stepping in place (Fraix *et al.*, 2013) and correlate with speed during actual walking (Thevathasan *et al.*, 2012). Our results agree on certain points with the recent report by Tattersall *et al.* (2014), who also observed that the majority of PPN neurons are modulated during imaginary gait. However, they did not find that imagery modulated alpha- or beta-band oscillations, which contrasts with our observations of sustained power increases in these frequency bands. This difference may be due to targeting differences, as we showed that task-related modulations are spatially restricted within the PPN. Taken together, these results suggest that the PPN area is normally active during locomotion in humans. The specific roles remain unclear, although functions including motor planning and attention that are common to both real and imaginary gait are likely possibilities.

Our data support the hypothesis that the PPN may be an appropriate DBS target for treating DOPA-resistant gait disorders. We demonstrated a marked spatial specificity of task-related responses during locomotor imagery within the PPN, which may be useful for targeting this structure during surgery as it has poorly defined boundaries that are not visible using current imaging techniques. Moreover, the diversity of responses in the PPN suggests that DBS of this area likely influences a wide range of functions, which may account for the heterogeneity of clinical results from PPN-DBS obtained thus far. Currently, the best strategy for selecting patients that could benefit from PPN-DBS remains unknown. Low-frequency stimulation of the PPN is thought to activate neurons, and one possibility is that PPN-DBS is effective in those patients with less severe degeneration of the PPN cholinergic neurons. It will be important in the future to understand the relationship between preserved cholinergic function and PPN-DBS effectiveness.

The PPN modulations we observed are potentially related to processes common to both gait and visuomotor imagery. Indeed, we did not observe significant differences in PPN spiking activity according to changes in imaginary gait speed, nor did we observe significant differences in local field potential modulations between imaginary gait and object motion. This raises the intriguing possibility that PPN activity changes signify processes including visual or kinaesthetic imagery, or sustained attention (Kinomura *et al.*, 1996; Paus *et al.*, 1997; Androulidakis *et al.*, 2008) involved in imagining movement. This is in line with evidence implicating the PPN in a number of general functions, including regulating arousal and sleep (Steriade and McCarley, 1990; Urbano *et al.*, 2012) and linking appetitive and aversive outcomes with behavioural responses (Bechara and van der Kooy, 1989; Winn, 2008; Okada and Kobayashi, 2013; Hong and Hikosaka, 2014), which may be mediated via rich connectivity with non-motor brain areas (Chiba *et al.*, 2001). For example, manipulating mesencephalic locomotor region activity can induce startle and escape responses in addition to locomotion (Mori *et al.*, 1989; Condé *et al.*, 1998), and PPN lesions can disrupt performance in certain associative learning tasks despite leaving abilities such as feeding and basic movement intact (Condé *et al.*, 1998; Winn, 2008). These results indicate that PPN functions extend beyond driving locomotor pattern generation or regulating postural tonus, and suggest that the PPN supports processes that are necessary for adaptive locomotion but that may not be gait-specific *per se*.

We also showed, for the first time in humans to our knowledge, that PPN neurons can be strongly activated by visual stimuli, which in our case were task instructions. In postsurgical recordings, these visual stimuli induced transient broad-band changes in local field potential power that extended well into the gamma band. Similarly sharp responses have been observed in the PPN of monkeys performing visually guided saccades (Okada and Kobayashi, 2009; Hong and Hikosaka, 2014), and may be mediated by direct projections from cortical areas such as the frontal

or supplementary eye fields (Matsumura *et al.*, 2000), or from subcortical structures like the superior colliculus (Redgrave *et al.*, 1988). These visual responses appeared distinct from overt motor modulations, which we also observed in spiking activity and local field potentials during button pressing, in agreement with observations that PPN neurons can be modulated during movements outside of any locomotor context (Matsumura *et al.*, 1997; Weinberger *et al.*, 2008; Okada and Kobayashi, 2009; Shimamoto *et al.*, 2010; Tsang *et al.*, 2010; Thompson and Felsen, 2013; Hong and Hikosaka, 2014; Tattersall *et al.*, 2014). PPN visual activity may play a role in increasing alertness or attention to visual stimuli relevant for task performance by influencing cortical processing via ascending projections (Steriade and McCarley, 1990; Lee *et al.*, 2014). These ascending projections may account for reports that PPN-DBS patients experience enhanced alertness during stimulation (Stefani *et al.*, 2013). Such a function likely extends beyond the visual modality, as PPN neurons can also be modulated at short latency by auditory (Reese *et al.*, 1995; Dormont *et al.*, 1998), vestibular (Aravamuthan and Angelaki, 2012), nociceptive (Carlson *et al.*, 2004) and somatosensory (Yeh *et al.*, 2010) stimuli, suggesting that this structure integrates a variety of ongoing sensory information that may be useful for adapting locomotor behaviour to environmental demands (Rossignol *et al.*, 2006). Further experiments are necessary to determine whether individual neurons integrate multimodal sensory information, and how these responses are related to preparatory, associative or cognitive processes linking sensory stimuli and movement.

We used a locomotor imagery task with the eyes closed to isolate the activity changes from potentially confounding visual stimuli. Importantly, the visual responses we observed in the PPN when the eyes were open were transient, and we observed task-related changes that were sustained throughout imaginary gait with the eyes closed, well after the transient visual responses. Moreover, our postsurgical recordings showed that sustained task-related changes were primarily in the alpha and beta bands that were spatially localized within the PPN area. Together with the fact that the patients performed the imaginary gait task correctly, these results argue against the interpretation that the activity changes exclusively from closing the eyes. Supporting this are functional imaging results using imaginary gait with the eyes closed showing blood oxygenation level-dependent changes in the PPN area in healthy volunteers (Jahn *et al.*, 2008; Karachi *et al.*, 2012) and patients with Parkinson's disease (Snijders *et al.*, 2011; Crémers *et al.*, 2012). In these experiments, all conditions contrasted were performed with the eyes closed, indicating that the PPN was modulated by locomotor imagery.

The involvement of the STN during gait appears different, with most task-related modulations occurring during button pressing. This agrees with observations that STN neurons are modulated during voluntary movements, which reflects regulation of basal ganglia inhibition around movement initiation (Matsumura *et al.*, 1992; Wichmann *et al.*, 1994; Hutchison *et al.*, 1998; Williams *et al.*, 2005; Hanson *et al.*, 2012). Few STN neurons were modulated during the imaginary gait epoch, suggesting that the STN may not be specifically active during gait, consistent with the lack of STN modulation during functional imaging of imaginary (Snijders *et al.*, 2011; Crémers *et al.*, 2012; Karachi *et al.*, 2012) or real gait (Hanakawa *et al.*, 1999; La Fougère *et al.*, 2010). Note that the STN is active during imaginary arm movements in patients with Parkinson's disease (Kühn *et al.*, 2006), suggesting that we might have observed STN modulation during imaginary gait if this structure is involved during real gait. The fact that we observed little activity in the STN during imaginary gait constitutes indirect evidence that the STN may not be involved in gait *per se*. However, in the locomotor imagery experiments cited above, gait was relatively automatic, with subjects walking or imagining gait at constant speed without obstacles. Thus, we may have observed relatively few responsive STN neurons as our task did not involve motor or cognitive conflict or a need to switch from automatic behaviour, situations that may specifically engage the STN (Aron and Poldrack, 2006; Frank *et al.*, 2007; Isoda and Hikosaka, 2008). Indeed, the STN is differentially activated in Parkinsons's disease patients with freezing of gait (Vercruysse *et al.*, 2014) as well as in patients with Parkinson's disease navigating a virtual environment with cognitive loading that induced motor arrests (Shine *et al.*, 2013). Such complex situations likely arise during natural locomotion, raising the possibility that the PPN and STN can interact during natural locomotor behaviour to adapt automatic gait programs to internal and external needs.

There is strong evidence that the PPN and STN interact. In Parkinson's disease, high frequency STN stimulation ($>100$ Hz) alleviates dopamine-sensitive motor symptoms (tremor, rigidity and akinesia), likely through a combination of effects local to the STN as well as effects distributed across brain networks (Kringelbach *et al.*, 2007; Lozano and Lipsman, 2013). Curiously, at these frequencies dopamine-resistant gait disorders can be aggravated, whereas reducing the STN stimulation frequency ($<100$ Hz) can mildly improve these gait disorders while worsening dopamine-sensitive motor symptoms in certain patients (Moreau *et al.*, 2008). The mechanisms underlying this reversal are not understood, but one possibility is that high frequency STN stimulation worsens dopamine-resistant gait disorders in patients with Parkinson's disease by aggravating PPN dysfunction, possibly through direct projections (Lavoie and Parent, 1994; Neagu *et al.*, 2013). Moreover, PPN lesions in parkinsonian monkeys mitigate dopamine-sensitive motor symptoms while at the same time inducing gait disorders (Grabli *et al.*, 2013). These results highlight a close relationship between these two nuclei in Parkinson's disease, and suggest that the PPN and STN likely interact during natural locomotion, perhaps providing a route for the state of the locomotor system to influence the basal ganglia.

# Acknowledgements

We are grateful to the patients for their participation. We thank Dr S. Gallais for managing the anaesthesiology; A. Buot, A. Demain, A. El Helou, C. Ewenczyk, V. Marchal and J. Sellers for training the patients and help collecting the data; and Drs C. François and J. Yelnik for feedback and help in targeting the PPN.

# Funding

This study was supported by the Institut National de la Santé et de la Recherche Médicale et Direction Générale de l'Organisation des Soins (INSERM-DGOS), a grant from the Thierry and Annick Desmarest Foundation to C.K. and B.L., an ATIP-Avenir grant and a grant from the Mairie de Paris to B.L., and a grant from the Régie Autonome des Transports Parisiens (RATP) to M.L.W.


# Supplementary material

Supplementary material is available at *Brain* online.

# References


Androulidakis AG, Mazzone P, Litvak V, Penny W, Dileone M, Gaynor LMFD, et al. Oscillatory activity in the pedunculopontine area of patients with Parkinson's disease. Exp Neurol 2008; 211: 59–66.

Aravamuthan BR, Angelaki DE. Vestibular responses in the macaque pedunculopontine nucleus and central mesencephalic reticular formation. Neuroscience 2012; 223: 183–99.

Aron AR, Poldrack RA. Cortical and subcortical contributions to Stop signal response inhibition: role of the subthalamic nucleus. J Neurosci 2006; 26: 2424–33.

Bakker M, de Lange FP, Stevens JA, Toni I, Bloem BR. Motor imagery of gait: a quantitative approach. Exp Brain Res 2007; 179: 497–504.

Bardinet E, Bhattacharjee M, Dormont D, Pidoux B, Malandain G, Schüpbach M, et al. A three-dimensional histological atlas of the human basal ganglia. II. Atlas deformation strategy and evaluation in deep brain stimulation for Parkinson disease. J Neurosurg 2009; 110: 208–19.

Bechara A, van der Kooy D. The tegmental pedunculopontine nucleus: a brain-stem output of the limbic system critical for the conditioned place preferences produced by morphine and amphetamine. J Neurosci 1989; 9: 3400–9.

Bejjani BP, Dormont D, Pidoux B, Yelnik J, Damier P, Arnulf I, et al. Bilateral subthalamic stimulation for Parkinson's disease by using three-dimensional stereotactic magnetic resonance imaging and electrophysiological guidance. J Neurosurg 2000; 92: 615–25.

Benjamini Y, Hochberg Y. Controlling the False Discovery Rate: A Practical and Powerful Approach to Multiple Testing. J R Stat Soc Ser B 1995; 57: 289–300.

Bohnen NI, Müller MLTM, Koeppe RA, Studenski SA, Kilbourn MA, Frey KA, et al. History of falls in Parkinson disease is associated with reduced cholinergic activity. Neurology 2009; 73: 1670–6.

Carlson JD, Iacono RP, Maeda G. Nociceptive excited and inhibited neurons within the pedunculopontine tegmental nucleus and cuneiform nucleus. Brain Res 2004; 1013: 182–7.

Chiba T, Kayahara T, Nakano K. Efferent projections of infralimbic and prelimbic areas of the medial prefrontal cortex in the Japanese monkey, Macaca fuscata. Brain Res 2001; 888: 83–101.

Condé H, Dormont JF, Farin D. The role of the pedunculopontine tegmental nucleus in relation to conditioned motor performance in the cat. II. Effects of reversible inactivation by intracerebral microinjections. Exp Brain Res 1998; 121: 411–8.

Crémers J, D'Ostilio K, Stamatakis J, Delvaux V, Garraux G. Brain activation pattern related to gait disturbances in Parkinson's disease. Mov Disord 2012; 27: 1498–505.

Demain A, Westby GWM, Fernandez-Vidal S, Karachi C, Bonneville F, Do MC, et al. High-level gait and balance disorders in the elderly: a midbrain disease? J Neurol 2014; 261: 196–206.

Dormont JF, Condé H, Farin D. The role of the pedunculopontine tegmental nucleus in relation to conditioned motor performance in the cat. I. Context-dependent and reinforcement-related single unit activity. Exp Brain Res 1998; 121: 401–10.

Eidelberg E, Walden JG, Nguyen LH. Locomotor control in macaque monkeys. Brain 1981; 104: 647–63.

Ferraye MU, Debû B, Fraix V, Goetz L, Ardouin C, Yelnik J, et al. Effects of pedunculopontine nucleus area stimulation on gait disorders in Parkinson's disease. Brain 2010; 133: 205–14.

La Fougère C, Zwergal A, Rominger A, Förster S, Fesl G, Dieterich M, et al. Real versus imagined locomotion: a [18F]-FDG PET-fMRI comparison. Neuroimage 2010; 50: 1589–98.

Fraix V, Bastin J, David O, Goetz L, Ferraye M, Benabid A-L, et al. Pedunculopontine nucleus area oscillations during stance, stepping and freezing in Parkinson's disease. PLoS One 2013; 8: e83919.

Frank MJ, Samanta J, Moustafa AA, Sherman SJ. Hold your horses: impulsivity, deep brain stimulation, and medication in parkinsonism. Science 2007; 318: 1309–12.

Garcia-Rill E, Skinner RD, Fitzgerald JA. Activity in the mesencephalic locomotor region during locomotion. Exp Neurol 1983; 82: 609–22.

Grabli D, Karachi C, Folgoas E, Monfort M, Tande D, Clark S, et al. Gait disorders in parkinsonian monkeys with pedunculopontine nucleus lesions: a tale of two systems. J Neurosci 2013; 33: 11986–93.

Grabli D, Karachi C, Welter M-L, Lau B, Hirsch EC, Vidailhet M, et al. Normal and pathological gait: what we learn from Parkinson's disease. J Neurol Neurosurg Psychiatry 2012; 83: 979–85.

Hanakawa T, Katsumi Y, Fukuyama H, Honda M, Hayashi T, Kimura J, et al. Mechanisms underlying gait disturbance in Parkinson's disease: a single photon emission computed tomography study. Brain 1999; 122: 1271–82.

Hanson TL, Fuller AM, Lebedev MA, Turner DA, Nicolelis MAL. Subcortical neuronal ensembles: an analysis of motor task association, tremor, oscillations, and synchrony in human patients. J Neurosci 2012; 32: 8620–32.

Hirsch EC, Graybiel AM, Duyckaerts C, Javoy-Agid F. Neuronal loss in the pedunculopontine tegmental nucleus in Parkinson disease and in progressive supranuclear palsy. Proc Natl Acad Sci USA 1987; 84: 5976–80.

Hong S, Hikosaka O. Pedunculopontine tegmental nucleus neurons provide reward, sensorimotor, and alerting signals to midbrain dopamine neurons. Neuroscience 2014; 282: 139–55.

Hutchison WD, Allan RJ, Opitz H, Levy R, Dostrovsky JO, Lang AE, et al. Neurophysiological identification of the subthalamic nucleus in surgery for Parkinson's disease. Ann Neurol 1998; 44: 622–8.

Isoda M, Hikosaka O. Role for subthalamic nucleus neurons in switching from automatic to controlled eye movement. J Neurosci 2008; 28: 7209–18.

Jahn K, Deutschländer A, Stephan T, Kalla R, Wiesmann M, Strupp M, et al. Imaging human supraspinal locomotor centers in brainstem and cerebellum. Neuroimage 2008; 39: 786–92.

Jellinger K. The pedunculopontine nucleus in Parkinson's disease, progressive supranuclear palsy and Alzheimer's disease. J Neurol Neurosurg Psychiatry 1988; 51: 540–3.

Karachi C, André A, Bertasi E, Bardinet E, Lehéricy S, Bernard FA. Functional parcellation of the lateral mesencephalus. J Neurosci 2012; 32: 9396–401.

Karachi C, Grabli D, Bernard FA, Tandé D, Wattiez N, Belaid H, et al. Cholinergic mesencephalic neurons are involved in gait and postural disorders in Parkinson disease. J Clin Invest 2010; 120: 2745–54.

Kinomura S, Larsson J, Gulyás B, Roland PE. Activation by attention of the human reticular formation and thalamic intralaminar nuclei. Science 1996; 271: 512–5.

Kringelbach ML, Jenkinson N, Owen SLF, Aziz TZ. Translational principles of deep brain stimulation. Nat Rev Neurosci 2007; 8: 623–35.

Kühn AA, Doyle L, Pogosyan A, Yarrow K, Kupsch A, Schneider G-H, et al. Modulation of beta oscillations in the subthalamic area during motor imagery in Parkinson's disease. Brain 2006; 129: 695–706.

Lavoie B, Parent A. Pedunculopontine nucleus in the squirrel monkey: projections to the basal ganglia as revealed by anterograde tract-tracing methods. J Comp Neurol 1994; 344: 210–31.

Lee AM, Hoy JL, Bonci A, Wilbrecht L, Stryker MP, Niell CM. Identification of a brainstem circuit regulating visual cortical state in parallel with locomotion. Neuron 2014; 83: 455–66.

Limousin P, Krack P, Pollak P, Benazzouz A, Ardouin C, Hoffman D, et al. Electrical stimulation of the subthalamic nucleus in advanced Parkinson's disease. N Engl J Med 1998; 339: 1105–11.

Lozano AM, Lipsman N. Probing and regulating dysfunctional circuits using deep brain stimulation. Neuron 2013; 77: 406–24.

Maillet A, Thobois S, Fraix V, Redouté J, Le Bars D, Lavenne F, et al. Neural substrates of levodopa-responsive gait disorders and freezing in advanced Parkinson's disease: a kinesthetic imagery approach. Hum Brain Mapp 2015; 36: 959–80.

Matsumura M, Kojima J, Gardiner TW, Hikosaka O. Visual and oculomotor functions of monkey subthalamic nucleus. J Neurophysiol 1992; 67: 1615–32.

Matsumura M, Nambu A, Yamaji Y, Watanabe K, Imai H, Inase M, et al. Organization of somatic motor inputs from the frontal lobe to the pedunculopontine tegmental nucleus in the macaque monkey. Neuroscience 2000; 98: 97–110.

Matsumura M, Watanabe K, Ohye C. Single-unit activity in the primate nucleus tegmenti pedunculopontinus related to voluntary arm movement. Neurosci Res 1997; 28: 155–65.

Mazzone P, Lozano A, Stanzione P, Galati S, Scarnati E, Peppe A, et al. Implantation of human pedunculopontine nucleus: a safe and clinically relevant target in Parkinson's disease. Neuroreport 2005; 16: 1877–81.

Mitra P, Bokil H. Observed brain dynamics. New York: Oxford University Press; 2007.

Moreau C, Defebvre L, Destée a, Bleuse S, Clement F, Blatt JL, et al. STN-DBS frequency effects on freezing of gait in advanced Parkinson disease. Neurology 2008; 71: 80–4.

Mori S, Sakamoto T, Ohta Y, Takakusaki K, Matsuyama K. Site-specific postural and locomotor changes evoked in awake, freely moving intact cats by stimulating the brainstem. Brain Res 1989; 505: 66–74.

Moro E, Hamani C, Poon Y-Y, Al-Khairallah T, Dostrovsky JO, Hutchison WD, et al. Unilateral pedunculopontine stimulation improves falls in Parkinson's disease. Brain 2010; 133: 215–24.

Neagu B, Tsang E, Mazzella F, Hamani C, Moro E, Hodaie M, et al. Pedunculopontine nucleus evoked potentials from subthalamic nucleus stimulation in Parkinson's disease. Exp Neurol 2013; 250: 221–7.

Okada KI, Kobayashi Y. Characterization of oculomotor and visual activities in the primate pedunculopontine tegmental nucleus during visually guided saccade tasks. Eur J Neurosci 2009; 30: 2211–23.

Okada KI, Kobayashi Y. Reward prediction-related increases and decreases in tonic neuronal activity of the pedunculopontine tegmental nucleus. Front Integr Neurosci 2013; 7: 36.

Olszewski J, Baxter D. Cytoarchitecture of the human brain stem. Philadelphia: Lippincott; 1954.

Orlovsky G, Deliagina T, Grillner S. Neural Control of Locomotion: from Mollusc to Man. London: Oxford University Press; 1999.

Pahapill PA, Lozano AM. The pedunculopontine nucleus and Parkinson's disease. Brain 2000; 123 (Pt 9): 1767–83.

Paus T, Zatorre RJ, Hofle N, Caramanos Z, Gotman J, Petrides M, et al. Time-related changes in neural systems underlying attention and arousal during the performance of an auditory vigilance task. J Cogn Neurosci 1997; 9: 392–408.

Piallat B, Chabardès S, Torres N, Fraix V, Goetz L, Seigneuret E, et al. Gait is associated with an increase in tonic firing of the sub-cuneiform nucleus neurons. Neuroscience 2009; 158: 1201–5.

Plaha P, Gill SS. Bilateral deep brain stimulation of the pedunculopontine nucleus for Parkinson's disease. Neuroreport 2005; 16: 1883–7.

Le Ray D, Juvin L, Ryczko D, Dubuc R. Supraspinal control of locomotion: the mesencephalic locomotor region. Prog Brain Res 2011; 188: 51–70.

Redgrave P, Dean P, Mitchell IJ, Odekunle A, Clark A. The projection from superior colliculus to cuneiform area in the rat. I. Anatomical studies. Exp Brain Res 1988; 72: 611–25.

Reese NB, Garcia-Rill E, Skinner RD. Auditory input to the pedunculopontine nucleus: II. Unit responses. Brain Res Bull 1995; 37: 265–73.

Rolland AS, Karachi C, Muriel MP, Hirsch EC, François C. Internal pallidum and substantia nigra control different parts of the mesopontine reticular formation in primate. Mov Disord 2011; 26: 1648–56.

Rossignol S, Dubuc R, Gossard JP. Dynamic sensorimotor interactions in locomotion. Physiol Rev 2006; 86: 89–154.

Shik M, Severin F, Orlovsky G. Control of walking and running by means of electric stimulation of the midbrain. Biofizika 1966; 11: 659–66.

Shimamoto SA, Larson PS, Ostrem JL, Glass GA, Turner RS, Starr PA. Physiological identification of the human pedunculopontine nucleus. J Neurol Neurosurg Psychiatry 2010; 81: 80–6.

Shimazaki H, Shinomoto S. Kernel bandwidth optimization in spike rate estimation. J Comput Neurosci 2010; 29: 171–82.

Shine JM, Matar E, Ward PB, Bolitho SJ, Gilat M, Pearson M, et al. Exploring the cortical and subcortical functional magnetic resonance imaging changes associated with freezing in Parkinson's disease. Brain 2013; 136: 1204–15.

Skinner RD, Garcia-Rill E. The mesencephalic locomotor region (MLR) in the rat. Brain Res 1984; 323: 385–9.

Snijders AH, Leunissen I, Bakker M, Overeem S, Helmich RC, Bloem BR, et al. Gait-related cerebral alterations in patients with Parkinson's disease with freezing of gait. Brain 2011; 134: 59–72.

Snijders AH, van de Warrenburg BP, Giladi N, Bloem BR. Neurological gait disorders in elderly people: clinical approach and classification. Lancet Neurol 2007; 6: 63–74.

Stefani A, Lozano AM, Peppe A, Stanzione P, Galati S, Tropepi D, et al. Bilateral deep brain stimulation of the pedunculopontine and subthalamic nuclei in severe Parkinson's disease. Brain 2007; 130: 1596–607.

Stefani A, Peppe A, Galati S, Bassi MS, D'Angelo V, Pierantozzi M. The serendipity case of the pedunculopontine nucleus low-frequency brain stimulation: chasing a gait response, finding sleep, and cognition improvement. Front Neurol 2013; 4: 68.

Steriade M, McCarley R. Brainstem control of wakefulness and sleep. New York: Plenum Press; 1990.

Székely GJ, Rizzo ML. Energy statistics: A class of statistics based on distances. J Stat Plan Inference 2013; 143: 1249–72.

Takakusaki K, Habaguchi T, Ohtinata-Sugimoto J, Saitoh K, Sakamoto T. Basal ganglia efferents to the brainstem centers controlling postural muscle tone and locomotion: a new concept for

understanding motor disorders in basal ganglia dysfunction. Neuroscience 2003; 119: 293–308.

Tattersall TL, Stratton PG, Coyne TJ, Cook R, Silberstein P, Silburn PA, et al. Imagined gait modulates neuronal network dynamics in the human pedunculopontine nucleus. Nat Neurosci 2014; 17: 449–54.

Thevathasan W, Pogosyan A, Hyam JA, Jenkinson N, Foltynie T, Limousin P, et al. Alpha oscillations in the pedunculopontine nucleus correlate with gait performance in parkinsonism. Brain 2012; 135: 148–60.

Thompson JA, Felsen G. Activity in mouse pedunculopontine tegmental nucleus reflects action and outcome in a decision-making task. J Neurophysiol 2013; 110: 2817–29.

Tsang EW, Hamani C, Moro E, Mazzella F, Poon YY, Lozano A. M, et al. Involvement of the human pedunculopontine nucleus region in voluntary movements. Neurology 2010; 75: 950–9.

Urbano FJ, Kezunovic N, Hyde J, Simon C, Beck P, Garcia-Rill E. Gamma band activity in the reticular activating system. Front Neurol 2012; 3: 6.

Vercruysse S, Spildooren J, Heremans E, Wenderoth N, Swinnen SP, Vandenberghe W, et al. The neural correlates of upper limb motor blocks in parkinson's disease and their relation to freezing of gait. Cereb Cortex 2014; 24: 3154–66.

Weinberger M, Hamani C, Hutchison WD, Moro E, Lozano AM, Dostrovsky JO. Pedunculopontine nucleus microelectrode recordings in movement disorder patients. Exp Brain Res 2008; 188: 165–74.

Welter ML, Houeto JL, Tezenas du Montcel S, Mesnage V, Bonnet AM, Pillon B, et al. Clinical predictive factors of subthalamic stimulation in Parkinson's disease. Brain 2002; 125: 575–83.

Wichmann T, Bergman H, DeLong MR. The primate subthalamic nucleus. I. Functional properties in intact animals. J Neurophysiol 1994; 72: 494–506.

Williams ZM, Neimat JS, Cosgrove GR, Eskandar EN. Timing and direction selectivity of subthalamic and pallidal neurons in patients with Parkinson disease. Exp Brain Res 2005; 162: 407–16.

Winn P. Experimental studies of pedunculopontine functions: are they motor, sensory or integrative? Parkinsonism Relat Disord 2008; 14 (Suppl 2): S194–8.

Yeh IJ, Tsang EW, Hamani C, Moro E, Mazzella F, Poon YY, et al. Somatosensory evoked potentials recorded from the human pedunculopontine nucleus region. Mov Disord 2010; 25: 2076–83.

Yelnik J, Bardinet E, Dormont D, Malandain G, Ourselin S, Tandé D, et al. A three-dimensional, histological and deformable atlas of the human basal ganglia. I. Atlas construction based on immunohistochemical and MRI data. Neuroimage 2007; 34: 618–38.

Zanos TP, Mineault PJ, Pack CC. Removal of spurious correlations between spikes and local field potentials. J Neurophysiol 2011; 105: 474–86.

Zrinzo L, Zrinzo L V, Tisch S, Limousin PD, Yousry TA, Afshar F, et al. Stereotactic localization of the human pedunculopontine nucleus: atlas-based coordinates and validation of a magnetic resonance imaging protocol for direct localization. Brain 2008; 131: 1588–98.

Zweig RM, Jankel WR, Hedreen JC, Mayeux R, Price DL. The pedunculopontine nucleus in Parkinson's disease. Ann Neurol 1989; 26: 41–6.

# AXE 1. IMPLICATION DE LA MLR A UN STADE AVANCEE DE LA MALADIE DE PARKINSON

# *CADRE THÉORIQUE*

## A. ATTEINTES NEURONALES DANS LA MALADIE DE PARKINSON

La maladie de Parkinson est caractérisée par des symptômes moteurs bien connus: la rigidité, l'akinésie et le tremblement de repos (Lang et Lozano, 1998a,b). Sur le plan physiopathologique, ces manifestations cliniques sont directement liées à la dégénérescence des neurones dopaminergiques de la SNc. Cette évolution est lente, et les symptômes apparaissent généralement lorsque la perte neuronale dopaminergique est supérieure à 80%. La Levodopa (L-dopa), permettant de corriger le déficit dopaminergique, reste le traitement médicamenteux de référence afin d'améliorer les symptômes de la MP. La réponse clinique à la L-dopa est en général très satisfaisante au début de la maladie, pendant une période d'environ 5 à 7 ans (considérée comme la « lune de miel thérapeutique »). Puis apparaissent fréquemment des complications motrices à long terme, telles que les fluctuations motrices et les dyskinésies. L'administration d'agonistes dopaminergiques est proposée comme traitement précoce de la maladie avec un plus faible risque de développer des dyskinésies, mais pouvant induire une aggravation des troubles du comportement. Aussi chez les patients souffrant d'une maladie sévère et de complications de la dopa-thérapie, la stimulation cérébrale profonde (SCP) du NST est proposée avec de très bons résultats améliorant considérablement la qualité de vie (Benabid et al., 1994; Limousin et al., 1995a,b; Welter et al., 2014).

Des atteintes du système nerveux central autres que celle des neurones dopaminergiques ont été mises en évidence. Les neurones noradrénergiques du *locus coeruleus (Mann, 1983; Chan-Palay et Asan, 1989; Gesi et al., 2000)*, les neurones sérotoninergiques des noyaux du raphé (Halliday et al., 1990), les neurones cholinergiques du *nucleus basalis* de Meynert (Arendt et al., 1983; Nakano et Hirano, 1984; Rogers et al., 1985), les neurones orexinergiques de l'hypothalamus (Fronczek et al., 2007; Thannickal et al., 2007), les neurones glutamatergiques des noyaux parafasciculaire et centro-median du thalamus (Henderson et al., 2000), font partie des nombreux systèmes pouvant être altérés.

Les lésions histologiques décrites au sein des neurones dopaminergiques sont des inclusions appelées anciennement Corps de Lewy, et qui correspondent à une accumulation

d'alpha-synucleine phosphorylée, entraînant une altération du cytosquelette des neurones atteints. Différents stades de la maladie ont été décrits (Braak et al., 2003; Braak et al., 2004; Jellinger, 2012), en fonction des systèmes neuronaux atteints. Selon Braak, la MP évoluerait en 6 stades par une progression lente avec un gradient caudo-rostral (Braak et al., 2004) (figure 7). Les deux premiers touchent particulièrement les noyaux olfactifs et le tronc cérébral inférieur, responsables des syndromes prodromiques (anosmie, troubles du sommeil, troubles digestifs et dépression). A partir de l'étape 3 les symptômes moteurs apparaissent avec la dégénérescence des neurones DA de la SNc, et l'atteinte du tronc cérébral supérieur (PPN). Au stade 4, d'autres structures sous-corticales, limbiques et associatives, telles que l'amygdale et l'hippocampe ainsi qu'une partie du cortex, sont atteintes. A ce stade les neurones DA de la SNc sont très sévèrement touchés avec la triade des symptômes moteurs (akinésie, tremblement et rigidité). Enfin dans les stades finaux 5 et 6, les lésions se propagent sur l'ensemble du cortex (cortex prémoteur, moteur, préfrontal), et vers l'ensemble du tronc cérébral (dont la MLR), avec le tableau symptomatique clinique complet de la MP très évoluée.

Figure 7: Description des stades de la Maladie de Parkinson
*d'après Braak et al (2004)*

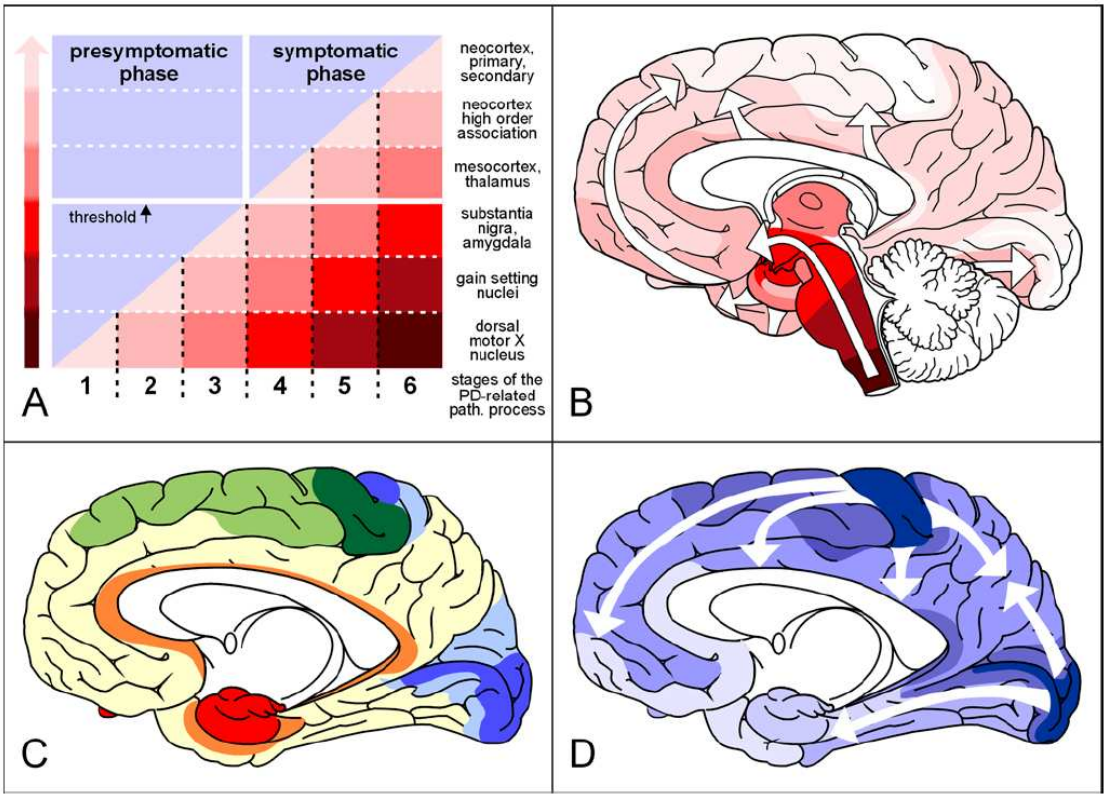

## B. DÉGÉNÉRESCENCE DES NEURONES CHOLINERGIQUES DU PPN

Les troubles de la marche et de l'équilibre survenant à un stade avancé de la maladie sont généralement dopa-résistants, et ne répondent pas à la SCP du NST. Ceci renforce l'idée d'une atteinte des systèmes non-dopaminergiques dans la pathogénèse de ces symptômes. Dans ce contexte, de nombreuses études se sont intéressées à la MLR et plus particulièrement au PPN, du fait de ses connexions avec les GB et de son rôle dans la locomotion (Pahapill et Lozano, 2000).

Nous avons vu en introduction qu'il existe une perte neuronale cholinergique importante du PPN prédominant dans la pars compacta (Hirsch et al., 1987; Jellinger, 1988) (figure 8). L'importance de cette perte est corrélée à la sévérité de la perte des neurones dopaminergiques de la SNc (Zweig et al., 1989), et à la sévérité de la maladie (selon la classification de Hoehn et Yahr) (Rinne et al., 2008). Nous avons montré dans notre équipe que cette perte est plus marquée de façon significative chez les patients parkinsoniens chuteurs (Karachi et al., 2010) (figure 9).

Par ailleurs il a été mis en évidence une perte modérée associée des neurones GABAergiques du PPN chez les patients parkinsoniens (Pienaar , 2013).

Ces données peuvent permettre de mieux comprendre la physiopathologie de ces symptômes, dont les conséquences physiques et psychosociales sont majeures sur la qualité de vie des patients parkinsoniens et sur l'espérance de vie (Kempster et al., 2010; Moore et al., 2007), avec en première ligne la perte d'autonomie et l'institutionnalisation (Bloem et al., 2004).

Figure 8: Dégénérescence des neurones cholinergiques du PPN dans la Maladie de Parkinson
*d'après Hirsch et al (1987)*

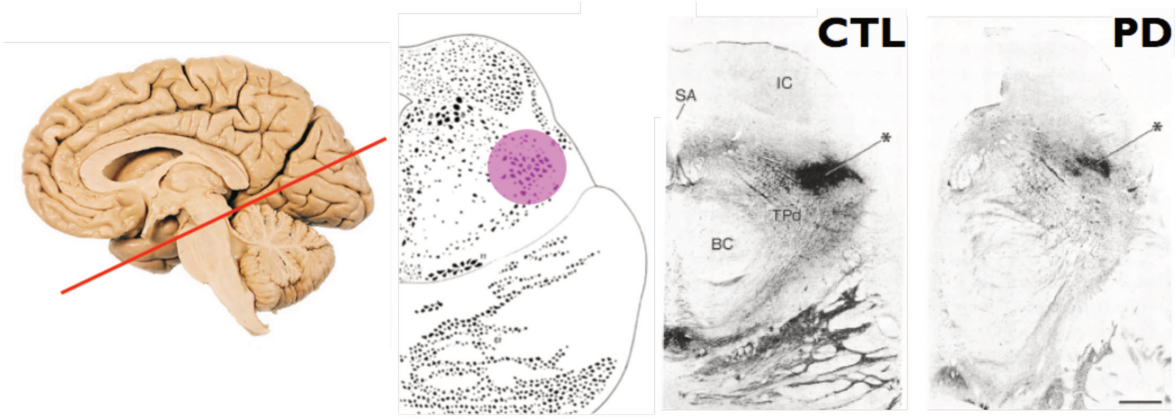


Figure 9: Corrélation entre la perte des neurones cholinergiques du PPN et la présence de chutes chez les patients parkinsoniens
*d'après Karachi et al (2010)*

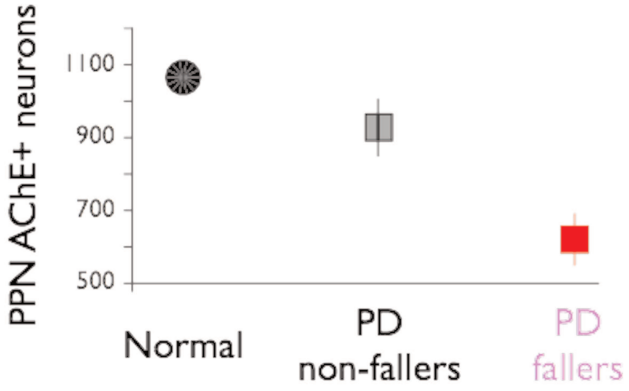

Complétant ces résultats histologiques, des études en PET chez les patients parkinsoniens ont mis en évidence une altération de l'activité cholinergique au niveau thalamique uniquement chez les patients chuteurs, et au niveau cortical prédominant chez ces mêmes patients (Bohnen et al., 2009). Par contre il n'y avait pas de différences sur l'innervation dopaminergique chez les 2 groupes de patients, chuteurs et non chuteurs. Sur une étude similaire en PET, la diminution de l'innervation cholinergique était de plus corrélée à la diminution de la vitesse de marche chez les patients parkinsoniens (Bohnen et al., 2013).

Aussi, des agonistes cholinergiques ont été testés chez les patients parkinsoniens, mais leurs effets sur les symptômes restent modestes, y compris sur la fréquence des chutes (Katzenschlager et al., 2003) (Li et al., 2015). De plus, ils sont associés à un ensemble d'effets secondaires périphériques qui limitent leur utilisation. Le développement d'agents ayant une action spécifique positive sur les récepteurs cholinergiques muscariniques pourrait apporter un réel bénéfice et améliorer les troubles de la marche et de la posture. Par ailleurs il pourrait aussi y avoir un effet potentiel sur le système dopaminergique en stimulant les neurones dopaminergiques de la SNc via les projections cholinergiques du PPN (Mena-Segovia et al., 2008).

## C. RÔLES DU PPN DANS LA POSTURE ET LA LOCOMOTION À L'ÉTAT PARKINSONIEN

### 1. Données expérimentales chez l'animal rendu parkinsonien

Une lésion dopaminergique chez l'animal, le plus souvent sélectionné jeune, n'entraine pas de mort neuronale au sein du PPN. Elle peut néanmoins modifier l'activité métabolique des neurones du PPN, même si les données de la littérature sont contradictoires sur l'effet induit. En effet, une augmentation de l'activité neuronale dans le PPN a été montrée chez les rats 6-OHDA (Breit et al., 2001; 2005; Jeon et al., 2003), alors qu'une diminution a été observée chez le singe intoxiqué par le MPTP (Gomez-Gallego et al., 2007). Par ailleurs, chez des singes âgés rendus parkinsoniens, des troubles de la posture et de l'équilibre sont présents, et de plus associés à une perte modérée de neurones cholinergiques dans le PPN, contrairement aux singes jeunes rendus parkinsoniens (Karachi et al., 2010).

Chez le singe intoxiqué par le 1-methyl-4-phenyl-1,2,3,6-tetrahydropyridine (MPTP), la modulation des neurones du PPN par des micro-injections d'un antagoniste GABA (bicuculline) (Nandi et al., 2002a), ou par stimulation unilatérale à basse fréquence du PPN, induit une amélioration de l'akinésie observée, celui-ci étant additif s'il est associé à un traitement dopaminergique (Jenkinson et al., 2004). La même stimulation unilatérale du PPN chez un singe à l'état contrôle a montré des résultats variables sur le tonus musculaire (Nandi et al., 2002b). Les symptômes induits diffèrent en fonction de la fréquence de stimulation: à haute fréquence (>100 Hz) il existe un trouble du contrôle postural et une akinésie, alors qu'à des fréquences plus basses (<45 Hz) on observe un tremblement sans anomalie posturale.

Enfin, permettant d'obtenir un modèle au plus proche d'un stade avancé de la MP, un modèle primate a été développé au sein de l'équipe (Grabli et al., 2013) associant chez un même singe des lésions dopaminergiques par injection de MPTP à des lésions cholinergiques du PPN par injection de toxine spécifique. Les animaux présentaient à la fois un syndrome parkinsonien classique, et des troubles de la posture et de l'équilibre surajoutés ne répondant pas au traitement dopaminergique. Ces troubles posturaux étaient similaires à ceux observés chez les singes avec une lésion du PPN cholinergique seule (Karachi et al., 2010). Ces résul-

tats soulignent le rôle complexe des systèmes dopaminergiques et cholinergiques dans la genèse des troubles de la posture et de l'équilibre, qui sont interconnectés mais fonctionnent aussi indépendamment l'un de l'autre. En parallèle, nous avons montré que seuls des singes âgés présentaient une perte de neurones cholinergiques du PPN après injections de MPTP (Karachi et al., 2010; Grabli et al., 2013). Ainsi l'association de ces 2 lésions permet d'avoir un modèle primate se rapprochant d'un stade avancé de la MP, qui pourrait permettre d'étudier la physiopathologie des différents symptômes dopa-résistants présents à ce stade de la maladie et surtout servir de modèle pré thérapeutique.

## 2. Stimulation de la MLR chez les patients parkinsoniens

### *a) Résultats cliniques*

La cible du PPN a été proposée par plusieurs équipes afin de traiter les troubles de la marche et de la posture dopa-résistants. Les premières études ont rapporté des effets cliniques prometteurs. L'équipe de Mazzone a été la première à montrer un bénéfice sur les scores moteurs (signes cardinaux et signes axiaux) par la stimulation bilatérale à basse fréquence du PPN (10Hz) chez deux patients parkinsoniens, associée à une implantation bilatérale dans le NST (Mazzone et al., 2005). A la même période a été publiée une seconde étude après implantation bilatérale dans le PPN chez deux patients parkinsoniens, avec un effet spécifique sur les troubles posturaux et de la marche pour une stimulation à basse fréquence (20-25Hz), en ON et OFF médication (Plaha et Gill, 2005).

Par la suite différentes équipes ont observé des résultats plus mitigés, avec un faible nombre de patients inclus. De plus cette population de patients est hétérogène et diffère entre les études: implantation unilatérale dans le PPN (Moro et al., 2010), bilatérale associée avec des électrodes dans le NST (Stefani et al., 2007; Ferraye et al., 2010; Khan et al., 2011) ou bilatérale dans le PPN (Thevathasan et al., 2011; 2012; Welter et al., 2015). Ces deux dernières études, réalisées en aveugle, ont cependant mis en évidence un effet objectif de la stimulation à basse fréquence sur les paramètres spécifiques de freezing et d'instabilité posturale. Une autre étude plus récente a analysé les effets à plus long terme de la stimulation unilatérale du PPN, à 2 ans et 4 ans (Mestre et al., 2016). Si l'équipe conclut à un effet positif

à 2 ans sur le freezing et les chutes, cet effet ne perdurerait pas lors de l'évaluation à 4 ans. Concernant la stimulation uni ou bilatérale, il apparaît que la stimulation bilatérale à basse fréquence soit la plus efficace (Thevathasan et al., 2012; Nosko et al., 2014).

Une des difficultés majeures d'interprétation de ces études est que la cible stimulée n'est pas similaire entre les équipes comme nous l'avons vu en introduction. Certaines décrivent en effet le noyau sub-cunéiforme comme la principale région impliquée dans la locomotion (Piallat et al., 2009), ou la région dorsale au PPNc (Ferraye et al., 2010), d'autres des cibles nettement plus profondes que le PPN, se situant sous la jonction ponto-mésencéphalique (Thevathasan et al., 2011; Thevathasan et al., 2012) (figure 10).

Il est ainsi difficile d'interpréter les résultats de la littérature, d'autant qu'il n'existe pas encore de paramètre prédictif de réponse positive à la stimulation du PPN, équivalent au test à la L-dopa pour la stimulation du NST. Un outil prédictif permettrait évidemment une meilleure sélection des patients pouvant bénéficier de cette chirurgie. Enfin, compliquant particulièrement l'analyse des résultats, les troubles de la marche et de la posture sont épisodiques et dépendent fortement du contexte et de l'environnement (Giladi et Nieuwboer, 2008; Giladi et al., 2013), rendant l'évaluation pertinente difficile en milieu hospitalier d'autant plus que les protocoles de recherche nécessitent une certaine rigidité et une évaluation aveugle (Chee et al., 2009).

Figure 10: Localisation des électrodes de SCP dans le PPN selon les équipes
*respectivement d'après Mazzone et al (2005), Plaha et Gill (2005)*
*et Thevathasan et al (2011)*

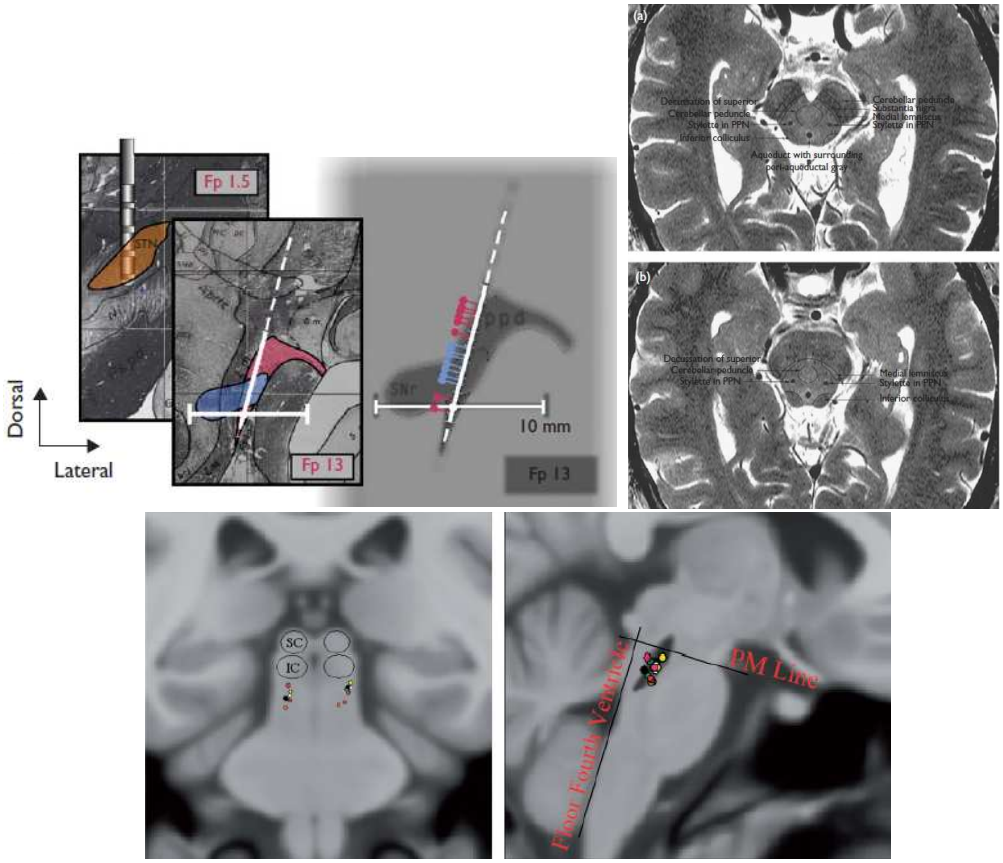


**En conclusion,** les dernières études montrent que 50% des patients ayant des troubles de la marche dopa-résistants avec freezing et chutes, implantés dans le PPN, ont une diminution de la fréquence des chutes d'environ 30% et une amélioration objective de leur qualité de vie.

### b) Données électrophysiologiques

Chez l'homme, des enregistrements électrophysiologiques de la région du PPN ont pu être réalisés au cours des procédures chirurgicales d'implantation d'électrode de stimulation profonde chez les patients parkinsoniens. Les premières descriptions rapportent une modification de l'activité neuronale lors des mouvements passifs ou actifs du membre supérieur controlatéral (Weinberger et al., 2008). La marche réelle ne pouvant être réalisée au cours de la procédure opératoire, des conditions de marche mimée ou imaginaire ont été effectuées. Ainsi l'équipe de Grenoble a montré une augmentation de la fréquence de décharge au cours de la tâche de marche mimée pour les neurones localisés dans le noyau sub-cunéiforme (Piallat et al., 2009). Cependant la localisation anatomique réelle des neurones enregistrés reste difficile à déterminer, notamment entre le noyau sub-cunéiforme et la limite dorsale du PPN. Plus récemment, des enregistrements ont mis en évidence des neurones au sein du PPN s'activant différemment en fonction des tâches: mobilisation passive du membre supérieur ou marche imaginaire (Tattersall et al., 2014). Cela suggère la mise en jeu de circuits différents activant soit l'intégration sensorielle et proprioceptive (tâche de mobilisation passive), soit l'initiation de la locomotion (marche imaginaire).

De façon similaire, les analyses électrophysiologiques réalisées chez les patients implantés dans notre centre sont en faveur d'une implication du PPN dans la locomotion allant au-delà du simple générateur de pattern de marche (Lau et al., 2015). En effet, lors des enregistrements du PPN au bloc opératoire, des neurones différents vont s'activer lors de la marche imaginaire, pendant la mobilisation active du membre supérieur, ou lors de la stimulation visuelle (figure 11). Il apparait donc que la majorité des neurones au sein du PPN répondent à plusieurs événements distincts de la tâche confirmant le rôle intégrateur de cette région.

Figure 11: Localisation des neurones du PPN activés
au cours des différentes tâches (visuelle, marche imaginaire, motrice)
*d'après Lau et al (2015)*

*Visuelle* *Marche imaginaire* *Motricité*

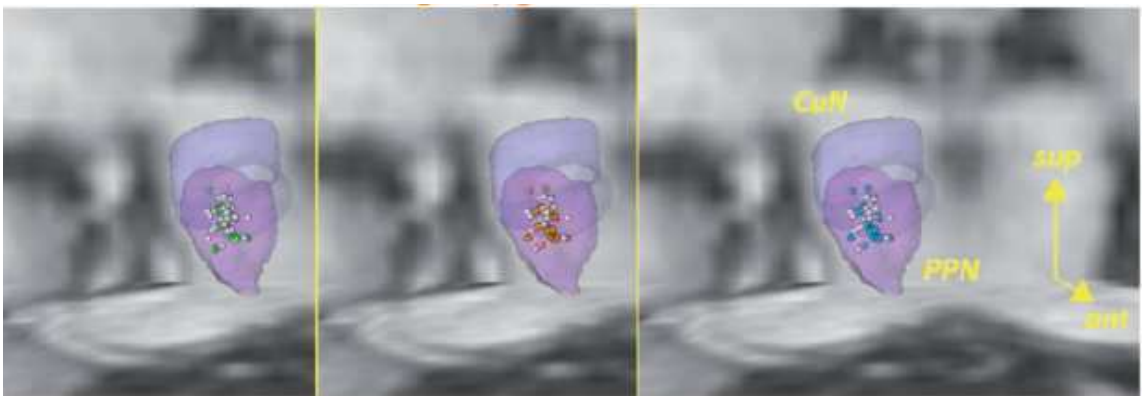

## D. Rôle du PPN dans les troubles du sommeil à l'état parkinsonien

Chez les patients parkinsoniens, les troubles du sommeil sont présents dans plus de 75% des cas, et sont plus fréquents chez les patients ayant une atteinte sévère (Lees et al., 1988). Ils associent principalement une somnolence diurne excessive (voire des attaques de sommeil), une diminution du temps et de l'efficacité du sommeil, un nombre accru de réveils nocturnes, et des parasomnies dont les troubles du comportement pendant le sommeil paradoxal (RBD) (Gagnon et al., 2002; Hobson et al., 2002; Rye, 2006; Wailke et al., 2011; Yong et al., 2011). Leur origine est multifactorielle, mais inclus en grande partie une dégénérescence des centres régulateurs du sommeil. En particulier, comme nous l'avons détaillé précédemment, de nombreuses données de la littérature convergent vers un rôle clé des neurones cholinergiques du PPN dans la régulation du sommeil paradoxal et de l'éveil.

De plus, les études cliniques récentes chez les patients parkinsoniens implantés dans le PPN montrent une amélioration nette des troubles du sommeil et de la vigilance diurne avec une stimulation à basse fréquence (Arnulf et al., 2010; Peppe et al., 2012). Cet effet prédomine sur l'architecture du sommeil et sur le sommeil paradoxal. Il est spécifique de la stimulation du PPN, et n'est pas reproduit avec la stimulation du NST. Par ailleurs, l'évaluation en journée a montré chez un patient qu'un arrêt brutal de la stimulation à basse fréquence était systématiquement suivi d'un très bref épisode de sommeil paradoxal (Arnulf et al., 2010). Au contraire, la stimulation à haute fréquence du PPN induit une phase de sommeil lent chez les patients (Arnulf et al., 2010) et semble majorer la somnolence diurne (Nosko et al., 2014).

Dans notre centre, l'étude du sommeil des patients parkinsoniens implantés dans le PPN a montré aussi un effet sur le sommeil paradoxal, en particulier chez un patient. La stimulation à basse fréquence du PPN entraîne chez ce patient une augmentation significative du temps passé en sommeil paradoxal en comparaison avec la condition OFF stimulation (passant de 0% en OFF à 49% ON stimulation). De plus, ceci correspond au double du temps de sommeil paradoxal habituel chez un sujet contrôle (Floyd et al., 2007). Ce phénomène de sommeil paradoxal supra-normal a été décrit transitoirement après privation de sommeil (Hornung et al., 2006), mais n'a encore jamais été rapporté chez les patients parkinsoniens. Nous pouvons faire l'hypothèse que la stimulation à basse fréquence du PPN active les

axones cholinergiques de projection vers le locus subcoeruleus permettant de déclencher du sommeil paradoxal. Par ailleurs, il est intéressant de noter qu'il s'agit aussi du patient ayant le meilleur effet sur les symptômes moteurs y compris la marche et la posture (Welter et al., 2015), supposant des mécanismes physiopathologiques communs.

Figure 12: Evolution du temps de sommeil paradoxal selon les conditions de stimulation après SCP du PPN chez un même patient *d'après Welter et al* (2015)

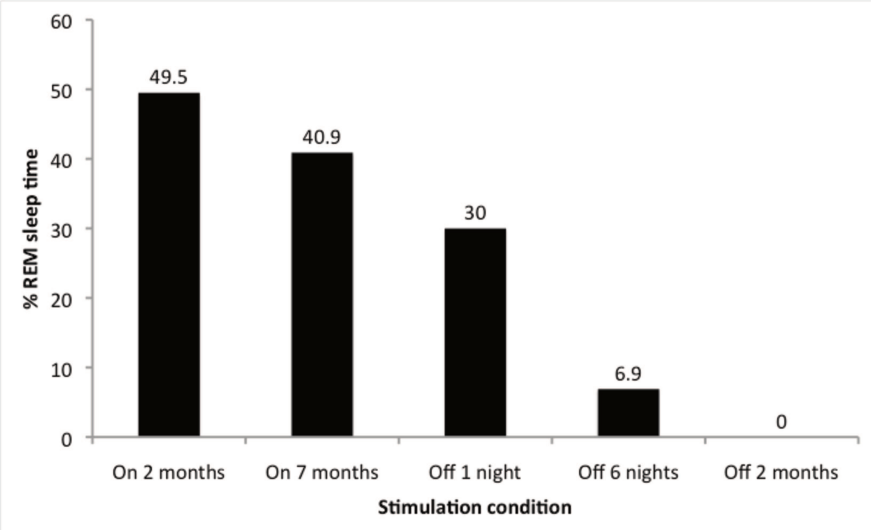

Figure 13: Evolution du score moteur et du freezing
chez un même patient (triangle noir) après SCP du PPN
*d'après Welter et al (2015)*

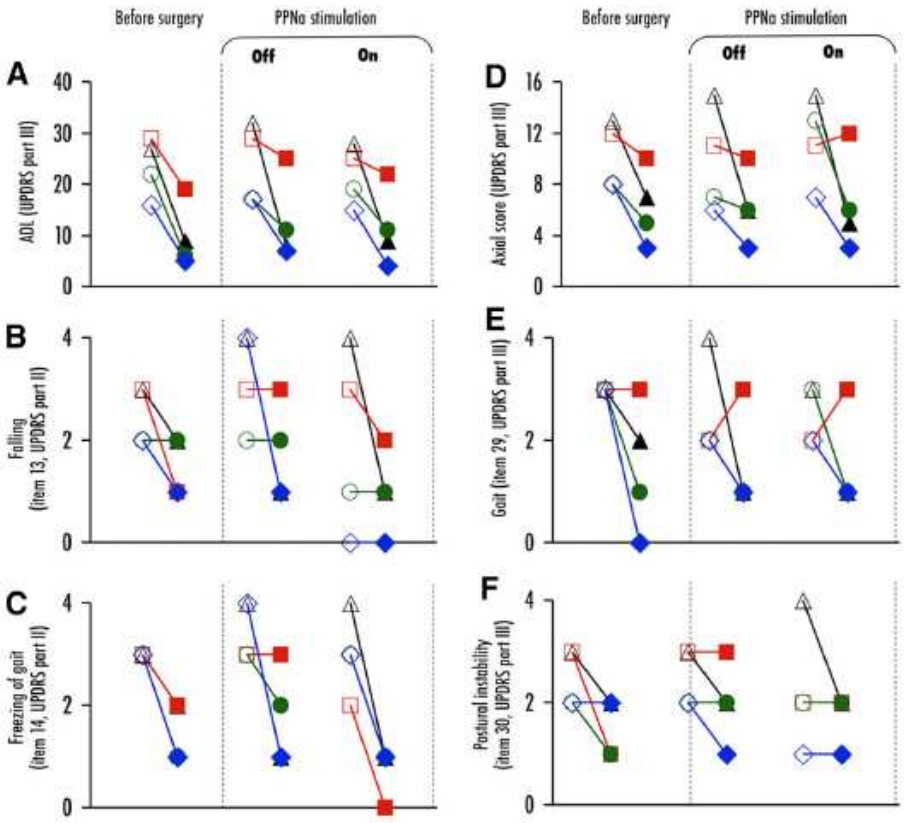

# *OBJECTIFS DE L'APPROCHE COMPORTE-MENTALE*

Nous avons précédemment montré dans l'équipe l'implication des neurones cholinergiques du PPN dans la survenue des troubles de la marche et de la posture en utilisant un modèle primate de maladie de Parkinson à un stade avancé. En utilisant ce même modèle, nous avons cherché à montrer l'implication des neurones cholinergiques dans la genèse des troubles du sommeil à l'état parkinsonien.

L'objectif principal de notre étude a été d'analyser les troubles du sommeil développés chez le singe rendu parkinsonien, puis l'effet des traitements dopaminergiques, et enfin l'effet que provoquerait une lésion cholinergique du PPN surajoutée.

L'objectif secondaire de ce travail a été d'analyser l'effet de l'administration de la mélatonine sur les troubles du sommeil induits chez le singe à l'état parkinsonien.

Les résultats de ce travail ont fait l'objet de deux publications (Belaid et al., 2014; Belaid et al., 2015), et sont résumés ici.

# *SYNTHÈSE DES RÉSULTATS OBTENUS*

## A. INTRODUCTION

L'origine des troubles du sommeil des patients parkinsoniens est probablement multifactorielle, impliquant à la fois la maladie elle-même, mais aussi des lésions non-dopaminergiques des centres régulateurs du sommeil, et enfin les effets des traitements dopaminergiques et agonistes dopaminergiques (Arnulf et al., 2002). Les conséquences des traitements DA sur le sommeil et la vigilance chez les patients parkinsoniens sont en effet variables et parfois opposées en fonction de la sévérité de la bradykinésie nocturne, de l'horaire de prise et de la nature de la molécule (levodopa vs agonistes DA). Ainsi les agonistes DA pris au cours de la journée peuvent induire une somnolence importante voire des attaques de sommeil, avec un effet majoré en fonction du dosage (Hobson et al., 2002; Arnulf, 2005), alors que la L-dopa va avoir un effet opposé (Bliwise et al., 2012). Chez le singe rendu parkinsonien, un agoniste sélectif D1 peut améliorer le sommeil paradoxal et la somnolence diurne excessive, alors qu'un agoniste D2 n'aura aucun effet (Hyacinthe et al., 2014). De plus, des lésions non dopaminergiques entrainent une dégénérescence des centres impliqués dans la régulation veille-sommeil et du sommeil paradoxal, principalement le locus coeruleus et les neurones cholinergiques du PPN (Hirsch et al., 1987; Jellinger, 1988). Dans cette hypothèse, des études ont montré une amélioration des troubles du sommeil par SCP chez les patients parkinsoniens implantés dans le PPN pour traiter les troubles de la marche dopa-résistants (Arnulf et al., 2010; Peppe et al., 2012). Ces résultats soulèvent la question du rôle de la dégénérescence des neurones cholinergiques dans la genèse des troubles du sommeil du patient parkinsonien. Les données de la littérature à partir des modèles animaux sont insuffisantes, et aucune étude n'a analysé l'effet spécifique d'une lésion cholinergique du PPN sur les troubles du sommeil dans un modèle de MP. Le modèle primate intoxiqué au MPTP a déjà été utilisé pour explorer les troubles du sommeil dans le cadre de la MP (Barraud et al., 2009), et par ailleurs un modèle primate de MP avancé associant des lésions DA et des lésions cholinergiques du PPN a été développé dans notre équipe (Grabli et al., 2013). En utilisant ce modèle, notre objectif est ainsi d'analyser les troubles du sommeil induits chez le singe MPTP, puis l'effet des traitements dopaminergiques, et enfin l'effet

d'une lésion cholinergique du PPN surajoutée.

Parallèlement, nous avons étudié l'effet de la mélatonine administrée en association avec le traitement dopaminergique sur les troubles du sommeil. En effet la mélatonine, synthétisée principalement par la glande pinéale, est connue pour jouer un rôle clé dans la régulation du rythme circadien veille-sommeil. L'administration de mélatonine chez l'homme peut modifier le cycle circadien (Zhdanova et al., 1997; Arendt et Skene, 2005), et améliorer la qualité du sommeil dans diverses pathologies chroniques (Campos et al., 2004; Pandi-Perumal et al., 2005). Chez les patients parkinsoniens, la sécrétion de mélatonine est diminuée (Breen et al., 2014; Videnovic et al., 2014), de même que l'expression des récepteurs de la mélatonine dans la SN (Adi et al., 2010). La supplémentation en mélatonine chez ces patients permet d'améliorer l'efficacité du sommeil ainsi que la qualité du sommeil (Dowling et al., 2005), bien qu'il n'y ait pas toujours de modification polysomnographique (Medeiros et al., 2007). De plus certaines études de modèles animaux ont montré un effet de la mélatonine dans la prévention de la mort des neurones dopaminergiques (Absi et al., 2000; Dabbeni-Sala et al., 2001) bien que cet effet ne soit pas toujours retrouvé (Morgan et Nelson, 2001; van der Schyf et al., 2000). L'objectif de cette étude est donc aussi d'étudier l'effet de la mélatonine associée au traitement dopaminergique sur les troubles du sommeil chez ce même modèle primate de MP, comparativement au traitement dopaminergique seul (résumé du protocole expérimental figure 15).

## B. MÉTHODOLOGIE

### 1. Enregistrement polysomnographique

L'étude a été réalisée chez 4 macaques hébergés selon les conditions standards (12 h cycle lumière/obscurité, extinction des lumières à 20h). Des enregistrements polysomnographiques sur des périodes de 24h ont été obtenus grâce à un transmetteur par radio-télémétrie qui permet de mesurer les signaux d'électroencéphalographie (EEG), d'électro-oculographie (EOG) et d'électromyographie (EMG). Nous avons obtenu des enregistrements à l'état contrôle, à l'état parkinsonien, pendant le traitement dopaminergique, avec traitement dopaminergique associé à la mélatonine, et enfin après lésion du PPN. Des

hypnogrammes permettent l'identification de l'éveil actif et avec ondes alpha, du sommeil léger (stades 1 et 2), du sommeil profond (stades 3 et 4) et du sommeil paradoxal. Différents paramètres ont ensuite été calculés pour chaque période nocturne de 12h: le temps de sommeil total (TST), la durée de chaque stade, le temps d'éveil après endormissement (WASO), l'efficacité du sommeil, et la latence de survenue du sommeil paradoxal (temps entre l'endormissement et le premier stade de sommeil paradoxal). De plus, des enregistrements vidéo étaient effectués simultanément aux enregistrements polysomnographiques.

## 2. Lésions dopaminergique et cholinergique

Une administration progressive de MPTP (0.2 à 0.4 mg/kg en IM) a été réalisée jusqu'à l'apparition de l'ensemble des symptômes parkinsoniens. La sévérité des symptômes a été évaluée par une échelle motrice (Herrero et al., 1993) et l'activité spontanée a été quantifiée en utilisant un système digitalisé automatique de mesure d'activité (VigiePrimates, Viewpoint). Après évaluation du sommeil à l'état parkinsonien, avec traitement dopaminergique seul puis associant la mélatonine, des lésions stéréotaxiques du PPN ont été réalisées par injection de toxine afin de léser spécifiquement les neurones cholinergiques (Clark et al., 2007) (figure 14). Les injections ont été unilatérales chez 2 singes et bilatérale chez un 3ème animal.

Figure 14: Injection stéréotaxique de toxine dans le PPN chez un singe

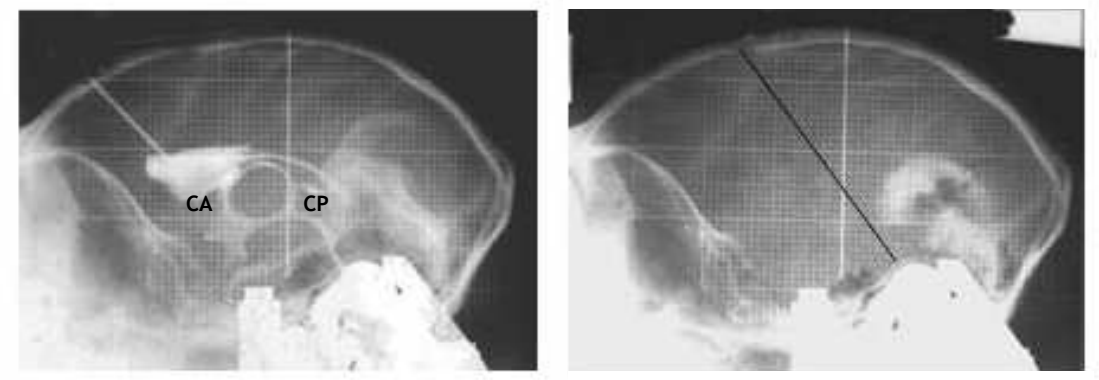

### 3. Traitement dopaminergique et administration de mélatonine

La L-dopa (Modopar Dispersible, 20 mg/kg) a été administrée oralement 2 fois par jour pendant une période de 8 à 12 jours. L'enregistrement polysomnographique a été démarré après avoir obtenu un effet optimal et stable. L'administration de mélatonine (10 µg/kg) associée à la L-dopa a été effectuée durant 5 jours consécutifs (2h avant l'extinction des lumières). L'enregistrement polysomnographique n'a été réalisé qu'après cette période.

Un test de Kruskal–Wallis puis de Mann–Whitney U a été appliqué pour la comparaison des paramètres du sommeil enregistrés dans chaque condition expérimentale.

Figure 15: Protocole expérimental d'étude du sommeil chez un même singe
*(nombre de sessions à l'état contrôle, après injection de MPTP, avec L-dopa /mélatonine et après lésion du PPN)*

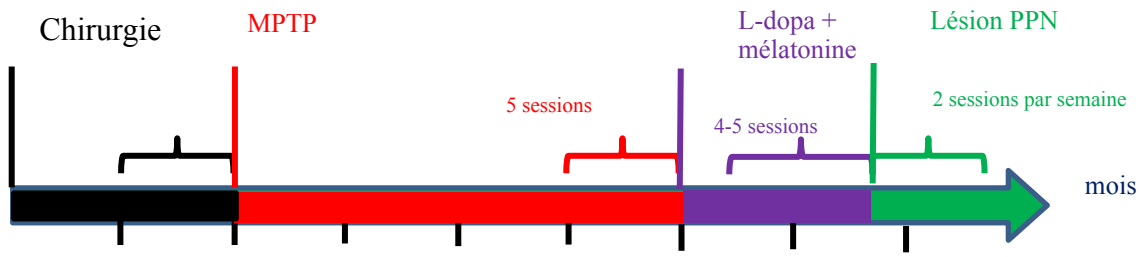

### 4. Immunohistochimie et analyse des données

Après euthanasie, prélèvement et coupe des cerveaux, un immunomarquage à la tyrosine hydroxylase (TH) a été réalisé sur une série de coupes au niveau de la SN et un marquage à la nicotinamide adénine dinucléotide phosphate diaphorase (NADPH) a été réalisé sur une autre série de coupe au niveau du PPN. La quantification des neurones TH positifs, NADPH positifs a été réalisée par stéréologie semi-automatique Ces données ont ensuite été comparées à celles de 5 macaques contrôles précédemment analysées selon la même technique (Karachi et al., 2010; Grabli et al., 2013). Nous avons obtenu une perte de 85% de corps cellulaires TH+ dans la SNc après intoxication des animaux par le MPTP ($p<0.001$ test de Mann-Whitney).

## C. Résultats après lésions dopaminergiques et du PPN

### 1. Cycle veille-sommeil à l'état contrôle puis parkinsonien

Le temps de sommeil des macaques à l'état basal était en moyenne de 42% sur 24h. Le sommeil paradoxal représentait 21.9% et le sommeil lent 23.8% du temps de sommeil total.

La première injection de MPTP a provoqué une réduction majeure du sommeil paradoxal, une diminution du sommeil lent, et une fragmentation du sommeil. Après stabilisation du syndrome parkinsonien, de nombreux épisodes de somnolence diurne sont apparus, avec une diminution de l'efficacité du sommeil et une augmentation du nombre de réveils nocturnes.

## 2. Cycle veille-sommeil après administration de L-dopa/mélatonine

L'administration de L-dopa seule a partiellement amélioré les symptômes parkinsoniens ainsi que l'ensemble des troubles du sommeil (figure 16).

L'administration de la mélatonine associée à la L-dopa durant 5 jours a eu un effet globalement bénéfique sur de nombreux paramètres du sommeil par rapport à la L-dopa seule. On a noté en particulier une réduction significative du temps d'éveil nocturne et de la latence d'endormissement et tendance à une amélioration du TST et de l'efficacité du sommeil. Cependant, aucun effet n'a été noté sur la somnolence diurne ou sur l'architecture du sommeil comparé à la L-dopa seule.

Figure 16: Modification du sommeil à l'état parkinsonien
et après administration de L-dopa

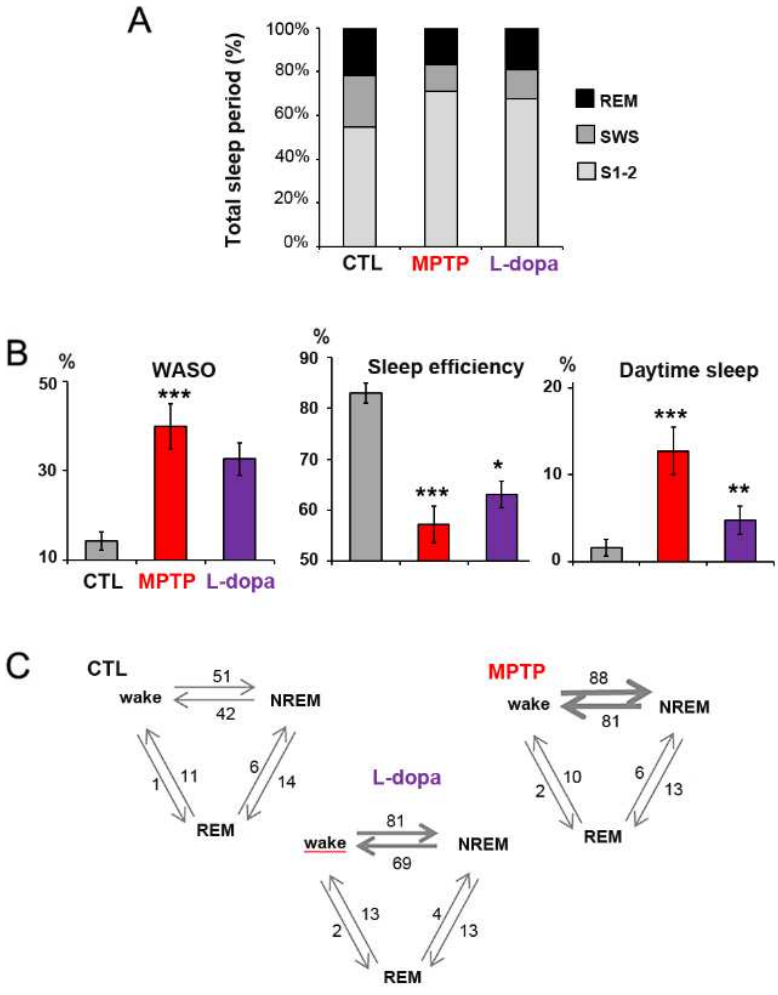

## 3. Cycle veille-sommeil après lésion cholinergique du PPN

Une lésion des neurones cholinergiques du PPN chez les 3 singes a provoqué une fragmentation du sommeil avec une augmentation du nombre de réveils nocturnes, une diminution de l'efficacité du sommeil, du sommeil lent et du sommeil paradoxal par rapport à l'état parkinsonien. Ces troubles du sommeil se sont améliorés progressivement environ 1 à 3 semaines après la lésion, parallèlement à la récupération des symptômes posturaux et de la marche, pour revenir à l'état antérieur à la lésion du PPN. Une discrète amélioration de l'efficacité du sommeil et une diminution des réveils nocturnes a même été constatée 3 semaines après la lésion (figure 17).

Figure 17: Résumé des hypnogrammes pour chaque condition expérimentale chez un même singe

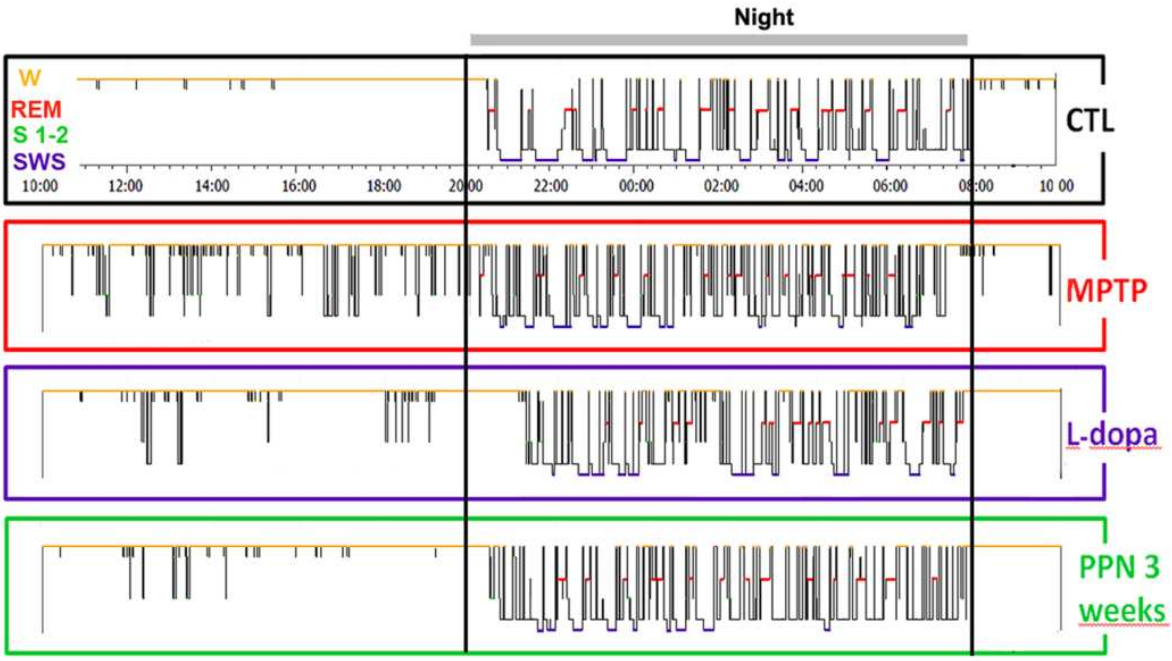

## D. Discussion et Conclusions

L'étude longitudinale du sommeil chez un même singe a permis de mettre en évidence les troubles induits par une lésion dopaminergique et leur amélioration par l'administration de L-dopa et de mélatonine. Une discrète amélioration du sommeil a également été observée à distance d'une lésion cholinergique du PPN surajoutée.

A l'état contrôle, les caractéristiques du sommeil que nous avons enregistré chez les macaques adultes sont similaires à ceux décrits dans la littérature (Hsieh et al., 2008; Barraud et al., 2009) et peu différents de celles décrites chez l'homme. L'état parkinsonien est caractérisé par une diminution de l'efficacité du sommeil, avec une réduction majeure du sommeil lent et du sommeil paradoxal, et une majoration de l'insomnie et du nombre de réveils nocturnes, confirmant les données de la littérature chez les singes intoxiqués au MPTP (Almirall et al., 1999; Barraud et al., 2009; Hyacinthe et al., 2014) et chez les patients parkinsoniens à un stade avancé de la maladie (Wailke et al., 2011; Yong et al., 2011). Ces données suggèrent qu'une atteinte dopaminergique pure entraine une altération du sommeil, et que le système dopaminergique est directement impliqué dans la régulation du cycle veille-sommeil et du sommeil paradoxal. Par ailleurs, nos résultats montrent que les singes parkinsoniens développent une somnolence diurne excessive (Rye, 2010), dont l'importance est corrélée à la sévérité des symptômes parkinsoniens. Les troubles du sommeil précédant souvent les symptômes moteurs de la maladie (Abbott et al., 2005), la somnolence diurne pourrait ainsi être un marqueur précoce du déficit dopaminergique (Arnulf et al., 2002).

L'administration de L-dopa améliore les symptômes moteurs, diminue les réveils nocturnes, et a un effet positif sur l'architecture du sommeil. Une réduction de la bradykinésie au cours des réveils nocturnes a également été rapportée chez les patients parkinsoniens sous traitement dopaminergique, mais sans impact sur l'altération de l'architecture du sommeil, (Wailke et al., 2011). Le fait que les macaques utilisés soient jeunes, avec une durée de traitement dopaminergique courte, et sans atteinte des autres systèmes impliqués dans le sommeil après injections de MPTP, pourrait expliquer ces différences.

Par ailleurs nous avons montré que l'association de la mélatonine avec la L-dopa avait un meilleur effet sur les troubles du sommeil que l'administration de L-dopa seule. Ces

résultats sont en accord avec les données chez les patients parkinsoniens montrant une amélioration de la qualité et du temps de sommeil avec une prise de mélatonine au coucher (Dowling et al., 2005). De même, un bénéfice a été rapporté pour les patients souffrant de RBD (Kunz et Bes, 1997; Takeuchi et al., 2001). La mélatonine jouant un rôle de promoteur de sommeil, nous avons effectivement observé un endormissement plus rapide chez nos animaux parkinsoniens, comme rapporté chez les singes à l'état contrôle (Zhdanova et al., 2002), et chez l'homme (Stone et al., 2000). L'absence d'effet de la mélatonine sur l'architecture du sommeil chez nos singes parkinsoniens, contrairement à ce qui est décrit chez les patients parkinsoniens (Medeiros et al., 2007), pourrait être due à un traitement de trop courte durée.

Une lésion cholinergique surajoutée du PPN chez les singes intoxiqués par le MPTP a induit des troubles du sommeil aigus et transitoires, ainsi qu'une activité oscillatoire pendant la période d'éveil similaire à celle rapportée après lésion de la formation réticulée chez le chat (Denoyer et al., 1991) ou après administration d'un agent anticholinergique (Longo, 1956). Les troubles du sommeil induits se sont ensuite progressivement améliorés avec un retour aux valeurs antérieures à la lésion du PPN, impliquant l'existence de processus de compensation qui restent peu connus. Les neurones cholinergiques résiduels du PPN ou du noyau segmental latéro-dorsal adjacent jouent probablement un rôle dans ces processus de compensation. Les systèmes noradrénergique du locus coeruleus et sérotoninergique du raphé, qui participent également à la régulation du sommeil, pourraient contribuer à la normalisation des symptômes.

Enfin, un des principaux résultats obtenus est l'amélioration de la qualité du sommeil des singes parkinsoniens 3 semaines après la lésion du PPN. L'hypothèse avancée serait que la lésion du PPN induise une réduction des projections excitatrices vers le NST, qui est hyperactif dans la MP. Une réversion de l'hyperactivité du NST chez le rat 6-OHDA après lésion du PPN a en effet déjà été mise en évidence (Breit et al., 2006).

Les résultats cliniques chez les patients implantés dans le PPN ont montré qu'une stimulation à haute fréquence induisait un état de sommeil profond, alors qu'une stimulation à basse fréquence améliorait l'éveil avec un effet bénéfique sur la qualité du sommeil (Arnulf et al., 2010; Peppe et al., 2012). Bien que la comparaison soit difficile, nos résultats suggèrent

néanmoins que l'effet obtenu chez les patients parkinsoniens implantés dans le PPN résulterait de la stimulation à la fois des neurones cholinergiques et non cholinergiques. Des études expérimentales supplémentaires restent nécessaires afin de déterminer l'ensemble des circuits neuronaux responsables des troubles du sommeil chez les patients parkinsoniens.

**En conclusion,** l'association de lésions dopaminergiques et cholinergiques du PPN chez le singe a permis de caractériser les troubles du sommeil dans un modèle primate de MP avancée. Cette approche a montré l'amélioration du sommeil après traitement par L-dopa et par la mélatonine, et l'implication du PPN cholinergique dans la régulation du cycle veille-sommeil.

Neurobiology of Disease

# Sleep Disorders in Parkinsonian Macaques: Effects of L-Dopa Treatment and Pedunculopontine Nucleus Lesion

**Hayat Belaid,[1] Joëlle Adrien,[1] Elodie Laffrat,[1] Dominique Tandé,[1] Carine Karachi,[1] David Grabli,[1] Isabelle Arnulf,[2] Stewart D. Clark,[3] Xavier Drouot,[4] Etienne C. Hirsch,[1] and Chantal François[1]**

[1]Institut National de la Santé et de la Recherche Médicale Unité Mixte de Recherche-S975, Université Pierre et Marie Curie Paris 06, Unité Mixte de Recherche-S975, CNRS Unité Mixte de Recherche 7225, and Centre de Recherche-Institut du Cerveau et de la Moelle, Groupe Hospitalier Pitié-Salpêtrière, 75013 Paris, France, [2]Service des pathologies du sommeil, Assistance Publique-Hôpitaux de Paris, Groupe Pitié-Salpêtrière, 75013 Paris, France, [3]Department of Pharmacology and Toxicology, University at Buffalo, Buffalo, New York 14214, and [4]Physiology Department, CHU de Poitiers, 8600 Poitiers, France

**Patients with Parkinson's disease (PD) display significant sleep disturbances and daytime sleepiness. Dopaminergic treatment dramatically improves PD motor symptoms, but its action on sleep remains controversial, suggesting a causal role of nondopaminergic lesions in these symptoms. Because the pedunculopontine nucleus (PPN) regulates sleep and arousal, and in view of the loss of its cholinergic neurons in PD, the PPN could be involved in these sleep disorders. The aims of this study were as follows: (1) to characterize sleep disorders in a monkey model of PD; (2) to investigate whether L-dopa treatment alleviates sleep disorders; and (3) to determine whether a cholinergic PPN lesion would add specific sleep alterations. To this end, long-term continuous electroencephalographic monitoring of vigilance states was performed in macaques, using an implanted miniaturized telemetry device. 1-Methyl-4-phenyl-1,2,3,6-tetrahydropyridine treatment induced sleep disorders that comprised sleep episodes during daytime and sleep fragmentation and a reduction of sleep efficiency at nighttime. It also induced a reduction in time spent in rapid eye movement (REM) sleep and slow-wave sleep and an increase in muscle tone during REM and non-REM sleep episodes and in the number of awakenings and movements. L-Dopa treatment resulted in a partial but significant improvement of almost all sleep parameters. PPN lesion induced a transient decrease in REM sleep and in slow-wave sleep followed by a slight improvement of sleep quality. Our data demonstrate the efficacy of L-dopa treatment in improving sleep disorders in parkinsonian monkeys, and that adding a cholinergic PPN lesion improves sleep quality after transient sleep impairment.**

*Key words:* **cholinergic neurons; L-dopa; macaques; Parkinson's disease; pedunculopontine nucleus; sleep disorders**

## Introduction

Patients with Parkinson's disease (PD) experience a range of symptoms, including significant sleep disturbances, with excessive daytime sleepiness and "sleep attacks," insomnia, reduced total sleep time and sleep efficiency, rapid eye movement (REM) sleep behavior disorder, and a marked increase in the number of nocturnal awakenings compared with healthy controls (Gagnon et al., 2002; Hobson et al., 2002; Rye, 2006; Wailke et al., 2011; Yong et al., 2011). Whether sleep disorders are generated by the disease itself, dopaminergic (DA) treatment, or non-DA lesions is incompletely known (Arnulf et al., 2002). The effects of DA drugs on sleep and alertness in PD patients are variable and sometimes opposite, depending on the level of nocturnal bradykinesia, the time of intake, and the nature of the drug (i.e., levodopa vs DA agonist). DA agonists taken during daytime may cause severe sleepiness and sleep attacks (Arnulf, 2005, Hobson et al., 2002), with sleepiness increased by increasing dosage, whereas L-dopa has the opposite effect (Bliwise et al., 2012). In parkinsonian macaques, selective D1 receptor agonist was recently reported to improve REM sleep and excessive daytime sleepiness, whereas D2 receptor agonist revealed no effect (Hyacinthe et al., 2014).

Degenerative changes in PD also affect non-DA structures involved in the regulation of arousal and REM sleep, such as the noradrenergic locus ceruleus system and the cholinergic pedunculopontine nucleus (PPN) system, known to degenerate in advanced PD (Hirsch et al., 1987; Jellinger, 1988). Recently, changes in sleep quality were reported in patients with PD with severe gait disorders, who had been implanted with electrodes for deep brain stimulation applied to the PPN (Arnulf et al., 2010; Peppe et al., 2012), thus raising the question of a role of PPN neuronal loss in the sleep abnormalities associated with PD. However, data in the literature on animal models are not conclusive, and no study has evaluated the effect of a specific cholinergic PPN lesion on sleep disorders observed in parkinsonian models. The development of animal models, such as the monkey rendered parkinsonian with 1-methyl-4-phenyl-1,2,3,6-tetrahydropyridine (MPTP), is a key element to understanding the pathophysiology of sleep disorders in patients with PD. The relevance of MPTP-treated macaques for exploring the sleep deficits that occur in PD has already been

Received Jan. 15, 2014; revised May 23, 2014; accepted May 29, 2014.

Author contributions: C.F. designed research; H.B., E.L., D.T., C.K., I.A., X.D., and C.F. performed research; S.D.C. and C.F. contributed unpublished reagents/analytic tools; H.B., J.A., and C.F. analyzed data; H.B., J.A., C.K., D.G., I.A., E.C.H., and C.F. wrote the paper.

This work was supported by "Laboratoires Servier" from the program "Investissements d'avenir" (ANR-10-IAIHU-06) and National Institutes of Health Grant R00DA024754. We thank Nick Barton for language editing.

The authors declare no competing financial interests.

Correspondence should be addressed to Dr. Chantal François, Centre de Recherche-Institut du Cerveau et de la Moelle, Unité Mixte de Recherche-S975, Hôpital de la Salpêtrière, 47 bd de l'Hôpital, 75013, Paris, France. E-mail: chantal.francois@upmc.fr.

DOI:10.1523/JNEUROSCI.0181-14.2014

 0270-6474/14/349124-10$15.00/0

**Table 1. Summary of the effect of MPTP intoxication and of subsequent L-dopa treatment on sleep parameters[a]**

| Treatment | TST min | Sleep efficiency | Night TST (100%) | | | WASO (%) | Wake (%) | Sleep onset to REM (min) | Daytime sleep (%) |
|---|---|---|---|---|---|---|---|---|---|
| | | | Stage 1–2 | SWS | REM | | | | |
| Control mean | 595.8 | 83.0 | 54.5 | 23.8 | 22.0 | 14.2 | 17.0 | 49.6 | 1.6 |
| SEM | 7.0 | 2.0 | 4.0 | 3.0 | 1.0 | 2.0 | 1.5 | 10.0 | 1.0 |
| MPTP mean | 410.5*** | 57.1*** | 67.4** | 12.5*** | 17.3*** | 40.0*** | 42.9*** | 101.5* | 12.8*** |
| SEM | 25.0 | 3.6 | 3.2 | 2.8 | 1.7 | 4.9 | 3.8 | 10.1 | 2.7 |
| L-Dopa mean | 452.9* | 63.1* | 64.9 | 13.2 | 19.1* | 32.4 | 37.0* | 98.8 | 5.8** |
| SEM | 18.1 | 2.6 | 4.1 | 3.4 | 1.3 | 3.7 | 2.6 | 10.8 | 1.6 |
| PPN 3w mean | 489.4 | 69.3 | 66.2 | 14.2 | 18.2 | 35.8 | 30.7 | 127.0 | 4.7 |
| SEM | 36 | 6.5 | 4.4 | 2.2 | 3.5 | 14.9 | 6.5 | 15.1 | 1.6 |

[a]Mean values of sleep parameters were calculated in 4 macaques in the control state, after MPTP intoxication, and then after L-dopa treatment, in 3 macaques 3 weeks (3w) after a unilateral PPN lesion and in one of these macaques after a second PPN lesion in the other hemisphere. MPTP values were compared with control values, and L-dopa values with MPTP values. Level of significance was given only in the case of statistical significance for each individual.
*$p < 0.05$; **$p < 0.01$; ***$p < 0.001$: Kruskal–Wallis test followed by Mann–Whitney *U* test in the event of statistically significant differences.

demonstrated (Barraud et al., 2009). Moreover, we reported that the combination of DA and PPN lesions in monkeys enabled us to reproduce a close model of advanced PD (Grabli et al., 2013). Using this approach, our aim was to investigate whether sleep deficits in PD reflect the disease itself or the side effects of DA medications, or other degenerative features, such as cell loss in non-DA structures. For this purpose, we implanted a miniaturized telemetry device to perform long-term continuous electroencephalographic monitoring of vigilance states in unrestrained macaques at baseline (control state), after MPTP intoxication, with L-dopa treatment, and then after cholinergic PPN lesion.

## Materials and Methods

*Animals.* The study was performed on 4 adult male macaque monkeys (*Macaca fascicularis*) and was performed in strict accordance with the European Union Directive of 2010 (Council Directive 2010/63/EU) for the care and use of laboratory animals. The authorization for conducting our experiments was approved by the Committee on the Ethics of Animal Experiments (agreement Ce5/2012/049). The animals were kept under standard conditions (12 h light/dark cycle [light off at 20:00 h], 23°C, and 50% humidity). Monkeys weighed 4–6 kg and were 3–5 years of age.

*Apparatus.* Macaques were chronically implanted with a radio-telemeter transmitter for continuous and long-term recording. The transmitter implant consisted of a sterile, disk-shaped, three-channel biopotential device (D70-EEE, Data Sciences International) for measuring electroencephalography (EEG), electro-oculography (EOG), and electromyography (EMG) signals. Extending from the transmitter body were flexible leads consisting of one ground lead and 3 channels. Biopotential signals were transmitted to two receivers mounted on the primate cage and then forwarded to a data exchange matrix serving as a multiplexer and connected through a ribbon cable to a computer for data recording and storage.

*Transmitter implantation.* After premedication with 0.05 ml/kg Robinul and 10 mg/kg ketamine given intramuscularly, animals were intubated and anesthetized with isoflurane (1%–2%). Analgesia was provided on the day of surgery by a single intramuscular injection of 2 mg/kg Tolfedine (tolfenamic acid, 4%). The transmitter was implanted within the abdominal muscle layers. The electrode biopotential leads were tunneled subcutaneously to the skull. Two EEG electrodes were screwed unilaterally into the skull 10 mm lateral to the midline: one above the frontal cortex and the other 30 mm more posterior (EEG channel). Two electrodes for EOG were affixed at the level of the orbital arch bone unilaterally: one at the top and the other on the external side (EOG channel). The two EMG leads were sutured to the neck musculature. After surgery, animals were returned to their home cage and allowed to recover for 3 weeks. Buprenorphine (Buprecare, 0.02 mg/kg i.m.) and prophylactic antibiotic cover (Clamoxyl, 20 mg/kg) were provided for 2 weeks postoperatively.

*MPTP intoxication.* All MPTP injections (0.2–0.4 mg/kg, in NaCl 0.9%) were intramuscular and were performed under light anesthesia (ketamine 0.4–0.5 mg/kg). A progressive administration protocol was used, with injections performed at an interval of 3–7 d until the emergence of all parkinsonian symptoms. Intoxication was stopped once all the motor parkinsonian symptoms had appeared.

*Dopaminergic therapy.* For levodopa (L-dopa) testing, doses of levodopa with benserazide at a ratio of 4:1 (Modopar Dispersible, Roche) were given orally. The dosage required to alleviate motor abnormalities in the MPTP-treated monkeys was 20 mg/kg, as already reported in the literature (Bezard et al., 1997), and was given twice per day (at 10:00 h and at 14:00 h), with an effect that lasted for between 3 h 30 min and 4 h after administration. As L-dopa has a long bioavailability at the beginning of the disease, no medication was given after 18:00 h. Our aim was to obtain a long duration benefit of L-dopa after some days of treatment, as that reported in PD patients, who gradually improve on L-dopa therapy. Such an improvement generally requires 9 d to achieve a maximum response (Barbato et al., 1997). Specifically, each animal received L-dopa treatment twice daily for 8–12 d, and the sleep recording was only performed afterward.

*Motor score.* The severity of parkinsonism before, during, and after MPTP intoxication and after L-dopa treatment was evaluated in the home cage using a rating scale. This scale includes 7 items (spontaneous activity, bradykinesia, tremor, freezing, posture, balance deficit, and feeding) (Herrero et al., 1993b), rated between 0 (normal) and 3 (maximal disability), with a total score out of 21. Evaluations were performed by the same observer every 2 d after the first injection of MPTP and until the day the animal was killed. Spontaneous activity was also quantified using an automated activity digitalizing system (VigiePrimates, Viewpoint).

*PPN lesion.* We performed PPN lesions stereotaxically on three MPTP-treated monkeys according to the procedure previously described (Karachi et al., 2010). We used injections of a fusion of diphtheria toxin and the peptide urotensin II (10 $\mu$l, 20%). This fusion toxin was developed to specifically kill cholinergic neurons of the PPN (Clark et al., 2007), which have previously been shown in rodents to express the urotensin II receptor (Clark et al., 2001). Lesions were performed unilaterally in a total of three macaques, and in one of these macaques a second PPN lesion was added in the other hemisphere.

*Sleep data.* For each of the four animals, sleep recordings were performed in the home cage during a 24 h period, always starting at 10:00 h. During this 24 h period, the light was on from 8:00 h to 20:00 h. Two 24 h recording sessions per week were performed over several weeks in each experimental condition: 5 recordings at baseline (i.e., control state, 3 weeks after surgery), one recording at day 1 after the first MPTP injection, 5 recordings after MPTP treatment (2 months after the last MPTP injection), and 4 or 5 recordings during L-dopa therapy (sleep recordings starting 8–12 d after the beginning of L-dopa therapy). Two 24 h recording sessions were also performed in three MPTP-treated animals 1, 2, and 3 weeks after each PPN lesion.

The polysomnographic signals were transmitted to a receiver and then to an acquisition device (Dataquest A.R.T., Data Sciences International). Software (Neuroscore, Data Sciences International) was used for sleep scoring to obtain hypnograms. Sleep–wake stage scoring was performed in 20 s epochs so that the whole epoch was assigned to one stage. The

vigilance stages identified were "active wake," "wake" (with $\alpha$ waves), "light sleep" (Stage 1 and Stage 2 pooled together), "slow-wave sleep" (SWS) (Stage 3 and Stage 4 pooled together) and "rapid eye movement" (REM) sleep. Non-REM sleep (NREM) included sleep Stages 1–4. As unconventional sleep stages, also named dissociate sleep stages (e.g., NREM sleep with rapid eye movements, or REM sleep without atonia) may occur in parkinsonism, sleep recordings were reviewed by clinicians (I.A., X.D.) trained to score PD sleep in humans. Two categories of muscle tone during REM sleep time were distinguished for the 20 s REM epochs: complete atonia and increased muscle tone for >50% of the epoch.

Artifacts, occasionally produced by excessive movements during wakefulness, were excluded from analyses. They represented no more than 2% of total recording time. The following parameters were calculated for each 12-hour period of darkness: total sleep time (TST), duration of each stage, wake time after sleep onset (WASO), sleep efficiency, REM sleep latency (time from nighttime start to REM sleep onset), and daytime sleep. The number of sleep transitions between wake, NREM, and REM stages was also quantified. All macaques were videotaped during the 24 h sleep recordings, video and sleep data being recorded synchronously.

*Immunohistochemistry.* All macaques were deeply anesthetized and intracardially perfused with 4% PFA in PBS. Brains were removed, immersed in 30% sucrose in PBS, and then frozen and cut into 50-$\mu$m-thick sections transversally. Series of regularly interspaced (500 $\mu$m apart) fresh-frozen sections of macaque brains were processed for tyrosine hydroxylase (TH) immunohistochemistry (François et al., 1999). Another series of regularly interspaced (500 $\mu$m apart) sections were processed for NADPH diaphorase histochemistry as previously described (Hirsch et al., 1987).

*Data analysis.* The extent of DA denervation was assessed by counting $TH^+$ neurons on 8 regularly interspaced nigral sections (every 500 $\mu$m) covering the anteroposterior extent of the structure. The sections were matched anatomically in each of the brains while verifying that the cross-sections of the substantia nigra were similar in all individuals. Estimation of the total number of DA neurons was performed using a semiautomatic stereology system with a computer-based system (Mercator, ExploraNova). The number of $TH^+$ neurons in the locus coeruleus and the number of $NADPH^+$, non-$NADPH^+$, and Nissl-stained neurons in both the PPN and the adjacent cuneiform nucleus were also counted using the same method and were expressed as the number of cells per $mm^3$. These data were compared with those obtained from 5 intact macaques (*M. fascicularis*) from previous studies (Karachi et al., 2010; Grabli et al., 2013) and whose brain sections were processed under the same conditions.

*Statistical analysis.* A Mann–Whitney rank-sum test was performed to determine the loss of $TH^+$ neurons between MPTP-treated animals and controls. A Kruskal–Wallis test, followed by a Mann–Whitney *U* test in the event of statistically significant differences, was applied for the comparison of sleep parameters at baseline, after MPTP intoxication, and after L-dopa treatment for each animal. Level of significance was given only in case of statistical significance for each individual. Results with $p \leq 0.05$ were considered significant for all the analyses. Data are presented as mean ± SEM.

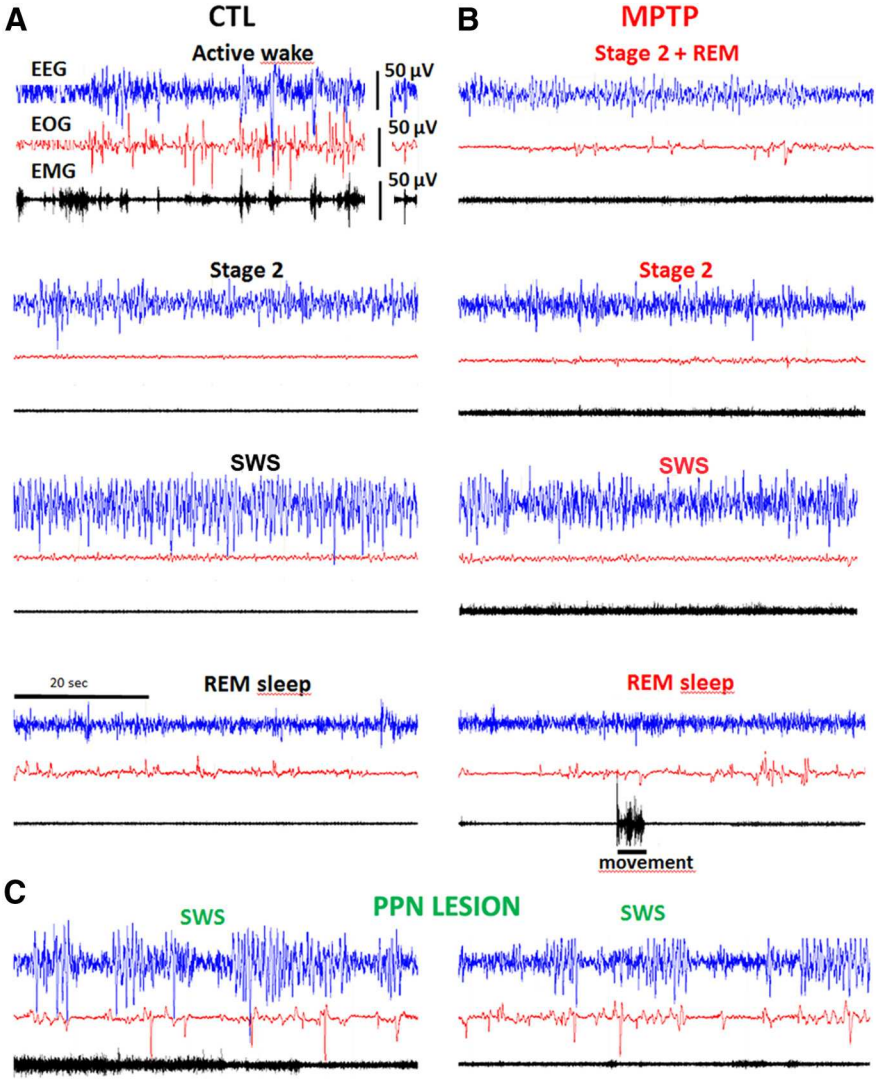


**Figure 1.** Examples of 1 min polysomnographic recordings. ***A***, At baseline (control state, CTL). ***B***, After MPTP intoxication. ***C***, At 1 week after further PPN lesion. Blue represents EEG; red represents EOG; black represents EMG. Note the existence, after MPTP, of eye movements during Stage 2 (top right: Stage 2 + REM), and of movements during Stage 2 and REM sleep, and the occurrence, after PPN lesion, of ample $\delta$ frequencies on EEG and increased muscle tone.

**Table 2. Motor scores obtained after MPTP intoxication ($n = 4$), under L-dopa treatment ($n = 4$), and 3 weeks after PPN lesion ($n = 3$)[a]**

| Monkey ID | MPTP | L-Dopa | PPN lesion |
|---|---|---|---|
| 1 | 10 | 2.5 | — |
| 2L | 13 | 2.5 | NR |
| 3R | 8,5 | 2 | 6,5 |
| 3L | 8,5 | 2 | 6 |
| 4L | 10 | 2 | 7,5 |

[a]The motor score of the most severely disabled macaque (2) was not recorded (NR) after PPN lesion in the left (L) hemisphere because of severe disequilibrium and falls. No PPN lesion was performed for animal 1. R, right.

## Results

### Basal sleep–wake states

Sleep parameters were recorded for 3–4 weeks to assess the baseline sleep/wakefulness patterns and features. Sleep measures are shown in Table 1. During wakefulness, $\alpha$ waves (8–12 Hz), commonly occurring in relaxed wakefulness in humans, were rarely observed (Fig. 1*A*). Sleep spindles of 14–16 Hz and high-amplitude K-complexes were common in Stage 2 NREM sleep. Rapid eye movements were frequently present in the EOG. The EMG activ-

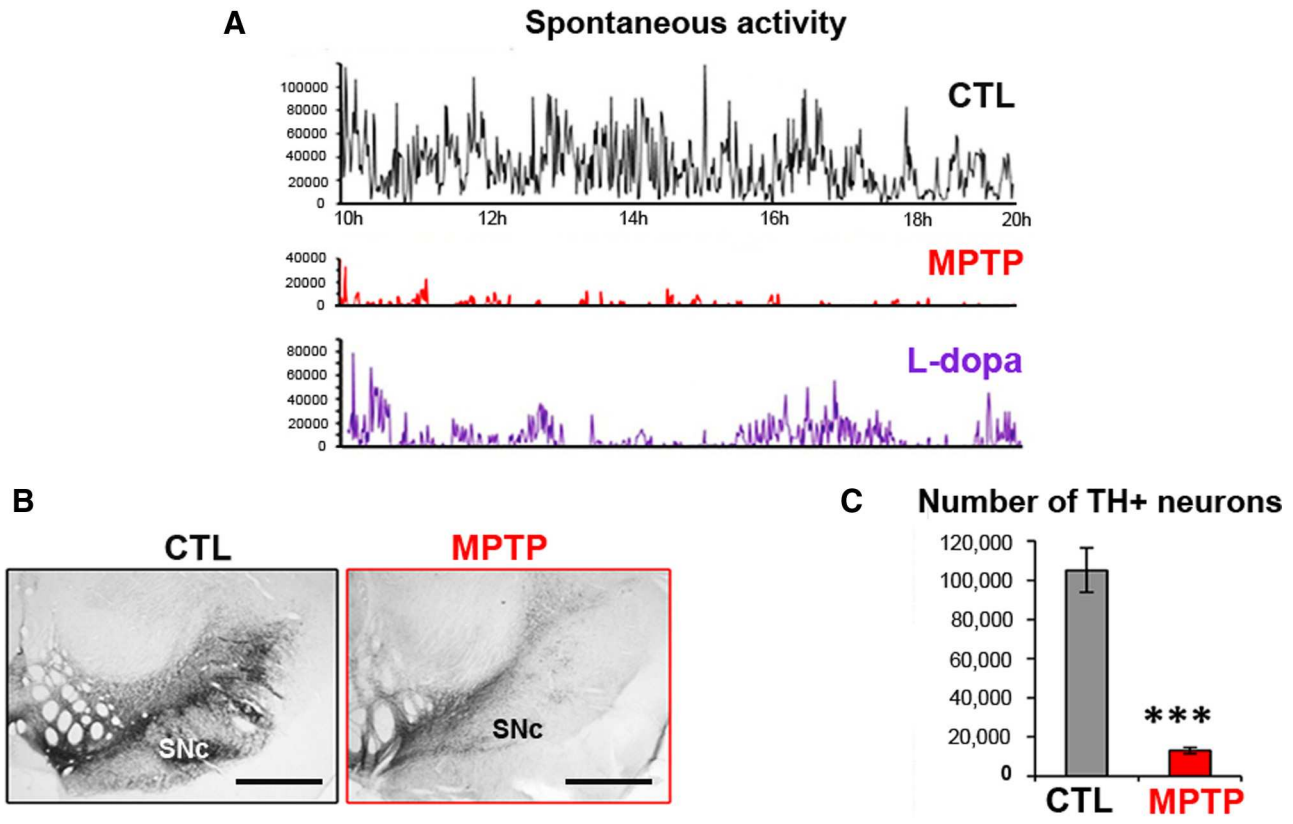


**Figure 2.** Measurement of motor disability and assessment of DA lesion within the mesencephalon of MPTP-treated macaques. ***A***, Examples of 10 h daytime recording of spontaneous activity of MPTP-treated Macaque 3 during the control (CTL) state, after MPTP intoxication, then after L-dopa medication. L-Dopa treatment (bottom graph) was given at 10 h and at 14 h. ***B***, Example of TH immunostaining in the mesencephalon of a control macaque and an MPTP-treated macaque. Scale bar, 2 mm. ***C***, Graphic representation of the number of $TH^+$ neurons in the substantia nigra pars compacta (SNc) in the 4 MPTP-treated macaques and 5 controls. ***$p < 0.001$ (Mann–Whitney rank-sum test).

ity recorded from posterior neck muscles was at its lowest level during REM sleep.

The macaques slept for 42% of the 24 h, mostly during the night. During the dark period, REM sleep occupied 21.9 ± 1.0% of the TST and was more abundant at the end of the night. SWS represented 23.8 ± 3.0% of the TST, was more frequently observed at the beginning of the night, and was more abundant in the 2 young animals (3.5 years) than in the older ones (5 years). A reduced amount of sleep, consisting exclusively of light sleep episodes (Stages 1 and 2), was observed during the daytime (1.6 ± 1.0% of the 12 h).

### Parkinsonian symptoms and DA cell loss

After MPTP intoxication, monkeys progressively developed motor symptoms: hypokinesia (freezing, bradykinesia, and reduction of spontaneous activity), rigidity, tremor, and postural disturbances. After stabilization of symptoms (6 weeks after the last MPTP injection), all the monkeys developed severe parkinsonism and scored between 8 and 13 on a scale of 21 (Table 2). For example, the spontaneous activity of the animals was reduced by ~85% (Fig. 2*A*). L-Dopa treatment partially reversed parkinsonism, with a decrease of the scores on the parkinsonian rating scale and an increase in spontaneous activity in all MPTP-treated monkeys (Fig. 2*A*).

Microscopic examination showed that the number of TH-immunoreactive cell bodies was dramatically reduced in the substantia nigra pars compacta of MPTP-treated macaques (Fig. 2*B*) compared with 5 control animals. Quantitative assessment revealed a statistically significant loss of 85% (105,187 ± 5193 neurons vs 15,512 ± 2995 neurons, $p < 0.001$, Mann–Whitney *U* test) (Fig. 2*C*). A statistically significant loss of 19% of $TH^+$ neurons was also observed in the ventral tegmental area (19,024 ± 7572 neurons vs 13,171 ± 3290 neurons, $p = 0.015$, Mann–Whitney *U* test). Because the locus ceruleus has a role in sleep–wake control and its noradrenergic neurons degenerate in PD, we quantified $TH^+$ neurons in the locus coeruleus of our animals. No statistically significant loss of $TH^+$ neurons occurred in the locus coeruleus (7906 ± 89 neurons vs 7307 ± 259 neurons, $p = 0.28$, Mann–Whitney *U* test).

### Effects of MPTP intoxication and then of L-dopa treatment upon sleep architecture

Major sleep impairments appeared during the night after the first MPTP injection (data not shown). The most striking changes observed consisted of a drastic reduction of REM sleep (3.9 ± 4.6% vs 21.9 ± 1.0%, $p < 0.01$), with large variations between animals (loss ranging from 32% to 99%), a decrease of 15% in TST and of 48% in SWS stage, and an increase in sleep fragmentation.

After stabilization of PD symptoms, thus 1–2 months after the last MPTP injection, sleep parameters were modified both quantitatively (Table 1) and qualitatively (Figs. 2, 3, and 4) compared with baseline. Episodes of sleepiness occurred in daytime (from 1.6 ± 1.0% of light NREM sleep to 12.8 ± 2.5% of the 12 daytime hours, $p < 0.001$), appearing less frequently in the less disabled macaques. During the night, MPTP-treated monkeys exhibited decreased sleep efficiency (from 83.2 ± 2.0% to 58.9 ± 3.5%, $p < 0.001$), and increased sleep fragmentation, as assessed by the increase in the number of stage transitions and of awakenings (Fig.

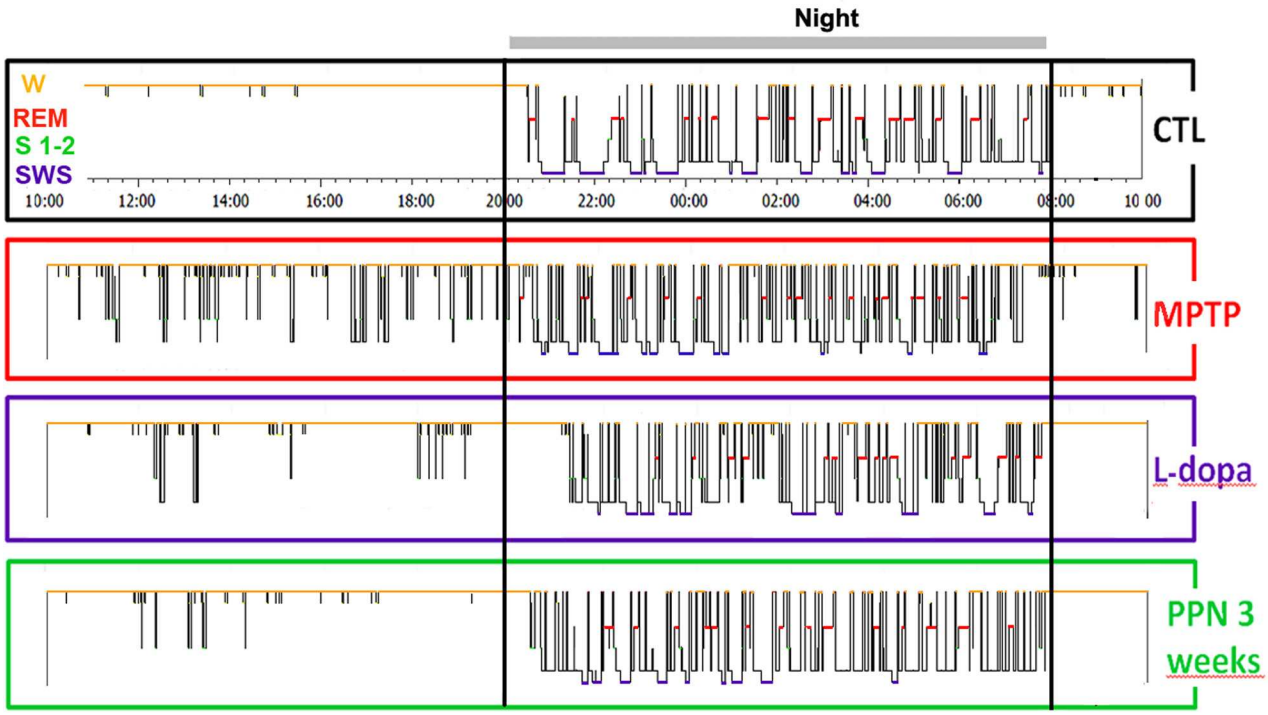


**Figure 3.** Examples of hypnograms of 24 h recordings in Macaque 3 at baseline (CTL), 1 month after MPTP intoxication, after 1 week of L-dopa treatment, and 3 weeks after subsequent PPN lesion. MPTP intoxication induced sleep episodes during the day and the impairment of sleep organization with marked sleep fragmentation and awakenings during the night. L-Dopa had a beneficial effect on daytime and nighttime sleep. A subsequent PPN lesion resulted in a better sleep quality 3 weeks after the lesion than after MPTP intoxication alone.

4*C*). The time spent in SWS and in REM sleep was reduced (from 23.8 ± 3.0% to 12.2 ± 2.8% of the TST, $p < 0.001$; and from 21.9 ± 1.0% to 16.8 ± 1.5% of the TST for REM sleep, $p < 0.001$). REM sleep latency increased from 50 ± 10 min to 105 ± 10 min ($p < 0.05$) (Fig. 4*A*).

L-Dopa given at a therapeutic dose (20 mg/kg twice daily) and after habituation over 8–12 d of treatment alleviated the motor symptoms during 3–4 h after treatment and induced in parallel a significant sleep improvement (Fig. 3). Daytime sleepiness was reduced from 12.8 ± 2.5% before L-dopa to 4.8 ± 1.6% of the 12 h ($p < 0.01$) (Table 1). L-Dopa treatment induced slight but significant effects in the number of stage transitions and awakenings, the relative time awake, WASO, TST, and REM sleep time ($p < 0.05$) (Fig. 4*A–C*), the effects being more pronounced in the most severely disabled macaque. Improvement was also observed for NREM sleep, but the effect was not statistically significant.

### Effects of MPTP intoxication and then of L-dopa treatment on muscle tone and movements during sleep

Muscle tone increased during nighttime and daytime sleep after MPTP intoxication (Figs. 2*B* and 5). This increase developed progressively during the first month after the last MPTP injection and then decreased slightly after stabilization of symptoms but never disappeared. It was characterized by the occurrence of high-amplitude EMG bouts during REM and NREM sleep. REM with muscle tone during >50% of an epoch occupied 17 ± 2% of the REM sleep time (which was never observed during the control state). Abnormal epochs containing rapid eye movements during light NREM sleep (indicative of a dissociate stage between NREM and REM sleep) were observed during 7 ± 2% of light NREM sleep. They most often occurred before the onset of REM sleep episodes (Figs. 2*B*, top, and 5).

MPTP also increased the number of movements and the number of awakenings during sleep. Loss of balance during sleep was observed, which sometimes led monkeys to sleep lying on the floor (which never happened in the control state), and even to fall from their nest. Although falls were observed in one animal on awakening from REM sleep, no abnormal movements or behaviors could be detected during REM sleep. Enhanced muscle tone during REM sleep and an increased number of movements were obvious 1 month after stabilization of parkinsonian symptoms and were slightly decreased but still visible up to 6 months after MPTP intoxication. Daytime L-dopa treatment tended to restore normal sleep-related hypotonia during both nighttime and daytime sleep (Fig. 5), but this finding was not statistically significant.

### Effects of PPN lesion on sleep architecture

A PPN lesion was performed unilaterally in three MPTP-treated macaques. Quantitative assessment revealed a loss of 17% of $NADPH^+$ neurons in the first macaque, 27% in the second, and 26% in the third compared with 5 control animals (Fig. 6*A*). The loss of noncholinergic neurons in the PPN was 5%, 15%, and 7%, respectively, and in the adjacent cuneiform nucleus was 5%, 11%, and 10%, respectively. These lesions impaired gait and worsened postural parameters, beginning 2 d after the lesion and being maximal 4–7 d after the lesion. When axial motor symptoms were maximal, muscle tone of limbs was markedly decreased on the side contralateral to the lesion but increased on the side ipsilateral, as previously described (Grabli et al., 2013).

Sleep was evaluated without L-dopa medication. We observed an increase in sleep fragmentation compared with the MPTP state (data not shown) and in nighttime wake, and a decrease in sleep efficiency, SWS, and REM sleep (Fig. 6*B*). Moreover, PPN

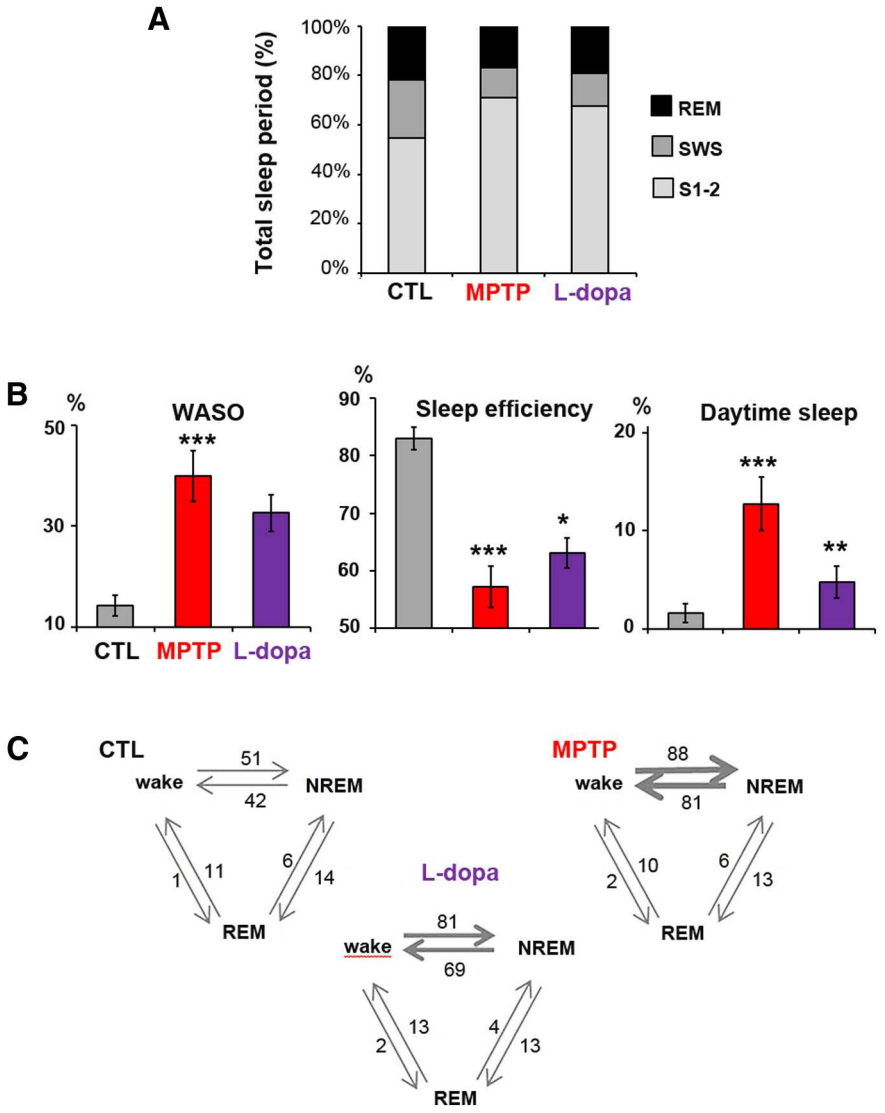


**Figure 4.** Sleep disorders after MPTP intoxication and partial improvement after L-dopa treatment. ***A***, Comparison of the contribution of REM, Stages 1 and 2 and SWS, expressed as a percentage of the total sleep period in the 4 macaques in the control state (CTL), after MPTP intoxication, and after L-dopa treatment. ***B***, Histograms showing increase in duration of WASO, reduction of sleep efficiency (ratio of total sleep time to the 12 h of nighttime), and development of daytime sleepiness (expressed as percentage of time spent asleep during the 12 h of daytime), and their improvement after L-dopa treatment. ***C***, Transitions between wake, NREM, and REM periods. The mean number of transitions is given and is represented by the thickness of the arrows. The number of transitions between wake and NREM stages was increased after MPTP intoxication and improved slightly after L-dopa treatment.

lesion induced δ wave activity occurring during wake time in the three animals (Fig. 2*C*), as assessed on videotapes. These sleep disorders progressively improved from 1 to 3 weeks after PPN lesion (Fig. 3), similarly to the partial recovery from gait disorders. Three weeks after PPN lesion, all sleep parameters had returned to values before the PPN lesion, with a slight increase in sleep efficiency, and a decrease of awakenings during the night. However, the most severely disabled macaque was still unable to sleep in his usual sitting position, which most likely interfered with the sleep–wake cycle. Because of severe disequilibrium and falls, he was killed 3 weeks after PPN lesion. A second PPN lesion was performed contralaterally in one of the two other macaques. This second lesion induced a statistically significant and specific loss of 77% of $NADPH^+$ neurons compared with control animals, accompanied by a negligible 2%–3% loss of noncholinergic neurons in the PPN and in the cuneiform nucleus. A slight, transient decrease in REM sleep and SWS was observed a week after the lesion, without δ wave activity during wake time. Again, the animal slept slightly better 3 weeks after the second PPN lesion than after MPTP intoxication, with a slight increase in sleep efficiency, and a decrease of awakenings during the night (Fig. 6*B*).

## Discussion

In this study, we showed that L-dopa treatment improved sleep disturbances induced by MPTP intoxication in macaques. Further cholinergic PPN lesion enhanced sleep quality. To our knowledge, this is the first longitudinal study in which sleep parameters were analyzed in the same monkey during the control state, after MPTP intoxication, under L-dopa treatment, and after PPN lesion. Because normal sleep architecture may vary across subjects, this experimental approach allows a precise description of the pathological state compared with the control state.

At baseline, nocturnal sleep parameters in the adult macaques of the present study were similar to those already described (Hsieh et al., 2008; Barraud et al., 2009). The first MPTP injection induced a dramatic decrease in SWS and REM sleep, as previously reported (Barraud et al., 2009). These symptoms increased after the stabilization of parkinsonian symptoms but without returning to the baseline score. On the whole, reduced sleep efficiency as well as a marked increase in insomnia and the number of nocturnal awakenings were observed. All these sleep disturbances were similar to those reported in MPTP-treated macaques (Almirall et al., 1999; Barraud et al., 2009; Hyacinthe et al., 2014) and in patients with advanced PD (Wailke et al., 2011; Yong et al., 2011), whereas sleep is not altered in *de novo* patients (Brunner et al., 2002; Kaynak et al., 2005). Our MPTP-treated macaques were markedly disabled and displayed a severe DA neuronal loss in the substantia nigra and a much smaller but significant DA degeneration in the ventral tegmental area as previously reported (Mounayar et al., 2007), and are therefore reminiscent of advanced PD. In addition, because a robust increase in the firing rate of DA neurons of the ventral tegmental area occurs during REM sleep (Dahan et al., 2007), the DA lesion in our MPTP-treated monkeys might account for the reduction of REM sleep, supporting the involvement of the DA system in the regulation of the sleep–wake cycle.

Although most of the sleep disorders in our parkinsonian macaques were similar to those described in parkinsonian patients, one element lacking was REM sleep behavior disorder (RBD). Indeed, the only movements observed during REM sleep were falls or awakenings; no abnormal behavior or violent movement

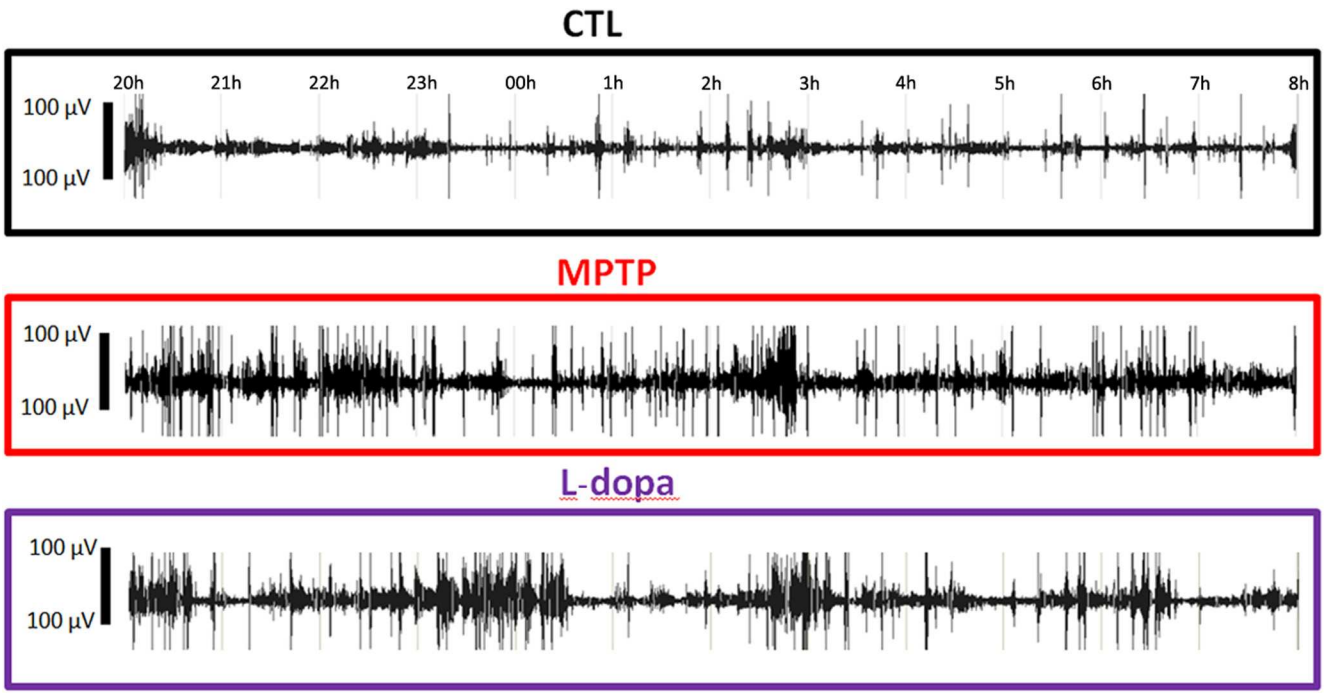


**Figure 5.** Examples of EMG recordings during the 12 h of nighttime sleep, at baseline (CTL) (first line), after MPTP intoxication (second line), and after L-dopa treatment in Macaque 2. The increase in muscle tone and in the number of movements that developed in the MPTP state was slightly improved after L-dopa treatment.

was observed, despite the fact that muscle tone was enhanced. The neuronal origin of RBD in PD might be a dysfunction of the subcoeruleus nucleus because it was reported to control atonia during REM sleep (Boeve et al., 2007), and to display a significant decrease in signal intensity on magnetic resonance images obtained in PD patients with RBD (García-Lorenzo et al., 2013). Therefore, the lack of RBD in our parkinsonian macaques might be the result of the absence of lesion within the locus coeruleus, as we and others observed (Herrero et al., 1993a). Moreover, the increased muscle tone during REM sleep in our MPTP-treated macaques may be equivalent to REM sleep without atonia in patients with PD (Gagnon et al., 2002; Arnulf, 2012). Similarly, Verhave et al. (2011) reported an enhancement of muscle tone during REM sleep in MPTP-treated marmosets, but no increase in phasic muscle tone (twitching) and no abnormal behavior. Together, these results suggest that DA deficiency increases tonic muscle activity during REM sleep (loss of atonia) but does not affect either the phasic or behavioral components during this sleep state.

Our results in MPTP-treated macaques show that L-dopa treatment not only decreased the number of movements and nocturnal awakenings but also had a beneficial effect on sleep architecture. L-Dopa was also found to be effective in patients with advanced PD for treating nighttime bradykinesia during awakenings but had no impact on the otherwise altered sleep structure and even induced a trend toward decreased total sleep period (Wailke et al., 2011). Several reasons may explain this discrepancy. First, all our animals were young and were treated with L-dopa twice a day for 8–12 d. In contrast, L-dopa is administered in middle-aged patients and for years. Thus, age effects and pharmacokinetics might be different in the patients and our monkeys. It is thus possible that L-dopa was still bioavailable at night at a dose sufficiently low to induce beneficial effects on sleep architecture in our animals, whereas the dosage has to be suitably adapted to the dopaminergic deficiency in each individual patient. Second, sleep recordings under L-dopa treatment in our macaques were directly compared with those obtained after MPTP intoxication and before any L-dopa medication. These conditions are impossible to reproduce in PD patients because sleep recordings under L-dopa are compared with those obtained after withdrawal of levodopa for no more than 24 h. It is also possible that the existence of non-DA lesions in PD limits the positive effect of L-dopa medication.

All our MPTP-treated macaques displayed an increase in daytime sleepiness, as also reported previously (Rye, 2010). Such symptoms cannot be solely a consequence of DA treatment because they were observed in the absence of L-dopa in MPTP-treated macaques and they often precede PD by several years in patients (Abbott et al., 2005). Daytime sleepiness would rather be an early marker of DA loss in humans and the first consequence of DA deficiency (Arnulf et al., 2002). The fact that daytime sleep was increased with motor disability and was decreased by L-dopa treatment further supports a direct role of dopamine in stimulating arousal systems. This is consistent with previous findings that high levels of levodopa were associated with increased alertness in parkinsonian patients (Arnulf et al., 2002; Bliwise et al., 2012). This raises the hypothesis that DA deficiency plays a role in the physiopathology of excessive daytime sleepiness. However, it should be kept in mind that patients with a higher levodopa equivalent dosage have a more advanced-stage disease.

A PPN lesion in our MPTP-treated macaques without L-dopa medication induced acute, transient, sleep disturbances, which were more severe in the most disabled macaque. These acute disturbances may be explained by postural deficits that resulted from PPN lesion and most likely interfered with the sleep–wake cycle. A temporary induction of δ wave activity during wake time resulted from PPN lesion in our MPTP-treated macaques, as already reported after destruction of the reticular formation in cats (Denoyer et al., 1991) or after administration of an anticholinergic compound (Longo, 1956). This reinforces the hypothesis

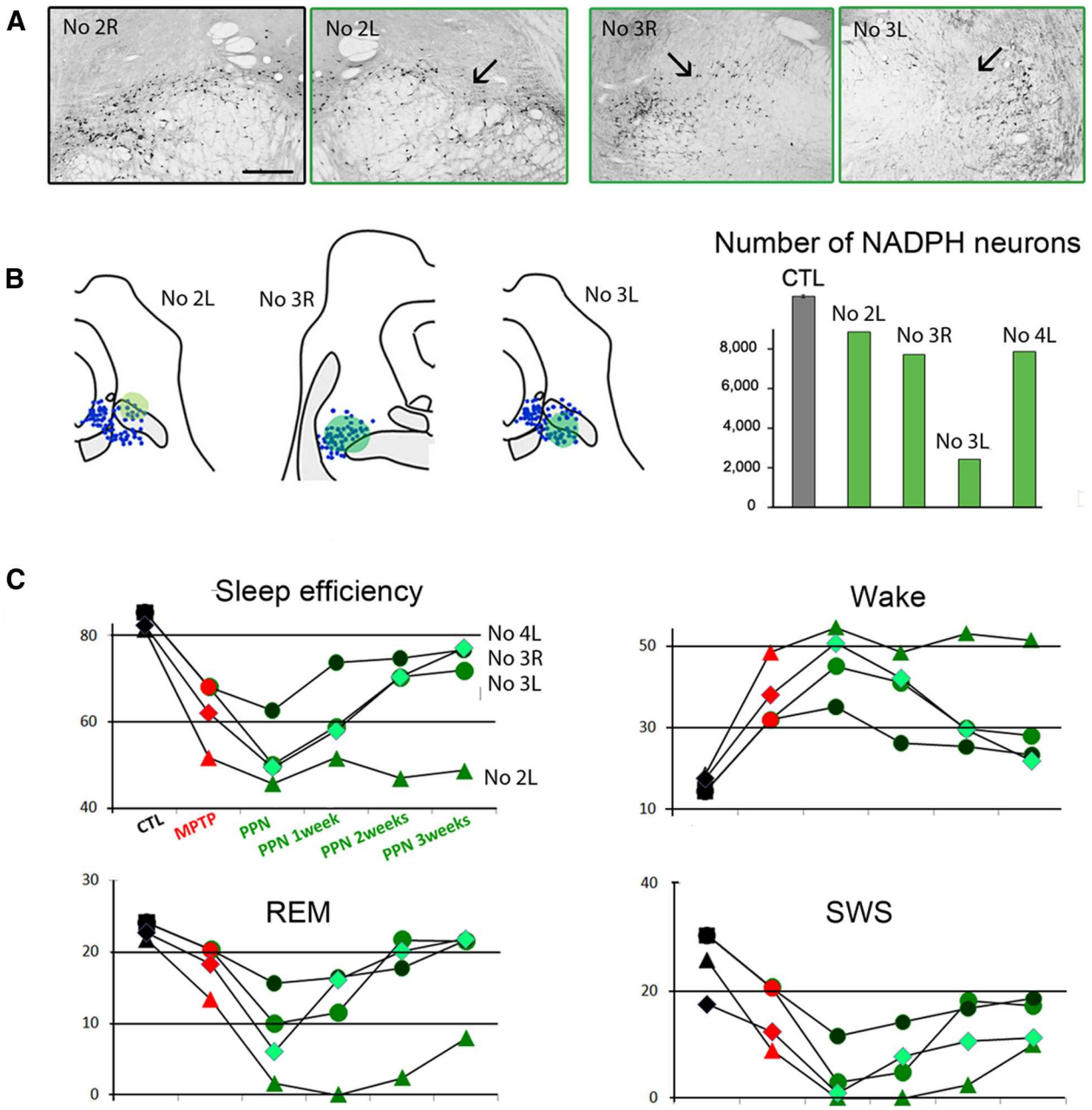


**Figure 6.** Effect of PPN lesion on sleep in three MPTP-treated macaques. ***A***, Photomicrographs of PPN sections labeled for NADPH histochemistry, showing the toxin injection site into the PPN (arrow) in the left (L) side of Macaque 2 and in both sides of Macaque 3 compared with the right (R) unlesioned side of Macaque 2. ***B***, Left, NADPH $^{+}$ neurons (blue) were mapped in two lesioned animals. Each dot represents an NADPH $^{+}$ neuron. Right, Quantification of the total number of NADPH $^{+}$ neurons in the PPN showing the neuronal loss for unilaterally lesioned macaques (Macaques 2 and 4), and for bilaterally lesioned macaque (Macaque 3). ***C***, Values of relevant sleep parameters in the three macaques 1–3 weeks after PPN lesion compared with control (CTL) and MPTP values. Note a decrease of sleep efficiency, REM sleep and SWS, and an increase of nighttime awakenings (wake). These disorders were much more severe in Macaque 2 than in Macaques 3 and 4. These parameters progressively returned to values observed after MPTP treatment, except for Macaque 2, which was therefore killed 3 weeks after PPN lesion. Scale bar: ***A***, 1 mm.

that the cholinergic activation of the cortex, by the PPN projections to the thalamocortical pathway, results in a suppression of slow δ waves and induction of cortical arousal.

The fact that sleep disturbances progressively returned to values observed before the PPN lesion, at least in the less severely parkinsonian animals, suggests that compensatory processes had occurred. Transient effects of PPN lesions on REM sleep have also been reported in cats (Webster and Jones, 1988). Postlesion compensatory mechanisms are still poorly understood, but they may involve the remaining cholinergic neurons of the PPN or of the adjacent laterodorsal tegmental nucleus. Noradrenergic neurons of the locus coeruleus and the serotoninergic neurons of the raphe nucleus, which both participate in sleep regulation, also degenerate in parkinsonian patients. The remaining neurons may also take over to compensate for the loss of cholinergic PPN neurons. Thus, the lack of changes in sleep, and in particular in REM sleep, 3 weeks after PPN lesion in our MPTP-intoxicated macaques, as reported in normal cats 2 weeks after discrete PPN lesion (Shouse and Siegel, 1992), suggests that other systems involved in sleep control were spared.

One of the main findings of our study is that PPN lesion slightly improved sleep quality after 3 weeks. This is reminiscent of our previous observations that PPN lesion improved motor symptoms in MPTP-treated macaques (Grabli et al., 2013). It is possible that PPN lesion results in a reduction of its excitatory

outputs to the subthalamic nucleus, which is overactive in PD. Indeed, a reversal of subthalamic nucleus hyperactivity has also been reported after PPN lesion in a 6-hydroxydopamine rat model (Breit et al., 2006). This would suggest that improvement of sleep quality after PPN lesion is a consequence of a reduction in nighttime bradykinesia. In this context, recent clinical data obtained in parkinsonian patients who were implanted with electrodes for deep-brain stimulation of the PPN to treat severe gait disorders indicate that sleep was strongly modified by PPN stimulation. Whereas high-frequency PPN stimulation induced NREM sleep, low-frequency stimulation increased alertness during the daytime and produced a long-term improvement of nighttime sleep (Arnulf et al., 2010; Peppe et al., 2012). It is difficult to compare these data with those obtained in MPTP-treated macaques after PPN lesion. However, our data suggest that the effects obtained in patients are the result of stimulation of both cholinergic and noncholinergic neuronal populations. Additional experiments are needed to determine the neuronal circuits that mediate parkinsonian sleep disorders.

In conclusion, combining DA and PPN lesions in macaques allowed us to characterize sleep disorders in a model of advanced PD. Using this approach, we demonstrated an improvement of sleep quality after L-dopa therapy and the involvement of the PPN in the regulation of the sleep/wake cycle.

## References


Abbott RD, Ross GW, White LR, Tanner CM, Masaki KH, Nelson JS, Curb JD, Petrovitch H (2005) Excessive daytime sleepiness and subsequent development of Parkinson disease. Neurology 65:1442–1446. CrossRef Medline

Almirall H, Pigarev I, de la Calzada MD, Pigareva M, Herrero MT, Sagales T (1999) Nocturnal sleep structure and temperature slope in MPTP treated monkeys. J Neural Transm 106:1125–1134. CrossRef Medline

Arnulf I (2005) Excessive daytime sleepiness in parkinsonism. Sleep Med Rev 9:185–200. CrossRef Medline

Arnulf I (2012) REM sleep behavior disorder: motor manifestations and pathophysiology. Mov Disord 27:677–689. CrossRef Medline

Arnulf I, Konofal E, Merino-Andreu M, Houeto JL, Mesnage V, Welter ML, Lacomblez L, Golmard JL, Derenne JP, Agid Y (2002) Parkinson's disease and sleepiness: an integral part of PD. Neurology 58:1019–1024. CrossRef Medline

Arnulf I, Ferraye M, Fraix V, Benabid AL, Chabardès S, Goetz L, Pollak P, Debû B (2010) Sleep induced by stimulation in the human pedunculopontine nucleus area. Ann Neurol 67:546–549. CrossRef Medline

Barbato L, Stocchi F, Monge A, Vacca L, Ruggieri S, Nordera G, Marsden CD (1997) The long-duration action of levodopa may be due to a postsynaptic effect. Clin Neuropharmacol 20:394–401. CrossRef Medline

Barraud Q, Lambrecq V, Forni C, McGuire S, Hill M, Bioulac B, Balzamo E, Bezard E, Tison F, Ghorayeb I (2009) Sleep disorders in Parkinson's disease: the contribution of the MPTP non-human primate model. Exp Neurol 219:574–582. CrossRef Medline

Bezard E, Imbert C, Deloire X, Bioulac B, Gross CE (1997) A chronic MPTP model reproducing the slow evolution of Parkinson's disease: evolution of motor symptoms in the monkey. Brain Res 766:107–112. CrossRef Medline

Bliwise DL, Trotti LM, Wilson AG, Greer SA, Wood-Siverio C, Juncos JJ, Factor SA, Freeman A, Rye DB (2012) Daytime alertness in Parkinson's disease: potentially dose-dependent, divergent effects by drug class. Mov Disord 27:1118–1124. CrossRef Medline

Boeve BF, Silber MH, Saper CB, Ferman TJ, Dickson DW, Parisi JE, Benarroch EE, Ahlskog JE, Smith GE, Caselli RC, Tippman-Peikert M, Olson EJ, Lin SC, Young T, Wszolek Z, Schenck CH, Mahowald MW, Castillo PR, Del Tredici K, Braak H (2007) Pathophysiology of REM sleep behaviour disorder and relevance to neurodegenerative disease. Brain 130:2770–2788. CrossRef Medline

Breit S, Lessmann L, Unterbrink D, Popa RC, Gasser T, Schulz JB (2006) Lesion of the pedunculopontine nucleus reverses hyperactivity of the subthalamic nucleus and substantia nigra pars reticulata in a 6-hydroxydopamine rat model. Eur J Neurosci 24:2275–2282. CrossRef Medline

Brunner H, Wetter TC, Hogl B, Yassouridis A, Trenkwalder C, Friess E (2002) Microstructure of the non-rapid eye movement sleep electroencephalogram in patients with newly diagnosed Parkinson's disease: effects of dopaminergic treatment. Mov Disord 17:928–933. CrossRef Medline

Clark SD, Nothacker HP, Wang Z, Saito Y, Leslie FM, Civelli O (2001) The urotensin II receptor is expressed in the cholinergic mesopontine tegmentum of the rat. Brain Res 923:120–127. CrossRef Medline

Clark SD, Alderson HL, Winn P, Latimer MP, Nothacker HP, Civelli O (2007) Fusion of diphtheria toxin and urotensin II produces a neurotoxin selective for cholinergic neurons in the rat mesopontine tegmentum. J Neurochem 102:112–120. CrossRef Medline

Dahan L, Astier B, Vautrelle N, Urbain N, Kocsis B, Chouvet G (2007) Prominent burst of firing neurons in the ventral tegmental area during paradoxical sleep. Neuropsychopharmacology 32:1232–1241. CrossRef Medline

Denoyer M, Sallanon M, Buda C, Kitahama K, Jouvet M (1991) Neurotoxic lesion of the mesencephalic reticular formation and/or the posterior hypothalamus does not alter waking in the cat. Brain Res 539:287–303. CrossRef Medline

François C, Yelnik J, Tandé D, Agid Y, Hirsch EC (1999) Dopaminergic cell group A8 in the monkey: anatomical organization and projections to the striatum. J Comp Neurol 414:334–347. CrossRef Medline

Gagnon JF, Bédard MA, Fantini ML, Petit D, Panisset M, Rompré S, Carrier J, Montplaisir J (2002) REM sleep behavior disorder and REM sleep without atonia in Parkinson's disease. Neurology 59:585–589. CrossRef Medline

García-Lorenzo D, Longo-Dos Santos C, Ewenczyk C, Leu-Semenescu S, Gallea C, Quattrocchi G, Pita Lobo P, Poupon C, Benali H, Arnulf I, Vidailhet M, Lehericy S (2013) The coeruleus/subcoeruleus complex in rapid eye movement sleep behaviour disorders in Parkinson's disease. Brain 136:2120–2129. CrossRef Medline

Grabli D, Karachi C, Folgoas E, Monfort M, Tande D, Clark S, Civelli O, Hirsch EC, François C (2013) Gait disorders in parkinsonian monkeys with pedunculopontine nucleus lesions: a tale of two systems. J Neurosci 33:11986–11993. CrossRef Medline

Herrero MT, Hirsch EC, Javoy-Agid F, Obeso JA, Agid Y (1993a) Differential vulnerability to 1-methyl-4-phenyl-1,2,3,6-tetrahydropyridine of dopaminergic and cholinergic neurons in the monkey mesopontine tegmentum. Brain Res 624:281–285. CrossRef Medline

Herrero MT, Perez-Otaño I, Oset C, Kastner A, Hirsch EC, Agid Y, Luquin MR, Obeso JA, Del Rio J (1993b) GM-1 ganglioside promotes the recovery of surviving midbrain dopaminergic neurons in MPTP-treated monkeys. Neuroscience 56:965–972. CrossRef Medline

Hirsch EC, Graybiel AM, Duyckaerts C, Javoy-Agid F (1987) Neuronal loss in the pedunculopontine tegmental nucleus in Parkinson disease and in progressive supranuclear palsy. Proc Natl Acad Sci U S A 84:5976–5980. CrossRef Medline

Hobson DE, Lang AE, Martin WW, Razmy A, Rivest J, Fleming J (2002) Excessive daytime sleepiness and sudden-onset sleep in Parkinson disease: a survey by the Canadian Movement Disorder Group. JAMA 287:455–463. CrossRef Medline

Hsieh KC, Robinson EL, Fuller CA (2008) Sleep architecture in unrestrained rhesus monkeys (Macaca mulatta) synchronized to 24-hour light-dark cycles. Sleep 31:1239–1250. Medline

Hyacinthe C, Barraud Q, Tison F, Bezard E, Ghorayeb I (2014) D1 receptor agonist improves sleep–wake parameters in experimental parkinsonism. Neurobiol Dis 63:20–24. CrossRef Medline

Jellinger K (1988) The pedunculopontine nucleus in Parkinson's disease, progressive supranuclear palsy and Alzheimer's disease. J Neurol Neurosurg Psychiatry 51:540–543. CrossRef Medline

Karachi C, Grabli D, Bernard FA, Tandé D, Wattiez N, Belaid H, Bardinet E, Prigent A, Nothacker HP, Hunot S, Hartmann A, Lehéricy S, Hirsch EC, François C (2010) Cholinergic mesencephalic neurons are involved in gait and postural disorders in Parkinson disease. J Clin Invest 120:2745–2754. CrossRef Medline

Kaynak D, Kiziltan G, Kaynak H, Benbir G, Uysal O (2005) Sleep and sleepiness in patients with Parkinson's disease before and after dopaminergic treatment. Eur J Neurol 12:199–207. CrossRef Medline

Longo VG (1956) Effects of scopolamine and atropine electroencephalographic and behavioral reactions due to hypothalamic stimulation. J Pharmacol Exp Ther 116:198–208. Medline

Mounayar S, Boulet S, Tandé D, Jan C, Pessiglione M, Hirsch EC, Féger J, Savasta M, François C, Tremblay L (2007) A new model to study compensatory mechanisms in MPTP-treated monkeys exhibiting recovery. Brain 130:2898–2914. CrossRef Medline

Peppe A, Pierantozzi M, Baiamonte V, Moschella V, Caltagirone C, Stanzione P, Stefani A (2012) Deep brain stimulation of pedunculopontine tegmental nucleus: role in sleep modulation in advanced Parkinson disease patients: one-year follow-up. Sleep 35:1637–1642. CrossRef Medline

Rye DB (2006) Excessive daytime sleepiness and unintended sleep in Parkinson's disease. Curr Neurol Neurosci Rep 6:169–176. CrossRef Medline

Rye D (2010) Seeing beyond one's nose: sleep disruption and excessive sleepiness accompany motor disability in the MPTP treated primate. Exp Neurol 222:179–180. CrossRef Medline

Shouse MN, Siegel JM (1992) Pontine regulation of REM sleep components in cats: integrity of the pedunculopontine tegmentum (PPT) is important for phasic events but unnecessary for atonia during REM sleep. Brain Res 571:50–63. CrossRef Medline

Verhave PS, Jongsma MJ, Van den Berg RM, Vis JC, Vanwersch RA, Smit AB, Van Someren EJ, Philippens IH (2011) REM sleep behavior disorder in the marmoset MPTP model of early Parkinson disease. Sleep 34:1119–1125. CrossRef Medline

Wailke S, Herzog J, Witt K, Deuschl G, Volkmann J (2011) Effect of controlled-release levodopa on the microstructure of sleep in Parkinson's disease. Eur J Neurol 18:590–596. CrossRef Medline

Webster HH, Jones BE (1988) Neurotoxic lesions of the dorsolateral pontomesencephalic tegmentum-cholinergic cell area in the cat: II. Effects upon sleep–waking states. Brain Res 458:285–302. CrossRef Medline

Yong MH, Fook-Chong S, Pavanni R, Lim LL, Tan EK (2011) Case control polysomnographic studies of sleep disorders in Parkinson's disease. PLoS One 6:e22511. CrossRef Medline

Sleep Medicine 16 (2015) 1245–1251

Contents lists available at ScienceDirect

Sleep Medicine

journal homepage: www.elsevier.com/locate/sleep

Review Article

# Effect of melatonin on sleep disorders in a monkey model of Parkinson's disease

Hayat Belaid, Joelle Adrien, Carine Karachi, Etienne C. Hirsch, Chantal François *

*Sorbonne Universités, UPMC Univ Paris 06, INSERM, CNRS, UM75, U1127, UMR 7225, ICM, F-75013 Paris, France*

ARTICLE INFO

*Article history:*
Received 30 March 2015
Received in revised form 21 May 2015
Accepted 2 June 2015
Available online 14 July 2015

*Keywords:*
Melatonin
Parkinson's disease
Sleep disorders
MPTP (1-methyl-4-phenyl-1,2,3,6-tetrahydropyridine)
Macaques
Monkeys

ABSTRACT

*Objectives:* To evaluate and compare the effects of melatonin and levodopa (L-dopa) on sleep disorders in a monkey model of Parkinson's disease.
*Materials and methods:* The daytime and nighttime sleep patterns of four macaques that were rendered parkinsonian by administration of 1-methyl-4-phenyl-1,2,3,6-tetrahydropyridine (MPTP) were recorded using polysomnography in four conditions: at baseline, during the parkinsonian condition; after administration of L-dopa, and after administration of a combination of melatonin with L-dopa.
*Results:* It was confirmed that MPTP intoxication induces sleep disorders, with sleep episodes during daytime and sleep fragmentation at nighttime. L-dopa treatment significantly reduced the awake time during the night and tended to improve all other sleep parameters, albeit not significantly. In comparison to the parkinsonian condition, combined treatment with melatonin and L-dopa significantly increased total sleep time and sleep efficiency, and reduced the time spent awake during the night in all animals. A significant decrease in sleep latencies was also observed in three out of four animals. Compared with L-dopa alone, combined treatment with melatonin and L-dopa significantly improved all these sleep parameters in two animals. On the other hand, combined treatment had no effect on sleep architecture and daytime sleep.
*Conclusion:* These data demonstrated, for the first time, objective improvement on sleep parameters of melatonin treatment in MPTP-intoxicated monkeys, showing that melatonin treatment has a real therapeutic potential to treat sleep disturbances in people with Parkinson's disease.


## 1. Introduction

People with Parkinson's disease (PD) experience significant sleep disturbances, including excessive daytime sleepiness, insomnia with reduced total sleep time and sleep efficiency, and an increased number of nocturnal awakenings. Moreover, 15–60% of people with PD have rapid eye movement (REM) sleep behavior disorder, which consists of excessive motor activity during dreaming in association with loss of skeletal muscle atonia of REM sleep [1,2]. The effects of dopaminergic drugs on sleep and alertness in people with PD are difficult to analyze because they may improve sleep quality, partly through reducing motor symptoms, but also increase daytime sleepiness and cause insomnia. To date, there is no specific medication known to be effective in alleviating these specific sleep disorders without adverse effects such as reduced cognitive function and alertness. In this context, melatonin is an interesting agent used to induce drowsiness and sleep, and may improve sleep disturbances.

Melatonin, which is mainly synthesized by the pineal gland, is known to play a key role in the circadian regulation of sleep and wakefulness. Exogenous melatonin can shift the phase of the human circadian clock [3,4], improving subjective sleep quality in various pathologies [5,6]. In people with PD, the expression of melatonin receptors is decreased in the substantia nigra [7] and melatonin secretion is reduced [8,9], leading to a blunted circadian rhythm. Administration of melatonin to these people has been found to increase sleep efficiency [10] and improve subjective sleep quality, whereas the polysomnographic (PSG) features remain unchanged [11]. The possibility that melatonin administration is effective in preventing dopaminergic cell death in experimental models of PD has been supported by some studies [12,13] but contradicted by others [14,15], whereas intraventricular implants of melatonin have been shown to increase the severity of motor symptoms [16].

1-Methyl-4-phenyl-1,2,3,6-tetrahydropyridine (MPTP)-intoxicated macaques develop sleep disorders that mimic those of people with PD [17,18]. It has previously been shown that levodopa (L-dopa) treatment in parkinsonian macaques, given twice a day and after habituation over 8–12 days, has a beneficial effect on almost all sleep parameters, including sleep architecture, but not on sleep and REM sleep latencies [18]. The aims of the present study were to characterize the effect of combined treatment with melatonin and

* Corresponding author. Sorbonne Universités, UPMC Univ Paris 06, INSERM, CNRS, UM75, U1127, UMR 7225, ICM, F-75013 Paris, France. Tel.: +33 1 57 27 45 40; fax: +33 1 57 27 47 82.
*E-mail address:* chantal.francois@upmc.fr (C. François).

http://dx.doi.org/10.1016/j.sleep.2015.06.018
1389-9457/

L-dopa on sleep disorders in this monkey model of PD using polysomnography (PSG), and to compare these effects to those obtained with L-dopa alone.

## 2. Materials and methods

### 2.1. Animals and sleep recordings

The study was performed on four adult male macaques (*Macaca fascicularis*) and was carried out in strict accordance with the European Community Council Directive of 2010 (2010/63/UE) for care and use of laboratory animals. The study was approved by the Committee on the Ethics of Animal Experiments (Charles Darwin, agreement no. Ce5/2012/049). All surgery was performed under general anesthesia and analgesia, and all efforts were made to minimize the number of animals used and their suffering.

Macaques were chronically implanted under deep anesthesia with a radio-telemetry transmitter (D70-EEE, Data Sciences International, St Paul, MN) for continuous recording of electroencephalography (EEG), electrooculography (EOG), and electromyography (EMG) signals, as previously described [18]. Briefly, the animals were anesthetized with isoflurane (1–2%) and received analgesia (2 mg/kg Tolfedine, tolfenamic acid, 4%). The transmitter was implanted and two EEG electrodes were screwed unilaterally into the skull 10 mm lateral to the midline (one above the frontal cortex and the other 30 mm more posterior). Two electrodes for EOG were unilaterally affixed at the level of the orbital arch bone (one at the top and the other on the external side). The two EMG leads were sutured to the neck musculature. After surgery, buprenorphine (Buprecare, 0.02 mg/kg IM) and prophylactic antibiotic cover (Clamoxyl, 20 mg/kg) were provided for two weeks postoperatively. The animals were allowed to recover for three weeks.

Software (Neuroscore, Data Sciences International, St Paul, MN) was used for sleep scoring to obtain hypnograms. Sleep–wake stage scoring was performed in 20-s epochs so that the whole epoch could be assigned to one of four different stages: 'wake', 'light sleep' (stages 1 and 2 pooled together), 'slow-wave sleep' (stages 3 and 4 pooled together), and 'REM sleep'. The following parameters were calculated for each 12-h period of darkness: total sleep time, duration of each stage, sleep efficiency (ratio between the total sleep time and the 12-h nighttime), sleep onset latency (time from nighttime start [20:00] to sleep onset), and REM latency (time from nighttime start to REM sleep onset). Sleep episodes during daytime were measured for a 12-h period from 08:00 to 20:00 in the same conditions.

### 2.2. Drugs

Intramuscular (IM) MPTP injections (0.2–0.4 mg/kg) were given every three to seven days, and intoxication was stopped once all of the motor parkinsonian symptoms had appeared [18]; thus, two to six weeks after the first injection. Parkinsonian symptoms had stabilized one to two months after the last MPTP injection (Fig. 1A). These symptoms were assessed two months after the last MPTP injection by a rating scale that included seven items rated between 0 and 3 [19]. L-dopa treatment consisted of oral doses of L-dopa (Modopar Dispersible, Roche, 20 mg/kg) once a day at midday for two weeks. The treatment schedule for melatonin included administration of an oral dose of L-dopa (20 mg/kg) at midday, then administration of melatonin (10 µg/kg) given 2 h before lights-off time [20] for a period of five consecutive days. This dose of melatonin was chosen based on the previous results showing that this physiological dose induced earlier sleep onset time and longer sleep period time, but did not significantly affect nighttime sleep efficiency in normal macaques [20].

### 2.3. Experimental protocol

A 3-week period was allowed for recovery from surgery, after which 24-h recording sessions, starting at 10:00 (lights on from 08:00 to 20:00), were obtained for each animal in the home cage at each experimental condition: five recordings at baseline (control state); five to six recordings after MPTP treatment (two months after the last MPTP injection), as previously described [18]; three to four recordings performed after administration of L-dopa alone; then one recording performed after administration of melatonin in addition to L-dopa (melatonin + L-dopa) (after five consecutive days of this same treatment). Following a 3-day washout, a last recording session was performed after administration of L-dopa to ensure that sleep parameters returned to values before combined treatment with melatonin and L-dopa. The timeline of sleep recording sessions is presented in Fig. 1B.

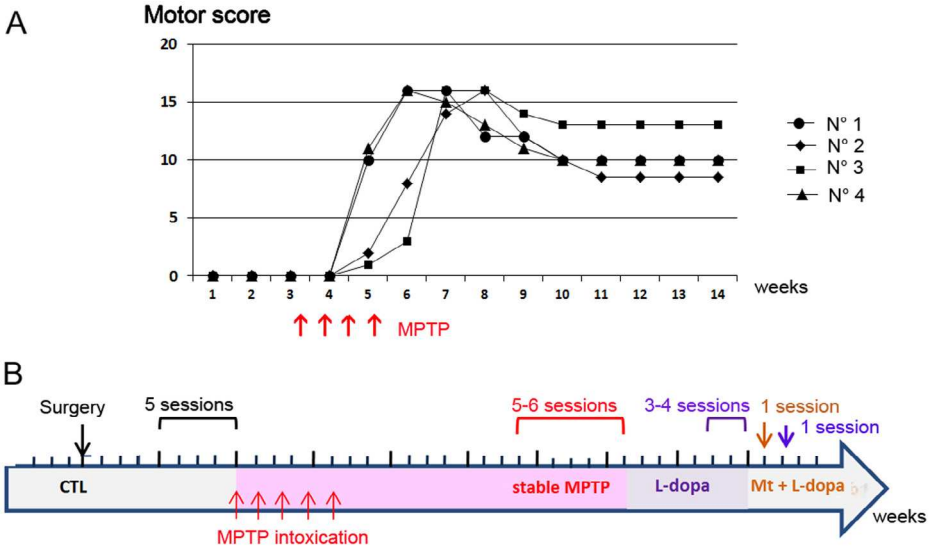


**Fig. 1.** (A) Evolution of motor score during intoxication until stabilization of symptoms for four monkeys. (B) Timeline of sleep recording sessions. Sleep recording sessions were carried out during the control (CTL) state, after MPTP treatment, after administration of L-dopa alone, and then after combined treatment with melatonin and L-dopa (Mt + L-dopa).

### 2.4. Statistical analysis

The values of each sleep parameter were normalized to control conditions. A repeated-measures analysis of variance on ranks with Dunnett's post hoc method (SigmaPlot version 11 computer software) was used to compare sleep parameters at baseline, after MPTP intoxication, after L-dopa administration, and after combined treatment with melatonin and L-dopa in the same individuals. However, statistical power was limited due to the low number of animals, and intra-individual statistical comparisons were thus also performed. For that purpose, because the present study focused on the effect of the combined treatment, with melatonin and L-dopa compared with the effect of L-dopa alone and of MPTP intoxication for each animal, a comparison of an observed mean (the mean of the values obtained for each sleep parameter after L-dopa alone or in the MPTP condition) was realized with a theoretical value obtained for each parameter after combined treatment with melatonin and L-dopa [21,22]. The level of significance was only given in case of statistical significance for each individual. Results with $p \leq 0.05$ were considered significant for all analyses. Data are presented as means ± SD.

## 3. Results

### 3.1. Assessment of motor symptoms and sleep disorders in MPTP-intoxicated macaques

The MPTP administration induced severe parkinsonian motor symptoms that stabilized one to two months after the last MPTP injection in all macaques and persisted over months. The parkinsonian motor score reached a mean of 10 (10.4 ± 1.9, range 8.5–13) out of a maximum total of 21 (Table 1). MPTP-treated macaques displayed sleep disorders that included sleep episodes during daytime and sleep fragmentation at nighttime (Figs. 2 and 3A,B). A reduction in total sleep time, in time spent in slow-wave sleep and REM sleep, and an increase in the number of movements and awakenings were also observed, as previously described [17,18].

### 3.2. Effect of L-dopa on motor disability and sleep disorders

L-dopa given at a therapeutic dose (20 mg/kg) once a day alleviated the motor symptoms for 3–4 h (78%, from 10.4 ± 1.9 to 2.2 ± 0.3 out of a total of 21, $p < 0.05$). L-dopa tended to reduce daytime sleep (–51%) but did not reach significance (7.3 ± 3.8 min vs 13.2 ± 5.2 min of the 12 h of daytime, $p = 0.29$). During the following night, L-dopa slightly, but significantly, reduced the percentage of wake time (–12%) and tended to improve all other sleep parameters, such as the slow-wave sleep (+13%) and REM sleep (+8%) percentages at nighttime (Figs. 2 and 3C). Sleep recording performed without L-dopa 24 h later showed that none of the sleep values differed from those observed during the MPTP condition (not shown). Values of standard deviations calculated for all sleep parameters during MPTP and L-dopa conditions were compared with those calculated during the control period. No statistical difference in standard deviation was observed, reflecting similar night-to-night variability across treatment modalities.

### 3.3. Effect of combined treatment with melatonin and L-dopa on parkinsonian motor symptoms and sleep disorders

Combined treatment with melatonin and L-dopa over five consecutive days had no benefit on motor symptoms compared with L-dopa alone (2.0 ± 0.8 vs 2.2 ± 0.3 out of a total of 21) (Table 1), and did not result in any adverse effects during daytime. Daytime sleep was not improved by the combined treatment with melatonin and L-dopa compared with L-dopa alone (7.3 ± 3.8 min vs 6.5 ± 3.2 min, $p = 0.19$) or the parkinsonian condition (7.3 ± 3.8 min vs 13.9 ± 5.3 min, $p = 0.19$) (Table 1, Fig. 3D). During nighttime, combined treatment had an overall favorable effect on many sleep parameters (Tables 1 and 2, Figs. 2 and 3D). It significantly increased total sleep time and sleep efficiency in all four MPTP-intoxicated animals (+23%) and in two animals when compared with L-dopa alone (+14%) (sleep efficiency, MPTP 57.7 ± 6.1%; L-dopa 61.8 ± 4.5%; melatonin + L-dopa 70.8 ± 5.6%, $p < 0.05$). It significantly reduced the percentage of wake time (–30%) in all MPTP-intoxicated animals, and in two animals when compared with L-dopa (–21%) (MPTP 42.9 ± 5.9%; L-dopa 37.9 ± 5.3%; melatonin + L-dopa 29.8 ± 3.6%, $p < 0.05$). Finally, sleep onset latency was reduced in three animals compared with the parkinsonian condition (–25%) and in two animals compared with L-dopa alone (–27%) (MPTP 43.2 ± 6.4 min; L-dopa 41.5 ± 7.5 min; melatonin + L-dopa 30.5 ± 5.7 min) (Table 2). However, sleep offset was not affected by the treatment. A last recording session was performed after a 3-day washout. In the three out four animals in which data could be exploited, it was observed that all sleep parameters returned to the values before combined treatment with melatonin and L-dopa (Tables 1 and 2).

### 3.4. Effect of combined treatment with melatonin and L-dopa on sleep architecture

The combined treatment with melatonin and L-dopa had no significant effect on sleep architecture compared with L-dopa alone.

**Table 1**
Summary of the effect on sleep parameters of MPTP intoxication and of subsequent treatment with L-dopa alone, and then with melatonin combined with L-dopa in four macaques, and finally after a 3-day washout in three of them.

| | CTL $n = 4$ | MPTP $n = 4$ | L-dopa alone $n = 4$ | Melatonin + L-dopa $n = 4$ | L-dopa 2 $n = 3$ |
|---|---|---|---|---|---|
| Motor score | 0 | 10.4 ± 1.9*** | 2.2 ± 0.3 | 2.0 ± 0.8$ | 2.2 ± 0.3 |
| TST (min) | 597 ± 12 | 414 ± 45* | 447 ± 35 | 508 ± 42$ | 450 ± 27 |
| Efficiency (%) | 83.3 ± 1.6 | 57.7 ± 6.1*** | 61.8 ± 4.5 | 70.8 ± 5.6$ | 62.9 ± 3.0 |
| Wake time (%) | 17.0 ± 1.8 | 42.9 ± 5.9*** | 37.9 ± 5.3# | 29.8 ± 3.6$ | 37.1 ± 2.9 |
| S1-S2 (%) | 52.1 ± 4.0 | 64.7 ± 7.8** | 61.3 ± 10.4 | 58.7 ± 16.2 | 70.1 ± 2.6 |
| SWS (%) | 23.8 ± 6.1 | 12.5 ± 5.3*** | 13.1 ± 4.7 | 15.1 ± 5.7 | 12.6 ± 0.9 |
| REM (%) | 22.0 ± 1.7 | 17.3 ± 3.0*** | 19.5 ± 3.1 | 18.8 ± 3.2 | 17.3 ± 2.7 |
| Sleep onset latency (min) | 19.2 ± 7.2 | 43.2 ± 6.4 | 41.5 ± 7.5 | 30.5 ± 5.7 | 42.3 ± 4.9 |

*Abbreviations:* L-dopa, levodopa; MPTP, 1-methyl-4-phenyl-1,2,3,6-tetrahydropyridine; REM, rapid eye movement; S1-S2, stages 1 and 2 pooled together (light sleep); SWS, slow-wave sleep; TST, total sleep time.
Each column represents mean values (±SD) derived from all nights of sleep recordings per each study period in all macaques. A recording after a 3-day washout period was performed after the combined treatment with melatonin and L-dopa phase (L-dopa 2).
* $p < 0.05$; **$p < 0.01$ and ***$p < 0.005$, MPTP vs control (CTL) values.
\# $p < 0.05$, L-dopa alone vs MPTP values.
§$p < 0.05$ and §§$p < 0.01$, Melatonin + L-dopa vs L-dopa alone values.
$ Melatonin + L-dopa vs MPTP values. Repeated-measures analysis of variance on ranks followed by Dunnett's post hoc test.

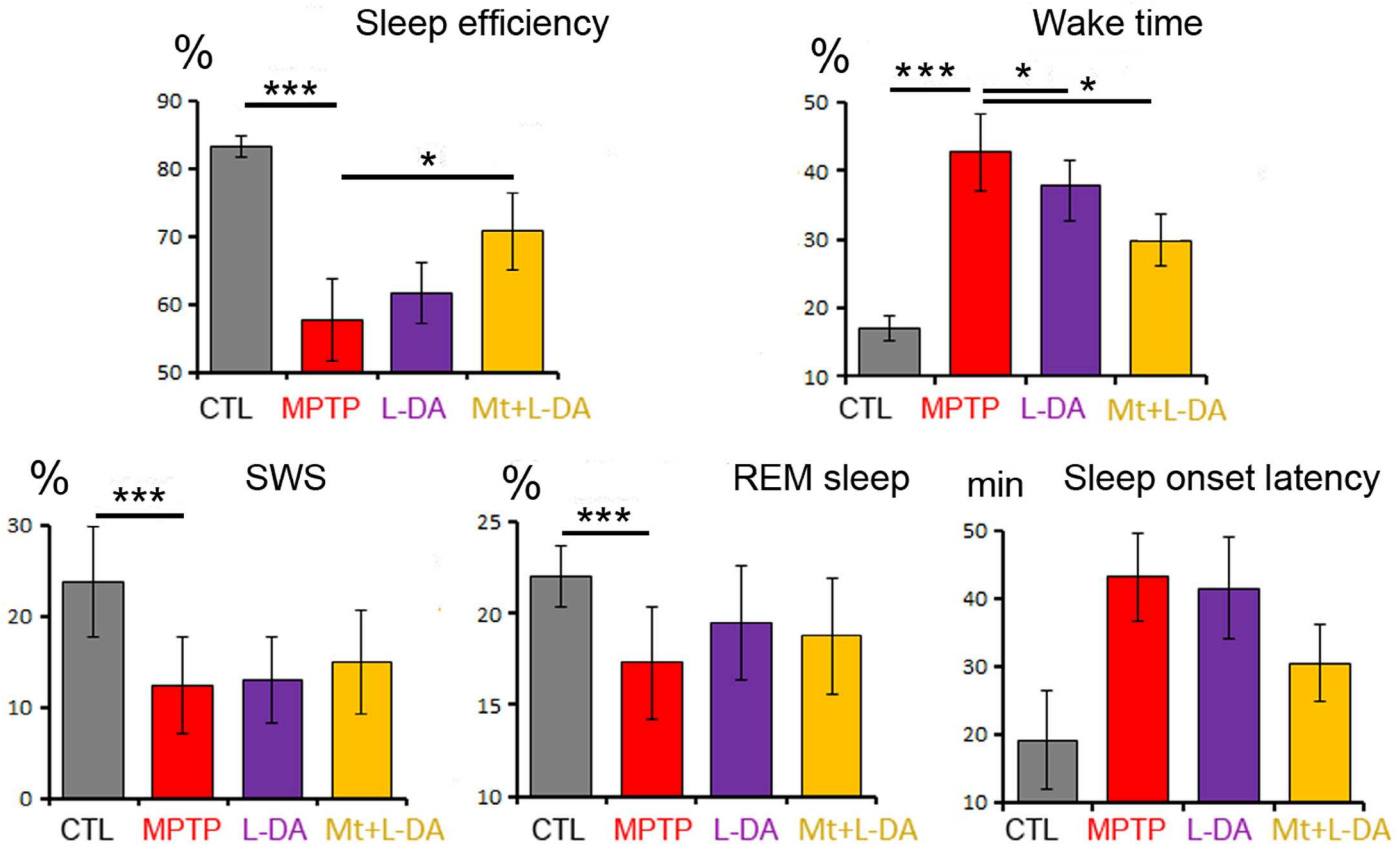


**Fig. 2.** Sleep disorders after MPTP intoxication, L-dopa administration and combined treatment with melatonin and L-dopa. Histograms showing reduction of sleep efficiency (ratio of total sleep time to the 12 h of nighttime), increase in wake time during nighttime, reduction in slow-wave sleep (SWS) and rapid eye movement (REM) sleep, and increase in sleep onset latency after MPTP intoxication. All these parameters tended to improve after L-dopa administration (L-DA), and mostly after combined treatment with melatonin and L-dopa (Mt + L-DA). Repeated-measures analysis of variance on ranks followed by Dunnett's post hoc test. CTL, control.

Only a tendency for an increase in slow-wave sleep percentage was observed (+14%, 15.1 ± 5.7% vs 13.1 ± 4.7%), which was significant for only one monkey. Slow-wave sleep percentage was, however, significantly increased in two animals when compared with the MPTP condition (+21%, 15.1 ± 5.7% vs 12.5 ± 5.3%) (Table 2).

## 4. Discussion

The present study demonstrated that administration of melatonin and L-dopa in MPTP-intoxicated monkeys improved sleep quality better than L-dopa alone. It increased total sleep time and sleep efficiency, and decreased the percentage of wake time and the sleep onset latency.

These results confirm that MPTP-intoxicated monkeys suffer from sleep disorders, as already reported [17,18]. These symptoms are similar to those observed in people with PD, especially in the advanced form of the disease [1,2]. It also confirmed that L-dopa tends to improve sleep parameters such as the relative time awake, sleep efficiency, and REM sleep time. The lack of significance was likely due to the low dose of L-dopa given, since a higher dose has already been shown to significantly alleviate sleep parameters, except sleep onset latency and slow-wave sleep [18]. The choice to administer low doses of L-dopa was dictated by the need to demonstrate an additional effect of the melatonin per se on these sleep parameters. In this study, the effect of melatonin alone was not evaluated because MPTP intoxication induced severe parkinsonian motor symptoms that had to be treated by L-dopa in order to not interfere with sleep.

The predominant finding of this study was that a combined treatment with melatonin and L-dopa can add benefit in alleviating sleep disorders in MPTP-intoxicated monkeys, with a significant increase in total sleep time and sleep efficiency and decrease in the time spent awake during nighttime. These results are consistent with previous studies showing that melatonin taken before bedtime by people with PD significantly improves the quality of sleep with increased nighttime sleep, as assessed by actigraphy [10]. Similar beneficial effects of melatonin were also reported in people suffering from REM sleep behavior disorder [23,24], which is a sleep symptom commonly encountered in parkinsonian people [9]. Another beneficial effect of the combination of melatonin and L-dopa administered to the animals was that it significantly advanced sleep onset in two of the four MPTP-intoxicated macaques compared with L-dopa alone, and in three macaques when compared with the parkinsonian condition. Such an improvement appears to be specific to melatonin because L-dopa alone, even given at a higher dose, had no effect on this specific sleep parameter [18]. It is interesting to note that latency to sleep onset was not improved for two MPTP-treated macaques, which developed the highest disability score with a slightly lower effect of L-dopa treatment on the motor symptoms. The effect of melatonin is thus possibly limited by the level of motor disability, implying that a beneficial effect could be obtained with a higher L-dopa dose associated with melatonin. These results fit well with the notion that melatonin can potentiate sleep initiation. Indeed, melatonin is a sleep-promoting hormone that induces an earlier sleep onset when administered 2 h before lights-off time in healthy monkeys [20], which is similar to observations

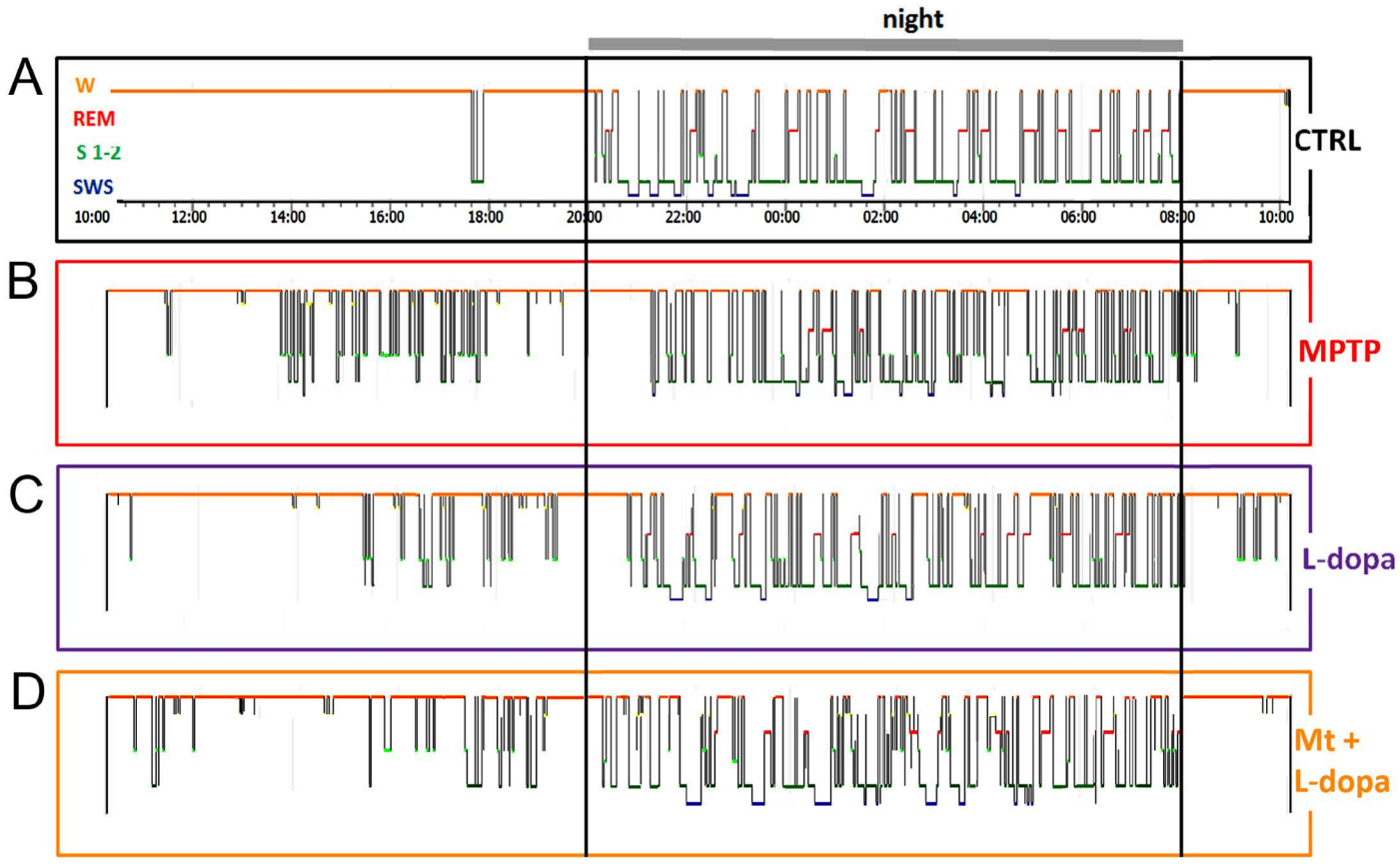


**Fig. 3.** Examples of hypnograms of 24-h recordings in macaque No. 3 at baseline (CTL) (A), six weeks after MPTP intoxication (B), after one week of L-dopa treatment once a day (C), and five days after combined treatment with melatonin and L-dopa (Mt + L-dopa) (D). MPTP intoxication induced sleep episodes during the day and marked sleep fragmentation and awakenings during the night. L-dopa had a small beneficial effect on daytime and nighttime sleep. A better sleep quality resulted from the combined treatment with melatonin and L-dopa compared with L-dopa alone and to the MPTP condition.

in healthy humans [3,25]. However, sleep offset was unaffected after melatonin treatment, as reported in normal macaques [20]. The presence of a regular light–dark cycle is likely to counteract any possible phase-shifting effects of the hormone.

On the contrary, no significant benefit on sleep architecture was observed in the animals, which is consistent with a previous finding that the PSG features remained unchanged after administration of melatonin in people with PD [11]. It is, however, possible that prolonging the duration of the combined treatment with melatonin and L-dopa in a larger number of animals would have induced a significant benefit on all sleep parameters, including sleep architecture. During daytime, melatonin had no effect on motor symptoms or daytime sleep. However, the dose of melatonin administered to the animals 2 h before lights off may not have sufficiently improved nighttime sleep quality to act on daytime sleepiness the day after. In that respect, it is interesting to note that for people with PD, 3 mg of melatonin given 1 h before bedtime did not affect daytime sleepiness [11], whereas a higher dose of 5 mg reduced it [10]. It can thus be hypothesized that a sufficient dose of melatonin is required to ensure a more physiological sleep–wake cycle, and to have a beneficial effect on daytime sleep.

It was reported that for people with PD, the timing of melatonin secretion onset or offset phases did not change, whereas circulating melatonin levels were reduced [8,9]. Moreover, these differences in melatonin levels were reported to significantly correlate with reduced slow-wave and REM sleep [8]. On the other hand, no melatonin deficit was observed in parkinsonian macaques, except that the amount released over a 24-h period varied with a peak at 06:00 compared with control animals [26]. In this study, however, MPTP-treated macaques did not receive L-dopa treatment, which may influence the amplitude and phase secretion of melatonin, as already suggested [27].

Previous results have suggested that administration of melatonin can prevent the deleterious effects of neurotoxins. This has been reported in neurotoxin models of PD [12,13,28], but is contradicted by other literature data [14,15,29]. It is possible that the neuroprotective effects of melatonin depend on its elevated circulating levels [15]. A better understanding of this neuroprotective aspect with experiments on blood dosage of melatonin in monkeys may help to understand the mechanisms underlying the benefit of melatonin, and thus to more precisely characterize its use in people with PD. Melatonin exerts its physiological, hypnotic and chronobiotic actions through MT1 and MT2 receptors expressed in different brain areas. The presence of these receptors has been demonstrated in the suprachiasmatic nucleus, which is considered as the major sleep–wake-cycle generating center. Exogenous melatonin may thus improve sleep disorders by its direct action on this central clock, influencing the amplitude of oscillations and the phase advance of the rhythm. MT1 and MT2 are also present in the dopaminergic pathways. These receptors exhibit decreased expression in people with PD [7], suggesting that the melatoninergic system might be involved in sleep disorders of PD. It would therefore be interesting to test the effects of melatonin in the presence of MT1 or MT2 receptor antagonist to characterize the melatonin receptor subtype involved in the improvement of sleep quality in MPTP-intoxicated monkeys. Further studies are thus needed to elucidate the role of melatonin and its receptors in the pathogenesis and treatment of PD.

**Table 2**
Intra-individual sleep parameters evaluated at baseline, after MPTP intoxication, and after subsequent treatment with L-dopa alone, and then with melatonin combined with L-dopa in four macaques, and finally after a 3-day washout in three of them.

| M. No. | CTL $n=4$ | MPTP $n=4$ | L-dopa alone $n=4$ | Melatonin + L-dopa $n=4$ | L-dopa 2 $n=3$ |
|---|---|---|---|---|---|
| No. 1 | | | | | |
| Motor score | 0 | 8.5 | 2 | 1 | |
| Sleep efficiency (%) | 100 ± 1.9 | 75.9 ± 3.8 | 78.1 ± 1.4 | 92.8**,§§ | |
| Wake time (%) | 14.6 ± 1.6 | 31.2 ± 3.2 | 31.3 ± 2.1 | 25.4*,§ | |
| SWS (%) | 30.3 ± 1.3 | 20.4 ± 0.9 | 20.0 ± 1.3 | 23.5*,§ | |
| REM (%) | 24.1 ± 0.4 | 20.7 ± 0.9 | 22.4 ± 1.5 | 19.5* | |
| Sleep onset latency (min) | 29.6 ± 2.3 | 54.1 ± 5.3 | 53.2 ± 7.9 | 36§ | |
| REM latency (min) | 45.7 ± 10.1 | 97.2 ± 26.1 | 106.7 ± 38.7 | 85§ | |
| No. 2 | | | | | |
| Motor score | 0 | 13 | 2.5 | 3 | 2.5 |
| Sleep efficiency (%) | 100 ± 5.6 | 62.5 ± 4.1 | 68.7 ± 3.3 | 82.1**,§ | 72.7 |
| Wake time (%) | 18.6 ± 4.6 | 49.3 ± 3.2 | 44.0 ± 2.7 | 33.1*,§ | 40.0 |
| SWS (%) | 26.1 ± 4.4 | 9.6 ± 0.9 | 12.4 ± 2.1 | 11.5 | 12.0 |
| REM (%) | 22.0 ± 1.5 | 14.3 ± 1.0 | 15.8 ± 3.1 | 15.5 | 15.3 |
| Sleep onset latency (min) | 22.0 ± 3.3 | 41.0 ± 12.8 | 41.5 ± 14.2 | 36 | 39 |
| REM latency (min) | 72.2 ± 24.6 | 106.0 ± 35.6 | 113.7 ± 27.6 | 98 | 114 |
| No. 3 | | | | | |
| Motor score | 0 | 10 | 2.5 | 2 | 2 |
| Sleep efficiency (%) | 100 ± 2.7 | 65.5 ± 2.3 | 73.5 ± 5.1 | 82.3§ | 71.6 |
| Wake time (%) | 16.5 ± 1.9 | 46.0 ± 2.1 | 39.3 ± 2.6 | 32.3§§ | 37.0 |
| SWS (%) | 23.2 ± 6.9 | 10.5 ± 5.1 | 9.2 ± 1.2 | 12.1 | 13.6 |
| REM (%) | 20.0 ± 1.7 | 15.2 ± 2.1 | 18.1 ± 3.2 | 17.2 | 16.4 |
| Sleep onset latency (min) | 11.4 ± 6.2 | 39.5 ± 7.1 | 38.7 ± 2.5 | 23*,§ | 48 |
| REM latency (min) | 57.6 ± 19.5 | 133.2 ± 41.9 | 112.7 ± 38.5 | 54 | 75 |
| No. 4 | | | | | |
| Motor score | 0 | 10 | 2 | 2 | 2 |
| Sleep efficiency (%) | 100 ± 3.4 | 73.0 ± 1.5 | 79.0 ± 5.5 | 82.7§§ | 79.8 |
| Wake time (%) | 18.3 ± 0.7 | 40.1 ± 2.1 | 37.0 ± 4.6 | 28.4§§ | 34.2 |
| SWS (%) | 15.8 ± 1.4 | 9.5 ± 1.1 | 11.0 ± 1.5 | 13.2§ | 12.2 |
| REM (%) | 22.0 ± 0.5 | 19.0 ± 1.0 | 21.6 ± 1.4 | 22.9§ | 20.3 |
| Sleep onset latency (min) | 13.8 ± 5.3 | 38.0 ± 3.7 | 32.7 ± 2.1 | 27*,§ | 40 |
| REM latency (min) | 30.8 ± 10.3 | 96.2 ± 14.6 | 53.0 ± 21.1 | 51§ | 33 |

*Abbreviations:* CTL, control; L-dopa, levodopa; MPTP, 1-methyl-4-phenyl-1,2,3,6-tetrahydropyridine; REM, rapid eye movement; SWS, slow-wave sleep.
Each column represents mean values (±SD) derived from all nights of sleep recordings per each study period. For each sleep parameter and for each animal, the mean of the values obtained after melatonin + L-dopa was compared to the value obtained after MPTP intoxication and after L-dopa alone using comparison of an observed mean with a theoretical value [21,22]. A recording after a 3-day washout period was performed after the combined treatment with melatonin and L-dopa phase (L-dopa 2).
* $p < 0.05$ and ** $p < 0.01$, melatonin + L-dopa vs MPTP values.
§ $p < 0.05$ and §§ $p < 0.01$, melatonin + L-dopa vs MPTP values.

In conclusion, this study provides experimental evidence that melatonin improves sleep disorders in parkinsonian monkeys. This finding supports the view that melatonin treatment has a therapeutic potential to treat sleep disturbances of people with PD.

## Financial disclosures

The authors declare that there are no financial interests that represent potential conflicts of interest.

## Conflict of interest

The authors declare no conflicts of interest.

The ICMJE Uniform Disclosure Form for Potential Conflicts of Interest associated with this article can be viewed by clicking on the following link: http://dx.doi.org/10.1016/j.sleep.2015.06.018.

## Acknowledgments

The research leading to these results has received funding from the program “Investissements d’avenir” ANR-10-IAIHU-06. The authors would like to thank Nick Barton for language editing.

## References

[1] Schrempf W, Brandt MD, Storch A, et al. Sleep disorders in Parkinson’s disease. J Parkinsons Dis 2014;4:211–21.
[2] Wailke S, Herzog J, Witt K, et al. Effect of controlled-release levodopa on the microstructure of sleep in Parkinson’s disease. Eur J Neurol 2011;18:590–6.
[3] Zhdanova IV, Lynch HJ, Wurtman RJ. Melatonin: a sleep-promoting hormone. Sleep 1997;20:899–907.
[4] Arendt J, Skene DJ. Melatonin as a chronobiotic. Sleep Med Rev 2005;9:25–39.
[5] Campos FL, Da Silva-Junior FP, De Bruin VM, et al. Melatonin improves sleep in asthma: a randomized, double-blind, placebo-controlled study. Am J Respir Crit Care Med 2004;170:947–51.
[6] Pandi-Perumal SR, Zisapel N, Srinivasan V, et al. Melatonin and sleep in aging population. Exp Gerontol 2005;40:911–25.
[7] Adi N, Mash DC, Ali Y, et al. Melatonin MT1 and MT2 receptor expression in Parkinson’s disease. Med Sci Monit 2010;16:BR 61–7.
[8] Breen DP, Vuono R, Nawarathna U, et al. Sleep and circadian rhythm regulation in early Parkinson disease. JAMA Neurol 2014;71:589–95.
[9] Videnovic A, Noble C, Reid KJ, et al. Circadian melatonin rhythm and excessive daytime sleepiness in Parkinson disease. JAMA Neurol 2014;71:463–9.
[10] Dowling GA, Mastick J, Colling E, et al. Melatonin for sleep disturbances in Parkinson’s disease. Sleep Med 2005;6:459–66.
[11] Medeiros CA, Carvalhedo De Bruin PF, Lopes LA, et al. Effect of exogenous melatonin on sleep and motor dysfunction in Parkinson’s disease. A randomized, double blind, placebo-controlled study. J Neurol 2007;254:459–64.
[12] Absi E, Ayala A, Machado A, et al. Protective effect of melatonin against the 1-methyl-4-phenylpyridinium-induced inhibition of complex I of the mitochondrial respiratory chain. J Pineal Res 2000;29:40–7.
[13] Dabbeni-Sala F, Di Santo S, Franceschini D, et al. Melatonin protects against 6-OHDA-induced neurotoxicity in rats: a role for mitochondrial complex I activity. FASEB J 2001;15:164–70.
[14] Van Der Schyf CJ, Castagnoli K, Palmer S, et al. Melatonin fails to protect against long-term MPTP-induced dopamine depletion in mouse striatum. Neurotox Res 2000;1:261–9.
[15] Morgan WW, Nelson JF. Chronic administration of pharmacological levels of melatonin does not ameliorate the MPTP-induced degeneration of the nigrostriatal pathway. Brain Res 2001;921:115–21.
[16] Willis GL, Armstrong SM. A therapeutic role for melatonin antagonism in experimental models of Parkinson’s disease. Physiol Behav 1999;66:785–95.

[17] Barraud Q, Lambrecq V, Forni C, et al. Sleep disorders in Parkinson's disease: the contribution of the MPTP non-human primate model. Exp Neurol 2009;219:574–82.
[18] Belaid H, Adrien J, Laffrat E, et al. Sleep disorders in parkinsonian macaques: effects of l-dopa treatment and pedunculopontine nucleus lesion. J Neurosci 2014;34:9124–33.
[19] Herrero MT, Perez-Otano I, Oset C, et al. GM-1 ganglioside promotes the recovery of surviving midbrain dopaminergic neurons in MPTP-treated monkeys. Neuroscience 1993;56:965–72.
[20] Zhdanova IV, Geiger DA, Schwagerl AL, et al. Melatonin promotes sleep in three species of diurnal nonhuman primates. Physiol Behav 2002;75:523–9.
[21] Crawford JR, Garthwaite PH. Investigation of the single case in neuropsychology: confidence limits on the abnormality of test scores and test score differences. Neuropsychologia 2002;40:1196–208.
[22] Crawford JR, Howell DC. Comparing an individual's test score against norms derived from small samples. Clin Neuropsychol 1998;12:482–6.
[23] Kunz D, Bes F. Melatonin effects in a patient with severe REM sleep behavior disorder: case report and theoretical considerations. Neuropsychobiology 1997;36:211–14.
[24] Takeuchi N, Uchimura N, Hashizume Y, et al. Melatonin therapy for REM sleep behavior disorder. Psychiatry Clin Neurosci 2001;55:267–9.
[25] Stone BM, Turner C, Mills SL, et al. Hypnotic activity of melatonin. Sleep 2000;23:663–9.
[26] Barcia C, Bautista V, Sanchez-Bahillo A, et al. Circadian determinations of cortisol, prolactin and melatonin in chronic methyl-phenyl-tetrahydropyridine-treated monkeys. Neuroendocrinology 2003;78:118–28.
[27] Fertl E, Auff E, Doppelbauer A, et al. Circadian secretion pattern of melatonin in Parkinson's disease. J Neural Transm Park Dis Dement Sect 1991;3:41–7.
[28] Antolin I, Mayo JC, Sainz RM, et al. Protective effect of melatonin in a chronic experimental model of Parkinson's disease. Brain Res 2002;943:163–73.
[29] Itzhak Y, Martin JL, Black MD, et al. Effect of melatonin on methamphetamine- and 1-methyl-4-phenyl-1,2,3,6-tetrahydropyridine-induced dopaminergic neurotoxicity and methamphetamine-induced behavioral sensitization. Neuropharmacology 1998;37:781–91.

# AXE 2. ETUDE ANATOMIQUE DE LA REGION LOCOMOTRICE MESENCEPHALIQUE

# *DIVERSITE ANATOMO-FONCTIONNELLE DE LA MLR*

## A. INTRODUCTION

Un certain nombre de travaux expérimentaux, essentiellement chez le rat et le chat, et dans une moindre mesure chez le singe, ont permis d'identifier les connexions du PPN (figure 18) et du CuN. Cependant l'absence de limites nettes, la présence de nombreux faisceaux de fibres et l'hétérogénéité des populations neuronales dans cette région mésencéphalique de la formation réticulée, rendent les résultats difficiles à interpréter et de nombreuses imprécisions persistent. Nous détaillerons ici essentiellement les données de la littérature existant chez le primate.

### 1. Hodologie du PPN

#### *a) Afférences*

Les afférences du PPN les plus connues et les plus denses sont celles provenant des ganglions de la base (GB), notamment des deux voies de sortie à savoir le Globus Pallidus interne (GPi) (Shink et al., 1997), et la Substantia Nigra pars reticulata (SNr) (Rolland et al., 2011). Les afférences du GPi proviennent principalement des neurones de type I (parent 2001), qui vont innerver aussi le noyau Ventral Antérieur et les noyaux intralaminaires du thalamus (dont les noyaux centre-médian (CM) et parafasciculaire (Pf)). Ces projections pallidales vers le PPN se composent d'axones relativement épais ayant un trajet assez direct avec peu de collatérales, suggérant une transmission rapide des informations. Le PPN reçoit aussi des afférences excitatrices glutamatergiques en provenance du NST (Parent et Smith, 1987; Smith et al., 1990), ainsi qu'une innervation dopaminergique (Rolland et al 2009). L'ensemble de ces afférences en provenance des GB se termine préférentiellement sur les neurones non cholinergiques de la MLR (environ 70%), quelle que soit l'espèce animale étudiée (Noda et Oka, 1986; Granata et Kitai, 1991; Spann et Grofova, 1991; Shink et al.,

1997; Rolland et al., 2011). Cependant, il reste à déterminer exactement où se terminent les afférences en provenance des GB au sein du PPN et / ou au sein noyau sub-cunéiforme décrit antérieurement par Olszewski et Baxter (Olszewski et Baxter, 1954).

Les neurones du PPN reçoivent également des afférences glutamatergiques en provenance des cortex moteurs (primaire, pré-moteur et aire motrice supplémentaire) chez le macaque (Matsumura et al., 2000), et à un moindre degré en provenance du cortex limbique (Chiba et al., 2001). Une seule étude réalisée chez le primate montre l'existence de projections en provenance des noyaux cérébelleux profonds (Hazrati et Parent, 1992). Par ailleurs des afférences provenant des segments cervicaux et lombaires de la moelle épinière ont été mises en évidence chez le rat (Grunwerg et al., 1992) et le chat (Hylden et al., 1985), faisant du PPN un relais potentiel pour les afférences sensorielles de la moelle épinière vers le thalamus. Enfin, une projection en provenance des neurones orexinergiques de l'hypothalamus a été mise en évidence chez le chat (Takakusaki et al., 2005) et le rongeur (Peyron et al., 1998; Nambu et al., 1999).

### b) Efférences

Il a été décrit des efférences ascendantes ou descendantes du PPN, bien que la plupart des neurones envoient des projections dans les deux sens.

Les projections ascendantes du PPN sont controlatérales pour 40% des neurones chez le primate (Lavoie et Parent, 1994b). Le PPN innerve de façon diffuse l'ensemble des noyaux du thalamus, mais avec une préférence pour les noyaux intralaminaires (dont les noyaux Pf et CM) et le noyau péri-thalamique (Lavoie et Parent, 1994b; Galvan et Smith, 2011). Chez le rat, ces projections proviennent essentiellement des neurones cholinergiques (Sofroniew et al., 1985; Hallanger et al., 1987; Rye et al., 1987; Steriade et al., 1988; Parent et Descarries, 2008), ceci n'étant pas encore démontré chez le primate. L'autre projection majeure du PPN chez le primate s'effectue vers l'ensemble des GB (Lavoie et Parent, 1994b,c), principalement le NST (Lavoie et Parent, 1994b) et la SNc (Charara et al., 1996), à un niveau moindre vers la SNr et le pallidum interne, et encore moindre le pallidum externe (Lavoie et Parent, 1994b). Le PPN modulerait ainsi la libération de dopamine (Mena-Segovia et al., 2008; Hong et Hikosaka, 2014). De très faibles projections vers le striatum (noyau accumbens, caudé et

putamen) ont également été observées chez le primate (Smith et Parent, 1986; Nakano et al., 1990; Lavoie et Parent, 1994b), alors qu'une forte innervation striatale a été décrite chez le rat ( Edley et Graybiel, 1983; Sofroniew et al., 1985; Woolf et Butcher, 1986; Scarnati et al., 1988; Steriade et al., 1988; Bevan et Bolam, 1995; Takakusaki et al., 1996).

Chez le primate ont été aussi montrées des projections descendantes vers la formation réticulée ponto-médullaire (Rolland et al., 2011) à l'origine du tractus réticulo-spinal (Sakai et al., 2009). Une faible proportion de ces efférences a été retrouvée au niveau de la moelle épinière (Garcia-Rill et Skinner, 1987b; Rolland et al., 2011).

Enfin, complétant ces données, des études d'imagerie utilisant les techniques de tractographie ont été effectuées chez le singe et chez l'homme, confirmant l'existence de fortes connexions entre le PPN, le cortex, le pallidum, le NST et le thalamus (Aravamuthan et al., 2007; 2009; Muthusamy et al., 2007).

Figure 18: Connectivité du PPN d'après les données de la littérature

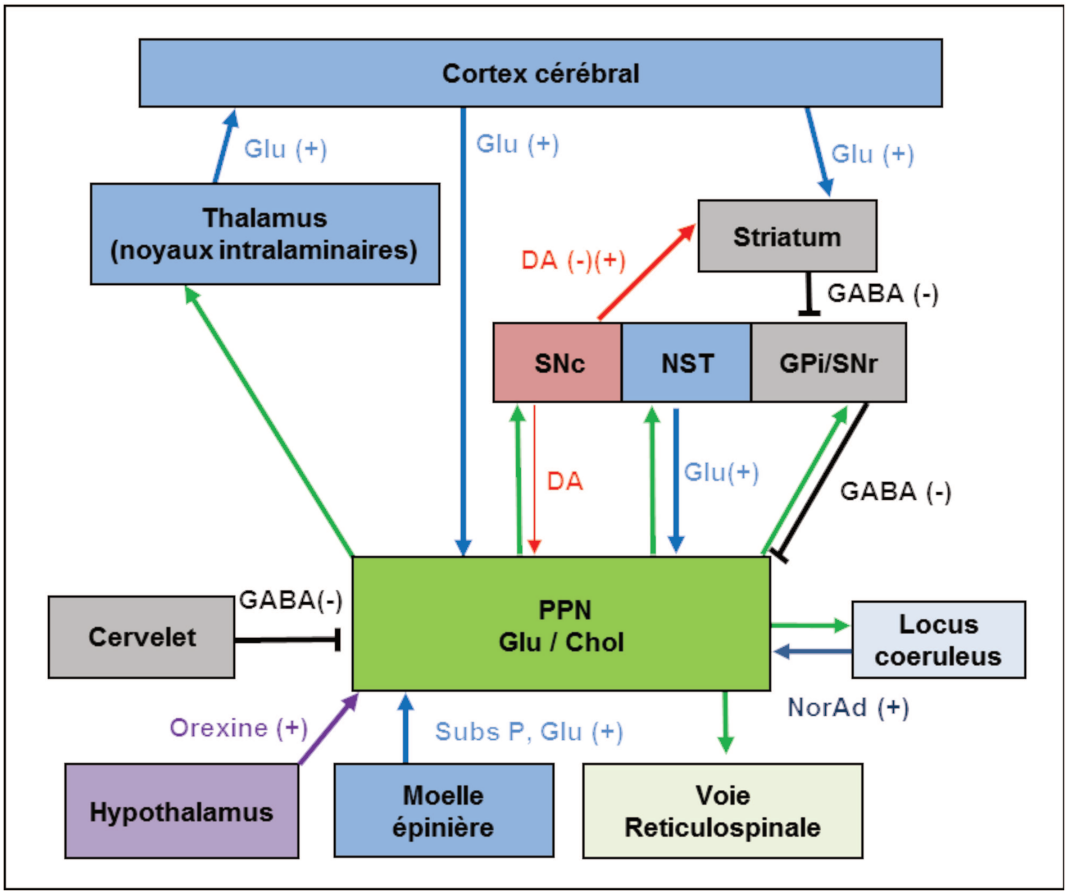

## 2. Hodologie du noyau Cunéiforme

Les afférences et efférences du CuN sont moins bien connues. Notre équipe a montré que le CuN reçoit des projections chez le primate essentiellement de la SNr, et très peu du GPi, contrairement au PPN, impliquant que les deux voies de sortie des GB contrôlent différentes régions de la MLR (Rolland et al., 2011). Ces résultats suggèrent donc que la voie SNr-CuN pourrait contrôler la posture axiale tandis que la voie GPi-PPN modulerait la motricité des membres et donc la locomotion. Une innervation dopaminergique du CuN a été également mise en évidence (Rolland et al., 2009) (figure 19). Une projection ascendante spino-mésencéphalique n'a été décrite que chez le rat (Menetrey et al., 1982; Veazey et Severin, 1982; Lima et Coimbra, 1989).

Il a été montré chez le primate des efférences ascendantes vers les neurones dopaminergiques de la SN (Hong et Hikosaka, 2014) et descendantes vers la formation réticulée ponto-bulbaire à l'origine du faisceau réticulo-spinal (Rolland et al., 2011).

Figure 19: Distribution de l'innervation dopaminergique
vers le CuN et le PPN
*d'après Rolland et al (2009)*

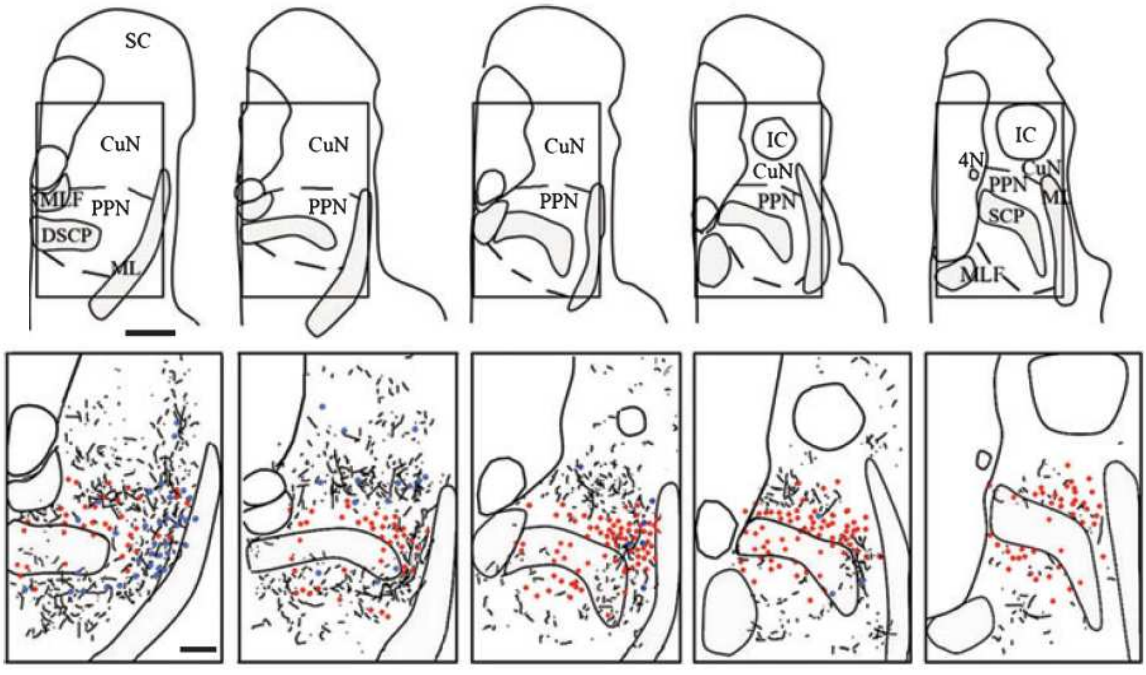

## B. OBJECTIFS

La MLR est impliquée dans diverses fonctions en plus de la locomotion, que nous avons rappelées précédemment. Chez l'homme, la SCP du PPN des patients parkinsoniens illustre bien la complexité fonctionnelle de cette région encore partiellement méconnue (Lau et al., 2015; Stefani et al., 2013; Tattersall et al., 2014). De plus, les rôles spécifiques du PPN et CuN restent peu identifiés, particulièrement chez le primate où les résultats expérimentaux sont même contradictoires. Ces ambiguïtés proviennent en partie de la difficulté de caractérisation anatomique précise du PPN et du CuN et de l'absence de limites nettes (Mena-Segovia et al., 2009; Wang et Morales, 2009). De plus, les connexions du PPN et surtout celles du CuN en fonction des territoires anatomo-fonctionnels n'ont jamais été étudiées avec précision.

Le but de cette étude est de définir l'anatomie hodologique du PPN et du CuN chez le singe et chez l'homme en fonction des trois grands territoires anatomo-fonctionnels. Nous avons ainsi identifié et comparé les connexions du PPN et du CuN par des techniques de traçage axonal chez le singe et par tractographie chez l'homme (Sebille et al., 2017). Les résultats obtenus chez l'homme ont fait l'objet d'un travail de thèse d'une autre étudiante (S. Sebille). Bien qu'illustrés, ils ne seront pas détaillés ici.

## C. MÉTHODOLOGIE

Les injections de Biotin Dextran Amine (BDA), traceur axonal à la fois antérograde et rétrograde, ont été effectuées chez 5 macaques, en utilisant l'approche stéréotaxique avec ventriculographie précédemment illustrée. Deux injections de BDA ont été effectuées dans le PPN (une antérieure et l'autre postérieure), et deux autres dans le CuN (une antérieure et l'autre postérieure). Une 5$^{ème}$ injection plus large incluant le PPN et le CuN a également été réalisée. Les singes ont été sacrifiés 13 jours après l'injection, et après extraction les cerveaux ont été coupés au microtome en coupes de 50 µm perpendiculaires à la ligne CA-CP.

La BDA a été révélée sur des coupes régulièrement espacées de 500 µm. Sur une 2$^{ème}$ série de coupes, la nicotinamide adenine dinucleotide phosphate diaphorase histochimie (NADPH) a été mise en évidence (Hirsch et al., 1987) afin d'identifier les neurones

cholinergiques du PPN et donc d'en délimiter les contours. La délimitation du CuN s'est effectuée en utilisant les repères anatomiques précédemment décrits. Les corps cellulaires et terminaisons nerveuses marqués par la BDA au sein des différentes structures ont été cartographiés à l'aide d'un logiciel d'analyse d'image (Mercator, ExploraNova). La délimitation des territoires anatomo-fonctionnels (sensori-moteur, associatif et limbique) au sein des différentes structures cérébrales d'intérêt s'est appuyée sur les données préalablement publiées dans la littérature.

L'étude de la connectivité du PPN et du CuN chez l'homme a été réalisée en parallèle, utilisant une méthodologie nouvelle de tractographie en IRM (Philippe et al., 2015).

## D. Synthèse des résultats obtenus

*Projections corticales*

Après injection dans le PPN, des corps cellulaires marqués rétrogrades ont été visualisés dans les aires corticales motrices (aires motrice primaire, pré-motrice, motrice supplémentaire et oculomotrice), avec une connexion plus forte vers le cortex moteur lorsque l'injection était située dans la partie antérieure du PPN. Des corps cellulaires marqués ont aussi été observés dans le cortex insulaire, et de façon moindre dans les aires corticales limbiques. La présence de terminaisons axonales marquées dans le PPN après injection de BDA dans l'aire corticale infralimbique (A10m) d'un autre animal a permis de confirmer les connections du PPN avec le cortex limbique.

La majorité des corps cellulaires rétrogrades marqués après injection dans le CuN ont été visualisés dans les aires corticales limbiques, et dans l'ensemble du cortex insulaire, ainsi qu'au niveau du cortex auditif et somato-sensoriel secondaire. A l'inverse du PPN, très peu de corps cellulaires ont été observés au niveau des cortex moteurs. L'injection du cortex infra limbique a permis de mettre en évidence des terminaisons marquées dans la partie la plus médio-ventrale du CuN.

*Projections vers les GB, thalamus et amygdale*

Les terminaisons du PPN ont été mises en évidence de façon homogène dans l'ensemble des 3 territoires anatomo-fonctionnels du NST, de la SN (surtout SNc et VTA) du

GPi, à un bien moindre degré du GPe, et très peu dans le striatum. Par ailleurs, de nombreuses terminaisons étaient marquées au niveau du basal forebrain (plus spécifiquement au sein de l'extended amygdala et du noyau central de l'amygdale), ainsi qu'au niveau des noyaux intralaminaires postérieurs du thalamus (CM et Pf).

Les terminaisons axonales marquées après injections dans le CuN ont été retrouvées dans les mêmes noyaux que le PPN, mais elles occupaient principalement les territoires limbiques de ces noyaux. Des amas denses de terminaisons s'étendaient ventralement au GPi, GPe, l'amygdale et le noyau central de l'amygdale.

Les résultats de tractographie chez l'homme ont retrouvé globalement la même connectivité du PPN et du CuN sur l'ensemble des ganglions de la base, l'amygdale, du thalamus et du cortex.

## E. Discussion et Conclusions

*Diversité des projections du PPN*

Le PPN apparaît fortement connecté aux GB chez le primate (Lavoie et Parent, 1994b; Shink et al., 1997; Aravamuthan et al., 2007; 2009; Muthusamy et al., 2007), cette innervation se faisant sur les 3 territoires anatomo-fonctionnels, et très peu sur le striatum, contrairement à ce qui a été décrit chez le rongeur (Dautan et al., 2014). Nos résultats chez le primate montrent aussi que le PPN est connecté aux aires corticales motrices, confirmant les résultats de littérature chez le singe par traçage axonal (Matsumura et al., 2000), et chez l'homme par tractographie (Aravamuthan et al., 2007; 2009; Muthusamy et al., 2007). Chez le singe, la partie antérieure du PPN est plus fortement connectée au cortex moteur, impliquant une organisation topographique au sein du PPN. Le PPN antérieur pourrait ainsi avoir un rôle prépondérant dans le contrôle de la locomotion chez le singe, confirmant aussi les résultats obtenus chez le rongeur, où seules les lésions situées à la partie antérieure induisaient une diminution de la locomotion spontanée (Alderson et al., 2008). Cependant il est difficile de faire une corrélation anatomique équivalente chez l'homme, les différences d'orientation du tronc cérébral ne permettant pas la même distinction antéro-postérieure au sein du PPN similaire à celle décrite chez les animaux. Ainsi, bien que cette région antérieure du PPN

semble être la cible à privilégier pour moduler la locomotion, il reste à déterminer quelle est la zone équivalente chez l'homme afin d'espérer améliorer la marche et de la posture des patients par SCP du PPN.

Nos résultats mettent aussi en évidence les nombreuses connexions non motrices du PPN. Les projections vers le thalamus notamment avaient été rapportées chez le rat (Barroso-Chinea et al., 2011), le chat (Pare et al., 1988) et le singe (Parent et al., 1988). Nous avons montré que le PPN projette vers l'ensemble des noyaux Pf et CM du thalamus. Ces noyaux intralaminaires sont le prolongement de la formation réticulée et font partie de la voie de projection ascendante vers les noyaux du thalamus jouant un rôle dans l'éveil cortical (Steriade et al., 1988). Ils ont de plus un rôle dans l'attention dirigée et les processus d'apprentissage (Galvan et Smith, 2011).

Le PPN reçoit aussi des afférences en provenance de l'ensemble du cortex insulaire, antérieur et postérieur. L'insula est bien connue pour avoir un rôle dans l'intégration de diverses informations liées à l'intéroception, en particulier viscérale, à la douleur, aux émotions négatives (dégout en particulier) mais aussi cognitives et socio-émotionnelles. Une cartographie fonctionnelle de l'insula a été réalisée grâce aux données de traçage chez le singe (Mesulam et Mufson, 1985; Augustine, 1996; Fudge et al., 2005) et en imagerie fonctionnelle chez l'homme (Kurth et al., 2010a,b). Ainsi le cortex insulaire postérieur est plutôt impliqué dans les fonctions somesthésiques. La partie antéro-dorsale de l'insula, de par ses connexions avec les cortex associatifs frontaux, est quant à elle surtout impliquée dans la mémoire de travail et l'attention (Augustine, 1996; Kurth et al., 2010b). De plus, cette région joue un rôle important dans les processus d'apprentissage et de prise de décision, particulièrement dans les situations d'incertitude ou à risque, processus sensibles à la punition (Singer et al., 2009, Palminteri et al., 2012). Enfin, le cortex insulaire antéro-basal, ayant des connexions avec l'amygdale et le cortex entorhinal, serait plutôt lié aux fonctions olfactives et socio-émotionnelles, dont l'empathie (Philips et al., 2003, Singer et al., 2006). Par ces afférences, le PPN intègre très probablement des informations très diverses allant de l'intéroception aux fonctions cognitives et socio-émotionnelles.

Le PPN reçoit d'autres sources d'informations limbiques, comme le montrent nos résultats avec la présence d'afférences directes des aires A10m et A25. Cela avait été précédemment décrit chez le primate par une seule étude (Chiba et al., 2001) et le rongeur ( Sesack et al., 1989; Semba et Fibiger, 1992), suggérant un rôle du PPN dans l'intégration des informations émotionnelles et motivationnelles. Renforçant cette hypothèse, une projection dense vers le noyau central de l'amygdale a été retrouvée chez le primate. Ce noyau reçoit des afférences provenant du complexe basolatéral de l'amygdale, qui a un rôle dans l'intégration des informations sensorielles, et va ensuite projeter vers l'hypothalamus latéral et la substance grise périaqueducale impliqués respectivement dans les réponses autonomique et comportementale liées à la peur (Ledoux et al., 1988, Sah et al., 2003). En effet il a été montré qu'une stimulation du noyau central de l'amygdale chez le rat va entraîner une réaction comportementale de peur même en l'absence de conditionnement préalable (Iwata et al., 1987).

En conclusion, l'analyse des projections suggère que le PPN a un rôle d'intégration des informations sensori-motrices, cognitives et émotionnelles, la partie antérieure du PPN chez le singe étant plutôt dévolue au contrôle moteur. La richesse de ces projections anatomiques permettent de mieux comprendre les données physiologiques acquises par notre équipe chez le patient puisqu'il a été montré qu'un même neurone du PPN pouvait intégrer des informations diverses à la fois motrices et non motrices. En effet la majorité des neurones enregistrés au sein du PPN modifiait leur décharge à la fois lors d'un mouvement actif du membre supérieur, lors de la présentation d'un stimulus visuel mais aussi pendant l'imagination de la marche, suggérant la complexité de la fonction du PPN (Lau et al., 2015) (figure 20).

Figure 20: Localisation des neurones activés pendant les différentes tâches (visuelle, marche imaginaire, motrice) dans le PPN et le NST de sujets parkinsoniens
*d'après Lau et al (2015)*

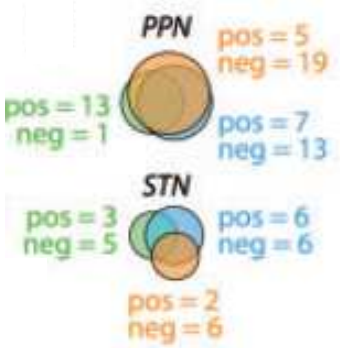


*Visuelle* *Motricité*

*Marche imaginaire*

*Connexions limbiques du CuN*

Nous avons montré pour la première fois que le CuN est préférentiellement connecté aux territoires limbiques des différents noyaux des GB (NST et GP) et du thalamus (noyau Pf) chez le primate. Ces résultats concordent avec les données rapportées pour le noyau mésencéphalique profond du rongeur (équivalent au CuN) (Rodriguez et al., 2001) avec des projections décrites uniquement vers la partie ventromédiale limbique du NST (Veazey et Severin, 1980). De plus, nos résultats montrent que le CuN va préférentiellement innerver la VTA, partie intégrante du système limbique dopaminergique, ainsi que le basal forebrain (extended amygdala) et le noyau central de l'amygdale. De plus, le CuN reçoit des projections du cortex limbique chez le primate et aussi associatif insulaire mais non moteur ce qui suggèrent que le CuN intègre prioritairement les informations émotionnelles et motivationnelles. D'autre part, le CuN, tout comme le PPN, a lui aussi une projection descendante vers la formation réticulée bulbaire du primate (Rolland et al., 2011), et pourrait donc jouer un rôle dans la modulation de l'activité locomotrice en fonctions des différentes intégrations limbiques.

Ces résultats anatomiques rejoignent les données physiologiques obtenues chez l'animal. En effet, il a été montré que des lésions du CuN chez le rat n'induisent pas d'effets

moteurs mais des changements comportementaux en réponse aux évènements renforçants (Allen et al., 1996), et des effets comparables à l'anxiété (réaction à la menace) (Walker et Winn, 2007). Ces données suggèrent que le CuN serait plutôt impliqué dans la production de mouvements réalisés dans certaines conditions et liées au contexte. Ainsi, il pourrait jouer un rôle central dans un circuit anatomique permettant d'avoir une réponse comportementale rapide vitale en cas d'évènements menaçants inattendus (Allen et al., 1996; Walker et Winn, 2007).

Le CuN représenterait donc au sein de la MLR une interface entre les systèmes limbique et moteur, afin d'adapter rapidement les réponses locomotrices à l'environnement, en particulier s'il est menaçant.

*Comparaison des connexions du PPN et du CuN chez l'homme*

Les résultats obtenus par tractographie chez l'homme ont montré des connexions en grande partie similaires à celles obtenues par traçage axonal chez le singe (figure 21 et 22). En effet, le PPN et le CuN sont fortement connectés à l'ensemble des GB, aux aires corticales sensori-motrices, associatives et limbiques, aux noyaux intralaminaires du thalamus et à l'amygdale. Il existe cependant quelques différences par rapport aux données chez le singe. Le CuN semble en effet connecté à l'ensemble des 3 territoires anatomo-fonctionnels chez l'homme, bien que celles des territoires limbiques prédominent. De même, des connexions entre les cortex moteurs et le CuN ont été mises en évidence chez l'homme contrairement aux résultats chez le singe. Ces différences pourraient être liées à la méthodologie utilisée, puisque les injections de traceur réalisées chez le singe ont été volontairement limitées afin d'avoir une meilleur précision dans la diffusion du traceur. Ainsi, des connexions du CuN avec les territoires sensori-moteurs auraient peut-être été mises en évidence chez le singe si les injections de traceurs avaient recouvert toute l'étendue du CuN. Par ailleurs cela pourrait aussi être lié à une différence anatomique entre l'homme et le singe, comme cela a été suggéré précédemment (Aravamuthan et al., 2008).

Figure 21: Connexions du PPN (rouge) et du CuN (bleu) avec le pallidum chez le singe et l'homme

*Représentation sur 2 coupes coronales du GP des terminaisons chez le singe (A) et du nombre de voxels chez l'homme (B)*

*C: Histogrammes représentant le pourcentage de voxels connectés chez l'homme*

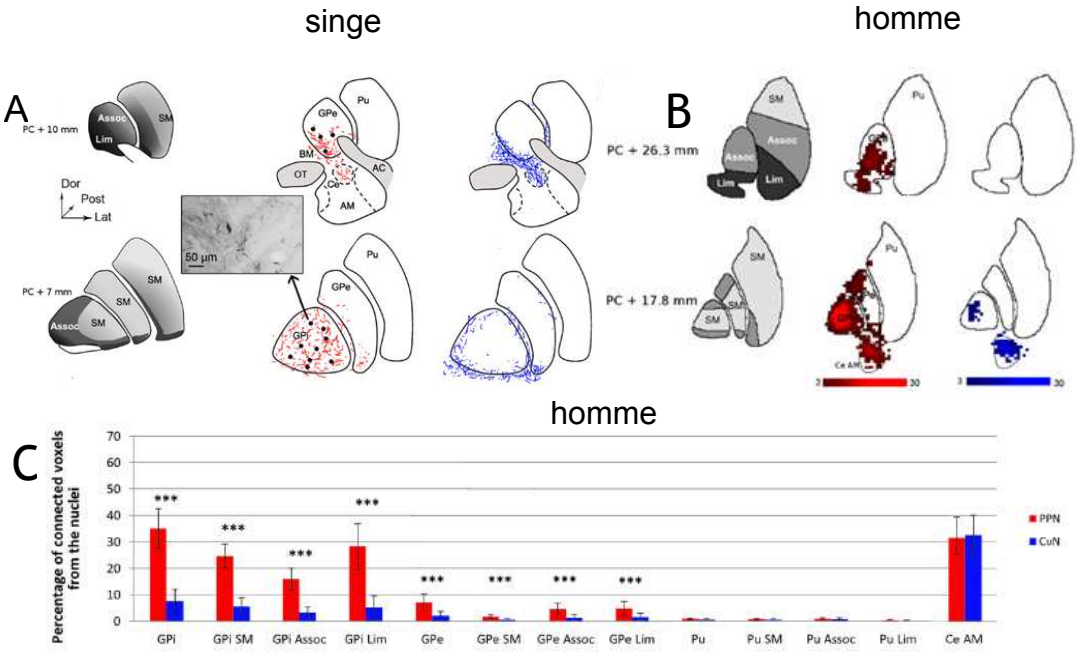

Figure 22: Connexions du PPN et du CuN avec le NST chez le singe et l'homme
*Représentation sur 3 coupes coronales du NST des terminaisons chez le singe (A) et du nombre de voxels chez l'homme (B)*
*C: Histogrammes représentant le pourcentage de voxels connectés chez l'homme*

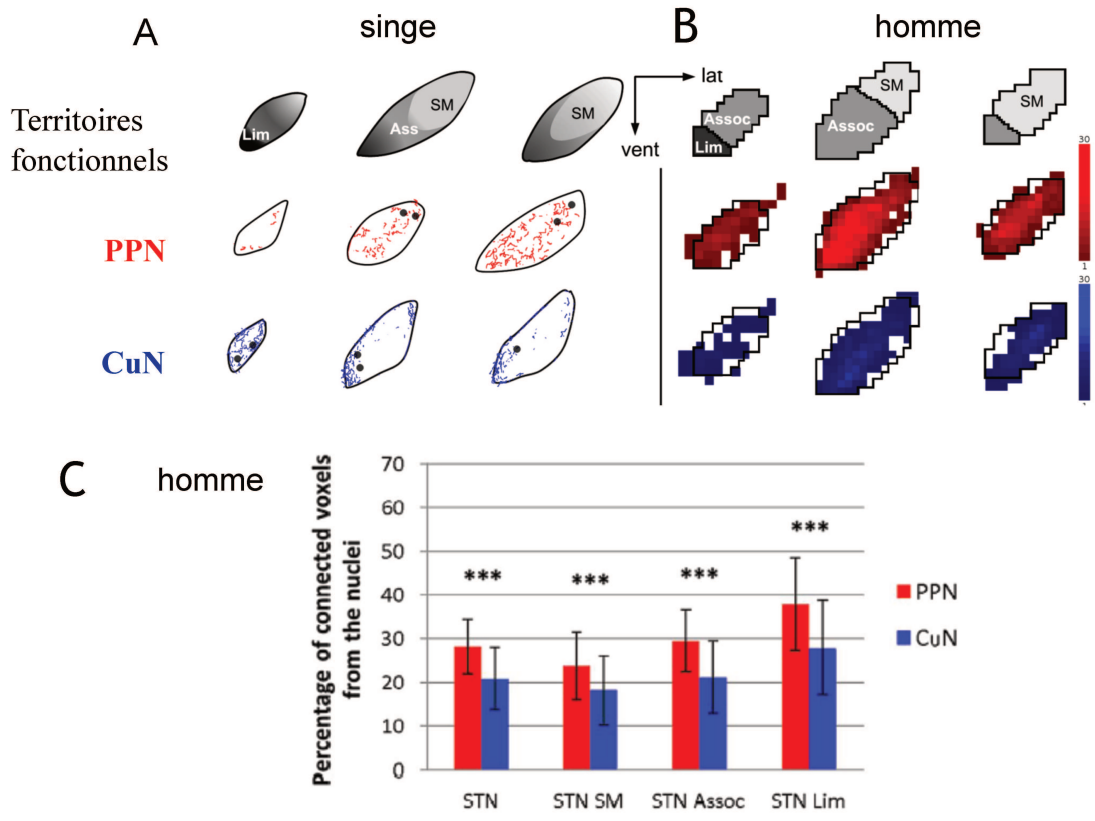

NeuroImage 147 (2017) 66–78

Contents lists available at ScienceDirect

NeuroImage

journal homepage: www.elsevier.com/locate/neuroimage

# Anatomical evidence for functional diversity in the mesencephalic locomotor region of primates

Sophie B. Sébille[a,c,1], Hayat Belaid[a,b,1], Anne-Charlotte Philippe[a,c], Arthur André[a,b], Brian Lau[a], Chantal François[a], Carine Karachi[a,b], Eric Bardinet[a,c,*]

[a] Sorbonne Universités, UPMC Univ Paris 06, CNRS, INSERM, APHP GH Pitié-Salpêtrière, Institut du cerveau et de la moelle épinière (ICM), F-75013 Paris, France
[b] Département de Neurochirurgie, Hôpital Pitie Salpêtrière, AP-HP, F-75013 Paris, France
[c] Centre de Neuro-Imagerie de Recherche (CENIR), Paris, France

ARTICLE INFO

*Keywords:*
Pedunculopontine nucleus
Cuneiform nucleus
Tract tracing
Monkey
Human
Tractography

ABSTRACT

The mesencephalic locomotor region (MLR) is a highly preserved brainstem structure in vertebrates. The MLR performs a crucial role in locomotion but also controls various other functions such as sleep, attention, and even emotion. The MLR comprises the pedunculopontine (PPN) and cuneiform nuclei (CuN) but their specific roles are still unknown in primates. Here, we sought to characterise the inputs and outputs of the PPN and CuN to and from the basal ganglia, thalamus, amygdala and cortex, with a specific interest in identifying functional anatomical territories. For this purpose, we used tract-tracing techniques in monkeys and diffusion weighted imaging-based tractography in humans to understand structural connectivity. We found that MLR connections are broadly similar between monkeys and humans. The PPN projects to the sensorimotor, associative and limbic territories of the basal ganglia nuclei, the centre median-parafascicular thalamic nuclei and the central nucleus of the amygdala. The PPN receives motor cortical inputs and less abundant connections from the associative and limbic cortices. In monkeys, we found a stronger connection between the anterior PPN and motor cortex suggesting a topographical organisation of this specific projection. The CuN projected to similar cerebral structures to the PPN in both species. However, these projections were much stronger towards the limbic territories of the basal ganglia and thalamus, to the basal forebrain (extended amygdala) and the central nucleus of the amygdala, suggesting that the CuN is not primarily a motor structure. Our findings highlight the fact that the PPN integrates sensorimotor, cognitive and emotional information whereas the CuN participates in a more restricted network integrating predominantly emotional information.

## 1. Introduction

The pedunculopontine nucleus (PPN) is located within the mesencephalic reticular formation of the upper brainstem. Together with the cuneiform nucleus (CuN), they have been named “the mesencephalic locomotor region” (MLR) because early studies showed that electrical stimulation of the MLR produces locomotion in various animal species (Garcia-Rill et al., 2014). Because of its anatomical location and the possibility to generate locomotor pattern, the MLR is considered to be a key generator of gait in the brain. However, the specific roles of the PPN and the CuN remain unclear, even if in decerebrate cat, stimulation of the CuN elicits locomotor patterns whereas stimulation of the PPN is able to change muscle tone (Takakusaki et al., 2003). Because the PPN and the CuN have no clear cut boundaries and are composed of clusters of various neuronal types (GABAergic, glutamatergic, cholinergic) (Mena-Segovia et al., 2009; Wang and Morales, 2009), their precise anatomical identification leads to divergence between authors and increases the confusion between these two nuclei.

*Abbreviations:* IV, trochlear nucleus; AC, anterior commissure; AM, amygdala; Ant, anterior; Assoc, associative territory; aud, auditory cortex; BC, brachium conjunctivum; BDA, biotine dextran amine; BM, nucleus basalis of Meynert; Ce, central nucleus of the amygdala; CM, centre median; cs, central sulcus; CuN, cuneiform nucleus; DBC, decussation of the brachium conjunctivum; DBS, deep brain stimulation, Dor: dorsal; FR, retroflex fascicle; DWI, diffusion-weighted imaging; GPi, internal pallidum; GPe, external pallidum; ia, anterior insula; IC, inferior colliculus; ins, insula; lat, lateral; Lim, limbic territory; MLF, medial longitudinal tract; MLR, mesencephalic locomotor region; NADPH, nicotinamide adenine dinucleotide phosphate; OT, optical tract; PAG, periaqueductal gray; PF, parafascicular nucleus; Post, posterior; PPN, pedunculopontine nucleus; Pu, putamen; SM, sensori-motor territory; SMA, supplementary motor area; SN, substantia nigra; STN, subthalamic nucleus; Sup, superior; temp, temporal cortex; VTA, ventral tegmental area.

* Correspondence to: Eric Bardinet, Institut du Cerveau et de la Moelle épinière, 47 boulevard de l'Hôpital, 75013 Paris, France.
*E-mail address:* eric.bardinet@upmc.fr (E. Bardinet).

[1] Authors contributed equally to this work.

http://dx.doi.org/10.1016/j.neuroimage.2016.12.011
Received 21 September 2016; Accepted 5 December 2016
Available online 09 December 2016
1053-8119/ 

Recently, deep brain stimulation (DBS) of the PPN area has been attempted in patients with Parkinson disease to improve gait disorders (Ferraye et al., 2009; Mazzone et al., 2005; Moro et al., 2010). Even if expected alleviation of gait remains disappointing, clinical and electrophysiological results strongly suggest that the MLR controls locomotion also in humans (Lau et al., 2015; Piallat et al., 2009; Tattersall et al., 2014). However, the precise implantation target within the MLR remains undefined, some suggests that DBS of the CuN should give better results than PPN DBS (Moro et al., 2010).

Besides locomotion, the MLR is known to control many other functions in the brain. As a part of the ascending reticular activating system, the PPN regulates sleep and arousal in rat (Datta, 2002; Steriade et al., 1990). Lesioning the rat PPN also affects attentional resources (Ainge et al., 2006; Okada et al., 2009), learning, reward and reinforcement processes (Inglis et al., 2001; Kozak et al., 2004; Steiniger and Kretschmer, 2004). PPN manipulations in rat are able to alter self-administration of nicotine and cocaine (Corrigall et al., 2002). In the macaque, PPN neurons send positive reward-related signals to nigral neurons where dopaminergic neurons are known to encode motivational values (Hong and Hikosaka, 2014; Okada and Kobayashi, 2013). In PD patients, DBS of the PPN has been shown to modulate non-motor functions. Indeed, PPN DBS could significantly improve sleep (Arnulf et al., 2010), executive functions and working memory (Stefani et al., 2013). These results emphasise the complex and integrative role of the PPN (Lau et al., 2015). The role of the CuN is much less known but this nucleus seems implicated in locomotion if related to aversive reactions, and in the perception of nociception in rodents (Allen et al., 1996). This result highlights the fact that the CuN is not just devoted to generating locomotion – it also integrates contextual information.

Analysis of the detailed connectivity of the MLR should help us understand the specific role that the PPN and CuN could play in motor, cognitive and emotional functions. Tract tracing studies in monkey have revealed that the PPN receives afferents from the motor cortices (Matsumura et al., 2000), from the output structures of the basal ganglia (internal pallidum (GPi) and substantia nigra (SN)) and from the subthalamic nucleus (STN) (Lavoie and Parent 1994a,b; Shink et al., 1997). The PPN ascending pathway projects to non-specific nuclei of the thalamus, in particular to the centre-median-parafascicular nuclei (CM-PF) (Parent et al., 1988; Steriade et al., 1988). The PPN descending outputs project to the ponto-bulbar reticulospinal formation (Rolland et al., 2011). Even if the connections of the CuN are less known, it has been demonstrated in monkey that the CuN only receives projections from the SN (Rolland et al., 2011) and projects back to various thalamic nuclei (Lavoie and Parent, 1994a), to dopaminergic neurons of the mesencephalon (Hong and Hikosaka, 2014), and to the reticulospinal formation (Rolland et al., 2011). Anatomical connectivity has also been explored *in vivo* in primates using diffusion weighted imaging (DWI). This technique is the only non-invasive method allowing access to white matter structural connectivity (Le Bihan et al., 1986) through tractography algorithms (Mori and van Zijl, 2002). Results of DWI-based analyses provide evidence for strong connections between the PPN and the cortex, pallidum, STN, thalamus and spinal cord in macaque and human (Aravamuthan et al., 2007; 2009; Muthusamy et al., 2007).

Altogether, these anatomical results provide insights into the complex connectivity of the MLR and its close relationship with basal ganglia. However, the delineation of the PPN remains controversial, the CuN connectivity remains poorly studied, and the connectivity of these two specific nuclei has not been determined in relation to the anatomo-functional subdivisions of different brain structures. This partial anatomical knowledge of the MLR limits our understanding of the specific role of the PPN and the CuN. The aim of our study was to examine the PPN and the CuN inputs and outputs focusing on how projection patterns relate to the cortical, basal-ganglia, amygdala and thalamic anatomo-functional territories that process sensorimotor, cognitive and emotional information. For this purpose, we used tract-tracing experiments in monkeys and DWI-based tractography in humans.

## 2. Material and methods

### 2.1. Monkeys and volunteers

All experiments were carried out in strict accordance with the European Community Council Directive of 2010 (2010/63/UE) for care and use of laboratory animals. The authorisation for conducting our experiments was approved by the local Committee on the Ethics of Animal Experiments. The animals were kept under standard conditions (12-h light/dark cycle [light on at 20 h], 23 °C and 50% humidity). We used five adult monkeys weighing between 2 and 5 kg (four *Macaca fascicularis*, MI53, MI58, MI82, MIW7 and one *Cercopithecus aethiops*, CA8). Both species are Old World monkeys, with comparable body size and brain development.

Data from 30 healthy volunteers (12 males, range 22 to 35 years) were included in this study, provided by the Human Connectome Project (HCP) (Van Essen et al., 2013). HCP experiments were performed in accordance with relevant guidelines and regulations and the experimental protocol was approved by the Institutional Review Board.

### 2.2. Tracer injections and analysis

All the procedures used have already been described in detail (Jan et al., 2000; Rolland et al., 2011). For all stereotaxic injections, we used biotin dextran amine (BDA, Sigma, St-Louis, MO) as an anterograde and retrograde tracer (10% in 0.01 M phosphate buffer saline). We made unilateral (CA8, MI58, MIW7) or bilateral (MI53) injections in the MLR at -3.5 to 4.5 mm from the Posterior Commissure (PC), 3 to 4 mm from the midline, and -6 to 7 mm below PC. We also performed one injection in the infralimbic cortex (MI82) at 12 mm from the frontal pole, 1 mm from the midline and at a depth of 8 mm from the dura.

Thirteen days after injections, animals were sacrificed, brains removed and cut on a freezing microtome into 50 µm coronal sections perpendicular to the Anterior Commissure (AC)-PC line. The BDA tracer was revealed on regularly spaced sections (500 µm) as previously described (Rolland et al., 2011). A second series of sections were first processed to precisely localise the BDA injections, and then processed with nicotinamide adenine dinucleotide phosphate diaphorase histochemistry (NADPH) to identify PPN cholinergic neurons (Hirsch et al., 1987). Representative sections distributed regularly over the whole extent of the regions studied were selected.

NADPH+ neurons were used to delimit the boundaries of the PPN, following criteria previously used (Rolland et al., 2011). For the delineation of the CuN, we used anatomical landmarks: medially, the periaqueductal grey matter, dorsally the colliculi, laterally the lateral lemniscus, and ventrally the PPN. Maps of the retrograde BDA-labelled cell bodies and anterograde labelled terminals (characterised by thin, varicose and bifurcating fibres) were drawn using a computer assisted image analysis (Mercator, ExploraNova, La Rochelle, France). Contralateral labelling was not considered. All the data obtained from the left side were flipped to the right side to simplify comparisons.

Brain structure functional territories were delineated from previous studies: in the STN (Karachi et al., 2009), in the SN (François et al., 1994), in the GPi and GPe (François et al., 2004), in the posterior intralaminar thalamic nuclei (centre median (CM), parafascicular nucleus (PF)) (Galvan and Smith, 2011). The ventral tegmental area (VTA), considered as a part of the limbic system, was delineated following criteria already described (François et al., 1999). An overview of the PPN and the CuN where the tracer was injected and their basal ganglia and thalamic target regions in monkey is summarized (Fig. 1A).

Since the injected amount of tracer was variable, no quantitative histological data were available in monkey.

### 2.3. Image acquisition and preprocessing

Three Tesla MRI acquisitions were performed and pre-processed by the HCP (Glasser et al., 2013; Sotiropoulos et al., 2013). A T1 weighted image was first collected with a 0.7 $mm^3$ resolution. A set of diffusion-weighted images (voxel size = 1.25 $mm^3$, 90 directions, b-value = 3000 $s/mm^2$) was then acquired.

We designed and used a methodological pipeline to estimate DWI-based connectivity (Philippe et al., 2015) of the PPN and CuN similar to the approaches used for studies of thalamic, striatal or subthalamic nucleus connectivity (Behrens et al., 2003; Draganski et al., 2008; Johansen-Berg et al., 2005; Lambert et al., 2012; Leh et al., 2007) that provide results consistent with histological findings. Our pipeline is summarised in supplementary figure 1 and its three main steps are detailed below.

### 2.4. Segmentation of regions of interest

The motor cortical areas were segmented using a Brodmann atlas (areas 4 and 6)[2]. The insula and limbic cortex were segmented with the Freesurfer *recon-all* pipeline (Destrieux et al., 2010). We applied an indicator function of the cortical ribbon to obtain homogenised cortical ROIs sizes.

To identify the basal ganglia and their anatomo-functional territories, we used our in-house 3D histological and deformable atlas (YeB atlas) (Bardinet et al., 2009; Yelnik et al., 2007).

The right and left PPN and CuN were manually segmented for the first ten subjects on the visualization of surrounding structures (inferior colliculus, medial and lateral lemniscus and the decussation of the superior cerebellar peduncle) (Fournier-Gosselin et al., 2013) using T1-weighted images and colored fractional anisotropy (FA) maps in order to visualize local fiber orientations. The corresponding ROIs were normalized and superimposed in the Montreal Neurological Institute (MNI) space (all HCP data are provided with MNI spatial normalization matrices), yielding probabilistic templates that were thresholded at 70% and provided PPN and CuN deterministic templates. Then, the template was applied (projected) onto the remaining 20 human brains of this study. Anatomical experts (CK, CF) carefully verified the delineation of the PPN and CuN on each side of each subject that have been produced by this automatic segmentation and manual corrections were performed if needed. Additionally, we checked the validity of these templates by back-projecting them onto the first ten human brains, and computing Dice coefficients between the manual delineations and the back-projected templates. We found Dice coefficients (Dice, 1945) ranging close to 1 (from 0.80 to 0.97), indicating a high similarity between the segmented masks.

We manually segmented the amygdala using T1-weighted images and the delineation from the 3rd edition of Mai's human brain atlas (Mai et al., 2007).

An overview of the regions of interest in human, including PPN and CuN, surrounding structures, and basal ganglia and thalamic nuclei, superimposed on T1-weighted and color FA (computed from diffusion MRI) images is summarised (Fig. 1B).

### 2.5. Probabilistic tractography

We estimated the distribution of fiber orientations present within each imaging voxel using the Constrained Spherical Deconvolution (CSD) framework (Tournier et al., 2007). Probabilistic CSD-based tractography was run in subject-specific native space using MRtrix software from a seed mask to a target mask. We applied probabilistic tractography from every voxel inside the PPN or CuN seed masks to the SN, VTA, GPe, GPi, Pu, STN, amygdala, CM, PF, area 4, area 6, insula and limbic cortices (parameters: 100 000 tracks, step length of 0.625 mm, curvature threshold of 45°, minimum tract length of 10 mm, maximum tract length of 250 mm and fiber orientation distribution amplitude cut-off of 0.1). When the CuN was the seed mask, PPN was used as an exclusion region to avoid PPN fibers passing dorsally through the CuN towards the basal ganglia.

We selected fibers extremities ending in target regions using the *test_ends_only* option of the *tckedit* command of MRtrix. For each voxel in a target, the number of extremities stopping in that voxel was counted to obtain a connectivity map. Finally, each map was thresholded at 20, meaning that only voxels which have received 20 or more fiber extremities are kept, and further binarised.

### 2.6. Statistical analysis

To compare connectivity results between PPN and CuN, we calculated the percentage of connected voxels from the target nuclei (total number of connected voxels divided by total number of the nuclei's voxels), or from their anatomo-functional territories for the putamen, GPe, GPi and STN. The variability is expressed as standard deviation. Comparisons of percentage values of connected voxels between PPN tractography and CuN tractography were performed using the Wilcoxon signed-rank test and MATLAB 2010b.

## 3. Results

### 3.1. Injections sites

In monkey, we performed two BDA injections into the PPN, one restricted to the anterior part (CA8) and one to the posterior part of the nucleus (MIW7). Similarly, we performed two BDA injections into the CuN, one restricted to the anterior part (MI58), and one to the posterior part of the nucleus (MI53, left side). A fifth larger injection including both PPN and CuN was also performed (MI53, right side) (Fig. 2A).

### 3.2. Cortical projections to the PPN and CuN

In monkey, numerous retrogradely labelled cell bodies were found in the premotor area (A6), supplementary motor area (A6), oculomotor area (A8), and in the primary motor area (A4) following PPN injections (Fig. 3A). A stronger connection with motor areas was observed with anterior (CA8) rather than with posterior PPN injections (MIW7). Labelled cell bodies were also observed in the anterior and posterior insular cortex (A12-13 and 16), with fewer in the cortical limbic area (A25).

To confirm the non-motor cortical projections to the PPN, BDA was injected in the infralimbic cortical area (A10m, MI82) (Fig. 2B). Anterogradely labelled terminals were seen in the dorsal, lateral and ventral parts of the PPN delimited using NADPH+ neurons (Fig. 2B). Consistent with previous reports (Chiba et al., 2001; Semba and Fibiger, 1992), numerous labelled fibers and terminals were also distributed in the adjacent dorsolateral tegmental nucleus, in the hypothalamus, and in the periaqueductal area (data not shown).

The great majority of the retrogradely labelled cell bodies following CuN injections were found in the limbic area (A25), and over the whole extent of the insular cortex (A12-13 and A16) (Fig. 2A). Very few cell bodies were encountered in the adjacent auditory and secondary somatosensory cortices (A1-2). Practically no labelled cell bodies were found in the premotor or motor cortices. The infralimbic cortical injection described above resulted in labelled terminals distributed in the most medio-ventral part of the CuN.

In the human subjects, connections of the PPN with the primary

[2] www.mccauslandcenter.sc.edu/mricro/mricro/lesion.html#brod

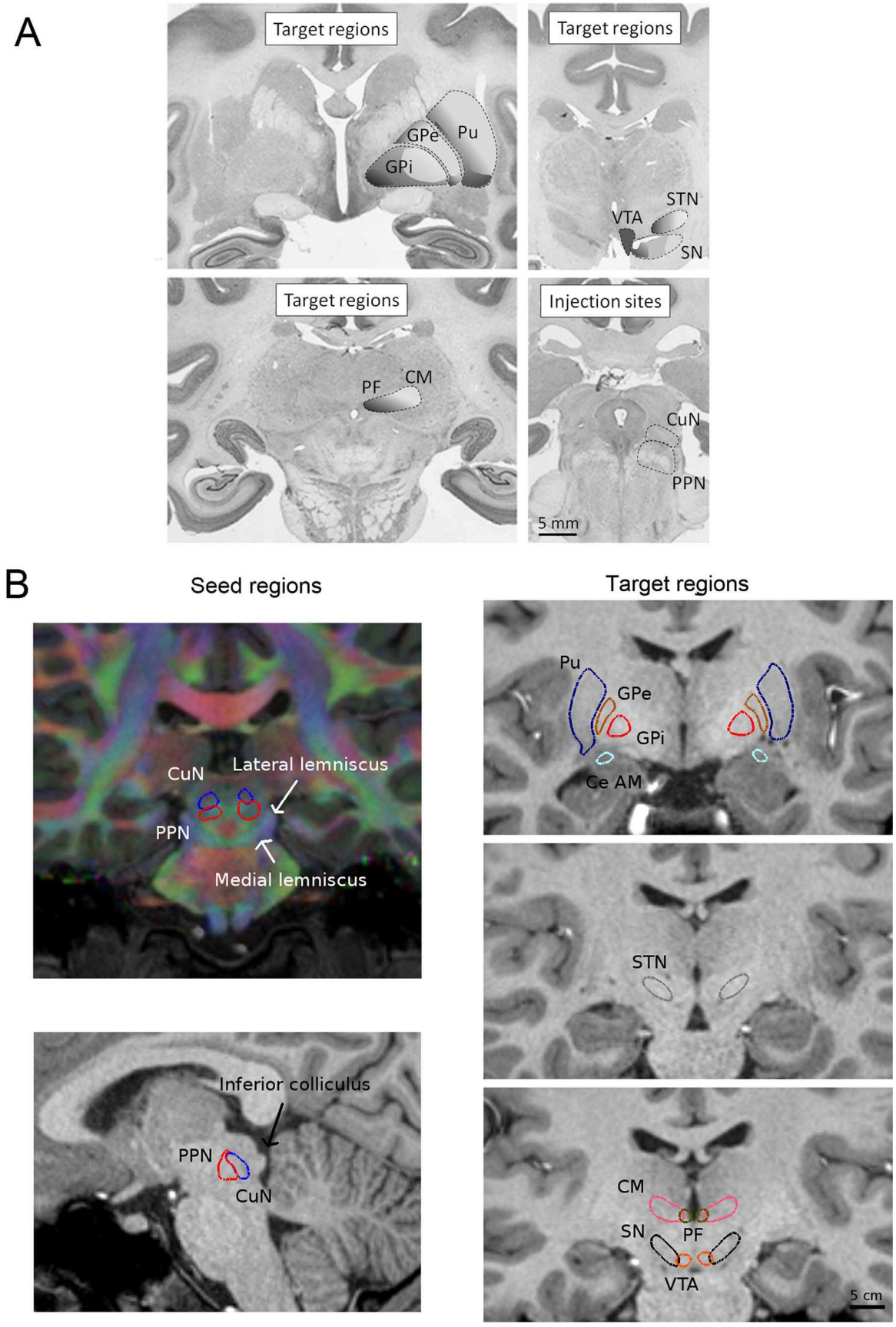


**Fig. 1.** (2-column): Overview of the PPN and CuN, and their basal ganglia and thalamic targets. (A) The PPN and CuN where the tracer was injected, and the basal ganglia and thalamic targets were represented on coronal sections counterstained with cresyl violet. The different anatomo-functional territories were also shown. (B) The same seed and target regions were shown on coronal and sagittal MRI slices in human. Left panel: coronal map of FA of the mesencephaleon including the PPN and CuN region. For abbreviations, see list.

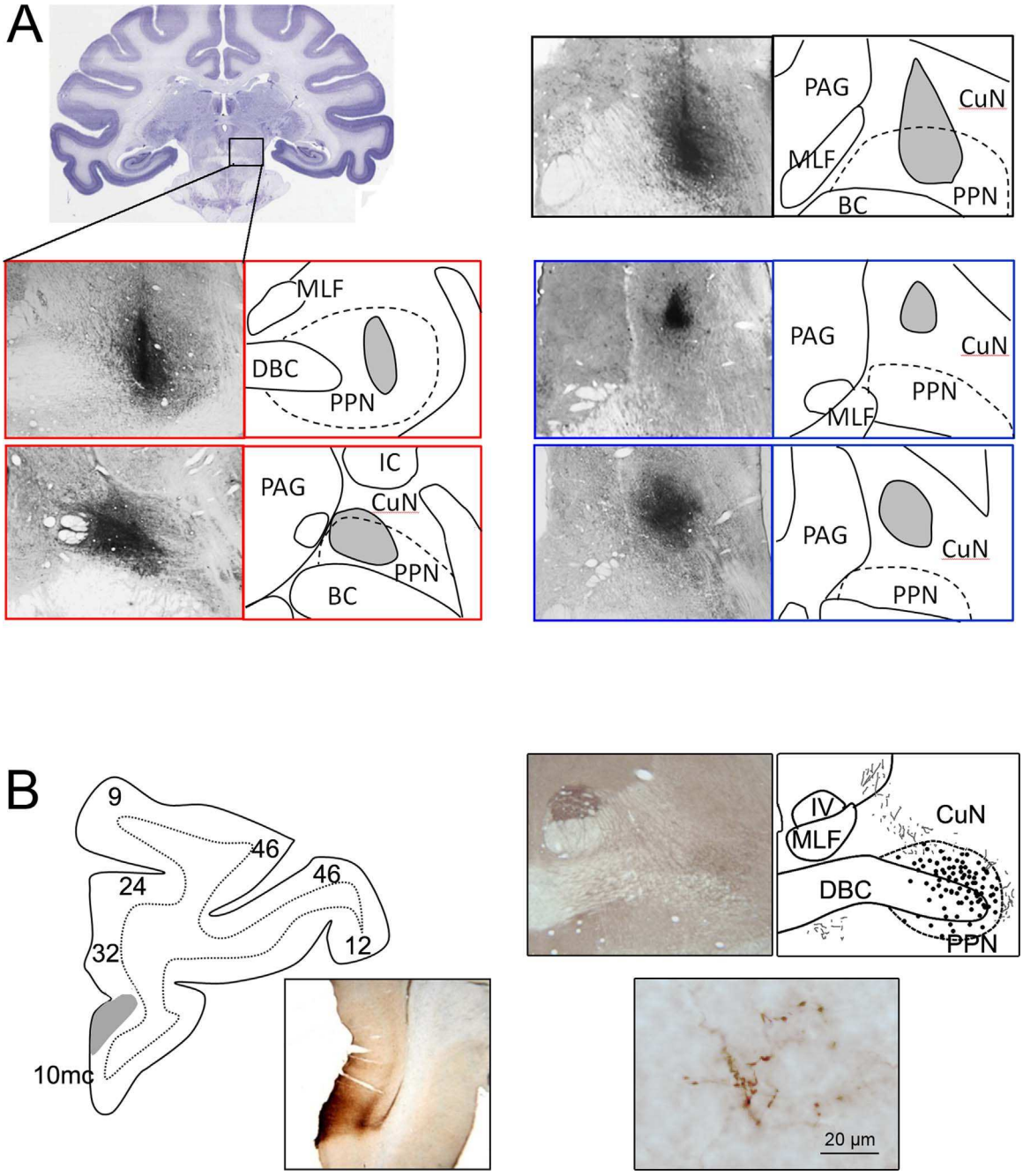


**Fig. 2.** (2-column): BDA injection sites in the mesencephalic locomotor region in macaques. (A) Maps showing sites confined to either the PPN (red) in two macaques, or to the CuN (blue) in two other macaques, or both (black) in another. The anatomical localisation of the PPN and CuN is shown in a Nissl-stained section (upper part). (B) Left, photograph and maps showing the BDA injection in the limbic cortical area 10mc in a macaque (MW7). Right, photomicrograph and map of anterogradely labelled terminals (grey lines) and NADPH-diaphorase neurons (black dots) on a brainstem coronal section following cortical BDA injection. The photomicrograph in the lower part shows labelled terminals at high magnification. For abbreviations, see list.

motor area (A4) and premotor area (A6) were found with slightly more connections with area A4 (66% of connected voxels from A4 versus 38% from A6) (Fig. 3B). A very weak connection was also observed between the PPN and the insular (4% of connected voxels) and limbic cortices (1% of connected voxels). The CuN also exhibited connections with the motor (A4) and premotor (A6) areas, but less dense than the PPN (66% of connected voxels from A4 and 38% from A6 for the PPN, compared to 54% from A4 versus 25% from A6 for the CuN) (Fig. 2B). We also observed weak connections between the CuN and the insular cortex (3% of connected voxels), but practically no connection was found with the limbic cortex (0.8% of connected voxels).

### *3.3. PPN and CuN projections to the basal ganglia and the adjacent amygdala in monkey*

In monkey, injections into the PPN of CA8, MIW7 and MI53 gave labelled terminals homogeneously distributed in the three anatomo-functional territories of the STN (Fig. 4A) with higher terminal density in MIW7 where the injection was posterior. All these PPN injections also resulted in numerous labelled terminals in the three anatomo-functional territories of the pallidum, the GPi being more strongly innervated than the GPe (Fig. 5A). A few labelled terminals were also found scattered within the ventral striatum and in the sensorimotor putamen. Labelled terminals were observed over the whole extent of

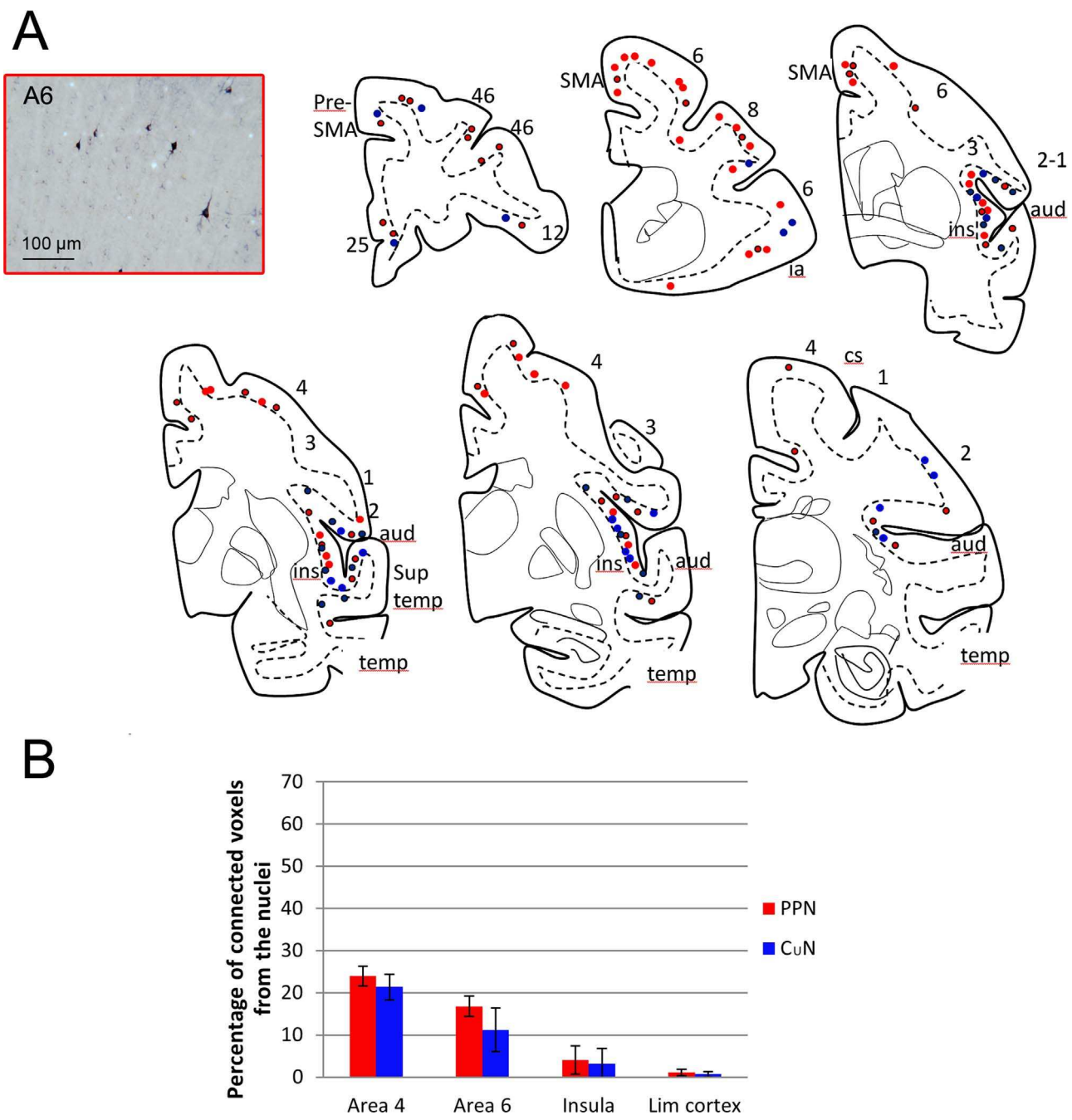


**Fig. 3.** (2-column): Cortical projections to the MLR (A) Left, photograph of retrogradely labelled neurons in area 6 (A6) after PPN injection in the macaque CA8. Right, Maps of retrogradely labelled neurons after BDA tracer injection in the PPN (red dots) and in the CuN (blue dots) on coronal sections of the brain ipsilateral to the injections shown in Fig 1 A. (B) Average results of connections of the PPN and CuN to cortical area 4, area 6, insula and limbic cortex in 30 human subjects. The error bars represent standard deviation. For abbreviations, see list.

the SN, the pars compacta (SNc) being more densely innervated than the pars reticulata (SNr), and the adjacent VTA (Fig. 6A). Anterior injection (case CA8) gave more labelled terminals in the SN than in the VTA, whereas the posterior injection (case MIW7) gave equal density of terminals in the SN and VTA. Numerous PPN labelled terminals were found in the basal forebrain of CA8 and MIW7, including the extended amygdala and the amygdala itself, specifically into the central nucleus (Fig. 5A). In all cases, a few retrogradely labelled cells were found inside the clusters of anterogradely labelled terminals.

CuN BDA injections of MI58 and MI53 resulted in an anterograde labelling in similar nuclei than after PPN injections. However, labelled terminals were mainly located in the anterior and medio-ventral limbic territories of the various nuclei. Indeed, a high density of labelled CuN terminals was observed in the most medial part of the STN (Fig. 4A), in the anse lenticularis surrounding the GPi (Fig. 5A) and in the VTA (extending to the proximal medio-dorsal part of the SNc) (Fig. 6A). Dense clusters of label extended ventrally to the GPi and GPe, in the extended amygdala and in the central nucleus of the amygdala.

Similarly to that observed following PPN injections, a few retrograde labelled cell bodies were found inside the clusters of anterogradely labelled terminals in the SN and in the STN after CuN injections (Fig. 4A, 6A).

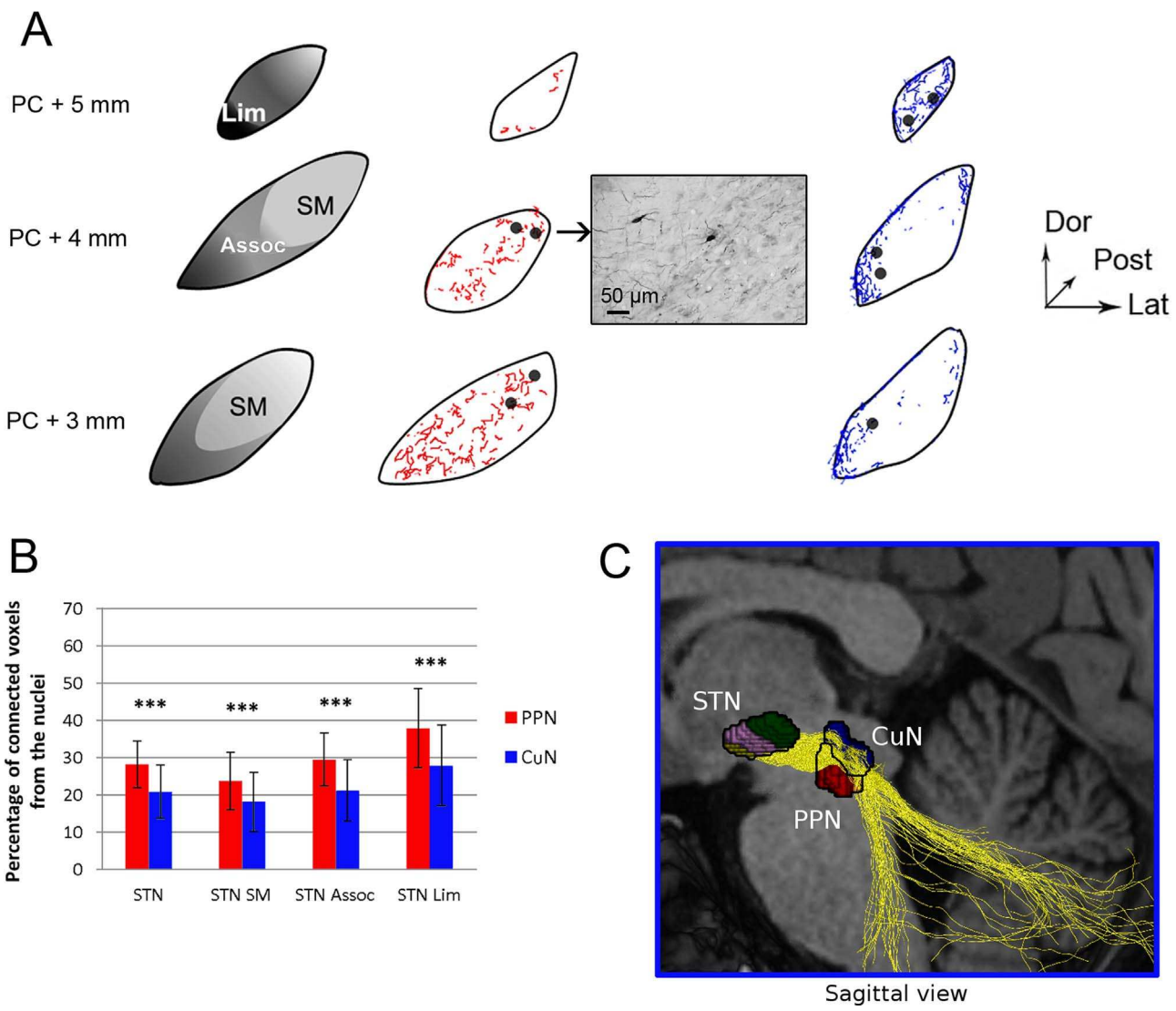


**Fig. 4.** (2-column): PPN (red) and CuN (blue) outputs to the STN. (A) Three representative coronal sections of monkey STN showing the functional territories delineated from (Karachi et al., 2009), and the distribution of labelled PPN terminals (middle column), and CuN terminals (last column) in one representative macaque. The three functional territories are represented as three shades of grey: dark for limbic territory (limb), intermediate for associative territory (assoc), and light for sensorimotor (SM). Black points represent retrogradely labelled cell bodies. Photomicrograph showing retrogradely labelled cell bodies within a region of anterogradely labelled axons after BDA injection in the CuN of macaque MI58. The antero-posterior position of all coronal sections is indicated with respect to the posterior commissure (PC). (**B**) Histograms showing percentages of connected voxels from the STN and its functional territories to the PPN and CuN, averaged in 30 human subjects. The error bars represent standard deviation. Note that the PPN is more connected to the STN (uniformly over its territories) than the CuN (Wilcoxon signed-rank test: *$p < 0.05$; **$p < 0.01$; ***$p < 0.001$). (**C**) Sagittal view of fibers (yellow) connecting the CuN and the limbic part of the STN. The sensorimotor, associative and limbic anatomo-functional territories of the human STN are represented in green, pink and yellow, respectively. For abbreviations, see list.

### *3.4. PPN and CuN projections to the basal ganglia and the adjacent amygdala in human*

In human subjects, we found strong PPN connections with the STN (28% of connected voxels), with lower number of connections of the associative compared to the limbic and sensorimotor territories of the STN (Fig. 4B). PPN connections were also found for the three anatomo-functional territories of the GP, predominantly the GPi (35% of connected voxels) (Fig. 5B, C). No PPN connection to the striatum was detected (0.7% of connected voxels) (Fig. 5B, C). We found that the PPN was also connected to the whole extent of the SN and the adjacent VTA (19% and 18% of connected voxels, respectively) (Fig. 6C, D). No precise delineation between the two nigral parts were possible because clusters of SNc neurons are deeply embedded within the SNr. The central nucleus of the amygdala was also strongly connected to the PPN (32% of connected voxels) (Fig. 5B, C).

Compared to the PPN, the number of connections identified between the CuN and the basal ganglia was lower for the STN, SN, GPi and GPe (21%, 15%, 7% and 2% of connected voxels, respectively). The CuN connections concerned the three anatomo-functional territories delineated in the different basal ganglia nuclei, but were denser in the limbic than in the associative and sensorimotor territories for the STN, SN and GPe, but not the GPi (Fig. 4B, C, 5B, C, 6 C, D). Again, nearly no connections were observed between the CuN and the striatum (0.6% of connected voxels) (Fig. 5B, C). The central nucleus of the amygdala also appeared strongly connected to the CuN (32% of connected voxels) (Fig. 5B, C).

### *3.5. PPN and CuN projections to the thalamus*

In the monkey, PPN labelled axons arborised mainly in the perithalamic, midline nuclei and in the posterior intralaminar nuclei. Prominent clusters of labelled terminals were observed in the three functional territories of these nuclei, thus in both the PF and the CM except its most lateral part (Fig. 6B). In comparison, CuN labelled axons were observed in the same thalamic nuclei, except that the PF

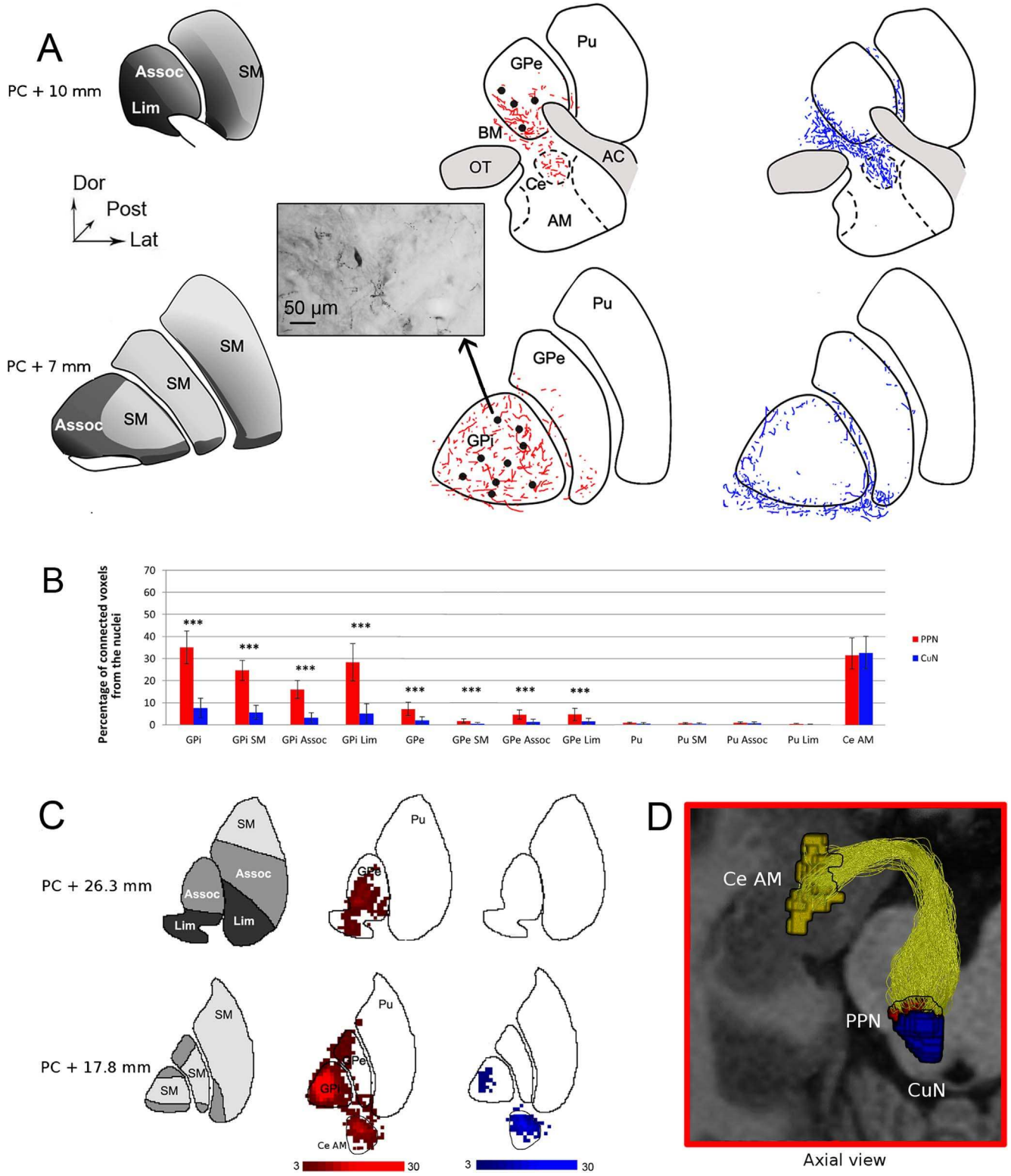


**Fig. 5.** (2-column): PPN (red) and CuN (blue) outputs to the pallidum, central nucleus of the amygdala and putamen. (A) Two representative coronal sections of monkey GPi, GPe and Pu showing the functional territories delineated from (François et al., 2004), and the distribution of labelled PPN terminals (middle column), and CuN terminals (last column) in one representative macaque. The three functional territories are represented as three shades of grey as in Fig. 3. Black points represent retrogradely labelled cell bodies. Photomicrograph showing a retrogradely labelled cell body within a region of anterogradely labelled axons after BDA injection into the GPi of macaque 58. Note that the PPN innervates the whole extent of the GPi, only partly the GPe, but not the Pu. In comparison, the CuN innervates the most ventral portion of the two segments of the pallidum, as well as the nucleus basalis of Meynert (BM) and the central nucleus (Ce) of the amygdala (AM). (B) Histograms showing percentages of connected voxels from the GPe and GPi, Ce of the AM, Pu and their functional territories to the PPN and CuN, averaged in 30 human subjects (Wilcoxon signed-rank test: *p < 0.05; **p < 0.01; ***p < 0.001). The error bars represent standard deviation. (**C**) Two representative coronal sections of human GPi, GPe, AM and Pu showing the functional territories segmented with the YeB atlas of 30 subjects, showing the distribution of connections from PPN (middle column), and CuN (last column) for the 30 subjects. The colorbars indicate the number of subject's overlapping in a particular voxel (ranging from 3 to 30). Numerous connections were observed between PPN and the GPi, with a large overlap between subjects (with a maximum of 28). Connections from the PPN or CuN to the GPe were also found but they were less numerous than to the GPi. Only very few connections from the PPN or CuN to the Pu were observed, with no overlap between subjects. (D) Axial view showing fibers (yellow) connecting the AM and the PPN with a relatively high curvature. For abbreviations, see list.

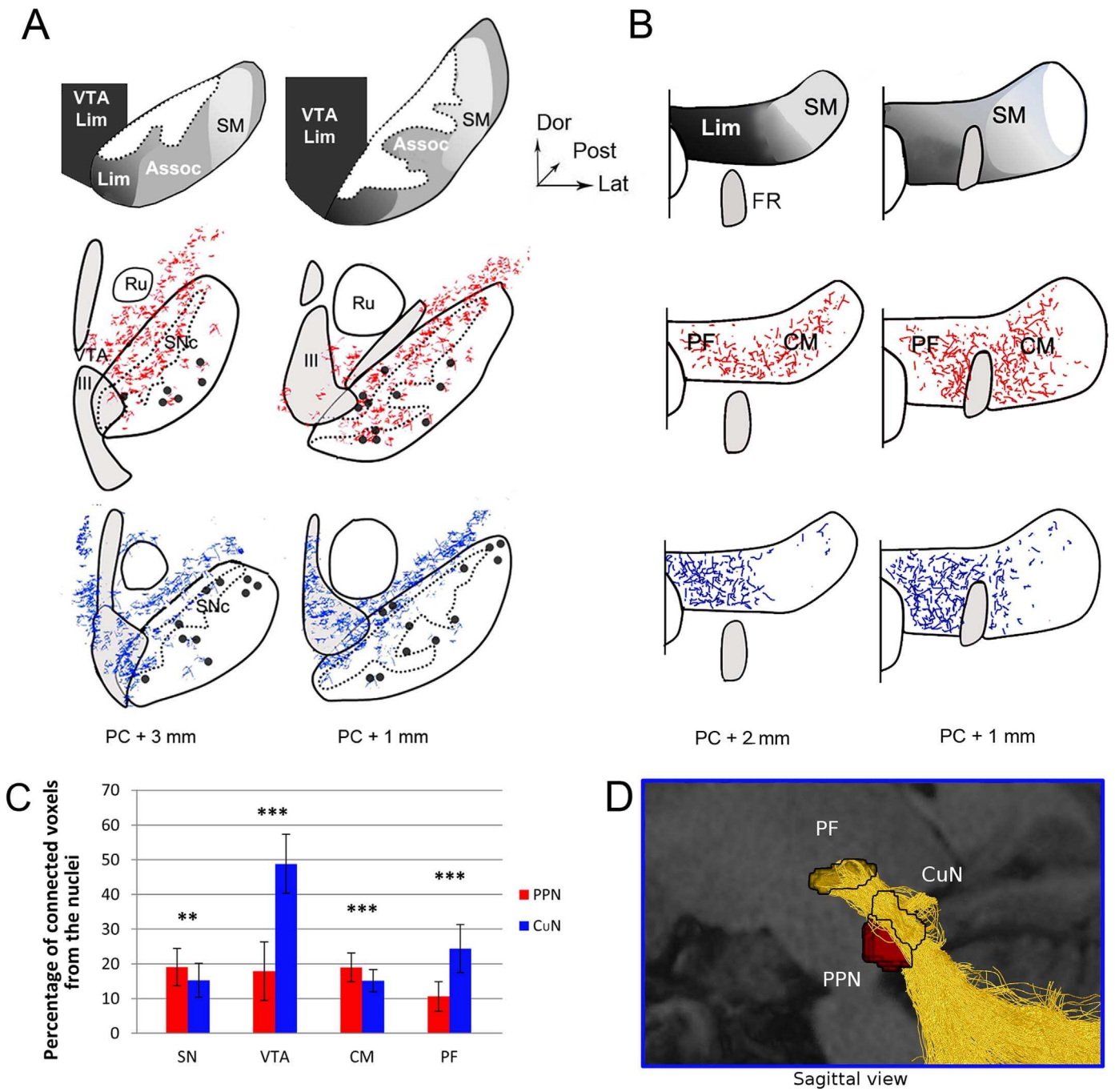


**Fig. 6.** (2-column): PPN and CuN outputs to the SN, VTA and the posterior intralaminar nuclei of the thalamus. (A) Three representative coronal sections of monkey SN showing the functional territories delineated from (François et al., 1994), and the distribution of labelled PPN terminals (middle row), and CuN terminals (lower row) in one representative macaque. The three functional territories are represented as three shades of grey as in Fig. 3. Note that the PPN mainly projects to the whole extent of the SN pars compacta (SNc), while the CuN mainly terminates in the VTA. Black points represent retrogradely labelled cell bodies (B) Three representative coronal sections of monkey CM-PF showing the functional territories delineated from (Galvan and Smith, 2011), and the distribution of labelled PPN terminals (middle row), and CuN terminals (lower row) in one representative macaque. The three functional territories are represented as three shades of grey as in Fig. 3. (C) Histograms showing percentages of connected voxels from the SN, VTA, CM and PF to the PPN and CuN, averaged in 30 human subjects. The error bars represent standard deviation. Note that more connections were observed between the CuN and the VTA and the PF than between the PPN and these same structures (Wilcoxon signed-rank test: *p < 0.05; **p < 0.01; ***p < 0.001). (D) Sagittal view showing fibers (yellow) connecting the PF and the CuN. For abbreviations, see list.

was more densely innervated than the CM (Fig. 6B).

In human subjects, the PPN was also found to be connected to both the PF and the CM (19% and 11% of connected voxels, respectively), whereas the CuN was more densely connected to the PF than the CM (24% and 15% of connected voxels, respectively) (Fig. 6C, D).

## 4. Discussion

Our study supports the view that both the PPN and the CuN project to the sensorimotor, associative and limbic anatomo-functional territories of the basal ganglia and the thalamus in monkeys and humans. The analysis of these projections highlights the fact that the PPN could act as an integrator of sensorimotor, cognitive and emotional information, with the anterior part of the PPN more devoted to motor control

in the monkey. In contrast, the CuN appears to participate in a more restricted network involving predominantly limbic brain regions.

### 4.1. Methodological considerations

Since the MLR is characterised by its high density of fibers of passage, our BDA injections in monkey could have labelled structures innervated by these fibers. In particular, the sensorimotor-related cortical areas labelled after these injections could be the sources of lower brainstem and spinal cord projections passing through the MLR. Being aware of this possibility, we performed very small injections to ascertain the position of the tracer within a given part of the chosen structure, avoiding contamination of adjacent structures. Because such injections resulted in retrograde labelled cell bodies in the motor cortices but not in sensory and frontal cortices which are the main sources of the descending projections, we considered that fibers of passage that could have been labelled did not provide significant false positives to our data. However, our small and specific injections did not completely fill the entire PPN or CuN, leading to fewer labelled terminals or retrograde cell bodies in the brain regions of interest.

We chose several methodological options inherent to the DWI-based tractography method. First, when building our PPN and CuN templates from our manually segmented ROIs, we had to fix a threshold to include only common voxels in order to be as specific as possible. The value of 70% was chosen because it leads to CuN and PPN volumes of 216 and 218 $mm^3$ (Olszewski and Baxter, 1954). Second, we used probabilistic tractography, which traces a large number of possible pathways from a set starting point. The advantages of probabilistic tractography are improved resolution of crossing tracts and sensitivity for curving fibers compared to deterministic algorithms (Tournier et al., 2012) that is particularly well adapted for studying the complex brainstem anatomical connectivity. We have chosen to illustrate fiber tracts originating from the PPN and CuN and descending to the cerebellum and the spinal cord that validate the specificity of the reconstructed tracts, as reported using diffusion MRI in macaque and human (Aravamuthan et al., 2007; 2009; Muthusamy et al., 2007) and axonal tracing in monkey (Rolland et al., 2011).

Due to the small size and complexity of the brainstem anatomy, there was a risk of partial volume effects. To minimize potential confounds, delineation of the seeds (PPN and CuN) was performed conservatively, meaning that only voxels clearly identified within the structures were included in the seeds. The anatomical landmarks, on the other hand, were identified on the T1-weighted MR image (for the inferior colliculus) with a voxel size of $0.7mm^3$, and on the color FA maps (for the medial and internal lemniscus, and decussation) with a voxel of $1.25mm^3$. Their identification was easy and accurate.

One limitation of the present study is that diffusion imaging was not performed on macaques injected with axonal tracer. We were thus unable to directly compare labeled fibers revealed on histological sections with corresponding tracts calculated from the in vivo data on the same animal. However, for now, histology still offers a resolution that is far beyond that of diffusion weighted images and enables a more precise delineation of fiber tracts (Bürgel et al. 2006). We were thus able to trace neuronal connections of the PPN and CuN on histological sections in monkey and to compare these data to diffusion MR images in human.

### 4.2. The PPN participates in motor, associative and limbic networks

The present data confirms that the PPN innervates the STN and the GP in primates as already reported using tract tracing (Shink et al., 1997; Lavoie and Parent 1994a) and tractography (Aravamuthan et al., 2007; 2009; Muthusamy et al., 2007). Our data demonstrate that PPN axons innervate the whole extent of these basal ganglia nuclei, including all the three anatomo-functional territories of each nucleus. Thus numerous labelled PPN fibers innervated the SNc and the adjacent limbic VTA in both monkey and human, as reported using tract tracing (Lavoie and Parent, 1994b) and tractography (Aravamuthan et al., 2008). The fact that no PPN connection to the nigra was previously been reported in humans (Aravamuthan et al., 2008) contrary to our present results is probably due to differences in the method used as we discussed above. Our results also show that a weak PPN-striatal projection exists in monkey as already reported (Nakano et al., 1990; Smith and Parent, 1986), but this connection was nearly undetectable in human compared to connections to other basal ganglia. Indeed, no PPN-striatal connection was previously shown in monkey and human (Aravamuthan et al., 2007; 2009; Muthusamy et al., 2007). This contrasts with the strong PPN-striatal projection reported in rodent (Dautan et al., 2014), suggesting an important role of this connection in rodent but not in primate.

Our data show that only the PPN and not the CuN drives the motor cortical components of the MLR in monkey and human. These motor cortical projections come from the primary, supplementary and pre-motor cortices, as well as the frontal eye fields. These motor projections were previously shown in human using tractography (Aravamuthan et al., 2007; 2009; Muthusamy et al., 2007) and in monkey using histological techniques (Matsumura et al., 2000). Here, we showed that the motor cortex has stronger connection to the anterior PPN than its posterior part in monkey, suggesting a topographical organization within the PPN itself. Moreover, anterior PPN axons densely innervated the SNc, whereas axons from the posterior PPN innervated mostly the limbic VTA. Similar antero-posterior topography of the nigral-PPN connection was also reported in rodent (Oakman et al., 1995). Whether such an antero-posterior topography exists in humans could not be examined in this diffusion-based study because we cannot differentiate fibers that terminate in the posterior part of the PPN and cross the anterior part from the ones that terminate in the anterior part.

We also showed that the whole PPN receives projections from associative and limbic cortices. In particular, the insular cortex (A12-13 and A16) gave projections to both the monkey and human PPN, suggesting that the PPN could integrate functions related to interoception and error processing. Limbic cortices have also been shown to project, although weakly, to the PPN in monkey (Chiba et al., 2001) and in rodent (Semba and Fibiger, 1992; Sesack et al., 1989), but we do not find this direct limbic projection in humans. It is possible that tractography sensitivity is too low to detect such weak cortical connections. However, the fact that anatomical differences exist between species has already been suggested (Aravamuthan et al., 2008) and this could be especially the case for limbic structures and connectivity.

The PPN is also part of a major ascending pathway through the non-specific nuclei of the thalamus (Steriade et al., 1988) known to modulate arousal. Our data showed that PPN axons innervate the limbic, associative and motor territories of the CM/PF nuclei of the thalamus, avoiding the most lateral part known to be interconnected with the motor cortex (Galvan and Smith, 2011). Moreover, the dense projection linking the PPN to the central nucleus of the amygdala that we observed in both monkey and human strengthens the notion that the PPN is not only a motor structure. The central nucleus of the amygdala is known to be the major output of the amygdala. This specific nucleus receives both direct and highly processed sensory information and is known to project to the hypothalamus and brainstem areas that mediate autonomic response and behavioural signs of fear (Sah et al., .2003). Because the CuN also densely projects to amygdala central nucleus, it is possible that the MLR as a whole could be crucial to generate escape behaviour in the context of locomotion.

### 4.3. The CuN is part of a limbic network

Here, we showed for the first time that the CuN is preferentially

connected to the limbic territory of the basal ganglia and thalamus in both species. In monkeys, the location of the labelled terminals coming from the CuN was preferentially within the limbic territories of the basal ganglia (STN and GP), and thalamus (PF nucleus). In humans, even if the CuN connections concerned the three anatomo-functional territories of these different basal ganglia nuclei, much denser connections were found in the limbic STN, SN and GPi. These results are in agreement with previous data obtained in rodents reporting a similar topography of the connections from the deep mesencephalic nucleus (equivalent of the cuneiform nucleus) (Rodríguez et al., 2001) to the ventromedial, limbic STN and GP (Veazey and Severin, 1980a). Moreover, the CuN preferentially innervated the limbic VTA and gave strong projections to the basal forebrain, extended amygdala and the central nucleus of the amygdala in both species. The CuN receives also cortical inputs from the insular cortex in both monkey and human, and from limbic cortices in monkey. Differences between monkey and human exist; the CuN also exhibited a few connections with motor cortical areas as well as associative and sensorimotor territories of the basal ganglia nuclei only in humans. This may be due to the fact that the whole CuN was not injected with the axonal tracer in monkey in order to avoid false positive as discussed above. However, as a whole, the CuN exhibits few connections with motor cortical areas as well as to associative and sensorimotor territories of the basal ganglia nuclei, which suggests that the CuN of the MLR is not primarily a motor structure.

### 4.4. Functional implications

The preferential link of the anterior PPN to motor network in monkey is consistent with the effects of experimental lesions restricted to the anterior PPN that reduce spontaneous locomotion in rat while posterior PPN lesions have no obvious motor consequences (Alderson et al., 2008). This suggests that the locomotor generator of the MLR might be located anteriorly in the PPN. Cholinergic neurons are known to be numerous in this anterior part of the PPN in monkey (Manaye et al., 1999), suggesting that these cholinergic PPN neurons could have a motor role. Consistent with this, specific lesions of PPN cholinergic neurons gave postural and locomotor deficits in monkey (Karachi et al., 2010). Moreover, PPN cholinergic cell loss in PD patients is correlated with falls (Karachi et al., 2010), leading consequently to a significant decrease in cholinergic concentration of the thalamus (Bohnen et al., 2009). However, the exact location of the cholinergic neuronal loss within the PPN remains to be determined in these PD patients. Taken together, these data suggest that the anterior PPN, should be the best target to improve locomotion in PD patients using DBS or future innovative therapy such as High Intensity Focused Ultrasound (HIFU) (Carpentier et al., 2016), or targeted pharmacologic therapy such as an acetylcholinesterase inhibitor (Henderson et al., 2016).

The PPN also belongs to non motor networks and plays a crucial role in sleep and arousal. Thus, PD patients with severe gait disorders report changes in sleep quality with PPN-DBS (Arnulf et al., 2010) and increased alertness (Stefani et al., 2013). Moreover, PPN neurons were reported to be strongly activated by visual stimuli, motor movement and imagined locomotion (Lau et al., 2015), showing that the PPN integrates many information sources at the scale of a single neuron.

While effective sites for chemically evoked locomotion in decerebrate cats are located within and around the CuN (Takakusaki et al., 2003), lesions of the CuN in intact rats do not produce locomotor deficits (Allen et al., 1996). However, CuN neurons that also project to the reticulospinal pathway in primate (Rolland et al., 2011), could modulate the activity of excitatory and inhibitory locomotor descending neurons. Thus, while the CuN might be critical for the production of movement in certain conditions, it does not appear to be a strictly locomotion generating centre (Walker and Winn, 2007), as we confirmed here by the analysis of its particular non-motor anatomical connections. Indeed, CuN lesions are able to produce behavioural changes in response to reinforcing events (Allen et al., 1996). Moreover, CuN lesions generate anxiety-like effects (reactions to threat) in rat (Walker and Winn, 2007), which is not the case when the lesion is restricted to the PPN (Winn, 2008). Thus the CuN is likely best understood in terms of its relationship with the organisation of defensive behaviours (Redgrave et al., 1987; Walker and Winn, 2007). Given its position as a major target of the ipsilateral descending projection from the superior colliculus as well as its role in mediating physiological responses to stress, it seems that the CuN is probably part of an anatomically low-level, rapid response system vital for dealing with unexpected threatening events (Allen et al., 1996; Walker and Winn, 2007). The CuN within the MLR could represent an interface between the limbic and the motor system able to adapt locomotor programs as fast as possible to the environmental environment.

## 5. Conclusion

Overall, our results suggest that MLR connectivity could form the anatomical basis for the integration of numerous and varied sources of information in order to generate and adapt locomotor behaviour to the environmental context. The PPN appears to be a structure where motor, cognitive and emotional information converge whereas the CuN serves to preferentially process emotional information.

## Funding sources for study

Research wad funded by "Investissements d'avenir" (investing in the future) program ANR-10-IAIHU-06, and the ATIP-Avenir program and Sanofi-Aventis R&D to BL. SS has been supported by the Bettencourt Schueller Foundation and by the National Agency for Research under the program "Investissements d'avenir" ANR-10-EQPX-15. Human data were provided by the Human Connectome Project, WU-Minn Consortium (Principal Investigators: David Van Essen and Kamil Ugurbil;1U54MH091657) funded by the 16 NIH Institutes and Centers that support the NIH Blueprint for Neuroscience Research; and by the McDonnell Center for Systems Neuroscience at Washington University.

## Financial disclosures

The authors declare that there are no financial considerations that represent potential conflicts of interest.

## Conflict of interest

The authors declare no conflicts of interest.

## Acknowledgements

The authors would like to thank Max Westby for language editing.

## Appendix A. Supporting information

Supplementary data associated with this article can be found in the online version at http://dx.doi.org/10.1016/j.neuroimage.2016.12.011.

## References

Ainge, J.A., Keating, G.L., Latimer, M.P., Winn, P., 2006. The pedunculopontine tegmental nucleus and responding for sucrose reward. Behav. Neurosci. 120, 563–570. http://dx.doi.org/10.1037/0735-7044.120.3.563.

Alderson, H.L., Latimer, M.P., Winn, P., 2008. A functional dissociation of the anterior and posterior pedunculopontine tegmental nucleus: excitotoxic lesions have differential effects on locomotion and the response to nicotine. Brain Struct. Funct. 213, 247–253. http://dx.doi.org/10.1007/s00429-008-0174-4.

Allen, L.F., Inglis, W.L., Winn, P., 1996. Is the cuneiform nucleus a critical component of

the mesencephalic locomotor region? An examination of the effects of excitotoxic lesions of the cuneiform nucleus on spontaneous and nucleus accumbens induced locomotion. Brain Res. Bull. 41, 201–210.
Aravamuthan, B.R., McNab, J.A., Miller, K.L., Rushworth, M., Jenkinson, N., Stein, J.F., Aziz, T.Z., 2009. Cortical and subcortical connections within the pedunculopontine nucleus of the primate Macaca mulatta determined using probabilistic diffusion tractography. J. Clin. Neurosci. 16, 413–420. http://dx.doi.org/10.1016/j.jocn.2008.03.018.
Aravamuthan, B.R., Muthusamy, K. a, Stein, J.F., Aziz, T.Z., Johansen-Berg, H., 2007. Topography of cortical and subcortical connections of the human pedunculopontine and subthalamic nuclei. Neuroimage 37, 694–705. http://dx.doi.org/10.1016/j.neuroimage.2007.05.050.
Aravamuthan, B.R., Stein, J.F., Aziz, T.Z., 2008. The anatomy and localization of the pedunculopontine nucleus determined using probabilistic diffusion tractography [corrected]. Br. J. Neurosurg. 22 (Suppl 1). http://dx.doi.org/10.1080/02688690802448251.
Arnulf, I., Ferraye, M., Fraix, V., Benabid, A.L., Chabardès, S., Goetz, L., Pollak, P., Debû, B., 2010. Sleep induced by stimulation in the human pedunculopontine nucleus area. Ann. Neurol. 67, 546–549. http://dx.doi.org/10.1002/ana.21912.
Bardinet, E., Bhattacharjee, M., Dormont, D., Pidoux, B., Malandain, G., Schüpbach, M., Ayache, N., Cornu, P., Agid, Y., Yelnik, J., 2009. A three-dimensional histological atlas of the human basal ganglia. II. Atlas deformation strategy and evaluation in deep brain stimulation for Parkinson disease. J. Neurosurg. 110, 208–219. http://dx.doi.org/10.3171/2008.3.17469.
Behrens, T.E.J., Johansen-Berg, H., Woolrich, M.W., Smith, S.M., Wheeler-Kingshott, C.A.M., Boulby, P.A., Barker, G.J., Sillery, E.L., Sheehan, K., Ciccarelli, O., Thompson, A.J., Brady, J.M., Matthews, P.M., 2003. Non-invasive mapping of connections between human thalamus and cortex using diffusion imaging. Nat. Neurosci. 6, 750–757. http://dx.doi.org/10.1038/nn1075.
Bohnen, N.I., Müller, M.L.T.M., Koeppe, R.A., Studenski, S.A., Kilbourn, M.A., Frey, K.A., Albin, R.L., 2009. History of falls in Parkinson disease is associated with reduced cholinergic activity. Neurology 73, 1670–1676. http://dx.doi.org/10.1212/WNL.0b013e3181c1ded6.
Bürgel, U., Amunts, K., Hoemke, L., Mohlberg, H., Gilsbach, J.M., Zilles, K., 2006. White matter fiber tracts of the human brain: three-dimensional mapping at microscopic resolution, topography and intersubject variability. Neuroimage 29, 1092–1105.
Carpentier, A., Canney, M., Vignot, A., Reina, V., Beccaria, K., Horodyckid, C., Karachi, C., Leclercq, D., Lafon, C., Chapelon, J.-Y., et al., 2016. Clinical trial of blood-brain barrier disruption by pulsed ultrasound. Sci. Transl. Med. 8, 343re2. http://dx.doi.org/10.1126/scitranslmed.aaf6086.
Chiba, T., Kayahara, T., Nakano, K., 2001. Efferent projections of infralimbic and prelimbic areas of the medial prefrontal cortex in the Japanese monkey, Macaca fuscata. Brain Res. 888, 83–101.
Corrigall, W.A., Coen, K.M., Zhang, J., Adamson, L., 2002. Pharmacological manipulations of the pedunculopontine tegmental nucleus in the rat reduce self-administration of both nicotine and cocaine. Psychopharmacol. (Berl.). 160, 198–205. http://dx.doi.org/10.1007/s00213-001-0965-2.
Datta, S., 2002. Evidence that REM sleep is controlled by the activation of brain stem pedunculopontine tegmental kainate receptor. J. Neurophysiol. 87, 1790–1798. http://dx.doi.org/10.1152/jn.00763.2001.
Dautan, D., Huerta-Ocampo, I., Witten, I.B., Deisseroth, K., Bolam, J.P., Gerdjikov, T., Mena-Segovia, J., 2014. A major external source of cholinergic innervation of the striatum and nucleus accumbens originates in the brainstem. J. Neurosci. 34, 4509–4518. http://dx.doi.org/10.1523/JNEUROSCI.5071-13.2014.
Destrieux, C., Fischl, B., Dale, A., Halgren, E., 2010. Automatic parcellation of human cortical gyri and sulci using standard anatomical nomenclature. Neuroimage 53, 1–15. http://dx.doi.org/10.1016/j.neuroimage.2010.06.010.
Dice, L.R., 1945. Measures of the amount of ecologic association between species. Ecology 26 (3), 297–302.
Draganski, B., Kherif, F., Klöppel, S., Cook, P. a, Alexander, D.C., Parker, G.J.M., Deichmann, R., Ashburner, J., Frackowiak, R.S.J., 2008. Evidence for segregated and integrative connectivity patterns in the human Basal Ganglia. J. Neurosci. 28, 7143–7152. http://dx.doi.org/10.1523/JNEUROSCI.1486-08.2008.
Ferraye, M.U., Debu, B., Fraix, V., Goetz, L., Ardouin, C., Yelnik, J., Henry-Lagrange, C., Seigneuret, E., Piallat, B., Krack, P., Le Bas, J.-F., Benabid, A.-L., Chabardes, S., Pollak, P., 2009. Effects of pedunculopontine nucleus area stimulation on gait disorders in Parkinson's disease. Brain 133, 205–214. http://dx.doi.org/10.1093/brain/awp229.
Fournier-Gosselin, M.-P., Lipsman, N., Saint-Cyr, J.A., Hamani, C., Lozano, A.M., 2013. Regional anatomy of the pedunculopontine nucleus: relevance for deep brain stimulation. Mov. Disord. 28, 1330–1336. http://dx.doi.org/10.1002/mds.25620.
François, C., Grabli, D., McCairn, K., Jan, C., Karachi, C., Hirsch, E.-C., Féger, J., Tremblay, L., 2004. Behavioural disorders induced by external globus pallidus dysfunction in primates II. Anatomical study. Brain 127, 2055–2070. http://dx.doi.org/10.1093/brain/awh239.
François, C., Yelnik, J., Percheron, G., Fénelon, G., 1994. Topographic distribution of the axonal endings from the sensorimotor and associative striatum in the macaque pallidum and substantia nigra. Exp. Brain Res. 102, 305–318.
François, C., Yelnik, J., Tandé, D., Agid, Y., Hirsch, E.C., 1999. Dopaminergic cell group A8 in the monkey: anatomical organization and projections to the striatum. J. Comp. Neurol. 414, 334–347. http://dx.doi.org/10.1002/(SICI)1096-9861(19991122)414:3 < 334::AID-CNE4 > 3.0.CO;2-X.
Galvan, A., Smith, Y., 2011. The primate thalamostriatal systems: anatomical organization, functional roles and possible involvement in Parkinson's disease. Basal Ganglia 1, 179–189. http://dx.doi.org/10.1016/j.baga.2011.09.001.
Garcia-Rill, E., Hyde, J., Kezunovic, N., Urbano, F.J., Petersen, E., 2014. The physiology of the pedunculopontine nucleus: implications for deep brain stimulation. J. Neural Transm. 122, 225–235. http://dx.doi.org/10.1007/s00702-014-1243-x.
Glasser, M.F., Sotiropoulos, S.N., Wilson, J.A., Coalson, T.S., Fischl, B., Andersson, J.L., Xu, J., Jbabdi, S., Webster, M., Polimeni, J.R., Van Essen, D.C., Jenkinson, M., 2013. The minimal preprocessing pipelines for the Human Connectome Project. Neuroimage 80, 105–124. http://dx.doi.org/10.1016/j.neuroimage.2013.04.127.
Henderson, E.J., Lord, S.R., Brodie, M.A., Gaunt, D.M., Lawrence, A.D., Close, J.C.T., Whone, A.L., Ben-Shlomo, Y., Allen, N., Schwarzel, A., et al., 2016. Rivastigmine for gait stability in patients with Parkinson's disease (ReSPonD): a randomised, double-blind, placebo-controlled, phase 2 trial. Lancet Neurol. 15, 249–258. http://dx.doi.org/10.1016/S1474-4422(15)00389-0.
Hirsch, E.C., Graybiel, a M., Duyckaerts, C., Javoy-Agid, F., 1987. Neuronal loss in the pedunculopontine tegmental nucleus in Parkinson disease and in progressive supranuclear palsy. Proc. Natl. Acad. Sci. U. S. A. 84, 5976–5980, (doi:VL - 84).
Hong, S., Hikosaka, O., 2014. Pedunculopontine tegmental nucleus neurons provide reward, sensorimotor, and alerting signals to midbrain dopamine neurons. Neuroscience 282C, 139–155. http://dx.doi.org/10.1016/j.neuroscience.2014.07.002.
Inglis, W.L., Olmstead, M.C., Robbins, T.W., 2001. Selective deficits in attentional performance on the 5-choice serial reaction time task following pedunculopontine tegmental nucleus lesions. Behav. Brain Res. 123, 117–131.
Jan, C., François, C., Tandé, D., Yelnik, J., Tremblay, L., Agid, Y., Hirsch, E., 2000. Dopaminergic innervation of the pallidum in the normal state, in MPTP-treated monkeys and in parkinsonian patients. Eur. J. Neurosci. 12, (4525–1535).
Johansen-Berg, H., Behrens, T.E.J., Sillery, E., Ciccarelli, O., Thompson, A.J., Smith, S.M., Matthews, P.M., 2005. Functional-anatomical validation and individual variation of diffusion tractography-based segmentation of the human thalamus. Cereb. Cortex 15, 31–39. http://dx.doi.org/10.1093/cercor/bhh105.
Karachi, C., Grabli, D., Baup, N., Mounayar, S., Tandé, D., François, C., Hirsch, E.C., 2009. Dysfunction of the subthalamic nucleus induces behavioral and movement disorders in monkeys. Mov. Disord. 24, 1183–1192. http://dx.doi.org/10.1002/mds.22547.
Karachi, C., Grabli, D., Bernard, F.A., Tandé, D., Wattiez, N., Belaid, H., Bardinet, E., Prigent, A., Nothacker, H.-P., Hunot, S., Hartmann, A., Lehéricy, S., Hirsch, E.C., François, C., 2010. Cholinergic mesencephalic neurons are involved in gait and postural disorders in Parkinson disease. J. Clin. Invest. 120, 2745–2754. http://dx.doi.org/10.1172/JCI42642.
Kozak, R., Bowman, E.M., Latimer, M.P., Rostron, C.L., Winn, P., 2004. Excitotoxic lesions of the pedunculopontine tegmental nucleus in rats impair performance on a test of sustained attention. Exp. Brain Res. 162, 257–264. http://dx.doi.org/10.1007/s00221-004-2143-3.
Lambert, C., Zrinzo, L., Nagy, Z., Lutti, A., Hariz, M., Foltynie, T., Draganski, B., Ashburner, J., Frackowiak, R., 2012. Confirmation of functional zones within the human subthalamic nucleus: patterns of connectivity and sub-parcellation using diffusion weighted imaging. Neuroimage 60, 83–94. http://dx.doi.org/10.1016/j.neuroimage.2011.11.082.
Lau, B., Welter, M.-L., Belaid, H., Fernandez Vidal, S., Bardinet, E., Grabli, D., Karachi, C., 2015. The integrative role of the pedunculopontine nucleus in human gait. Brain 138, 1284–1296. http://dx.doi.org/10.1093/brain/awv047.
Lavoie, B., Parent, A., 1994a. Pedunculopontine nucleus in the squirrel monkey: projections to the basal ganglia as revealed by anterograde tract-tracing methods. J. Comp. Neurol. 344, 210–231. http://dx.doi.org/10.1002/cne.903440204.
Lavoie, B., Parent, A., 1994b. Pedunculopontine nucleus in the squirrel monkey: cholinergic and glutamatergic projections to the substantia nigra. J. Comp. Neurol. 344, 232–241. http://dx.doi.org/10.1002/cne.903440205.
Le Bihan, D., Breton, E., Lallemand, D., Grenier, P., Cabanis, E., Laval-Jeantet, M., 1986. MR imaging of intravoxel incoherent motions: application to diffusion and perfusion in neurologic disorders. Radiology 161, 401–407. http://dx.doi.org/10.1148/radiology.161.2.3763909.
Leh, S.E., Ptito, A., Chakravarty, M.M., Strafella, A.P., 2007. Fronto-striatal connections in the human brain: a probabilistic diffusion tractography study. Neurosci. Lett. 419, 113–118. http://dx.doi.org/10.1016/j.neulet.2007.04.049.
Mai, J., Paxinos, G., Voss, T., 2007. Atlas of the Human Brain. Acad. P. Ed..
Manaye, K., Zweig, R., Wu, D., Hersh, L., De Lacalle, S., Saper, C., German, D., 1999. Quantification of cholinergic and select non-cholinergic mesopontine neuronal populations in the human brain. Neuroscience 89, 759–770. http://dx.doi.org/10.1016/S0306-4522(98)00380-7.
Matsumura, M., Nambu, A., Yamaji, Y., Watanabe, K., Imai, H., Inase, M., Tokuno, H., Takada, M., 2000. Organization of somatic motor inputs from the frontal lobe to the pedunculopontine tegmental nucleus in the macaque monkey. Neuroscience 98, 97–110.
Mazzone, P., Lozano, A., Stanzione, P., Galati, S., Scarnati, E., Peppe, A., Stefani, A., 2005. Implantation of human pedunculopontine nucleus: a safe and clinically relevant target in Parkinson's disease. Neuroreport 16, 1877–1881.
Mena-Segovia, J., Micklem, B.R., Nair-Roberts, R.G., Ungless, M.A., Bolam, J.P., 2009. GABAergic neuron distribution in the pedunculopontine nucleus defines functional subterritories. J. Comp. Neurol. 515, 397–408. http://dx.doi.org/10.1002/cne.22065.
Mori, S., van Zijl, P.C.M., 2002. Fiber tracking: principles and strategies - a technical review. NMR Biomed. 15, 468–480. http://dx.doi.org/10.1002/nbm.781.
Moro, E., Hamani, C., Poon, Y.-Y., Al-Khairallah, T., Dostrovsky, J.O., Hutchison, W.D., Lozano, A.M., 2010. Unilateral pedunculopontine stimulation improves falls in Parkinson's disease. Brain 133, 215–224. http://dx.doi.org/10.1093/brain/awp261.
Muthusamy, K.A., Aravamuthan, B.R., Kringelbach, M.L., Jenkinson, N., Voets, N.L., Johansen-Berg, H., Stein, J.F., Aziz, T.Z., 2007. Connectivity of the human pedunculopontine nucleus region and diffusion tensor imaging in surgical targeting.

J. Neurosurg. 107, 814–820. http://dx.doi.org/10.3171/JNS-07/10/0814.
Nakano, K., Hasegawa, Y., Tokushige, A., Nakagawa, S., Kayahara, T., Mizuno, N., 1990. Topographical projections from the thalamus, subthalamic nucleus and pedunculopontine tegmental nucleus to the striatum in the Japanese monkey, Macaca fuscata. Brain Res. 537, 54–68.
Oakman, S.A., Faris, P.L., Kerr, P.E., Cozzari, C., Hartman, B.K., 1995. Distribution of pontomesencephalic cholinergic neurons projecting to substantia nigra differs significantly from those projecting to ventral tegmental area. J. Neurosci. 15, 5859–5869.
Okada, K., Toyama, K., Inoue, Y., Isa, T., Kobayashi, Y., 2009. Different pedunculopontine tegmental neurons signal predicted and actual task rewards. J. Neurosci. 29, 4858–4870. http://dx.doi.org/10.1523/JNEUROSCI.4415-08.2009.
Okada, K.-I., Kobayashi, Y., 2013. Reward prediction-related increases and decreases in tonic neuronal activity of the pedunculopontine tegmental nucleus. Front. Integr. Neurosci. 7, 36. http://dx.doi.org/10.3389/fnint.2013.00036.
Olszewski, J., Baxter, D., 1954. Cytoarchitecture of the human brainstem. By Jerzy Olszewski and Donald Baxter. Published and distributed in North America for S. Karger by J. B. Lippincott Company, Philadelphia and Montreal. 1954. 199 pages. Price $16.00 (Reviewed by Gerhardt von Bonin). J. Comp. Neurol. 101. http://dx.doi.org/10.1002/cne.901010308.
Parent, A., Paré, D., Smith, Y., Steriade, M., 1988. Basal forebrain cholinergic and noncholinergic projections to the thalamus and brainstem in cats and monkeys. J. Comp. Neurol. 277, 281–301. http://dx.doi.org/10.1002/cne.902770209.
Philippe, A.-C., Sébille, S., François, C., Karachi, C., Valabregue, R., Lehéricy, S., Bardinet, E., 2015. Computation of diffusion-based pathway connectivity maps: a study of subthalamic nucleus connections. 21th Annu. Meet. Organ. Hum. Brain Mapp., Honol., USA..
Piallat, B., Chabardès, S., Torres, N., Fraix, V., Goetz, L., Seigneuret, E., Bardinet, E., Ferraye, M., Debu, B., Krack, P., Yelnik, J., Pollak, P., Benabid, A.L., 2009. Gait is associated with an increase in tonic firing of the sub-cuneiform nucleus neurons. Neuroscience 158, 1201–1205. http://dx.doi.org/10.1016/j.neuroscience.2008.10.046.
Redgrave, P., Mitchell, I.J., Dean, P., 1987. Further evidence for segregated output channels from superior colliculus in rat: ipsilateral tecto-pontine and tecto-cuneiform projections have different cells of origin. Brain Res. 413, 170–174.
Rodríguez, M., Abdala, P., Barroso-Chinea, P., González-Hernández, T., 2001. The deep mesencephalic nucleus as an output center of basal ganglia: morphological and electrophysiological similarities with the substantia nigra. J. Comp. Neurol. 438, 12–31.
Rolland, A.-S., Karachi, C., Muriel, M.-P., Hirsch, E.C., François, C., 2011. Internal pallidum and substantia nigra control different parts of the mesopontine reticular formation in primate. Mov. Disord. 26, 1648–1656. http://dx.doi.org/10.1002/mds.23705.
Sah, P., Faber, E.S.L., Lopez De Armentia, M., Power, J., 2003. The amygdaloid complex: anatomy and physiology. Physiol. Rev. 83, 803–834. http://dx.doi.org/10.1152/physrev.00002.2003.
Semba, K., Fibiger, H.C., 1992. Afferent connections of the laterodorsal and the pedunculopontine tegmental nuclei in the rat: a retro- and antero-grade transport and immunohistochemical study. J. Comp. Neurol. 323, 387–410. http://dx.doi.org/10.1002/cne.903230307.
Sesack, S.R., Deutch, A.Y., Roth, R.H., Bunney, B.S., 1989. Topographical organization of the efferent projections of the medial prefrontal cortex in the rat: an anterograde tract-tracing study with Phaseolus vulgaris leucoagglutinin. J. Comp. Neurol. 290, 213–242. http://dx.doi.org/10.1002/cne.902900205.
Shink, E., Sidibé, M., Smith, Y., 1997. Efferent connections of the internal globus pallidus in the squirrel monkey: ii. Topography and synaptic organization of pallidal efferents to the pedunculopontine nucleus. J. Comp. Neurol. 382, 348–363.
Smith, Y., Parent, A., 1986. Differential connections of caudate nucleus and putamen in the squirrel monkey (Saimiri sciureus). Neuroscience 18, 347–371.
Sotiropoulos, S.N., Jbabdi, S., Xu, J., Andersson, J.L., Moeller, S., Auerbach, E.J., Glasser, M.F., Hernandez, M., Sapiro, G., Jenkinson, M., Feinberg, D.A., Yacoub, E., Lenglet, C., Van Essen, D.C., Ugurbil, K., Behrens, T.E.J., 2013. Advances in diffusion MRI acquisition and processing in the Human Connectome Project. Neuroimage 80, 125–143. http://dx.doi.org/10.1016/j.neuroimage.2013.05.057.
Stefani, A., Peppe, A., Galati, S., Bassi, M.S., D'Angelo, V., Pierantozzi, M., 2013. The serendipity case of the pedunculopontine nucleus low-frequency brain stimulation: chasing a gait response, finding sleep, and cognition improvement. Front. Neurol. 4, 68. http://dx.doi.org/10.3389/fneur.2013.00068.
Steiniger, B., Kretschmer, B.D., 2004. Effects of ibotenate pedunculopontine tegmental nucleus lesions on exploratory behaviour in the open field. Behav. Brain Res. 151, 17–23. http://dx.doi.org/10.1016/j.bbr.2003.08.001.
Steriade, M., Datta, S., Paré, D., Oakson, G., Curró Dossi, R.C., 1990. Neuronal activities in brain-stem cholinergic nuclei related to tonic activation processes in thalamocortical systems. J. Neurosci. 10, 2541–2559.
Steriade, M., Paré, D., Parent, A., Smith, Y., 1988. Projections of cholinergic and non-cholinergic neurons of the brainstem core to relay and associational thalamic nuclei in the cat and macaque monkey. Neuroscience 25, 47–67.
Takakusaki, K., Habaguchi, T., Ohtinata-Sugimoto, J., Saitoh, K., Sakamoto, T., 2003. Basal ganglia efferents to the brainstem centers controlling postural muscle tone and locomotion: a new concept for understanding motor disorders in basal ganglia dysfunction. Neuroscience 119, 293–308. http://dx.doi.org/10.1016/S0306-4522(03)00095-2.
Tattersall, T.L., Stratton, P.G., Coyne, T.J., Cook, R., Silberstein, P., Silburn, P.A., Windels, F., Sah, P., 2014. Imagined gait modulates neuronal network dynamics in the human pedunculopontine nucleus. Nat. Neurosci. 17, 449–454. http://dx.doi.org/10.1038/nn.3642.
Tournier, J.D., Calamante, F., Connelly, A., 2012. MRtrix: diffusion tractography in crossing fiber regions. Int. J. Imaging Syst. Technol. 22, 53–66. http://dx.doi.org/10.1002/ima.22005.
Tournier, J.-D., Calamante, F., Connelly, A., 2007. Robust determination of the fibre orientation distribution in diffusion MRI: non-negativity constrained super-resolved spherical deconvolution. Neuroimage 35, 1459–1472. http://dx.doi.org/10.1016/j.neuroimage.2007.02.016.
Van Essen, D.C., Smith, S.M., Barch, D.M., Behrens, T.E.J., Yacoub, E., Ugurbil, K., 2013. The WU-Minn Human Connectome Project: an overview. Neuroimage 80, 62–79. http://dx.doi.org/10.1016/j.neuroimage.2013.05.041.
Veazey, R.B., Severin, C.M., 1980a. Efferent projections of the deep mesencephalic nucleus (pars lateralis) in the rat. J. Comp. Neurol. 190, 231–244. http://dx.doi.org/10.1002/cne.901900203.
Walker, S.C., Winn, P., 2007. An assessment of the contributions of the pedunculopontine tegmental and cuneiform nuclei to anxiety and neophobia. Neuroscience 150, 273–290. http://dx.doi.org/10.1016/j.neuroscience.2007.09.018.
Wang, H.-L., Morales, M., 2009. Pedunculopontine and laterodorsal tegmental nuclei contain distinct populations of cholinergic, glutamatergic and GABAergic neurons in the rat. Eur. J. Neurosci. 29, 340–358. http://dx.doi.org/10.1111/j.1460-9568.2008.06576.x.
Winn, P., 2008. Experimental studies of pedunculopontine functions: are they motor, sensory or integrative? Park. Relat. Disord. 14, S194–S198. http://dx.doi.org/10.1016/j.parkreldis.2008.04.030.
Yelnik, J., Bardinet, E., Dormont, D., Malandain, G., Ourselin, S., Tandé, D., Karachi, C., Ayache, N., Cornu, P., Agid, Y., 2007. A three-dimensional, histological and deformable atlas of the human basal ganglia. I. Atlas construction based on immunohistochemical and MRI data. Neuroimage 34, 618–638. http://dx.doi.org/10.1016/j.neuroimage.2006.09.026.

# *PLACE DU NST*

## A. INTRODUCTION

Le NST représente l'un des noyaux innervés massivement par les neurones cholinergique du PPN, comme souligné précédemment. Etant par ailleurs la cible de référence de stimulation cérébrale profonde pour la maladie de Parkinson (Limousin et al., 1995a,b), il était intéressant dans ce contexte d'analyser l'innervation cholinergique du PPN sur le NST.

*Rôles moteur et non-monteur du NST*

Le NST, composé essentiellement de neurones de projection glutamatergiques (Rinvik et Ottersen, 1993), est fortement interconnecté avec le pallidum interne et externe, et la SNr (Parent et Smith, 1987; Parent et al., 1989; Shink et al., 1997). Il reçoit également des informations corticales directes (voie hyperdirecte), faisant de ce noyau la deuxième voie d'entrée dans le système des GB (Nambu et al., 2002).

Le rôle moteur du NST a été démontré non seulement expérimentalement chez l'animal mais aussi par des exemples cliniques chez l'homme. Ainsi une lésion excitotoxique (Hammond et al., 1979), des micro-injections d'un antagoniste GABAergique (Crossman et al., 1984) ou une stimulation électrique à haute fréquence (Beurrier et al., 1997) du NST induisent des mouvements anormaux involontaires (hémiballisme) chez le singe. Chez le singe normal, 60 à 75 % des neurones enregistrés sont modulés par le mouvement volontaire et par les manipulations articulaires passives (Abosch et al., 2002). Une organisation somatotopique caractérisée par une représentation ventrale du membre inférieur et dorsale de la face a également été démontrée (DeLong et al., 1985; Georgopoulos et al., 1983; Wichmann et al., 1994; Baron et al., 2002).

De nombreuses études expérimentales et électrophysiologiques dans des modèles animaux de maladie de Parkinson ont montré que l'activité neuronale glutamatergique du NST est augmentée à l'état parkinsonien, qualifiant le NST d'hyperactif (Bergman et al., 1994). Cette hyperactivité irrégulière avec bursts semble jouer un rôle central dans le dysfonctionnement des GB à l'état parkinsonien (figures 23 et 24) (Galvan et Wichmann, 2008), associée à une synchronisation des décharges et des oscillations anormales, en

particulier dans les bandes de fréquence beta (Brown et Williams, 2005; Little et Brown, 2014).

Partant de ces constatations, des lésions du NST à l'acide iboténique ont été effectuées chez le primate rendu parkinsonien, avec une amélioration nette et prolongée de l'ensemble des symptômes induits par le MPTP (Bergman et al., 1990; Aziz et al., 1991). Des essais de stimulation à haute fréquence du NST chez le singe rendu parkinsonien ont amélioré les symptômes moteurs, avec une réversibilité à l'arrêt de la stimulation (Benazzouz et al., 1993). Rapidement les études cliniques chez l'homme ont montré l'efficacité de la stimulation à haute fréquence de la partie centrale et postéro-latérale du NST pour contrôler l'ensemble des symptômes dopa-sensibles des patients parkinsoniens (Benabid et al., 1994; Limousin et al., 1995a).

Figure 23: Organisation de la connectivité intrinsèque des GB et leurs altérations à l'état parkinsonien
*d'après Galvan et Wichmann (2008)*

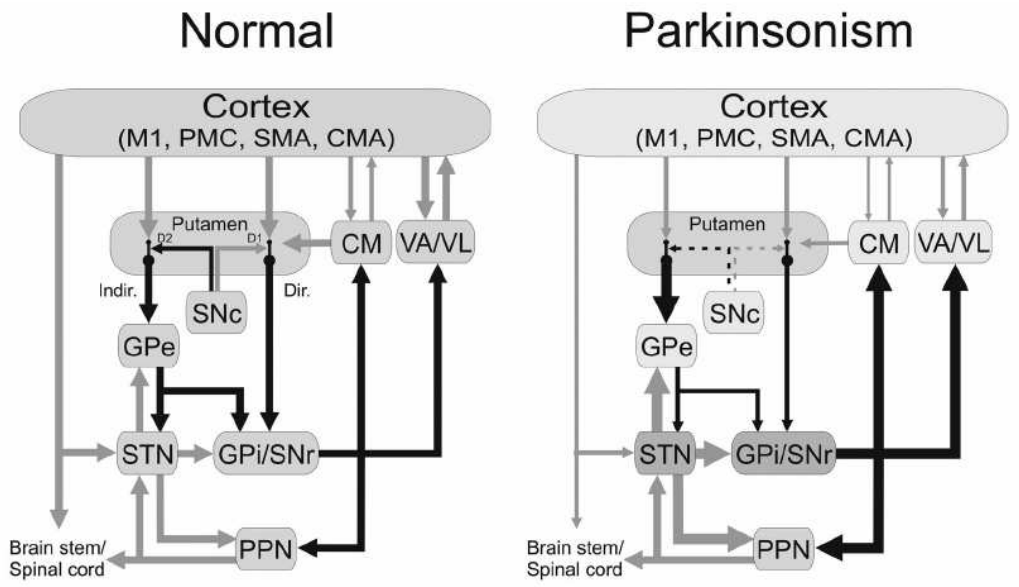

Figure 24: Modification du pattern d'activité du NST
à l'état parkinsonien
*d'après Galvan et Wichmann (2008)*

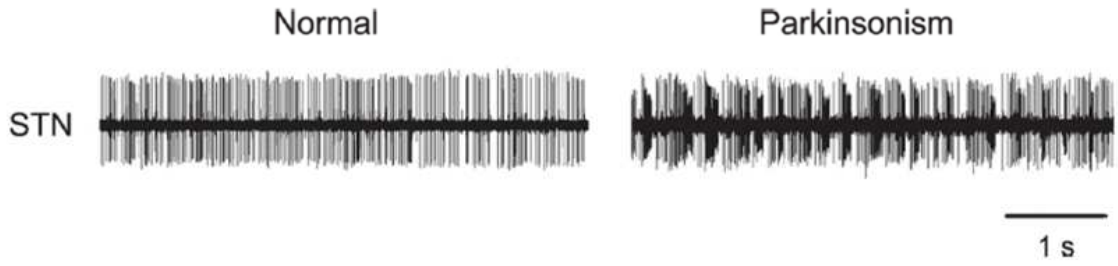


En plus de ce rôle moteur, de nombreuses études expérimentales et cliniques ont démontré le rôle du NST dans un contrôle comportemental plus large impliquant les processus cognitifs et émotionnels. En effet, sur le plan expérimental, des lésions bilatérales chez le rat induisent un déficit attentionnel et une augmentation des comportements impulsifs (Baunez et al., 1995; Baunez et Robbins, 1997). Chez le singe, des injections antérieures et ventro-médiales d'agonistes et d'antagonistes GABA (bicuculline, muscimol) au sein du NST provoquent des comportements anormaux de type stéréotypies/hyperactivité (Karachi et al., 2009). Chez l'homme, il a été décrit des symptômes psychiques (hypomanie principalement) chez des patients avec une lésion vasculaire de cette région (Trillet et al., 1995). De plus, il a été observé chez 2 patients parkinsoniens souffrant également de troubles obsessionnels compulsifs (TOC), une amélioration significative de leurs compulsions et obsessions après stimulation à haute fréquence du NST (Mallet et al., 2002). La localisation des électrodes était plus médiale ventrale et antérieure que la cible habituellement implantée pour traiter les symptômes parkinsoniens. Partant de cette constatation clinique, d'autres études ont cherché à confirmer l'intérêt de la stimulation du NST dans le traitement des TOC, sur des modèles animaux primates (Baup et al., 2008) et aussi chez l'homme (Mallet et al., 2008).

La variabilité des résultats cliniques obtenus après stimulation de différents secteurs du NST confirment l'existence de différents territoires anatomo-fonctionnels dévolus au traitement de différentes fonctions (figure 25).

Figure 25: Localisation du contact (rouge) induisant une hypomanie
et corrélation avec les territoires anatomo-fonctionnels du NST
*d'après Mallet et al (2007)*

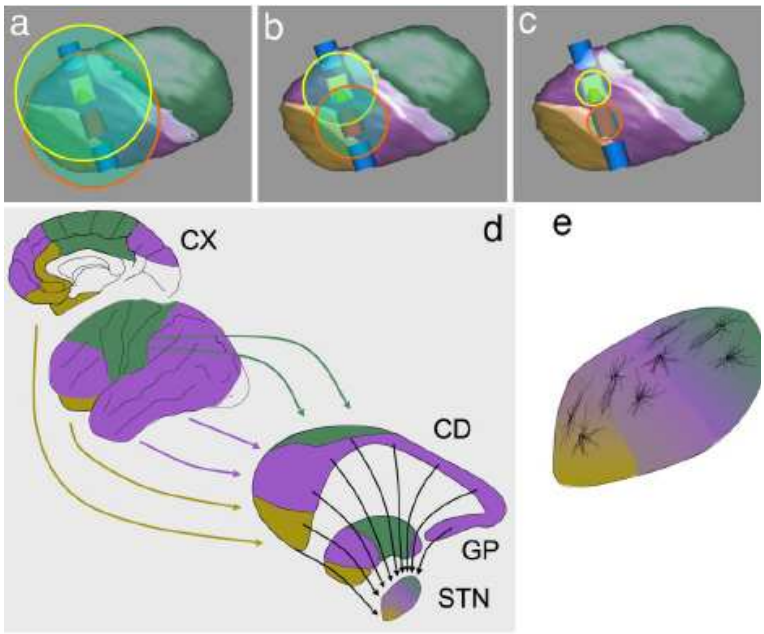

*Division anatomo-fonctionnelle du NST*

Une ségrégation du NST en différents territoires anatomo-fonctionnels a été mise en évidence par des études de traçage chez l'animal (figure 26), et de tenseur de diffusion chez l'homme. La première démonstration d'une somatotopie précise au sein du NST a été réalisée grâce au traçage axonal chez le singe, basée sur la topographie des projections corticales motrices. Les projections des cortex moteur primaire, AMS et cortex pré-moteur convergent vers la partie dorsale du NST (Nambu et al., 1996; Nambu et Llinas, 1997), et celles de l'aire FEF vont vers une partie plus ventrale (Matsumura et al., 1992). Des études plus récentes proposent une ségrégation fonctionnelle du NST se basant sur les projections en provenance non seulement du cortex mais aussi du GPe (Karachi et al., 2005; Lambert et al., 2012; Haynes et Haber, 2013). Celle-ci se résume en 3 principaux territoires anatomo-fonctionnels: postérieur et dorso-latéral intégrant des informations sensori-motrices, central intégrant des informations cognitives (territoire associatif), et antérieur et ventro-médial intégrant des informations émotionnelles et motivationnelles (territoire limbique).

Figure 26: Ségrégation fonctionnelle des projections du GPe vers le NST chez le singe
*d'après Karachi et al (2005)*

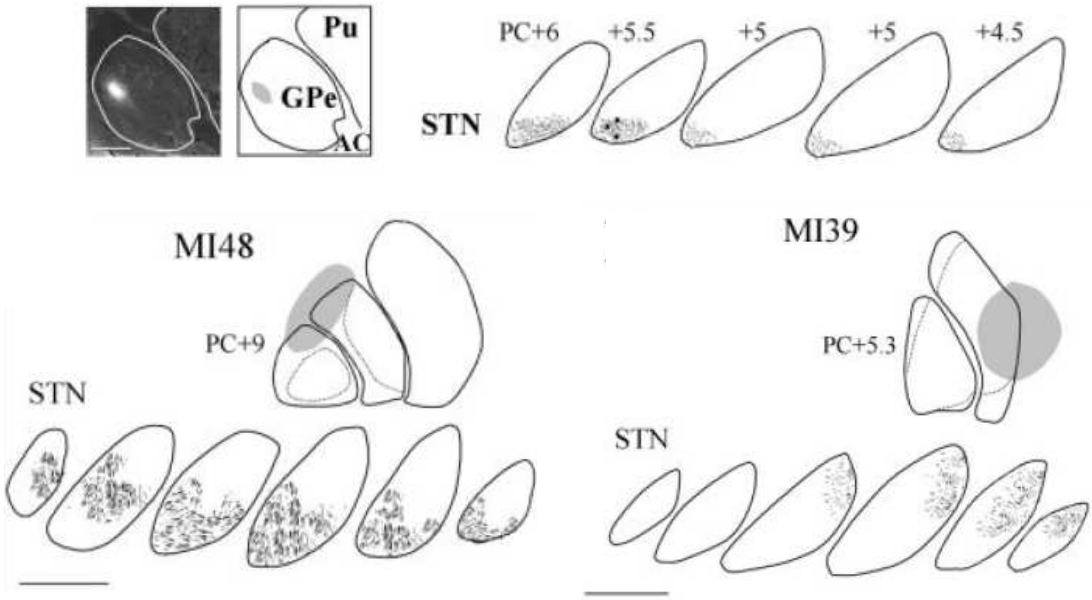

*Innervation dopaminergique et cholinergique du NST*

Le NST reçoit également de nombreuses innervations modulatrices à savoir cholinergique, dopaminergique et sérotoninergique, qui influencent très probablement le fonctionnement de ces trois territoires anatomo-fonctionnels.

L'innervation cholinergique du NST ne provient que du PPN et non du noyau basalis de Meynert. Cette innervation a été étudiée chez le rongeur (Jackson et Crossman, 1983; Scarnati et al., 1987; Semba et Fibiger, 1992), le singe (Lavoie et Parent 1994b) (figure 27) et l'homme (Mesulam et al., 1992). Chez le rat, cette innervation cholinergique caractérisée en microscopie optique et électronique est diffuse et homogène dans l'ensemble du NST (Bevan et Bolam, 1995). Chez le singe et l'homme, cette innervation a été décrite comme étant dense, mais sans précision quant à une distribution régionale particulière (Lavoie et Parent, 1994b). Il reste ainsi à déterminer si celle-ci est homogène chez le primate comme chez le rat, ou hétérogène comme cela a été observé dans d'autres noyaux des GB: globus pallidus chez le singe (Eid et al., 2014) ou la SNc chez l'homme (Mesulam et al., 1992). Ces résultats pourraient suggérer que l'innervation cholinergique du NST chez le primate soit distribuée différemment en fonction des territoires anatomo-fonctionnels.

De même, il est intéressant de rappeler que l'innervation dopaminergique que reçoit le NST a été décrite comme étant hétérogène. Cette innervation est nettement moins dense que la projection cholinergique. Initialement rapportée comme accessoire avec des connexions « en passant » du faisceau dopaminergique allant vers le striatum, elle a ensuite été mieux caractérisée et mise en évidence par des techniques histochimiques ou de traçage de voies axonales chez le rat (Brown et al., 1979; Gerfen et al., 1982; Lindvall et al., 1984; Campbell et al., 1985; Gauthier et al., 1999; Hassani et al., 1997), le chat (Meibach et Katzman, 1979), le singe (Lavoie et al., 1989; Francois et al., 2000; Smith et Kieval, 2000) et l'homme (Nobin et Bjorklund, 1973; Cossette et al., 1999; Hedreen, 1999; Augood et al., 2000). Cependant, on ne connaît pas de façon précise sa distribution en rapport avec les territoires anatomo-fonctionnels du NST. De plus cette innervation n'a jamais été caractérisée en microscopie électronique chez le primate.

Figure 27: Terminaisons cholinergiques du PPN
mises en évidence sur une coupe transverse du NST chez le singe
*d'après Lavoie et Parent (1994b)*

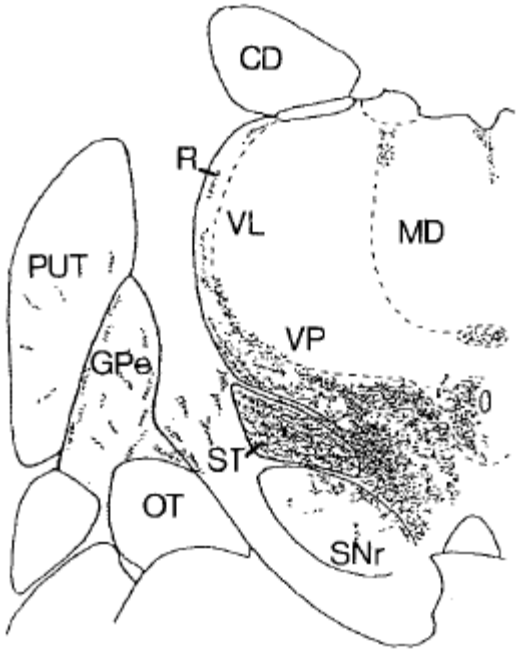

## B. Objectifs de l'étude

Le NST recevant des afférences modulatrices cholinergique, dopaminergique et sérotoninergique, leur effets sur le fonctionnement des trois territoires anatomo-fonctionnels ne sont pas connus. Malgré les nombreuses études de la littérature, l'ultrastructure de l'innervation cholinergique et dopaminergique du NST n'a été décrite que chez le rat (Bevan et Bolam, 1995; Cragg et al., 2004; Kita et Kita, 2011), et à peine évoquée chez le singe (Smith et Kieval, 2000). De plus, la topographie des afférences n'a pas été étudiée en fonction des trois territoires anatomo-fonctionnels.

L'objectif est donc ici de décrire la topographie, de quantifier et de caractériser l'innervation cholinergique et dopaminergique du NST en fonction des trois grands territoires anatomo-fonctionnels chez le singe et l'homme, et de comparer leur distribution et leur connexions synaptiques en microscopie optique et électronique.

## C. Méthodologie

### 1. Prélèvements post-mortem

Deux cerveaux humains ont été acquis par le département d'anatomie de l'université de médecine Paris V, chez des sujets ayant donné de leur vivant leur consentement au don du corps pour la science. Les cerveaux ont été obtenus selon les règles approuvées par le Comité National d'Ethique, et ne présentaient macroscopiquement pas de lésion visible, ni de dégénérescence de la SN. Cas 1: 65 ans, intervalle post-mortem 120 heures; Cas 2: 73 ans, intervalle post-mortem 55 heures. Après extraction du cerveau, chaque hémisphère a été coupé en blocs contenant l'ensemble du NST, qui ont été immédiatement fixés (immersion dans le paraformaldehyde (PFA) 4% pendant 72h à 4°C).

Deux cerveaux de macaque adulte ont été utilisés. Après sédation à la kétamine et morphine, puis anesthésie profonde à l'isoflurane, les animaux ont reçu une perfusion intracardiaque de PFA 4%. De petits blocs contenant le NST ont été coupés et fixés selon le même protocole que pour les cerveaux humains.

## 2. Procédures immunohistochimiques

Les blocs contenant le NST ont été coupés après congélation (coupes transverses de 50 µm). Les neurones et les fibres DA ont été mis en évidence par immunomarquage de la tyrosine hydroxylase (TH), et de la Choline Acétyl Transferase (ChAT). Brièvement, pour l'immunomarquage de la TH, après rinçages dans du tampon phosphate salin (PBS), les coupes ont été incubées dans une solution de PBS 0,1M contenant 20% de méthanol et 3% d'$H_2O_2$ pendant 15 min afin d'inhiber les péroxydases endogènes puis dans du sérum normal de cheval 33% afin de bloquer les sites de liaison non spécifiques des anticorps. Les coupes ont ensuite été incubées 48h à 4°C dans l'anticorps primaire anti-TH (fabriqué chez la souris; Immunostar) dilué au 1/5000ème dans du PBS 0,1M contenant 0,02% de thimérosal. A nouveau après rinçage, ces coupes ont été incubées pendant 1h30 dans l'anticorps secondaire biotinylé dirigé contre les immunoglobulines de souris (anticorps développé chez le cheval; Vector Laboratories) dilué au 1/250ème dans du PBS 0,1M. Enfin, la péroxydase a été révélée dans une solution de Diaminobenzidine (DAB) à 0,05%. Le temps de révélation est déterminé visuellement sous loupe binoculaire. Les coupes ont alors été rincées, montées sur lames gélatinées, séchées, déshydratées puis montées entre lame et lamelle avec du milieu de montage (Eukitt). La même procédure a été appliquée pour l'immunomarquage de la ChAT, avec des séries de coupes régulièrement espacées, incubées avec l'anticorps anti-ChAT (1/500; Merck Millipore) puis avec l'anticorps secondaire correspondant.

## 3. Méthode de quantification en microscopie optique

La délimitation du NST et la quantification des fibres marquées TH+ et ChAT+ dans le NST ont été réalisées grâce à un système d'analyse d'image semi-automatique (mercator, ExploraNova). Le NST a été délimité en excluant le faisceau dopaminergique dense longeant le noyau dorsalement, afin de restreindre la quantification aux axones entrant et se terminant dans le noyau. Afin de déterminer la distribution des terminaisons TH positives (TH+) et ChAT positives (ChAT+), le NST a été divisé en 4 parties et 6 sous-parties: n°1 pour la partie antérieure et ventro-médiale, n°2 pour la partie centrale subdivisée en centro-dorsale (n° 2d) et centro-ventrale (n° 2v), n°3 pour la partie latérale subdivisée en latéro-dorsale (n° 3d) et latéro-ventrale (n° 3v), et n°4 pour la partie postérieure et dorsolatérale (figure 28). La

quantification des terminaisons a été effectuée dans les différentes sous-parties sur 2 niveaux similaires antéro-postérieurs pour les NST du singe et humain (Bregma -10.35 mm and -11.25 mm pour le singe (Paxinos 2008) et sections 35 and 33 pour l'homme (Mai 1997)). La méthode de quantification consiste à déterminer le nombre de terminaisons TH+ et ChAT+ visualisées dans des cubes de 50 µm et 40µm d'épaisseur (100000 µm3), espacés de 200 µm et distribués aléatoirement au sein des différentes parties et sous-parties du NST. La visualisation s'est effectuée à un objectif de 63X (immersion à l'huile) dans chaque sous partie sur 2 coupes. Ont été comptées toutes les terminaisons axonales marquées situées à l'intérieur du volume quantifié ou croisant ses bords, sur l'ensemble de l'épaisseur de la coupe. Nous nous sommes principalement intéressés au nombre de terminaisons marquées fines et tortueuses correspondant aux terminaisons axonales, afin d'exclure les axones plus épais considérés comme les fibres de passage vers le pallidum et le striatum. Le nombre de volumes sélectionnés aléatoirement dans chaque sous-partie du NST a été déterminé au préalable, de telle sorte que l'addition d'un autre volume ne modifiait pas de plus de 5% la variation moyenne du nombre de terminaisons par volume. La densité des terminaisons TH+ et ChAT+ a été exprimée en nombre d'axones marqués par $mm^3$. Un test de Mann–Whitney a été effectué, d'abord pour analyser les différences entre les 2 macaques et les 2 humains pour chaque sous-partie du NST, puis afin de déterminer la densité des terminaisons dans l'ensemble des territoires du NST chez le macaque et l'homme. Aucune différence statistique n'a été observée entre les 2 NST de chaque espèce ($p > 0.05$), ce qui a permis de regrouper les résultats par espèce, aussi bien pour les terminaisons ChAT+ que TH+.

Figure 28: Subdivision du NST sur 3 coupes transverses chez le singe
*n°1: partie antérieure et ventro-médiale, n°2: partie centrale (centro-dorsale 2d et centro-ventrale 2v), n°3: partie latérale (latéro-dorsale 3d et latéro-ventrale 3v), n°4: partie postérieure et dorsolatérale*

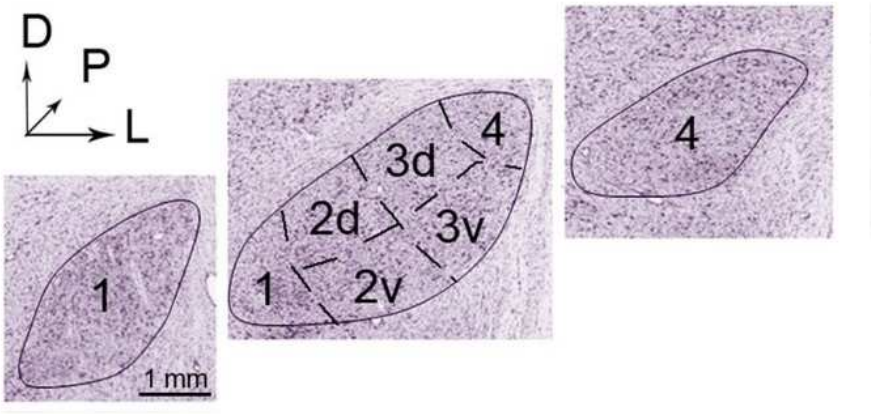


## 4. Analyse en microscopie électronique

Après révélation immunohistochimique TH ou ChAT, les coupes ont été post-fixées (osmium tetroxide 1%, incubé dans 1% d'uranyl acetate, déshydratées et immergées dans l'epon 812). Des coupes ultrafines ont été réalisées (70 nm d'épaisseur), et analysées au microscope électronique (JEOL 1200EX II).

La quantification des varicosités TH+ a été réalisée dans les parties antérieures et ventro-médiales (n°1) et centrales (n°2) chez le singe et l'homme, et celles des varicosités ChAT+ dans l'ensemble des sous-parties du NST. Le nombre de varicosités formant des contacts synaptiques ou non-synaptiques ont été comptés. Concernant les varicosités ayant des contacts synaptiques, la synapse a été classée comme symétrique ou asymétrique selon la spécialisation membranaire post-synaptique. L'analyse et la quantification des varicosités axonales ont été réalisées sur un minimum de 10 images d'axones sélectionnées aléatoirement pour chaque sujet et 30 pour chaque espèce.

# D. RÉSULTATS

## 1. Innervation dopaminergique du NST

Pour les deux espèces, de nombreux axones TH+ ont été mis en évidence, formant un épais faisceau se dirigeant à travers le champ de forel pré-rubral, courant le long de la limite dorsale du NST vers le striatum. L'observation en microscopie optique a mis en évidence que de ces axones venant du faisceau, beaucoup entrent dans le NST à la partie la plus antérieure et médio-ventrale, et à un moindre degré vers la partie centrale du noyau. En microscopie électronique, un grand nombre de ces axones TH+ apparaissent myélinisés, et ces fibres dopaminergiques myélinisées sont présentes dans la partie antérieure ventro-médiale (n°1), mais aussi dorsale du noyau. Des corps cellulaires et dendrites TH+ ont été observés dans la partie antérieure et ventro-médiale du NST, proche de la SNc, mais aussi dans la partie centro-dorsale (n°2d). Le nombre de corps cellulaires comptés sur 6 coupes TH+ reste très faible (2 à 3 chez le singe, et 6 chez l'homme). De fins axones TH+ avec terminaisons marquées ont été observés dans l'ensemble du NST. La densité de ces terminaisons était hétérogène avec un gradient (figure 29). En effet, la densité de terminaisons TH+ était élevée dans la partie antérieure et ventro-médiale du noyau ainsi que la partie dorsale (n°2d et 3d), et beaucoup plus faible dans la partie ventrale (n°2v et 3v). La densité des terminaisons TH+ était la plus élevée dans le territoire antérieur et ventro-médial, puis dans les 2 parties centro-dorsale et dorso-latérale ($p<0.001$ par rapport au n°1), dans le territoire postéro-latéral (n° 4) ($p<0.001$ par rapport au n°2d et 3d), et dans la partie ventrale (n° 2v/3v) ($p<0.001$ chez le singe et $<0.05$ chez l'homme par rapport au n°4). Par ailleurs, même si le gradient est similaire pour les deux espèces étudiées, la densité globale des terminaisons TH était 2 fois plus faible chez l'homme ($121 \pm 10 \times 10^3$ terminaisons/mm$^3$) que chez le singe ($238 \pm 15 \times 10^3$ terminaisons/mm$^3$).

Figure 29: Hétérogénéité de l'innervation dopaminergique du NST

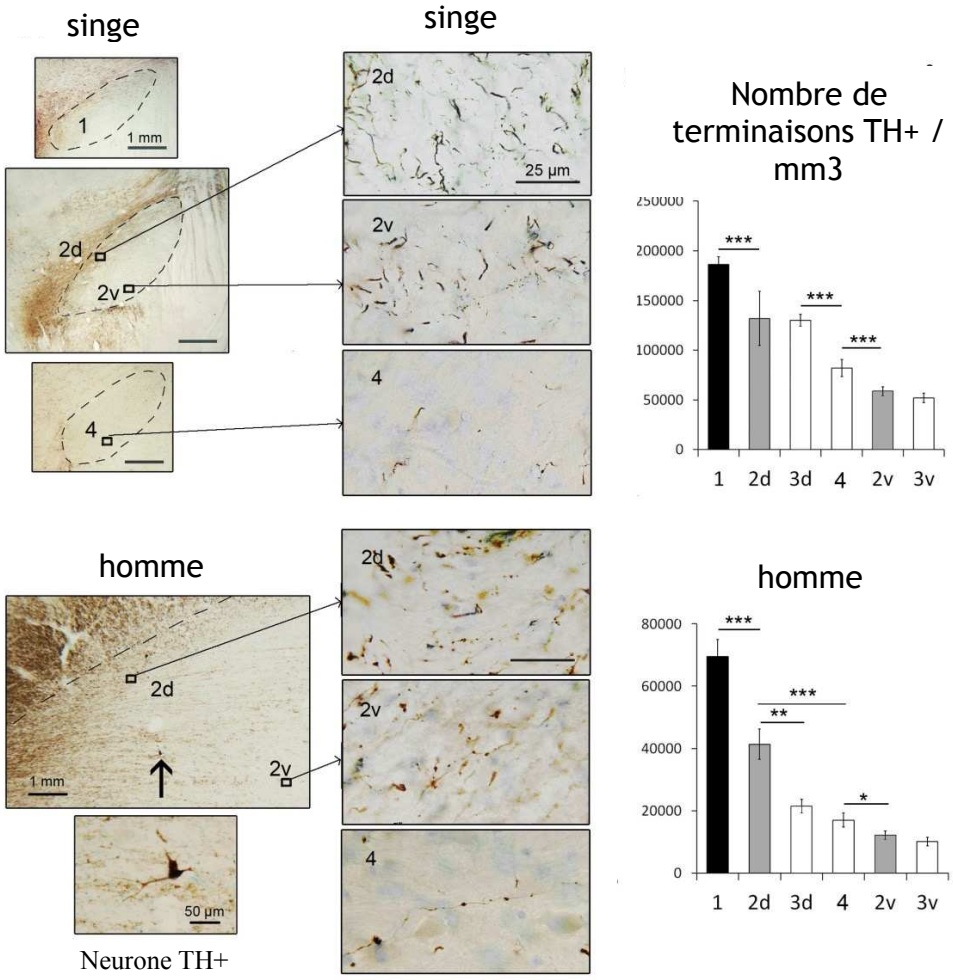


Neurone TH+

En microscopie électronique, un faible nombre de terminaisons TH+ établissaient des contacts synaptiques (31% et 28% de contacts synaptiques versus 69% et 72% de contacts non synaptiques chez le singe et chez l'homme). Ces contacts synaptiques correspondaient à des synapses symétriques (53% chez le singe; 59% chez l'homme) et asymétriques (47% chez le singe; 41% chez l'homme) (figures 30 et 31). Ils étaient visualisés dans l'ensemble du NST, mais prédominaient dans la partie antérieure ventro-médiale et dorsale. Des dendrites recevant à la fois des contacts synaptiques TH+ symétriques et asymétriques ont aussi été mis en évidence.

Figure 30: Marquage TH en microscopie électronique
*Axones TH myélinisés (A) et synapses asymétriques (B)*

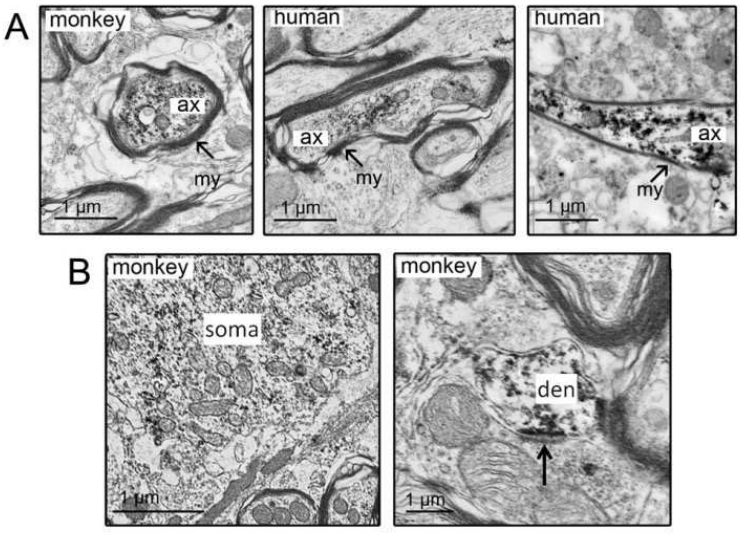

Figure 31: Marquage TH en microscopie électronique
*Axones non myélinisés formant des contacts non synaptiques (A), des synapses symétriques (B), et asymétriques (C)*

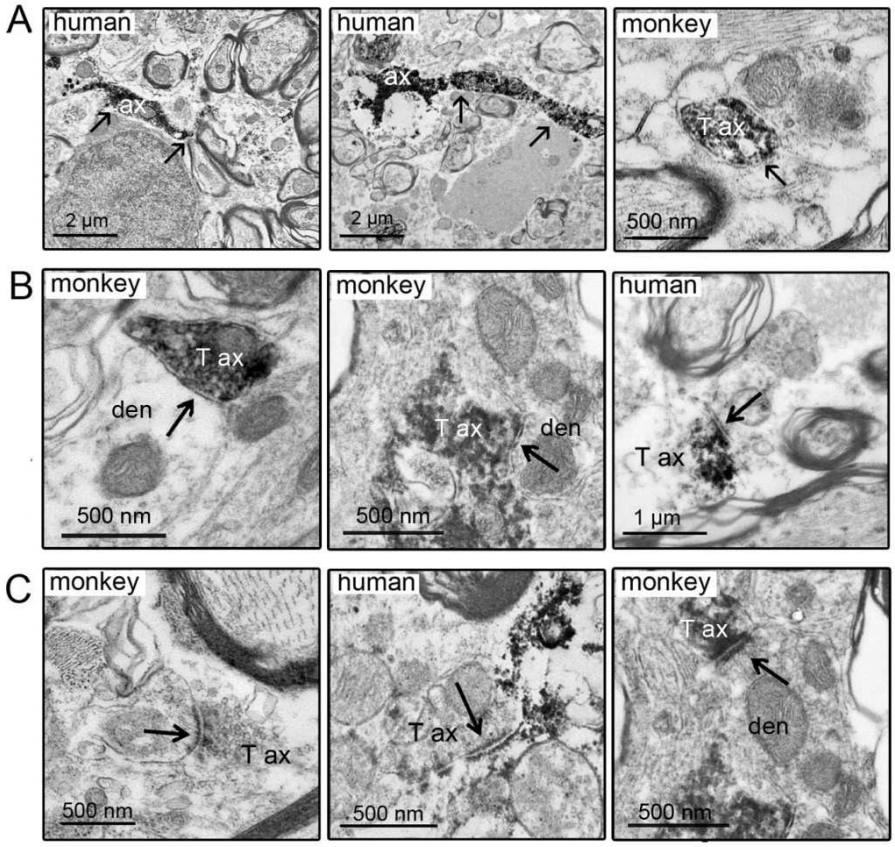

## 2. Innervation cholinergique du NST

Les axones cholinergiques ChAT+ s'étendent de la partie caudale et dorsale du NST avec une direction antérieure et ventrale, en émettant de petites varicosités. Contrairement à l'innervation TH+, la distribution des terminaisons ChAT+ est homogène dans l'ensemble du NST pour les deux espèces étudiées (figure 32). Nous avons quantifié 958 ± 99 x103 terminaisons par mm3 chez le singe et 740 ± 116 x103 terminaisons par mm3 chez l'homme. En microscopie électronique, de nombreuses varicosités ChAT+ établissaient des contacts avec les corps cellulaires et les dendrites de l'ensemble du NST (75% chez le singe; 71% chez l'homme) sans synapse visualisée. Seulement une minorité de terminaisons ChAT+ établissait des contacts synaptiques (25% chez le singe; 29% chez l'homme), surtout sur des dendrites non marquées et plus rarement sur des corps cellulaires (figure 33). Ces synapses étaient fréquemment asymétriques (85% chez le singe; 90% chez l'homme), et plus rarement symétriques (15% chez le singe; 10% chez l'homme).

Figure 32: Homogénéité de l'innervation cholinergique du NST chez le singe et l'homme en microscopie optique

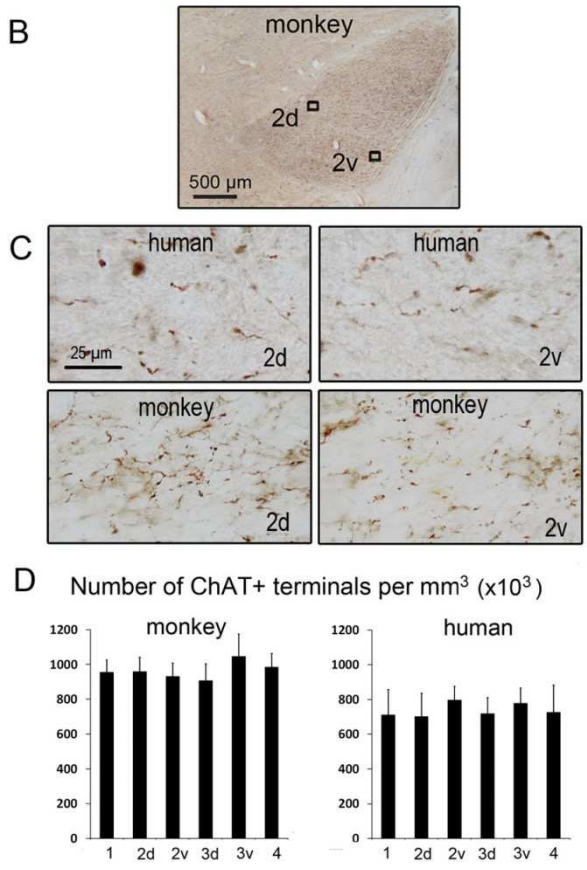

Figure 33: Marquage ChAT en microscopie électronique

*A: Axones non myélinisés*

*B: Synapses asymétriques chez le singe*

*C: Synapses asymétriques chez l'homme*

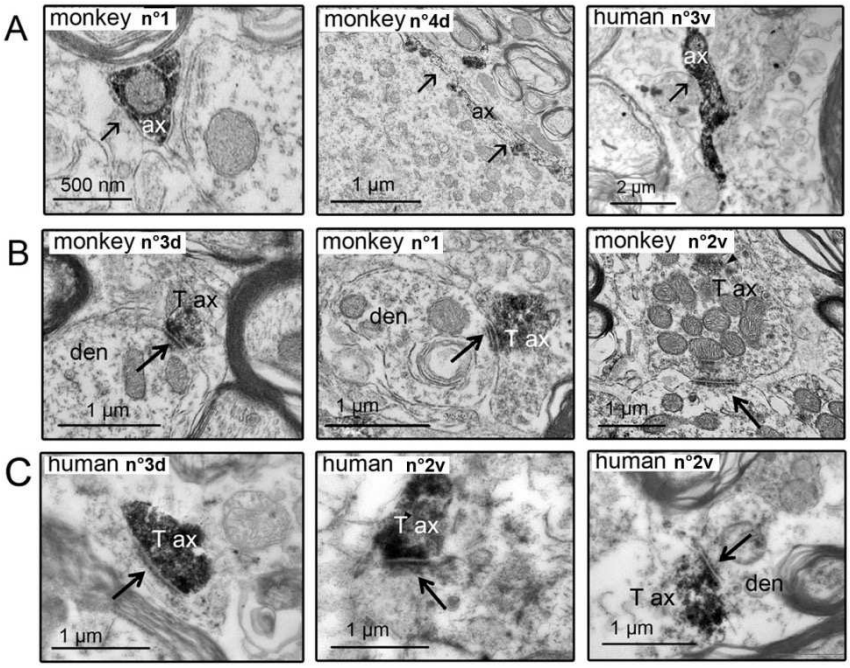

## E. Discussion et Conclusions

Les résultats obtenus montrent une innervation cholinergique homogène dans l'ensemble des territoires anatomo-fonctionnels du NST, alors que l'innervation dopaminergique est hétérogène avec un gradient de densité plus élevé dans la partie antérieure ventro-médiale correspondant au territoire limbique. Seul un faible nombre de terminaisons dopaminergiques et cholinergiques présentaient une spécialisation synaptique.

*Topographie de l'innervation cholinergique et dopaminergique du NST*

Les précédentes études ont décrit une innervation dopaminergique minime dans le NST du primate (Nobin et Bjorklund, 1973; Lavoie et al., 1989; Hedreen, 1999; Cossette et al., 1999; Augood et al., 2000; Francois et al., 2000; Smith et Kieval, 2000) associée à une faible concentration de dopamine libérée (Pifl et al., 1990). Nos résultats confirment cette densité faible de terminaisons TH+ dans le NST. Celle-ci est encore moindre chez l'homme par rapport au singe, avec une densité neuronale globale connue pour être plus faible aussi dans les autres noyaux des GB (Hardman et al., 2002) mais associée à une connectivité plus importante (Armstrong, 1990). Nous avons observé une hétérogénéité de l'innervation dopaminergique avec un gradient de densité plus élevé dans la partie correspondant au territoire anatomo-fonctionnel limbique. Cette innervation correspond à une densité élevée de terminaisons dopaminergiques avec même des corps cellulaires TH+ au sein du NST ventral et antérieur. La présence de corps cellulaires TH+ au sein du NST a aussi été montrée chez le chat (Meibach et Katzman, 1979) permettant une sécrétion locale de dopamine complétant celle provenant des terminaisons. En comparaison, l'innervation dopaminergique des parties dorsales correspondants aux territoires anatomo-fonctionnels associatif et sensori-moteur est beaucoup plus faible, sauf tout dorsalement juste sous-jacent au faisceau dopaminergique se dirigeant vers le striatum. Ces variations de densité anatomique suggèrent un rôle de la dopamine dans la régulation des informations émotionnelles et motivationnelles au sein du territoire limbique du NST.

Cependant la distribution des récepteurs dopaminergiques ne semble pas suivre le gradient de densité des terminaisons dopaminergiques. Aucun gradient n'a été retrouvé pour les récepteurs D1, D2 et D3 dans le NST chez le rat et le macaque par technique d'hybridation in

situ (Suzuki et al., 1998; Galvan et al., 2014), bien qu'une étude par RT-PCR chez le rat ait rapporté une densité plus élevée des récepteurs D1 dans la partie ventrale du NST (Flores et al., 1999). Chez le singe, les récepteurs D1 et D2 sont retrouvés sur les terminaisons axonales pré-synaptiques glutamatergiques et GABAergiques, et les récepteurs D5 sont plutôt exprimés au niveau post-synatique sur les dendrites des neurones du NST (Galvan et al., 2014). Notons que la dopamine sécrétée par les varicosités axonales TH+ sans spécialisation synaptique présentes au sein du territoire limbique peut diffuser secondairement vers les récepteurs dopaminergiques dans l'ensemble du NST. Cette transmission volumique (Agnati et al., 1986; Fuxe et al., 1988) représenterait un mode alternatif de transmission dopaminergique dans le NST, similaire à celui mis en évidence récemment dans le pallidum chez le singe (Eid et Parent, 2015).

Nous avons par ailleurs retrouvé une innervation cholinergique homogène dans l'ensemble du NST chez le singe et l'homme, contrairement aux résultats retrouvés dans le pallidum chez le singe (Eid et al., 2014). Cette innervation est dense, et la majorité des varicosités cholinergiques ne présentent pas de spécialisation synaptique, suggérant aussi un mode de transmission volumique cholinergique. La majorité des synapses observées étaient asymétriques, et donc très probablement excitatrices (Capozzo et al., 2009). Il a été montré que des récepteurs muscariniques (Feger et al., 1979; Xiang et al., 2012) et nicotiniques (Xiao et al., 2015) étaient distribués de façon homogène dans le NST de rongeurs. Il n'y a ainsi pas de différence significative de l'effet modulateur de l'acétylcholine selon les territoires anatomo-fonctionnels du NST.

*Particularités de l'innervation dopaminergique*

Environ deux tiers des synapses dopaminergiques du NST chez le primate étaient inhibitrices (symétriques), et un tiers excitatrices (asymétriques), ce qui est similaire aux données sur l'innervation dopaminergique du pallidum interne et externe chez le macaque (Eid et Parent, 2015). Chez le rat in vivo, des études de micro-injections d'agoniste dopaminergique montrent une inhibition de l'activité neuronale du NST (Campbell et al., 1985; Hassani et Feger, 1999), alors que l'application de dopamine exogène sur des coupes in vitro augmente l'activité des neurones du NST (Mintz et al., 1986; Ni et al., 2001; Zhu et al., 2002). Ainsi la modulation dopaminergique du NST apparaît complexe, associant des

synapses symétriques et asymétriques, et des récepteurs dopaminergiques synaptiques et non synaptiques.

Par ailleurs l'innervation dopaminergique du NST se caractérise par des axones myélinisés au sein du noyau. La présence d'axones dopaminergiques non myélinisés a été rapportée chez le rat dans le striatum (Freund et al., 1984; Pickel et al., 1992; Descarries et al., 1996; Hanley, 1996) et dans le NST (Cragg et al., 2004). Les axones dopaminergiques myélinisés ont été décrits dans la SN et le striatum chez le macaque et l'homme (Arsenault et al., 1988; Roberts, 1997; Kung et al., 1998) et dans le pallidum interne et externe chez le macaque (Eid et Parent, 2015). Dans le contexte de la MP, les neurones avec des axones myélinisés sont connus pour être préservés durant l'évolution de la maladie (Braak et al., 2004). Reste à déterminer si ces axones myélinisés présents dans le NST proviennent des neurones dopaminergiques préservés situés dans la partie dorsale de la substance noire et dans la VTA (Damier et al., 1999).

*Implications fonctionnelles*

Chez les patients parkinsoniens implantés dans le NST, des effets psychiatriques ont été observés lorsque l'électrode ou les contacts utilisés étaient situés dans la partie antérieure ventro-médiale du noyau (Dujardin et al., 2004; Volkmann et al., 2010; Welter et al., 2014). D'après nos résultats anatomiques, ces symptômes d'ordre limbique pourraient être expliqués en partie par une modulation de l'innervation dopaminergique par l'électrode de stimulation, d'autant que l'innervation dopaminergique est préservée dans le striatum limbique chez le patient parkinsonien (Kish 1988). Cette modulation des circuits émotionnels et motivationnels peut par ailleurs jouer un rôle dans l'effet positif de la stimulation du territoire limbique du NST pour le traitement des troubles obsessionnels compulsifs (Mallet et al., 2008; Chabardes et al., 2013). De plus les enregistrements électrophysiologiques, réalisés au cours d'un paradigme de catégorisation émotionnelle chez les patients parkinsoniens implantés, montraient une modification de l'activité du NST corrélée à la valence émotionnelle de l'image (plaisante, déplaisante ou neutre) (Buot et al., 2013), prédominant sur les contacts situés ventralement. En appliquant le même paradigme chez les patients TOC implantés dans le NST, il a été montré que l'amplitude de l'effet émotionnel variait en fonction de la valence plaisante du stimulus, encodé seulement pour les contacts situés dans la partie antéro-médiale

du NST (Buot et al., 2015). Ce résultat pourrait correspondre plus spécifiquement à la modulation dopaminergique du territoire anatomo-fonctionnel particulier du NST (figure 34).

Par ailleurs, la modulation du territoire sensori-moteur du NST par la SCP peut induire ou aggraver les troubles de la marche et de la posture chez les patients parkinsoniens. L'innervation cholinergique du NST provenant du PPN est dense et homogène (Lavoie et Parent, 1994b; Kita et Kita, 2011). Les neurones cholinergiques du PPN ayant un rôle central dans la locomotion et la posture, on peut supposer que la SCP du NST pourrait altérer rétrogradement la fonction du PPN, quelle que soit la localisation de l'électrode, entraînant ou aggravant les troubles de la marche.

Figure 34: Représentation des territoires anatomo-fonctionnels du NST (A) et corrélation avec le gradient d'innervation dopaminergique (B)

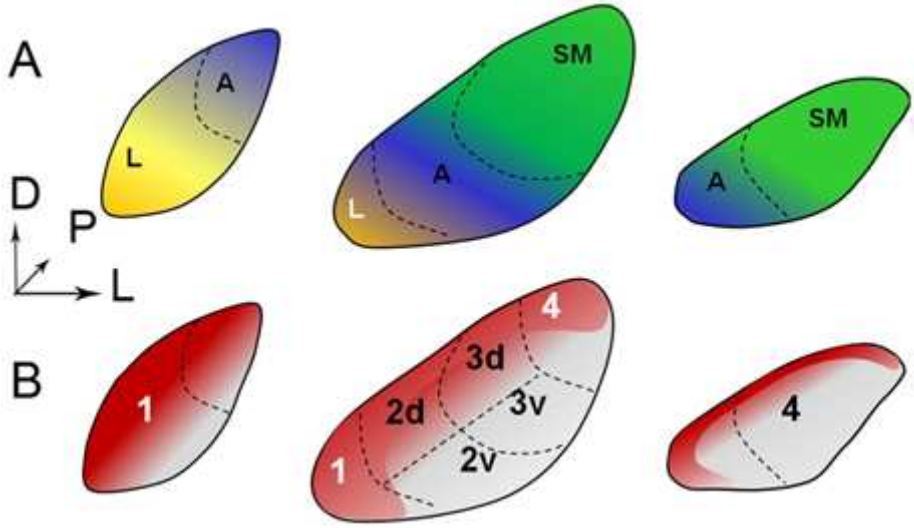

# PERSPECTIVES

L'étude de la MLR, nouvelle cible thérapeutique de la SCP, représente un challenge compte tenu de la complexité anatomique de cette région. Nos résultats sur la connectivité du PPN et du CuN chez le primate ont montré l'importance du rôle intégrateur du PPN, le CuN étant quant à lui plutôt connecté à des réseaux limbiques. Ainsi le PPN, de par ses connexions avec les territoires sensori-moteurs et associatifs, semble la cible à privilégier en SCP pour tenter d'améliorer les troubles de la marche et de l'équilibre chez les patients parkinsoniens à un stade avancé.

1. Sur le plan expérimental

Une étude portant sur le rôle fonctionnel respectif du PPN et du CuN dans la locomotion a été débutée au sein de l'équipe afin d'étayer ces données anatomiques. L'objectif de cette étude est de comparer les effets de lésions restreintes du CuN sur la posture et la locomotion chez le singe aux lésions cholinergiques spécifiques du PPN déjà réalisées dans l'équipe (Karachi et al., 2010). Une lésion bilatérale du CuN a déjà été effectuée chez un premier singe (figure 35), avec des symptômes associant une déviation de la tête, une rigidité du membre supérieur, et une augmentation de la vitesse de marche et de la hauteur du bassin. Ces résultats préliminaires orientent donc bien vers des fonctions distinctes du PPN et du CuN, mais nécessitent d'être confirmés sur un 2ème singe.

Figure 35: Représentation des lésions bilatérales du CuN (en rouge) chez un singe sur une coupe coronale cartographiée et modélisation tridimensionnelle

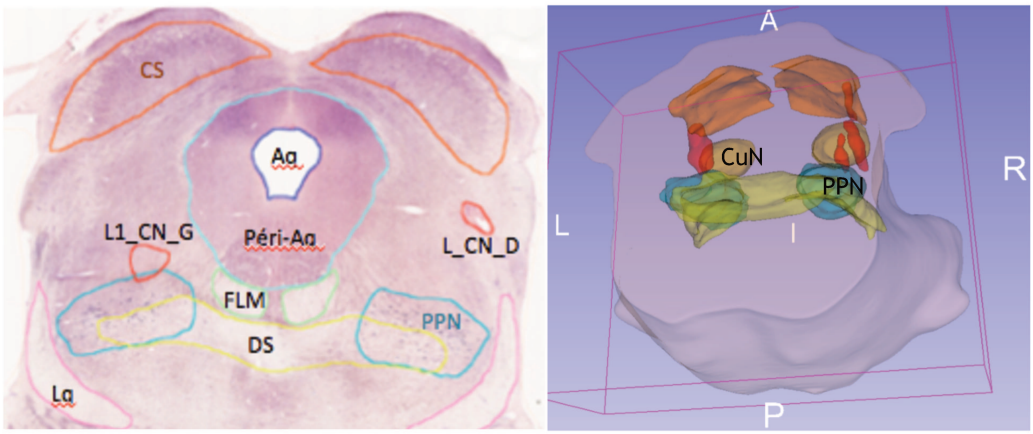

2. Sur le plan clinique

En clinique chez l'homme, un protocole de SCP de cette région est en cours dans l'équipe (GAITPARK), afin de comparer l'effet de la stimulation de plusieurs cibles sur des paramètres de marche et de posture chez douze patients. Les cibles testées sont le PPN, et plus profondément la jonction ponto-mésencéphalique, implantée avec de bons résultats par l'équipe d'Oxford (Thevathasan et al., 2011; 2012). Trois patients ont déjà été implantés, mais l'évaluation clinique n'est pas encore disponible (évaluation en double aveugle).

La connectivité du PPN et du CuN va être étudiée chez ces mêmes patients selon la même modalité que celle effectué chez les sujets sains (tractographie probabiliste (Philippe et al., 2015)), afin de comparer les éventuelles différences et déterminer si ces différences impliquent préférentiellement les territoires sensori-moteurs. Cette étude permettra également de visualiser une éventuelle altération de la connectivité de la MLR au cours de la MP.

De façon parallèle, pour opérer ces patients, nous développons un atlas du tronc cérébral, regroupant les données histologiques de densité des différentes populations neuronales et d'imagerie sur un espace commun. Un tel outil permettrait d'affiner le ciblage pour la SCP de cette région et ainsi espérer améliorer en partie les résultats cliniques obtenus sur la marche et la posture en réduisant l'imprécision anatomique du positionnement des électrodes. De plus la visualisation des faisceaux de fibres traversant cette région pourrait aussi guider les trajectoires et les contacts à activer afin de minimiser les effets indésirables et améliorer l'effet de la stimulation (figure 36).

En améliorant ainsi notre connaissance anatomique et fonctionnelle de la MLR, cette cible pourrait à terme être proposée pour d'autres indications, comme les troubles de la marche dans la population vieillissante ou encore les troubles du sommeil sévères dont souffrent certains patients. En effet notre étude a montré l'implication du PPN cholinergique dans la régulation des cycles veille-sommeil, et l'effet positif à distance d'une lésion chez le singe rendu parkinsonien. Des observations cliniques chez les patients implantés dans le PPN pour les troubles de la marche ont de même suggéré le bénéfice de la stimulation à basse fréquence sur l'architecture et la qualité du sommeil. Une étude expérimentale de stimulation du PPN chez le singe à l'état contrôle puis parkinsonien permettrait de préciser le rôle du PPN et le bénéfice attendu sur les troubles du sommeil, en utilisant la même technique d'évaluation du sommeil que celle que nous avons utilisée. Un projet est actuellement en cours à l'Institut

des Neurosciences de Grenoble sous la direction de Brigitte Piallat, avec une collaboration proposée entre nos équipes.

Figure 36: Atlas multimodal utilisé pour le ciblage du PPN
(représentation des électrodes et en rouge la densité des neurones cholinergiques)

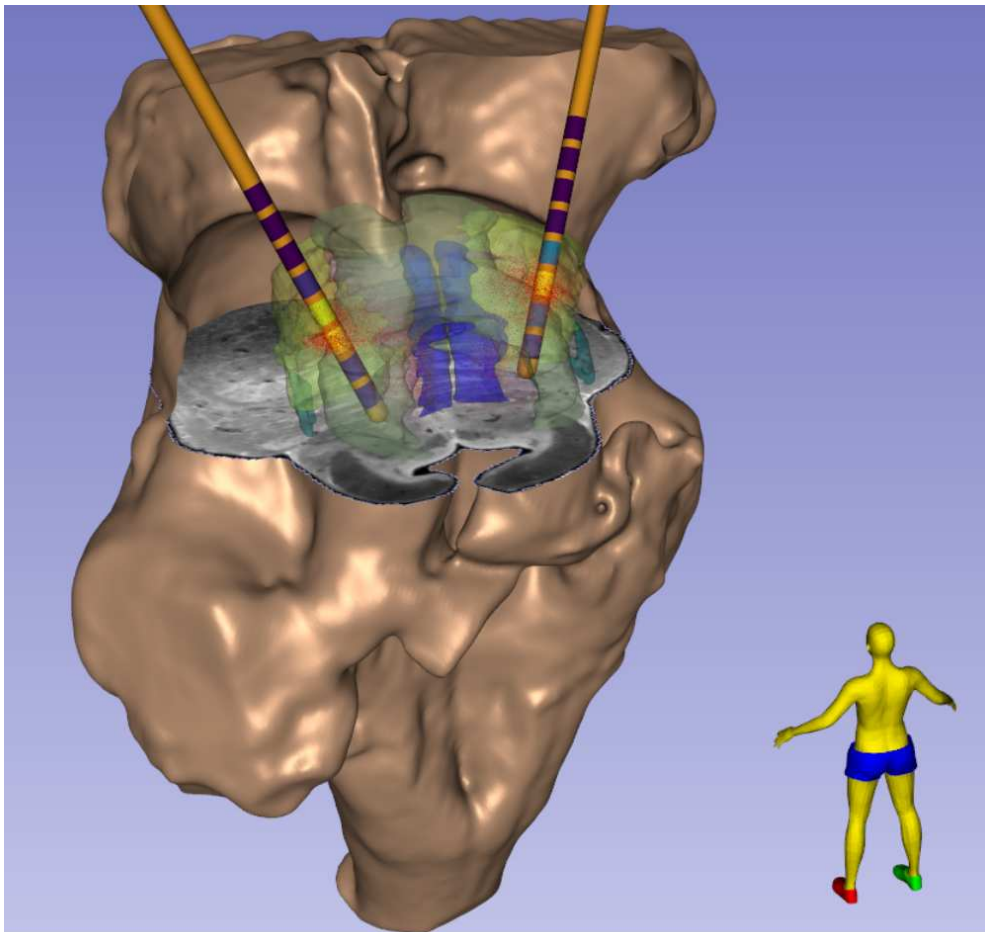

Cette démarche transversale associant les études anatomiques et comportementales chez le singe et chez l'homme peut s'appliquer pour tous les champs d'investigation. De nombreuses pathologies neurologiques, telles que la maladie d'Alzheimer, et psychiatriques, telles que la dépression ou les troubles du comportement agressif, représentent des enjeux médicaux, sociaux et économiques. En améliorant nos connaissances scientifiques fondamentales aussi bien sur le plan anatomiques que sur la compréhension des mécanismes physiopathologiques, les techniques de neurochirurgie fonctionnelle actuelle ou d'avenir pourront ainsi être développées avec le maximum de sécurité pour les patients.

# REFERENCES


Abbott RD, Ross GW, White LR, Tanner CM, Masaki KH, Nelson JS, et al. (2005). Excessive daytime sleepiness and subsequent development of Parkinson disease. *Neurology*. 65**,** 1442-6.

Abosch A, Hutchison WD, Saint-Cyr JA, Dostrovsky JO, et Lozano AM (2002). Movement-related neurons of the subthalamic nucleus in patients with Parkinson disease. *J Neurosurg*. 97**,** 1167-72.

Absi E, Ayala A, Machado A, et Parrado J (2000). Protective effect of melatonin against the 1-methyl-4-phenylpyridinium-induced inhibition of complex I of the mitochondrial respiratory chain. *J Pineal Res*. 29**,** 40-7.

Adi N, Mash DC, Ali Y, Singer C, Shehadeh L, et Papapetropoulos S (2010). Melatonin MT1 and MT2 receptor expression in Parkinson's disease. *Med Sci Monit*. 16**,** BR61-7.

Agnati LF, Fuxe K, Zoli M, Ozini I, Toffano G, et Ferraguti F (1986). A correlation analysis of the regional distribution of central enkephalin and beta-endorphin immunoreactive terminals and of opiate receptors in adult and old male rats. Evidence for the existence of two main types of communication in the central nervous system: the volume transmission and the wiring transmission. *Acta Physiol Scand*. 128**,** 201-7.

Alderson HL, Jenkins TA, Kozak R, Latimer MP, et Winn P (2001). The effects of excitotoxic lesions of the pedunculopontine tegmental nucleus on conditioned place preference to 4%, 12% and 20% sucrose solutions. *Brain Res Bull*. 56**,** 599-605.

Alderson HL, Latimer MP, Blaha CD, Phillips AG, et Winn P (2004). An examination of d-amphetamine self-administration in pedunculopontine tegmental nucleus-lesioned rats. *Neuroscience*. 125**,** 349-58.

Alderson HL, Latimer MP, et Winn P (2006). Intravenous self-administration of nicotine is altered by lesions of the posterior, but not anterior, pedunculopontine tegmental nucleus. *Eur J Neurosci*. 23**,** 2169-75.

Alderson HL, Latimer MP, et Winn P (2008). A functional dissociation of the anterior and posterior pedunculopontine tegmental nucleus: excitotoxic lesions have differential effects on locomotion and the response to nicotine. *Brain Struct Funct*. 213**,** 247-53.

Allen LF, Inglis WL, et Winn P (1996). Is the cuneiform nucleus a critical component of the mesencephalic locomotor region? An examination of the effects of excitotoxic lesions of the cuneiform nucleus on spontaneous and nucleus accumbens induced locomotion. *Brain Res Bull*. 41**,** 201-10.

Almirall H, Pigarev I, de la Calzada MD, Pigareva M, Herrero MT, et Sagales T (1999). Nocturnal sleep structure and temperature slope in MPTP treated monkeys. *J Neural Transm (Vienna)*. 106**,** 1125-34.

Appell PP, et Behan M (1990). Sources of subcortical GABAergic projections to the superior colliculus in the cat. *J Comp Neurol*. 302**,** 143-58.

Aravamuthan BR, Muthusamy KA, Stein JF, Aziz TZ, et Johansen-Berg H (2007). Topography of cortical and subcortical connections of the human pedunculopontine and subthalamic nuclei. *Neuroimage*. 37**,** 694-705.

Aravamuthan BR, Stein JF, et Aziz TZ (2008). The anatomy and localization of the pedunculopontine nucleus determined using probabilistic diffusion tractography [corrected]. *Br J Neurosurg*. 22 Suppl 1**,** S25-32.

Aravamuthan BR, McNab JA, Miller KL, Rushworth M, Jenkinson N, Stein JF, et al. (2009). Cortical and subcortical connections within the pedunculopontine nucleus of the primate Macaca mulatta determined using probabilistic diffusion tractography. *J Clin Neurosci*. 16**,** 413-20.

Arendt J, et Skene DJ (2005). Melatonin as a chronobiotic. *Sleep Med Rev*. 9**,** 25-39.

Arendt T, Bigl V, Arendt A, et Tennstedt A (1983). Loss of neurons in the nucleus basalis of Meynert in Alzheimer's disease, paralysis agitans and Korsakoff's Disease. *Acta Neuropathol*. 61**,** 101-8.

Armstrong E (1990). Evolution of the brain. In: The human nervous system. Vol., G. Paxinos, ed. eds. Academic Press, New York, pp. 1-16.

Arnulf I, Konofal E, Merino-Andreu M, Houeto JL, Mesnage V, Welter ML, et al. (2002). Parkinson's disease and sleepiness: an integral part of PD. *Neurology*. 58**,** 1019-24.

Arnulf I (2005). Excessive daytime sleepiness in parkinsonism. *Sleep Med Rev*. 9**,** 185-200.

Arnulf I, Ferraye M, Fraix V, Benabid AL, Chabardes S, Goetz L, et al. (2010). Sleep induced by stimulation in the human pedunculopontine nucleus area. *Ann Neurol*. 67**,** 546-9.

Arsenault MY, Parent A, Seguela P, et Descarries L (1988). Distribution and morphological characteristics of dopamine-immunoreactive neurons in the midbrain of the squirrel monkey (Saimiri sciureus). *J Comp Neurol*. 267**,** 489-506.

Augood SJ, Hollingsworth ZR, Standaert DG, Emson PC, et Penney JB, Jr. (2000). Localization of dopaminergic markers in the human subthalamic nucleus. *J Comp Neurol*. 421**,** 247-55.

Augustine JR (1996). Circuitry anf functional aspects of the insular lobe in primates including humans. *Brain Research Review*. 22**,** 229-244.

Aziz TZ, Peggs D, Sambrook MA, et Crossman AR (1991). Lesion of the subthalamic nucleus for the alleviation of 1- methyl-4-phenyl-1,2,3,6-tetrahydro-pyridine (MPTP)-induced parkinsonism in the primate. *Mov Disord*. 6**,** 288-292.

Aziz TZ, Davies L, Stein J, et France S (1998). The role of descending basal ganglia connections to the brain stem in parkinsonian akinesia. *Br J Neurosurg*. 12**,** 245-249.

Bakker M, De Lange FP, Helmich RC, Scheeringa R, Bloem BR, et Toni I (2008). Cerebral correlates of motor imagery of normal and precision gait. *Neuroimage*. 41**,** 998-1010.

Baron MS, Wichmann T, Ma D, et DeLong MR (2002). Effects of transient focal inactivation of the basal ganglia in parkinsonian primates. *The Journal of Neuroscience*. 22**,** 592-599.

Barraud Q, Lambrecq V, Forni C, McGuire S, Hill M, Bioulac B, et al. (2009). Sleep disorders in Parkinson's disease: the contribution of the MPTP non-human primate model. *Exp Neurol*. 219**,** 574-82.

Barroso-Chinea P, Rico AJ, Conte-Perales L, Gomez-Bautista V, Luquin N, Sierra S, et al. (2011). Glutamatergic and cholinergic pedunculopontine neurons innervate the thalamic parafascicular nucleus in rats: changes following experimental parkinsonism. *Brain Struct Funct*. 216**,** 319-30.

Baunez C, Nieoullon A, et Amalric M (1995). In a rat model of parkinsonism, lesions of the subthalamic nucleus reverse increases of reaction time but induce a dramatic premature responding deficit. *J Neurosci.* 15**,** 6531-6541.

Baunez C, et Robbins TW (1997). Bilateral lesions of the subthalamic nucleus induce multiple deficits in an attentional task in rats. *Eur. J Neurosci.* 9**,** 2086-2099.

Baup N, Grabli D, Karachi C, Mounayar S, Francois C, Yelnik J, et al. (2008). High-frequency stimulation of the anterior subthalamic nucleus reduces stereotyped behaviors in primates. *J Neurosci*. 28**,** 8785-8.

Beitz AJ (1982). The nuclei of origin of brain stem enkephalin and substance P projections to the rodent nucleus raphe magnus. *Neuroscience*. 7**,** 2753-68.

Belaid H, Adrien J, Laffrat E, Tande D, Karachi C, Grabli D, et al., (2014). Sleep disorders in Parkinsonian macaques: effects of L-dopa treatment and pedunculopontine nucleus lesion. *J Neurosci*. 34**,** 9124-33.

Belaid H, Adrien J, Karachi C, Hirsch EC, et Francois C (2015). Effect of melatonin on sleep disorders in a monkey model of Parkinson's disease. *Sleep Med*. 16**,** 1245-51.

Benabid AL, Pollak P, Gross C, Hoffmann D, Benazzouz A, Gao DM, et al. (1994). Acute and long-term effects of subthalamic nucleus stimulation in Parkinson's disease. *Stereotact Funct Neurosurg*. 62**,** 76-84.

Benazzouz A, Gross C, F,ger J, Boraud T, et Bioulac B (1993). Reversal of rigidity and improvement of motor performance by subthalamic high-frequency stimulation in MPTP-treated monkeys. *Eur. J Neurosci*. 5**,** 382-389.

Bergman H, Wichmann T, et DeLong MR (1990). Reversal of experimental parkinsonism by lesions of the subthalamic nucleus. *Science*. 249**,** 1436-1438.

Bergman H, Wichmann T, Karmon B, et DeLong MR (1994). The primate subthalamic nucleus. 2. Neuronal activity in the MPTP model of Parkinsonism. *Journal of Neurophysiology*. 72**,** 507-520.

Beurrier C, Bezard E, Bioulac B, et Gross C (1997). Subthalamic stimulation elicits hemiballismus in normal monkey. *NeuroReport*. 8**,** 1625-1629.

Bevan MD, et Bolam JP (1995). Cholinergic, GABAergic, and glutamate-enriched inputs from the mesopontine tegmentum to the subthalamic nucleus in the rat. *J Neurosci*. 15**,** 7105-20.

Bliwise DL, Trotti LM, Wilson AG, Greer SA, Wood-Siverio C, Juncos JJ, et al. (2012). Daytime alertness in Parkinson's disease: potentially dose-dependent, divergent effects by drug class. *Mov Disord*. 27**,** 1118-24.

Bloem BR, Hausdorff JM, Visser JE, et Giladi N (2004). Falls and freezing of gait in Parkinson's disease: a review of two interconnected, episodic phenomena. *Mov Disord*. 19**,** 871-84.

Bohnen NI, Muller MLTM, Koeppe RA, Studenski SA, Kilbourn MA, Frey KA, et al. (2009). History of falls in Parkinson disease is associated with reduced cholinergic activity. *Neurology*. 73**,** 1670-1676.

Bohnen NI, Frey KA, Studenski S, Kotagal V, Koeppe RA, Scott PJ, et al. (2013). Gait speed in Parkinson disease correlates with cholinergic degeneration. *Neurology*. 81**,** 1611-6.

Boucetta S, Cisse Y, Mainville L, Morales M, et Jones BE (2014). Discharge profiles across the sleep-waking cycle of identified cholinergic, GABAergic, and glutamatergic neurons in the pontomesencephalic tegmentum of the rat. *J Neurosci*. 34**,** 4708-27.

Braak H, Del Tredici K, Rub U, de Vos RA, Jansen Steur EN, et Braak E (2003). Staging of brain pathology related to sporadic Parkinson's disease. *Neurobiol Aging*. 24**,** 197-211.

Braak H, Ghebremedhin E, Rub U, Bratzke H, et Del Tredici K (2004). Stages in the development of Parkinson's disease-related pathology. *Cell Tissue Res*. 318**,** 121-34.

Breen DP, Vuono R, Nawarathna U, Fisher K, Shneerson JM, Reddy AB, et al. (2014). Sleep and circadian rhythm regulation in early Parkinson disease. *JAMA Neurol*. 71**,** 589-95.

Breit S, Bouali-Benazzouz R, Benabid AL, et Benazzouz A (2001). Unilateral lesion of the nigrostriatal pathway induces an increase of neuronal activity of the pedunculopontine nucleus, which is reversed by the lesion of the subthalamic nucleus in the rat. *Eur J Neurosci*. 14**,** 1833-42.

Breit S, Lessmann L, Benazzouz A, et Schulz JB (2005). Unilateral lesion of the pedunculopontine nucleus induces hyperactivity in the subthalamic nucleus and substantia nigra in the rat. *Eur J Neurosci*. 22**,** 2283-94.

Breit S, Lessmann L, Unterbrink D, Popa RC, Gasser T, et Schulz JB (2006). Lesion of the pedunculopontine nucleus reverses hyperactivity of the subthalamic nucleus and substantia nigra pars reticulata in a 6-hydroxydopamine rat model. *Eur J Neurosci*. 24**,** 2275-82.

Brown LL, Markman MH, Wolfson LI, Dvorkin B, Warner C, et Katzman R (1979). A direct role of dopamine in the rat subthalamic nucleus and an adjacent intrapeduncular area. *Science*. 206**,** 1416-8.

Brown P, et Williams D (2005). Basal ganglia local field potential activity: character and functional significance in the human. *Clin Neurophysiol*. 116**,** 2510-9.

Buot A, Welter ML, Karachi C, Pochon JB, Bardinet E, Yelnik J, et al. (2013). Processing of emotional information in the human subthalamic nucleus. *J Neurol Neurosurg Psychiatry*. 84**,** 1331-8.

Buot A, Lau B, Welter ML, Yelnik J, Bardinet E, Fernandez-Vidal S, et al. (2015). The subthalamic nucleus processes emotion: electrophysiological differences between Parkinson's Disease and Obsessive-Compulsive Disorder patients. *45th annual meeting of the Society for Neuroscience, abstract.*

Campbell GA, Eckardt MJ, et Weight FF (1985). Dopaminergic mechanisms in subthalamic nucleus of rat: analysis using horseradish peroxidase and microiontophoresis. *Brain Res*. 333**,** 261-70.

Campos FL, da Silva-Junior FP, de Bruin VM, et de Bruin PF (2004). Melatonin improves sleep in asthma: a randomized, double-blind, placebo-controlled study. *Am J Respir Crit Care Med*. 170**,** 947-51.

Capozzo A, Florio T, Confalone G, Minchella D, Mazzone P, et Scarnati E (2009). Low frequency stimulation of the pedunculopontine nucleus modulates electrical activity of subthalamic neurons in the rat. *J Neural Transm*. 116**,** 51-6.

Ceravolo R, Brusa L, Galati S, Volterrani D, Peppe A, Siciliano G, et al. (2011). Low frequency stimulation of the nucleus tegmenti pedunculopontini increases cortical metabolism in parkinsonian patients. *Eur J Neurol*. 18**,** 842-9.

Chabardes S, Polosan M, Krack P, Bastin J, Krainik A, David O, et al., (2013). Deep brain stimulation for obsessive-compulsive disorder: subthalamic nucleus target. *World Neurosurg*. 80**,** S31 e1-8.

Chan-Palay V, et Asan E (1989). Alterations in catecholamine neurons of the locus coeruleus in senile dementia of the Alzheimer type and in Parkinson's disease with and without dementia and depression. *J Comp Neurol*. 287**,** 373-92.

Charara A, Smith Y, et Parent A (1996). Glutamatergic inputs from the pedunculopontine nucleus to midbrain dopaminergic neurons in primates: Phaseolus vulgaris-leucoagglutinin anterograde labeling combined with postembedding glutamate and GABA immunohistochemistry. *J Comp Neurol*. 364**,** 254-66.

Chee R, Murphy A, Danoudis M, Georgiou-Karistianis N, et Iansek R (2009). Gait freezing in Parkinson's disease and the stride length sequence effect interaction. *Brain*. 132**,** 2151-60.

Chiba T, Kayahara T, et Nakano K (2001). Efferent projections of infralimbic and prelimbic areas of the medial prefrontal cortex in the Japanese monkey, *Macaca fuscata*. *Brain Res*. 888**,** 83-101.

Clark SD, Alderson HL, Winn P, Latimer MP, Nothacker HP, et Civelli O (2007). Fusion of diphtheria toxin and urotensin II produces a neurotoxin selective for cholinergic neurons in the rat mesopontine tegmentum. *J Neurochem*. 102**,** 112-20.

Clements JR, et Grant S (1990). Glutamate-like immunoreactivity in neurons of the laterodorsal tegmental and pedunculopontine nuclei in the rat. *Neurosci Lett*. 120**,** 70-3.

Clements JR, Toth DD, Highfield DA, et Grant SJ (1991). Glutamate-like immunoreactivity is present within cholinergic neurons of the laterodorsal tegmental and pedunculopontine nuclei. *Adv Exp Med Biol*. 295**,** 127-42.

Cossette M, Levesque M, et Parent A (1999). Extrastriatal dopaminergic innervation of human basal ganglia. *Neurosci Res*. 34**,** 51-4.

Costa A, Carlesimo GA, Caltagirone C, Mazzone P, Pierantozzi M, Stefani A, et al. (2010). Effects of deep brain stimulation of the peduncolopontine area on working memory tasks in patients with Parkinson's disease. *Parkinsonism Relat Disord*. 16**,** 64-7.

Cragg SJ, Baufreton J, Xue Y, Bolam JP, et Bevan MD (2004). Synaptic release of dopamine in the subthalamic nucleus. *Eur J Neurosci*. 20**,** 1788-802.

Crossman AR, Sambrook MA, et Jackson A (1984). Experimental hemichorea/hemiballismus in the monkey. Studies on the intracerebral site of action in a drug-induced dyskinesia. *Brain*. 107**,** 579-596.

Dabbeni-Sala F, Di Santo S, Franceschini D, Skaper SD, et Giusti P (2001). Melatonin protects against 6-OHDA-induced neurotoxicity in rats: a role for mitochondrial complex I activity. *FASEB J*. 15**,** 164-170.

Damier P, Hirsch EC, Agid Y, et Graybiel AM (1999). The substantia nigra of the human brain. II. Patterns of loss of dopamine-containing neurons in Parkinson's disease. *Brain*. 122**,** 1437-48.

Datta S (2002). Evidence that REM sleep is controlled by the activation of brain stem pedunculopontine tegmental kainate receptor. *J Neurophysiol*. 87**,** 1790-8.

Dautan D, Huerta-Ocampo I, Witten IB, Deisseroth K, Bolam JP, Gerdjikov T, et al. (2014). A major external source of cholinergic innervation of the striatum and nucleus accumbens originates in the brainstem. *J Neurosci*. 34**,** 4509-18.

DeLong MR, Crutcher MD, et Georgopoulos AP (1985). Primate globus pallidus and subthalamic nucleus: functional organization. *J Neurophy*. 53**,** 530-543.

Denoyer M, Sallanon M, Buda C, Kitahama K, et Jouvet M (1991). Neurotoxic lesion of the mesencephalic reticular formation and/or the posterior hypothalamus does not alter waking in the cat. *Brain Res*. 539**,** 287-303.

Descarries L, Watkins KC, Garcia S, Bosler O, et Doucet G (1996). Dual character, asynaptic and synaptic, of the dopamine innervation in adult rat neostriatum: a quantitative autoradiographic and immunocytochemical analysis. *J Comp Neurol*. 375**,** 167-86.

Deurveilher S, et Hennevin E (2001). Lesions of the pedunculopontine tegmental nucleus reduce paradoxical sleep (PS) propensity: evidence from a short-term PS deprivation study in rats. *Eur J Neurosci*. 13**,** 1963-76.

Dowling GA, Mastick J, Colling E, Carter JH, Singer CM, et Aminoff MJ (2005). Melatonin for sleep disturbances in Parkinson's disease. *Sleep Med*. 6**,** 459-66.

Dubuc R, Brocard F, Antri M, Fenelon K, Gariepy JF, Smetana R, et al. (2008). Initiation of locomotion in lampreys. *Brain Res Rev*. 57**,** 172-82.

Dujardin K, Blairy S, Defebvre L, Krystkowiak P, Hess U, Blond S, et al. (2004). Subthalamic nucleus stimulation induces deficits in decoding emotional facial expressions in Parkinson's disease. *J Neurol Neurosurg Psychiatry*. 75**,** 202-8.

Edley SM, et Graybiel AM (1983). The afferent and efferent connections of the feline nucleus tegmenti pedunculopontinus, pars compacta. *J Comp Neurol*. 217**,** 187-215.

Eid L, Parent A, et Parent M, (2014). Asynaptic feature and heterogeneous distribution of the cholinergic innervation of the globus pallidus in primates. *Brain Struct Funct*. 221:1139-55.

Eid L, et Parent M (2015). Morphological evidence for dopamine interactions with pallidal neurons in primates. *Front Neuroanat*. 9**,** 111.

Eidelberg E, Walden JG, et Nguyen LH (1981). Locomotor control in macaque monkeys. *Brain*. 104**,** 647-63.

Feger J, Hammond C, et Rouzaire-Dubois B (1979). Pharmacological properties of acetylcholine-induced excitation of subthalamic nucleus neurones. *Br J Pharmacol*. 65**,** 511-5.

Ferraye MU, Debu B, Fraix V, Goetz L, Ardouin C, Yelnik J, et al. (2010). Effects of pedunculopontine nucleus area stimulation on gait disorders in Parkinson's disease. *Brain*. 133**,** 205-14.

Flores G, Liang JJ, Sierra A, Martinez-Fong D, Quirion R, Aceves J, et al. (1999). Expression of dopamine receptors in the subthalamic nucleus of the rat: characterization using reverse transcriptase-polymerase chain reaction and autoradiography. *Neuroscience*. 91**,** 549-56.

Floyd JA, Janisse JJ, Jenuwine ES, et Ager JW (2007). Changes in REM-sleep percentage over the adult lifespan. *Sleep*. 30**,** 829-36.

Ford B, Holmes CJ, Mainville L, et Jones BE (1995). GABAergic neurons in the rat pontomesencephalic tegmentum: codistribution with cholinergic and other tegmental neurons projecting to the posterior lateral hypothalamus. *J Comp Neurol*. 363**,** 177-96.

Francois C, Savy C, Jan C, Tande D, Hirsch EC, et Yelnik J (2000). Dopaminergic innervation of the subthalamic nucleus in the normal state, in MPTP-treated monkeys, and in Parkinson's disease patients. *J Comp Neurol*. 425**,** 121-9.

Freund TF, Powell JF, et Smith AD (1984). Tyrosine hydroxylase-immunoreactive boutons in synaptic contact with identified striatonigral neurons, with particular reference to dendritic spines. *Neuroscience*. 13**,** 1189-215.

Fronczek R, Overeem S, Lee SY, Hegeman IM, van Pelt J, van Duinen SG, et al. (2007). Hypocretin (orexin) loss in Parkinson's disease. *Brain*. 130**,** 1577-85.

Fudge JL, Breitbart MA, Danish M, et Pannoni V (2005). Insular and gustatory inputs to the caudal ventral striatum in primates. *J Comp Neurol*. 490**,** 101-18.

Fuxe K, Cintra A, Agnati LF, Harfstrand A, et Goldstein M (1988). Studies on the relationship of tyrosine hydroxylase, dopamine and cyclic amp-regulated phosphoprotein-32 immunoreactive neuronal structures and d1 receptor antagonist binding sites in various brain regions of the male rat-mismatches indicate a role of d1 receptors in volume transmission. *Neurochem Int*. 13**,** 179-97.

Gagnon JF, Bedard MA, Fantini ML, Petit D, Panisset M, Rompre S, et al. (2002). REM sleep behavior disorder and REM sleep without atonia in Parkinson's disease. *Neurology*. 59**,** 585-9.

Galvan A, et Wichmann T (2008). Pathophysiology of parkinsonism. *Clin Neurophysiol*. 119**,** 1459-74.

Galvan A, et Smith Y (2011). The primate thalamostriatal systems: Anatomical organization, functional roles and possible involvement in Parkinson's disease. *Basal Ganglia*. 1**,** 179-189.

Galvan A, Hu X, Rommelfanger KS, Pare JF, Khan ZU, Smith Y, et al. (2014). Localization and function of dopamine receptors in the subthalamic nucleus of normal and parkinsonian monkeys. *J Neurophysiol*. 112**,** 467-79.

Garcia-Rill E (1986). The basal ganglia and the locomotor regions. *Brain Res*. 396**,** 47-63.

Garcia-Rill E, Houser CR, Skinner RD, Smith W, et Woodward DJ (1987). Locomotion-inducing sites in the vicinity of the pedunculopontine nucleus. *Brain Res Bull*. 18**,** 731-8.

Garcia-Rill E, et Skinner RD (1987a). The mesencephalic locomotor region. I. Activation of a medullary projection site. *Brain Res*. 411**,** 1-12.

Garcia-Rill E, et Skinner RD (1987b). The mesencephalic locomotor region. II. Projections to reticulospinal neurons. *Brain Res*. 411**,** 13-20.

Garcia-Rill E, Kinjo N, Atsuta Y, Ishikawa Y, Webber M, et Skinner RD (1990). Posterior midbrain-induced locomotion. *Brain Res Bull*. 24**,** 499-508.

Garcia-Rill E (1991). The pedunculopontine nucleus. *Prog Neurobiol*. 36**,** 363-89.

Garcia-Rill E, Homma Y, et Skinner RD (2004). Arousal mechanisms related to posture and locomotion: 1. Descending modulation. *Prog Brain Res*. 143**,** 283-90.

Garcia-Rill E, Heister DS, Ye M, Charlesworth A, et Hayar A (2007). Electrical coupling: novel mechanism for sleep-wake control. Sleep. 30, 1405-14.

Garcia-Rill E, et Skinner RD (1991). Modulation of rhythmic functions by the brainstem. In: Shimamura M, Grillner S, Edgerton VR, editors. Neurobiological basis of human locomotion. Tokyo: Japan Scientific Societies Press. p. 137–58.

Gauthier J, Parent M, Levesque M, et Parent A (1999). The axonal arborization of single nigrostriatal neurons in rats. Brain Res. 834, 228-32.

Georgopoulos AP, DeLong MR, et Crutcher MD (1983). Relations between parameters of step-tracking movements and single cell discharge in the globus pallidus and subthalamic nucleus of the behaving monkey. *J Neurosci*. 3**,** 1586-1598.

Gerfen CR, Staines WA, Arbuthnott GW, et Fibiger HC (1982). Crossed connections of the substantia nigra in the rat. *J Comp Neurol*. 207**,** 283-303.

Gesi M, Soldani P, Giorgi FS, Santinami A, Bonaccorsi I, et Fornai F (2000). The role of the locus coeruleus in the development of Parkinson's disease. *Neurosci Biobehav Rev*. 24**,** 655-68.

Geula C, Schatz CR, et Mesulam MM (1993). Differential localization of NADPH-diaphorase and calbindin-D28k within the cholinergic neurons of the basal forebrain, striatum and brainstem in the rat, monkey, baboon and human. *Neuroscience*. 54**,** 461-76.

Giladi N, et Nieuwboer A (2008). Understanding and treating freezing of gait in parkinsonism, proposed working definition, and setting the stage. *Mov Disord*. 23 Suppl 2**,** S423-5.

Giladi N, Horak FB, et Hausdorff JM (2013). Classification of gait disturbances: distinguishing between continuous and episodic changes. *Mov Disord*. 28**,** 1469-73.

Goetz L, Piallat B, Thibaudier Y, Montigon O, David O, et Chabardes S (2012). A non-human primate model of bipedal locomotion under restrained condition allowing gait studies and single unit brain recordings. *J Neurosci Methods*. 204**,** 306-17.

Goetz L, Piallat B, Bhattacharjee M, Mathieu H, David O, et Chabardes S (2016). On the Role of the Pedunculopontine Nucleus and Mesencephalic Reticular Formation in Locomotion in Nonhuman Primates. *J Neurosci*. 36**,** 4917-29.

Golestanirad L, Elahi B, Graham SJ, Das S, et Wald LL (2016). Efficacy and Safety of Pedunculopontine Nuclei (PPN) Deep Brain Stimulation in the Treatment of Gait Disorders: A Meta-Analysis of Clinical Studies. *Can J Neurol Sci*. 43**,** 120-6.

Gomez-Gallego M, Fernandez-Villalba E, Fernandez-Barreiro A, et Herrero MT (2007). Changes in the neuronal activity in the pedunculopontine nucleus in chronic MPTP-treated primates: an in situ hybridization study of cytochrome oxidase subunit I, choline acetyl transferase and substance P mRNA expression. *J Neural Transm*. 114**,** 319-26.

Grabli D, Karachi C, Folgoas E, Monfort M, Tande D, Clark S, et al. (2013). Gait disorders in parkinsonian monkeys with pedunculopontine nucleus lesions: a tale of two systems. *J Neurosci*. 33**,** 11986-93.

Granata AR, et Kitai ST (1991). Inhibitory substantia nigra inputs to the pedunculopontine neurons. *Exp Brain Res*. 86**,** 459-466.

Grillner S (1981). Control of locomotion in bipeds, tetrapods and fish. In: Handbook of Physiologydthe Nervous System II. Vol., V. Brooks, eds. American Physiological Society, Baltimore, , pp. 1199-236.

Grunwerg BS, Krein H, et Krauthamer GM (1992). Somatosensory input and thalamic projection of pedunculopontine tegmental neurons. *Neuroreport*. 3, 673-5.

Hallanger AE, Levey AI, Lee HJ, Rye DB, et Wainer BH (1987). The origins of cholinergic and other subcortical afferents to the thalamus in the rat. *J Comp Neurol*. 262(1), 105-24.

Halliday GM, Blumbergs PC, Cotton RG, Blessing WW, et Geffen LB (1990). Loss of brainstem serotonin- and substance P-containing neurons in Parkinson's disease. *Brain Res*. 510**,** 104-7.

Hammond C, Féger J, Bioulac B, et Souteyrand JP (1979). Experimental hemiballism in the monkey produced by unilateral kainic acid lesion, in corpus Luysii. *Brain Res*. 171**,** 577-580.

Hanley JJ, et Bolam JP (1996). Synaptology of the nigrostriatal protection in relation to the compartmental organization of the rat neostriatum. *Soc Neurosci Abstr.* 22**,** 413.

Hardman CD, Henderson JM, Finkelstein DI, Horne MK, Paxinos G, et Halliday GM (2002). Comparison of the basal ganglia in rats, marmosets, macaques, baboons, and humans: volume and neuronal number for the output, internal relay, and striatal modulating nuclei. *J Comp Neurol*. 445**,** 238-55.

Hassani OK, Francois C, Yelnik J, et Feger J (1997). Evidence for a dopaminergic innervation of the subthalamic nucleus in the rat. *Brain Res*. 749**,** 88-94.

Hassani OK, et Feger J (1999). Effects of intrasubthalamic injection of dopamine receptor agonists on subthalamic neurons in normal and 6-hydroxydopamine-lesioned rats: an electrophysiological and c-Fos study. *Neuroscience*. 92**,** 533-43.

Haynes WI, et Haber SN (2013). The organization of prefrontal-subthalamic inputs in primates provides an anatomical substrate for both functional specificity and integration: implications for Basal Ganglia models and deep brain stimulation. *J Neurosci*. 33**,** 4804-14.

Hazrati LN, et Parent A (1992). Projection from the deep cerebellar nuclei to the pedunculopontine nucleus in the squirrel monkey. *Brain Res*. 585**,** 267-71.

Hedreen JC (1999). Tyrosine hydroxylase-immunoreactive elements in the human globus pallidus and subthalamic nucleus. *J Comp Neurol*. 409**,** 400-10.

Henderson JM, Carpenter K, Cartwright H, et Halliday GM (2000). Loss of thalamic intralaminar nuclei in progressive supranuclear palsy and Parkinson's disease: clinical and therapeutic implications. *Brain*. 123**,** 1410-21.

Herrero MT, P,rez-Otano I, Oset C, Kastner A, Hirsch EC, Agid Y, et al. (1993). GM-1 ganglioside promotes the recovery of surviving midbrain dopaminergic neurons in MPTP-treated monkeys. *Neuroscience*. 56**,** 965-972.

Hirsch EC, Graybiel AM, Duyckaerts C, et Javoy-Agid F (1987). Neuronal loss in the pedunculopontine tegmental nucleus in parkinson disease and in progressive supranuclear palsy. P. roc. Natl. Acad. Sci. U. S. A. (Washington) 84**,** 5976-5980.

Hobson DE, Lang AE, Martin WR, Razmy A, Rivest J, et Fleming J (2002). Excessive daytime sleepiness and sudden-onset sleep in Parkinson disease: a survey by the Canadian Movement Disorders Group. *JAMA*. 287**,** 455-63.

Homs-Ormo S, Coll-Andreu M, Satorra-Marin N, Arevalo-Garcia R, et Morgado-Bernal I (2003). Effects of pedunculopontine tegmental nucleus lesions on emotional reactivity and locomotion in rats. *Brain Res Bull*. 59**,** 495-503.

Hong S, et Hikosaka O (2014). Pedunculopontine tegmental nucleus neurons provide reward, sensorimotor, and alerting signals to midbrain dopamine neurons. *Neuroscience*. 282**,** 139-155.

Hornung OP, Regen F, Schredl M, Heuser I, et Danker-Hopfe H (2006). Manipulating REM sleep in older adults by selective REM sleep deprivation and physiological as well as pharmacological REM sleep augmentation methods. *Exp Neurol*. 197**,** 486-94.

Hsieh KC, Robinson EL, et Fuller CA (2008). Sleep architecture in unrestrained rhesus monkeys (Macaca mulatta) synchronized to 24-hour light-dark cycles. *Sleep*. 31**,** 1239-50.

Hyacinthe C, Barraud Q, Tison F, Bezard E, et Ghorayeb I (2014). D1 receptor agonist improves sleep-wake parameters in experimental parkinsonism. *Neurobiol Dis*. 63**,** 20-4.

Hylden JL, Hayashi H, Bennett GJ, et Dubner R, (1985). Spinal lamina I neurons projecting to the parabrachial area of the cat midbrain. *Brain Res*. 336**,** 195-8.

Iseki K, Hanakawa T, Shinozaki J, Nankaku M, et Fukuyama H (2008). Neural mechanisms involved in mental imagery and observation of gait. *Neuroimage*. 41**,** 1021-31.

Iwata J, Chida K, et LeDoux JE (1987). Cardiovascular responses elicited by stimulation of neurons in the central amygdaloid nucleus in awake but not anesthetized rats resemble conditioned emotional responses. *Brain Res*. 418(1), 183-8.

Jackson A, et Crossman AR (1983). Nucleus tegmenti pedunculopontinus: efferent connections with special reference to the basal ganglia, studied in the rat by anterograde and retrograde transport of horseradish peroxidase. *Neuroscience*. 10**,** 725-65.

Jahn K, Deutschlander A, Stephan T, Kalla R, Wiesmann M, Strupp M, et al. (2008). Imaging human supraspinal locomotor centers in brainstem and cerebellum. *Neuroimage*. 39**,** 786-92.

Jellinger KA (1988). The pedunculopontine nucleus in Parkinson' s disease, progressive supranuclear palsy and Alzheimer' s disease. *J Neurol Neurosurg Psychiatry*. 51**,** 540-3.

Jellinger KA (2012) Neuropathology of sporadic Parkinson's disease: evaluation and changes of concepts. *Mov Disord*. 27, 8-30.

Jenkinson N, Nandi D, Miall RC, Stein JF, et Aziz TZ, (2004). Pedunculopontine nucleus stimulation improves akinesia in a Parkinsonian monkey. *Neuroreport*. 15**,** 2621-4.

Jeon MF, Ha Y, Cho YH, Lee BH, Park YG, et Chang JW (2003). Effect of ipsilateral subthalamic nucleus lesioning in a rat parkinsonian model: study of behavior correlated with neuronal activity in the pedunculopontine nucleus. *J Neurosurg*. 99**,** 762-7.

Jia HG, Yamuy J, Sampogna S, Morales FR, et Chase MH (2003). Colocalization of gamma-aminobutyric acid and acetylcholine in neurons in the laterodorsal and pedunculopontine tegmental nuclei in the cat: a light and electron microscopic study. *Brain Res*. 992**,** 205-19.

Jones BE (1993). The organization of central cholinergic systems and their functional importance in sleep-waking states. *Prog Brain Res*. 98**,** 61-71.

Kang Y, et Kitai ST (1990). Electrophysiological properties of pedunculopontine neurons and their postsynaptic responses following stimulation of substantia nigra reticulata. *Brain Res*. 535**,** 79-95.

Karachi C, Yelnik J, Tande D, Tremblay L, Hirsch EC, et Francois C (2005). The pallidosubthalamic projection: an anatomical substrate for nonmotor functions of the subthalamic nucleus in primates. *Mov Disord*. 20**,** 172-80.

Karachi C, Grabli D, Baup N, Mounayar S, Tande D, Francois C, et al. (2009). Dysfunction of the subthalamic nucleus induces behavioral and movement disorders in monkeys. *Mov Disord*. 24**,** 1183-92.

Karachi C, Grabli D, Bernard FA, Tande D, Wattiez N, Belaid H, et al. (2010). Cholinergic mesencephalic neurons are involved in gait and postural disorders in Parkinson disease. *J Clin Invest*. 120**,** 2745-54.

Karachi C, Andre A, Bertasi E, Bardinet E, Lehericy S, et Bernard FA (2012). Functional parcellation of the lateral mesencephalus. *J Neurosci*. 32**,** 9396-401.

Katzenschlager R, Sampaio C, Costa J, et Lees A (2003). Anticholinergics for symptomatic management of Parkinson's disease. *Cochrane Database Syst Rev*. CD003735.

Kelland MD, et Asdourian D (1989). Pedunculopontine tegmental nucleus-induced inhibition of muscle activity in the rat. *Behav Brain Res*. 34**,** 213-34.

Kempster PA, O'Sullivan SS, Holton JL, Revesz T, et Lees AJ (2010). Relationships between age and late progression of Parkinson's disease: a clinico-pathological study. *Brain*. 133**,** 1755-62.

Khan S, Mooney L, Plaha P, Javed S, White P, Whone AL, et al. (2011). Outcomes from stimulation of the caudal zona incerta and pedunculopontine nucleus in patients with Parkinson's disease. *Br J Neurosurg*. 25**,** 273-80.

Kinomura S, Larsson J, Gulyas B, et Roland PE (1996). Activation by attention of the human reticular formation and thalamic intralaminar nuclei. *Science*. 271**,** 512-5.

Kish SJ, Shannak K, et Hornykiewicz O (1988). Uneven pattern of dopamine loss in the striatum of patients with idiopathic Parkinson's disease. Pathophysiologic and clinical implications. *N Engl J Med*. 318**,** 876-80.

Kita T, et Kita H (2011). Cholinergic and non-cholinergic mesopontine tegmental neurons projecting to the subthalamic nucleus in the rat. *Eur J Neurosci*. 33**,** 433-43.

Kobayashi Y, Inoue Y, Yamamoto M, Isa T, et Aizawa H (2002). Contribution of pedunculopontine tegmental nucleus neurons to performance of visually guided saccade tasks in monkeys. *J Neurophysiol*. 88**,** 715-31.

Koch M, Kungel M, et Herbert H (1993). Cholinergic neurons in the pedunculopontine tegmental nucleus are involved in the mediation of prepulse inhibition of the acoustic startle response in the rat. *Exp Brain Res*. 97**,** 71-82.

Kojima J, Yamaji Y, Matsumura M, Nambu A, Inase M, Tokuno H, et al. (1997). Excitotoxic lesions of the pedunculopontine tegmental nucleus produce contralateral hemiparkinsonism in the monkey. *Neurosci Lett*. 226**,** 111-114.

Kroeger D, Ferrari LL, Petit G, Mahoney CE, Fuller PM, Arrigoni E, et al. (2017). Cholinergic, Glutamatergic, and GABAergic Neurons of the Pedunculopontine Tegmental Nucleus Have Distinct Effects on Sleep/Wake Behavior in Mice. *J Neurosci*. 37**,** 1352-1366.

Kung L, Force M, Chute DJ, et Roberts RC (1998). Immunocytochemical localization of tyrosine hydroxylase in the human striatum: a postmortem ultrastructural study. *J Comp Neurol*. 390**,** 52-62.

Kunz D, et Bes F (1997). Melatonin effects in a patient with severe REM sleep behavior disorder: case report and theoretical considerations. *Neuropsychobiology*. 36**,** 211-4.

Kurth F, Eickhoff SB, Schleicher A, Hoemke L, Zilles K, et Amunts K (2010a). Cytoarchitecture and probabilistic maps of the human posterior insular cortex. *Cereb Cortex*. 20**,** 1448-61.

Kurth F, Zilles K, Fox PT, Laird AR, et Eickhoff SB (2010b). A link between the systems: functional differentiation and integration within the human insula revealed by meta-analysis. *Brain Struct Funct*. 214**,** 519-34.

La Fougere C, Zwergal A, Rominger A, Forster S, Fesl G, Dieterich M, et al. (2010). Real versus imagined locomotion: a [18F]-FDG PET-fMRI comparison. *Neuroimage*. 50**,** 1589-98.

Lai YY, et Siegel JM (1990). Muscle tone suppression and stepping produced by stimulation of midbrain and rostral pontine reticular formation. *J Neurosci*. 10**,** 2727-34.

Lambert C, Zrinzo L, Nagy Z, Lutti A, Hariz M, Foltynie T, et al. (2012). Confirmation of functional zones within the human subthalamic nucleus: patterns of connectivity and sub-parcellation using diffusion weighted imaging. *Neuroimage*. 60**,** 83-94.

Lang AE, et Lozano AM, (1998a). Parkinson's disease. First of two parts. *N Engl J Med*. 339**,** 1044-53.

Lang AE, et Lozano AM, (1998b). Parkinson's disease. Second of two parts. *N Engl J Med*. 339**,** 1130-43.

Lau B, Welter ML, Belaid H, Fernandez Vidal S, Bardinet E, Grabli D, et al. (2015). The integrative role of the pedunculopontine nucleus in human gait. *Brain*.

Lavoie B, Smith Y, et Parent A (1989). Dopaminergic innervation of the basal ganglia in the squirrel monkey as revealed by tyrosine hydroxylase immunohistochemistry. *J Comp Neurol*. 289**,** 36-52.

Lavoie B, et Parent A, (1994a). Pedunculopontine nucleus in the squirrel monkey: distribution of cholinergic and monoaminergic neurons in the mesopontine tegmentum with evidence for the presence of glutamate in cholinergic neurons. *J Comp Neurol*. 344**,** 190-209.

Lavoie B, et Parent A (1994b). Pedunculopontine nucleus in the squirrel monkey: projections to the basal ganglia as revealed by anterograde tract-tracing methods. *J Comp Neurol*. 344**,** 210-231.

Lavoie B, et Parent A (1994c). Pedunculopontine nucleus in the squirrel monkey: cholinergic and glutamatergic projections to the substantia nigra. J Comp Neurol. 344, 232-241.

LeDoux JE, Iwata J, Cicchetti P, et Reis DJ (1988). Different projections of the central amygdaloid nucleus mediate autonomic and behavioral correlates of conditioned fear. J Neurosci. 8(7): 2517-29.

Le Ray D, Brocard F, Bourcier-Lucas C, Auclair F, Lafaille P, et Dubuc R (2003). Nicotinic activation of reticulospinal cells involved in the control of swimming in lampreys. *Eur J Neurosci*. 17**,** 137-48.

Lee AM, Hoy JL, Bonci A, Wilbrecht L, Stryker MP, et Niell CM (2014). Identification of a brainstem circuit regulating visual cortical state in parallel with locomotion. *Neuron*. 83**,** 455-466.

Lees AJ, Blackburn NA, et Campbell VL (1988). The nighttime problems of Parkinson's disease. *Clin Neuropharmacol*. 11**,** 512-9.

Li Z, Yu Z, Zhang J, Wang J, Sun C, Wang P, et Zhang J (2015). *Eur Neurol*. 74(1-2), 86-91.

Lima D, et Coimbra A (1989). Morphological types of spinomesencephalic neurons in the marginal zone (lamina I) of the rat spinal cord, as shown after retrograde labelling with cholera toxin subunit B. *J Comp Neurol*. 279**,** 327-39.

Limousin P, Pollak P, Benazzouz A, Hoffmann D, Broussolle E, Perret JE, et al. (1995a). Bilateral subthalamic nucleus stimulation for severe Parkinson's disease. *Mov Disord*. 10**,** 672-4.

Limousin P, Pollak P, Benazzouz A, Hoffmann D, Le Bas JF, Broussolle E, et al. (1995b). Effect of parkinsonian signs and symptoms of bilateral subthalamic nucleus stimulation. *Lancet*. 345**,** 91-5.

Lindvall O, Bjorklund A, et Skagerberg G (1984). Selective histochemical demonstration of dopamine terminal systems in rat di- and telencephalon: new evidence for dopaminergic innervation of hypothalamic neurosecretory nuclei. Brain Res. 306, 19-30.

Little S, et Brown P (2014). The functional role of beta oscillations in Parkinson's disease. *Parkinsonism Relat Disord*. Jan;20 Suppl 1:S44-8. Review.

Longo VG (1956). Effects of scopolamine and atropine electroencephalographic and behavioral reactions due to hypothalamic stimulation. *J Pharmacol Exp Ther*. 116**,** 198-208.

Maclaren DA, Wilson DI, et Winn P (2013). Updating of action-outcome associations is prevented by inactivation of the posterior pedunculopontine tegmental nucleus. *Neurobiol Learn Mem*. 102**,** 28-33.

Mallet L, Mesnage V, Houeto JL, Pelissolo A, Yelnik J, Behar C, et al. (2002). Compulsions, Parkinson's disease, and stimulation. *Lancet*. 360**,** 1302-1304.

Mallet L, Polosan M, Jaafari N, Baup N, Welter ML, Fontaine D, et al. (2008). Subthalamic nucleus stimulation in severe obsessive-compulsive disorder. *N Engl J Med*. 359**,** 2121-34.

Mann DM (1983). The locus coeruleus and its possible role in ageing and degenerative disease of the human central nervous system. *Mech Ageing Dev*. 23**,** 73-94.

Martinez-Gonzalez C, Bolam JP, et Mena-Segovia J (2011). Topographical organization of the pedunculopontine nucleus. *Front Neuroanat*. 5**,** 22.

Martinez-Gonzalez C, Wang HL, Micklem BR, Bolam JP, et Mena-Segovia J (2012). Subpopulations of cholinergic, GABAergic and glutamatergic neurons in the pedunculopontine nucleus contain calcium-binding proteins and are heterogeneously distributed. *Eur J Neurosci*. 35**,** 723-34.

Matsumura M, Kojima J, Gardiner TW, et Hikosaka O (1992). Visual and oculomotor functions of monkey subthalamic nucleus. *J Neurophysiol*. 67**,** 1615-32.

Matsumura M, Watanabe K, et Ohye C (1997). Single-unit activity in the primate nucleus tegmenti pedunculopontinus related to voluntary arm movement. *Neurosci Res*. 28**,** 155-165.

Matsumura M, Nambu A, Yamaji Y, Watanabe K, Imai H, Inase M, et al (2000). Organization of somatic motor inputs from the frontal lobe to the pedunculopontine tegmental nucleus in the macaque monkey. *Neuroscience*. 98**,** 97-110.

Matsumura M, et Kojima J (2001). The role of the pedunculopontine tegmental nucleus in experimental parkinsonism in primates. *Stereotact Funct Neurosurg*. 77**,** 108-15.

Mazzone P, Lozano A, Stanzione P, Galati S, Scarnati E, Peppe A, et al. (2005). Implantation of human pedunculopontine nucleus: a safe and clinically relevant target in Parkinson's disease. *Neuroreport*. 16**,** 1877-81.
Medeiros CA, Carvalhedo de Bruin PF, Lopes LA, Magalhaes MC, de Lourdes Seabra M, et de Bruin VM (2007). Effect of exogenous melatonin on sleep and motor dysfunction in Parkinson's disease. A randomized, double blind, placebo-controlled study. *J Neurol*. 254**,** 459-64.
Meibach RC, et Katzman R (1979). Catecholaminergic innervation of the subthalamic nucleus: evidence for a rostral continuation of the A9 (substantia nigra) dopaminergic cell group. *Brain Res*. 173**,** 364-8.
Mena-Segovia J, Sims HM, Magill PJ, et Bolam JP (2008). Cholinergic brainstem neurons modulate cortical gamma activity during slow oscillations. *J Physiol*. 586**,** 2947-60.
Mena-Segovia J, Micklem BR, Nair-Roberts RG, Ungless MA, et Bolam JP (2009). GABAergic neuron distribution in the pedunculopontine nucleus defines functional subterritories. *J Comp Neurol*. 515**,** 397-408.
Menetrey D, Chaouch A, Binder D, et Besson JM (1982). The origin of the spinomesencephalic tract in the rat: an anatomical study using the retrograde transport of horseradish peroxidase. *J Comp Neurol*. 206**,** 193-207.
Mestre TA, Sidiropoulos C, Hamani C, Poon YY, Lozano AM, Lang AE, et al. (2016). Long-term double-blinded unilateral pedunculopontine area stimulation in Parkinson's disease. *Mov Disord*. 31, 1570-74.
Mesulam MM.; Mufson EJ (1985). The insula of Reil in man and monkey. Architectonics, connectivity and function. In: Peters, A.; Jones, EG., editors. Cerebral cortex. Plenum Press; New York. p. 179-226.
Mesulam MM, Mufson EJ, Wainer BH, et Levey AI (1983). Central cholinergic pathways in the rat: an overview based on an alternative nomenclature (Ch1-Ch6). *Neuroscience*. 10**,** 1185-201.
Mesulam MM, Mufson EJ, Levey AI, et Wainer BH (1984). Atlas of cholinergic neurons in the forebrain and upper brainstem of the macaque based on monoclonal choline acetyltransferase immunohistochemistry and acetylcholinesterase histochemistry. *Neuroscience*. 12**,** 669-86.
Mesulam MM, Geula C, Bothwell MA, et Hersh LB (1989). Human reticular formation: cholinergic neurons of the pedunculopontine and laterodorsal tegmental nuclei and some cytochemical comparisons to forebrain cholinergic neurons. *J Comp Neurol*. 283**,** 611-33.
Mesulam MM, Mash D, Hersh L, Bothwell M, et Geula C (1992). Cholinergic innervation of the human striatum, globus pallidus, subthalamic nucleus, substantia nigra, and red nucleus. *J Comp Neurol*. 323**,** 252-68.
Mintz I, Hammond C, et Feger J (1986). Excitatory effect of iontophoretically applied dopamine on identified neurons of the rat subthalamic nucleus. *Brain Res*. 375**,** 172-5.
Miwa H, Fuwa T, Yokochi M, Nishi K, et Mizuno Y (1996). Injection of a GABA antagonist into the mesopontine reticular formation abolishes haloperidol-induced catalepsy in rats. *Neuroreport*. 7**,** 2475-8.
Moore O, Peretz C, et Giladi N (2007). Freezing of gait affects quality of life of peoples with Parkinson's disease beyond its relationships with mobility and gait. *Mov Disord*. 22**,** 2192-5.
Morgan WW, et Nelson JF (2001). Chronic administration of pharmacological levels of melatonin does not ameliorate the MPTP-induced degeneration of the nigrostriatal pathway. *Brain Res*. 921**,** 115-21.
Mori S, Sakamoto T, Ohta Y, Takakusaki K, et Matsuyama K (1989). Site-specific postural and locomotor changes evoked in awake, freely moving intact cats by stimulating the brainstem. *Brain Res*. 505**,** 66-74.
Moro E, Hamani C, Poon YY, Al-Khairallah T, Dostrovsky JO, Hutchison WD, et al. (2010). Unilateral pedunculopontine stimulation improves falls in Parkinson's disease. *Brain*. 133**,** 215-24.
Moruzzi G, et Magoun HW (1949). Brain stem reticular formation and activation of the EEG. *Electroencephalogr Clin Neurophysiol*. 1**,** 455-73.
MunroDavies LE, Winter J, Aziz TZ, et Stein JF (1999). The role of the pedunculopontine region in basal-ganglia mechanisms of akinesia. *Exp.Brain Res*. 129**,** 511-517.
Muthusamy KA, Aravamuthan BR, Kringelbach ML, Jenkinson N, Voets NL, Johansen-Berg H, et al. (2007). Connectivity of the human pedunculopontine nucleus region and diffusion tensor imaging in surgical targeting. *J Neurosurg*. 107**,** 814-20.
Nakano I, et Hirano A (1984). Parkinson's disease: neuron loss in the nucleus basalis without concomitant Alzheimer's disease. *Ann Neurol*. 15**,** 415-8.

Nakano K, Hasegawa Y, Tokushige A, Nakagawa S, Kayahara T, et Mizuno N (1990). Topographical projections from the thalamus, subthalamic nucleus and pedunculopontine tegmental nucleus to the striatum in the Japanese monkey, *Macaca fuscata*. *Brain Res*. 537**,** 54-68.

Nambu A, Takada M, Inase M, et Tokuno H (1996). Dual somatotopical representations in the primate subthalamic nucleus: Evidence for ordered but reversed body-map transformations from the primary motor cortex and the supplementary motor area. *J Neurosci*. 16**,** 2671-2683.

Nambu A, et Llinas R (1997). Morphology of globus pallidus neurons: Its correlation with electrophysiology in guinea pig brain slices. *J Comp Neurol*. 377, 85-94.

Nambu A, Tokuno H, et Takada M (2002). Functional significance of the cortico-subthalamo-pallidal 'hyperdirect' pathway. *Neurosci Res*. 43**,** 111-117.

Nambu T, Sakurai T, Mizukami K, Hosoya Y, Yanagisawa M, et Goto K (1999). Distribution of orexin neurons in the adult rat brain. *Brain Res*. 827**,** 243-60.

Nandi D, Aziz TZ, Giladi N, Winter J, et Stein JF (2002a). Reversal of akinesia in experimental parkinsonism by GABA antagonist microinjections in the pedunculopontine nucleus. *Brain*. 125**,** 2418-30.

Nandi D, Liu X, Winter JL, Aziz TZ, et Stein JF (2002b). Deep brain stimulation of the pedunculopontine region in the normal non-human primate. *J Clin Neurosci*. 9**,** 170-4.

Ni Z, Gao D, Bouali-Benazzouz R, Benabid AL, et Benazzouz A (2001). Effect of microiontophoretic application of dopamine on subthalamic nucleus neuronal activity in normal rats and in rats with unilateral lesion of the nigrostriatal pathway. *Eur J Neurosci*. 14**,** 373-81.

Nobin A, et Bjorklund A (1973). Topography of the monoamine neuron systems in the human brain as revealed in fetuses. *Acta Physiol Scand Suppl*. 388**,** 1-40.

Noda T, et Oka H (1986). Distribution and morphology of tegmental neurons receiving nigral inhibitory inputs in the cat: An intracellular HRP study. *J Comp Neurol*. 244**,** 254-266.

Nosko D, Ferraye MU, Fraix V, Goetz L, Chabardes S, Pollak P, et al. (2014). Low-frequency versus high-frequency stimulation of the pedunculopontine nucleus area in Parkinson's disease: a randomised controlled trial. *J Neurol Neurosurg Psychiatry*. 86, 674-9.

Oakman SA, Faris PL, Kerr PE, Cozzari C, et Hartman BK (1995). Distribution of pontomesencephalic cholinergic neurons projecting to substantia nigra differs significantly from those projecting to ventral tegmental area. *J Neurosci*. 15**,** 5859-69.

Okada K, Toyama K, Inoue Y, Isa T, et Kobayashi Y (2009). Different pedunculopontine tegmental neurons signal predicted and actual task rewards. *J Neurosci*. 29**,** 4858-70.

Okada K, et Kobayashi Y (2013). Reward prediction-related increases and decreases in tonic neuronal activity of the pedunculopontine tegmental nucleus. *Front Integr Neurosci*. 7**,** 36.

Okada K, et Kobayashi Y (2015). Rhythmic Firing of Pedunculopontine Tegmental Nucleus Neurons in Monkeys during Eye Movement Task. *PLoS One*. 10**,** e0128147.

Olszewski J, et Baxter D (1954). Cytoarchitecture of the human brain stem, Vol., Karger, S., New York.

Pahapill PA, et Lozano AM (2000). The pedunculopontine nucleus and Parkinson's disease. *Brain*. 123**,** 1767-83.

Palminteri S, Justo D, Jauffret C, Pavlicek B, Dauta A, Delmaire C, et al. (2012). Critical roles for anterior insula and dorsal striatum in punishment-based avoidance learning. *Neuron.* 76(5), 998-1009.

Pandi-Perumal SR, Zisapel N, Srinivasan V, et Cardinali DP (2005). Melatonin and sleep in aging population. Exp Gerontol. 40, 911-25.

Pare D, Smith Y, Parent A, et Steriade M (1988). Projections of brainstem core cholinergic and noncholinergic neurons of cat to intralaminar and reticular thalamic nuclei. *Neuroscience*. 25**,** 69-86.

Parent M, et Descarries L (2008). Acetylcholine innervation of the adult rat thalamus: distribution and ultrastructural features in dorsolateral geniculate, parafascicular, and reticular thalamic nuclei. *J Comp Neurol*. 511(5), 678-91.

Parent A, et Smith Y (1987). Organization of efferent projections of the subthalamic nucleus in the squirrel monkey as revealed by retrograde labeling methods. *Brain Res*. 436**,** 296-310.

Parent A, Pare D, Smith Y, et Steriade M (1988). Basal forebrain cholinergic and noncholinergic projections to the thalamus and brainstem in cats and monkeys. *J Comp Neurol*. 277**,** 281-301.

Parent A, Hazrati LN, Smith Y, Crossman AR, et Sambrook MA (1989). The subthalamic nucleus in primates. A neuroanatomical and immunohistochemical study. In: Neural mechanisms in disorders of movement. Vol., eds. John Libbey, London, pp. 29-35.

Peppe A, Pierantozzi M, Baiamonte V, Moschella V, Caltagirone C, Stanzione P, et al. (2012). Deep brain stimulation of pedunculopontine tegmental nucleus: role in sleep modulation in advanced Parkinson disease patients: one-year follow-up. *Sleep*. 35**,** 1637-42.

Peyron C, Tighe DK, van den Pol AN, de Lecea L, Heller HC, Sutcliffe JG, et al. (1998). Neurons containing hypocretin (orexin) project to multiple neuronal systems. *J Neurosci*. 18**,** 9996-10015.

Philippe AS, Sébille S, Francois C, Karachi C, Valabregue R, Lehéricy S, Bardinet E (2015). Computation of diffusion-based pathway connectivity map: a study of subthalamic nucleus connections. *21th Annu. Meet. Organ. Hum. Brain Mapping, Honolulu, USA*.

Phillips ML, Drevets WC, Rauch SL, Lane R (2003). Neurobiology of emotion perception I: the neural basis of normal emotion perception. *Biol Psychiatry*. 54, 504–514.

Piallat B, Chabardes S, Torres N, Fraix V, Goetz L, Seigneuret E, et al. (2009). Gait is associated with an increase in tonic firing of the sub-cuneiform nucleus neurons. *Neuroscience*. 158**,** 1201-5.

Pickel VM, Chan J, et Sesack SR (1992). Cellular basis for interactions between catecholaminergic afferents and neurons containing Leu-enkephalin-like immunoreactivity in rat caudate-putamen nuclei. *J Neurosci Res*. 31**,** 212-30.

Pienaar IS, Elson JL, Racca C, Nelson G, Turnbull DM, et Morris CM (2013). Mitochondrial abnormality associates with type-specific neuronal loss and cell morphology changes in the pedunculopontine nucleus in Parkinson disease. *Am J Pathol*. 183**,** 1826-40.

Pifl C, Bertel O, Schingnitz G, et Hornykiewicz O (1990). Extrastriatal dopamine in symptomatic and asymptomatic rhesus monkeys treated with 1-methyl-4-phenyl-1,2,3,6-tetrahydropyridine (MPTP). *Neurochem Int*. 17**,** 263-70.

Plaha P, et Gill SS (2005). Bilateral deep brain stimulation of the pedunculopontine nucleus for Parkinson's disease. *Neuroreport*. 16**,** 1883-7.

Pose I, Sampogna S, Chase MH, et Morales FR (2000). Cuneiform neurons activated during cholinergically induced active sleep in the cat. *J Neurosci*. 20**,** 3319-27.

Reese NB, Garcia-Rill E, et Skinner RD (1995). The pedunculopontine nucleus--auditory input, arousal and pathophysiology. *Prog Neurobiol*. 47**,** 105-33.

Rinne JO, Ma SY, Lee MS, Collan Y, et Roytta M (2008). Loss of cholinergic neurons in the pedunculopontine nucleus in Parkinson's disease is related to disability of the patients. *Parkinsonism Relat Disord*. 14**,** 553-7.

Rinvik E, et Ottersen OP (1993). Terminals of subthalamonigral fibres are enriched with glutamate-like immunoreactivity: an electron microscopic, immunogold analysis in the cat. *J Chem Neuroanat*. 6**,** 19-30.

Roberts RC, Kung L, Crosby K,et Chute DJ (1997). The immunocytochemical localization of tyrosine hydroxylase in the human substantia nigra: A postmortem ultrastructural study. *Schizophr Res.* 24**,** 41.

Rodriguez M, Abdala P, Barroso-Chinea P, et Gonzalez-Hernandez T (2001). The deep mesencephalic nucleus as an output center of basal ganglia: morphological and electrophysiological similarities with the substantia nigra. *J Comp Neurol*. 438**,** 12-31.

Rogers JD, Brogan D, et Mirra SS (1985). The nucleus basalis of Meynert in neurological disease: a quantitative morphological study. *Ann Neurol*. 17**,** 163-70.

Rolland AS, Tande D, Herrero MT, Luquin MR, Vazquez-Claverie M, Karachi C, et al. (2009). Evidence for a dopaminergic innervation of the pedunculopontine nucleus in monkeys, and its drastic reduction after MPTP intoxication. *J Neurochem*. 110**,** 1321-9.

Rolland AS, Karachi C, Muriel MP, Hirsch EC, et Francois C (2011). Internal pallidum and substantia nigra control different parts of the mesopontine reticular formation in primate. *Mov Disord*. 26**,** 1648-56.

Roseberry TK, Lee AM, Lalive AL, Wilbrecht L, Bonci A, et Kreitzer AC (2016). Cell-Type-Specific Control of Brainstem Locomotor Circuits by Basal Ganglia. *Cell*. 164**,** 526-37.

Rye DB (1997). Contributions of the pedunculopontine region to normal and altered REM sleep. Sleep. 20, 757-88.

Rye DB (2006). Excessive daytime sleepiness and unintended sleep in Parkinson's disease. Curr Neurol Neurosci Rep. 6, 169-76.

Rye DB (2010). Seeing beyond one's nose: sleep disruption and excessive sleepiness accompany motor disability in the MPTP treated primate. Exp Neurol. 222, 179-80.

Rye DB, Saper CB, Lee HJ, et Wainer BH (1987). Pedunculopontine tegmental nucleus of the rat: cytoarchitecture, cytochemistry, and some extrapyramidal connections of the mesopontine tegmentum. *J Comp Neurol*. 259(4), 483-528.

Sah P1, Faber ES, Lopez De Armentia M, et Power J. (2003). The amygdaloid complex: anatomy and physiology. Physiol Rev. 83(3):803-34.

Sakai ST, Davidson AG, et Buford JA (2009). Reticulospinal neurons in the pontomedullary reticular formation of the monkey (Macaca fascicularis). Neuroscience. 163, 1158-70.

Sakanaka M, Shibasaki T, et Lederis K (1987). Corticotropin releasing factor-like immunoreactivity in the rat brain as revealed by a modified cobalt-glucose oxidase-diaminobenzidine method. J Comp Neurol. 260, 256-98.

Samson HH, et Chappell A (2001). Injected muscimol in pedunculopontine tegmental nucleus alters ethanol self-administration. *Alcohol*. 23**,** 41-8.

Scarnati E, Gasbarri A, Campana E, et Pacitti C (1987). The organization of nucleus tegmenti pedunculopontinus neurons projecting to basal ganglia and thalamus: a retrograde fluorescent double labeling study in the rat. *Neurosci Lett*. 79**,** 11-6.

Scarnati E, Hajdu F, Pacitti C, et Tombol T (1988). An EM and Golgi study on the connection between the nucleus tegmenti pedunculopontinus and the pars compacta of the substantia nigra in the rat. *J Hirnforsch*. 29**,** 95-105.

Schrempf W, Brandt MD, Storch A, et Reichmann H (2014). Sleep disorders in Parkinson's disease. *J Parkinson Dis*. 4**,** 211-21.

Sebille SB, Belaid H, Philippe AC, Andre A, Lau B, Francois C, et al. (2017). Anatomical evidence of the functional diversity of the mesencephalic locomotor region in primate. *Neuroimage*. 147:66-78.

Semba K, et Fibiger HC (1992). Afferent connections of the laterodorsal and the pedunculopontine tegmental nuclei in the rat: a retro- and antero-grade transport and immunohistochemical study. *J Comp Neurol*. 323**,** 387-410.

Sesack SR, Deutch AY, Roth RH, et Bunney BS (1989). Topographical organization of the efferent projections of the medial prefrontal cortex in the rat: an anterograde tract-tracing study with Phaseolus vulgaris leucoagglutinin. *J Comp Neurol*. 290**,** 213-42.

Shik ML, Severin FV, et Orlovskii GN (1966). [Control of walking and running by means of electric stimulation of the midbrain]. *Biofizika*. 11**,** 659-66.

Shink E, Sidibe M, et Smith Y (1997). Efferent connections of the internal globus pallidus in the squirrel monkey: II. Topography and synaptic organization of pallidal efferents to the pedunculopontine nucleus. *J Comp Neurol*. 382**,** 348-63.

Shouse MN, et Siegel JM (1992). Pontine regulation of REM sleep components in cats: integrity of the pedunculopontine tegmentum (PPT) is important for phasic events but unnecessary for atonia during REM sleep. Brain Res. 571, 50-63.

Shute CC, et Lewis PR (1967). The ascending cholinergic reticular system: neocortical, olfactory and subcortical projections. Brain. 90, 497-520.

Singer T, Critchley, HD, et Preuschoff K (2009). A common role of insula in feelings, empathy and uncertainty. *Trends in Cognitive Sciences*. 13(8), 334-440.

Singer T, Seymour B, O'Doherty JP, Stephan KE, Dolan RJ, et Frith CD (2006). Empathic neural responses are modulated by the perceived fairness of others. Nature. 439(7075), 466-9.

Sirota MG, Di Prisco GV, et Dubuc R (2000). Stimulation of the mesencephalic locomotor region elicits controlled swimming in semi-intact lampreys. Eur J Neurosci. 12, 4081-92.

Smith Y, et Parent A (1986). Differential connections of caudate nucleus and putamen in the squirrel monkey (Saimiri sciureus). Neuroscience. 18, 347-71.

Smith Y, Hazrati LN, et Parent A (1990). Efferent projections of the subthalamic nucleus in the squirrel monkey as studied by the PHA-L anterograde tracing method. J Comp Neurol. 294, 306-323.

Smith Y, et Kieval JZ (2000). Anatomy of the dopamine system in the basal ganglia. *Trends Neurosci*. 23**,** S28-33.

Sofroniew MV, Priestley JV, Consolazione A, Eckenstein F, et Cuello AC (1985). Cholinergic projections from the midbrain and pons to the thalamus in the rat, identified by combined retrograde tracing and choline acetyltransferase immunohistochemistry. *Brain Res*. 329**,** 213-23.

Spann BM, et Grofova I (1991). Nigropedunculopontine projection in the rat: an anterograde tracing study with phaseolus vulgaris-leucoagglutinin (PHA-L). *J Comp Neurol*. 311**,** 375-388.
Stefani A, Lozano AM, Peppe A, Stanzione P, Galati S, Tropepi D, et al. (2007). Bilateral deep brain stimulation of the pedunculopontine and subthalamic nuclei in severe Parkinson's disease. *Brain*. 130**,** 1596-607.
Stefani A, Pierantozzi M, Ceravolo R, Brusa L, Galati S, et Stanzione P (2010). Deep brain stimulation of pedunculopontine tegmental nucleus (PPTg) promotes cognitive and metabolic changes: a target-specific effect or response to a low-frequency pattern of stimulation? *Clin EEG Neurosci*. 41**,** 82-6.
Stefani A, Peppe A, Galati S, Bassi MS, D'Angelo V, et Pierantozzi M (2013). The serendipity case of the pedunculopontine nucleus low-frequency brain stimulation: chasing a gait response, finding sleep, and cognition improvement. *Front Neurol*. 4**,** 68.
Steiniger B, et Kretschmer BD (2004). Effects of ibotenate pedunculopontine tegmental nucleus lesions on exploratory behaviour in the open field. *Behav Brain Res*. 151**,** 17-23.
Steriade M, Pare D, Parent A, et Smith Y (1988). Projections of cholinergic and non-cholinergic neurons of the brainstem core to relay and associational thalamic nuclei in the cat and macaque monkey. *Neuroscience*. 25**,** 47-67.
Steriade M, Datta S, Pare D, Oakson G, et Curro Dossi RC (1990). Neuronal activities in brain-stem cholinergic nuclei related to tonic activation processes in thalamocortical systems. *J Neurosci*. 10**,** 2541-59.
Steriade M, Dossi RC, Pare D, et Oakson G (1991). Fast oscillations (20-40 Hz) in thalamocortical systems and their potentiation by mesopontine cholinergic nuclei in the cat. *Proc Natl Acad Sci U S A*. 88**,** 4396-400.
Stone BM, Turner C, Mills SL, et Nicholson AN (2000). Hypnotic activity of melatonin. *Sleep*. 23**,** 663-9.
Suzuki M, Hurd YL, Sokoloff P, Schwartz JC, et Sedvall G (1998). D3 dopamine receptor mRNA is widely expressed in the human brain. *Brain Res*. 779**,** 58-74.
Takakusaki K, Shiroyama T, Yamamoto T, et Kitai ST (1996). Cholinergic and noncholinergic tegmental pedunculopontine projection neurons in rats revealed by intracellular labeling. *J Comp Neurol*. 371**,** 345-61.
Takakusaki K, Shiroyama T, et Kitai ST (1997). Two types of cholinergic neurons in the rat tegmental pedunculopontine nucleus: electrophysiological and morphological characterization. *Neuroscience*. 79**,** 1089-109.
Takakusaki K, Habaguchi T, Ohtinata-Sugimoto J, Saitoh K, et Sakamoto T (2003). Basal ganglia efferents to the brainstem centers controlling postural muscle tone and locomotion: a new concept for understanding motor disorders in basal ganglia dysfunction. *Neuroscience*. 119**,** 293-308.
Takakusaki K, Saitoh K, Harada H, Okumura T, et Sakamoto T (2004). Evidence for a role of basal ganglia in the regulation of rapid eye movement sleep by electrical and chemical stimulation for the pedunculopontine tegmental nucleus and the substantia nigra pars reticulata in decerebrate cats. *Neuroscience*. 124**,** 207-20.
Takakusaki K, Takahashi K, Saitoh K, Harada H, Okumura T, Kayama Y, et al. (2005). Orexinergic projections to the cat midbrain mediate alternation of emotional behavioural states from locomotion to cataplexy. *J Physiol*. 568**,** 1003-20.
Takeuchi N, Uchimura N, Hashizume Y, Mukai M, Etoh Y, Yamamoto K, et al. (2001). Melatonin therapy for REM sleep behavior disorder. *Psychiatry Clin Neurosci*. 55**,** 267-9.
Tattersall TL, Stratton PG, Coyne TJ, Cook R, Silberstein P, Silburn PA, et al. (2014). Imagined gait modulates neuronal network dynamics in the human pedunculopontine nucleus. *Nat Neurosci*. 17**,** 449-54.
Thannickal TC, Lai YY, et Siegel JM (2007). Hypocretin (orexin) cell loss in Parkinson's disease. *Brain*. 130**,** 1586-95.
Thevathasan W, Coyne TJ, Hyam JA, Kerr G, Jenkinson N, Aziz TZ, et al. (2011). Pedunculopontine nucleus stimulation improves gait freezing in Parkinson disease. *Neurosurgery*. 69**,** 1248-53.
Thevathasan W, Cole MH, Graepel CL, Hyam JA, Jenkinson N, Brittain JS, et al. (2012). A spatiotemporal analysis of gait freezing and the impact of pedunculopontine nucleus stimulation. *Brain*. 135**,** 1446-54.
Thompson JA, et Felsen G (2013). Activity in mouse pedunculopontine tegmental nucleus reflects action and outcome in a decision-making task. *J Neurophysiol*. 110**,** 2817-29.

Trillet M, Vighetto A, Croisile B, Charles N, et Aimard G (1995). [Hemiballismus with logorrhea and thymo-affective disinhibition caused by hematoma of the left subthalamic nucleus]. *Rev.Neurol. (Paris)*. 151**,** 416-419.
van der Schyf CJ, Castagnoli K, Palmer S, Hazelwood L, et Castagnoli N, Jr. (2000). Melatonin fails to protect against long-term MPTP-induced dopamine depletion in mouse striatum. *Neurotox Res*. 1**,** 261-9.
Van Dort CJ, Zachs DP, Kenny JD, Zheng S, Goldblum RR, Gelwan NA, et al. (2015). Optogenetic activation of cholinergic neurons in the PPT or LDT induces REM sleep. *Proc Natl Acad Sci U S A*. 112**,** 584-9.
Veazey RB, et Severin CM (1980). Efferent projections of the deep mesencephalic nucleus (pars medialis) in the rat. *J Comp Neurol*. 190**,** 245-58.
Veazey RB, et Severin CM (1982). Afferent projections to the deep mesencephalic nucleus in the rat. *J Comp Neurol*. 204**,** 134-50.
Velazquez-Moctezuma J, Gillin JC, et Shiromani PJ (1989). Effect of specific M1, M2 muscarinic receptor agonists on REM sleep generation. *Brain Res*. 503**,** 128-31.
Videnovic A, Noble C, Reid KJ, Peng J, Turek FW, Marconi A, et al. (2014). Circadian melatonin rhythm and excessive daytime sleepiness in Parkinson disease. *JAMA Neurol*. 71**,** 463-9.
Vincent SR, Satoh K, Armstrong DM, et Fibiger HC (1983). Substance P in the ascending cholinergic reticular system. *Nature*. 306**,** 688-91.
Vincent SR, Satoh K, Armstrong DM, Panula P, Vale W, et Fibiger HC (1986). Neuropeptides and NADPH-diaphorase activity in the ascending cholinergic reticular system of the rat. *Neuroscience*. 17**,** 167-82.
Vincent SR (2000). The ascending reticular activating system--from aminergic neurons to nitric oxide. *J Chem Neuroanat*. 18**,** 23-30.
Volkmann J, Daniels C, et Witt K (2010). Neuropsychiatric effects of subthalamic neurostimulation in Parkinson disease. *Nat Rev Neurol*. 6**,** 487-98.
Wailke S, Herzog J, Witt K, Deuschl G, et Volkmann J (2011). Effect of controlled-release levodopa on the microstructure of sleep in Parkinson's disease. *Eur J Neurol*. 18**,** 590-6.
Walker SC, et Winn P (2007). An assessment of the contributions of the pedunculopontine tegmental and cuneiform nuclei to anxiety and neophobia. *Neuroscience*. 150**,** 273-90.
Wang HL, et Morales M (2009). Pedunculopontine and laterodorsal tegmental nuclei contain distinct populations of cholinergic, glutamatergic and GABAergic neurons in the rat. *Eur J Neurosci*. 29**,** 340-58.
Webster HH, et Jones BE (1988). Neurotoxic lesions of the dorsolateral pontomesencephalic tegmentum-cholinergic cell area in the cat. II. Effects upon sleep-waking states. *Brain Res*. 458**,** 285-302.
Weinberger M, Hamani C, Hutchison WD, Moro E, Lozano AM, et Dostrovsky JO (2008). Pedunculopontine nucleus microelectrode recordings in movement disorder patients. *Exp Brain Res*. 188**,** 165-74.
Welter ML, Schupbach M, Czernecki V, Karachi C, Fernandez-Vidal S, Golmard JL, et al. (2014). Optimal target localization for subthalamic stimulation in patients with Parkinson disease. *Neurology*. 82**,** 1352-61.
Welter ML, Demain A, Ewenczyk C, Czernecki V, Lau B, El Helou A, et al. (2015). PPNa-DBS for gait and balance disorders in Parkinson's disease: a double-blind, randomised study. *J Neurol*. 262**,** 1515-25.
Wichmann T, Bergman H, et DeLong MR (1994). The primate subthalamic nucleus. 1. Functional properties in intact animals. *J Neurophysiol*. 72**,** 494-506.
Woolf NJ, et Butcher LL (1986). Cholinergic systems in the rat brain: III. Projections from the pontomesencephalic tegmentum to the thalamus, tectum, basal ganglia, and basal forebrain. *Brain Res Bull*. 16**,** 603-37.
Xiang Z, Thompson AD, Jones CK, Lindsley CW, et Conn PJ (2012). Roles of the M1 muscarinic acetylcholine receptor subtype in the regulation of basal ganglia function and implications for the treatment of Parkinson's disease. *J Pharmacol Exp Ther*. 340**,** 595-603.
Xiao C, Miwa JM, Henderson BJ, Wang Y, Deshpande P, McKinney SL, et al. (2015). Nicotinic receptor subtype-selective circuit patterns in the subthalamic nucleus. *J Neurosci*. 35**,** 3734-46.
Yong MH, Fook-Chong S, Pavanni R, Lim LL, et Tan EK (2011). Case control polysomnographic studies of sleep disorders in Parkinson's disease. *PLoS One*. 6**,** e22511.
Zhdanova IV, Lynch HJ, et Wurtman RJ (1997). Melatonin: a sleep-promoting hormone. *Sleep*. 20**,** 899-907.

Zhdanova IV, Geiger DA, Schwagerl AL, Leclair OU, Killiany R, Taylor JA, et al, (2002). Melatonin promotes sleep in three species of diurnal nonhuman primates. *Physiol Behav*. 75**,** 523-9.

Zhu ZT, Shen KZ, et Johnson SW (2002). Pharmacological identification of inward current evoked by dopamine in rat subthalamic neurons in vitro. *Neuropharmacology*. 42**,** 772-81.

Zweig RM, Jankel WR, Hedreen JC, Mayeux R, et Price DL (1989). The pedunculopontine nucleus in Parkinson's disease. *Ann Neurol*. 26**,** 41-46

# LISTE DES ABREVIATIONS

6-OHDA: 6-hydroxydopamine

BDA: Biotin dextran amine

CA: Commissure antérieure

ChAT: Choline Acétyl Transférase

CM: Noyau centro-médian

CP: Commissure postérieure

CuN: Noyau Cunéiforme

DA: Dopaminergique

DAB: Diaminobenzidine

EEG: Electroencéphalographie

EOG: Electro-oculographie

EMG: Electromyographie

FEF: Frontal eye field

GABA: acide γ-amino-butyrique

GB: Ganglions de la base

GPi: Globus pallidus interne

GPe: Globus pallidus externe

L-dopa: Levodopa

MLR: Région locomotrice mésencéphalique

MP: Maladie de Parkinson

MPTP: 1-methyl-4-phenyl-1,2,3,6-tetrahydropyridine

NADPH: nicotinamide adénine dinucléotide phosphate diaphorase

NST: Noyau Subthalamique

PBS: tampon phosphate salin

Pf: Noyau parafasciculaire

PPN: Noyau pédonculopontin

RBD: Rapid eye movement sleep Behavior Disorder

REM: Rapid eye movement

SCP: Stimulation cérébrale profonde

SNc: Substantia Nigra pars compacta

SNr: Substantia Nigra pars reticulata

SRAA: Système réticulé activateur ascendant

TOC: Troubles obsessionnels compulsifs

TH : Tyrosine hydroxylase

TST: Temps de sommeil total

VTA: Aire tegmentale ventrale

WASO : Wake after sleep onset

# TABLE DES ILLUSTRATIONS

# RESUME

En plus des signes cardinaux classiques, de nombreux patients parkinsoniens souffrent de troubles du sommeil sévères résistant aux traitements dopaminergiques. A un stade avancé de la maladie, apparaissent des troubles de la marche et de l'équilibre dopa-résistants. De nombreux résultats expérimentaux et cliniques orientent vers un dysfonctionnement de la région locomotrice mésencéphalique (MLR) du tronc cérébral, formée anatomiquement du noyau pédonculopontin (PPN) et du noyau cunéiforme (CuN). La stimulation cérébrale profonde à basse fréquence du PPN proposée aux patients parkinsoniens ayant des troubles de la marche majeurs modifie aussi la qualité et l'architecture du sommeil. Ainsi, un dysfonctionnement de ce noyau de la MLR pourrait expliquer au moins en partie, les troubles de la marche et les troubles du sommeil chez ces patients parkinsoniens. Afin d'étudier l'anatomie et le rôle respectif du PPN et du CuN à l'état normal et à l'état parkinsonien, ce projet de thèse a été mené en associant une étude comportementale et anatomique de la MLR.

**Axe comportemental.** Nous avons analysé les troubles du sommeil induits dans un modèle primate de maladie de Parkinson (MP) avancée, puis l'effet de traitement dopaminergique associé ou non à de la mélatonine, et enfin l'effet d'une lésion cholinergique du PPN surajoutée. Nos résultats montrent que les troubles du sommeil développés à l'état parkinsonien sont similaires à ceux observés chez les patients, et améliorés par l'administration de L-dopa et de mélatonine. La lésion surajoutée du PPN aggrave les troubles du sommeil en aigu, mais améliore légèrement la qualité du sommeil à distance de la lésion. **Axe anatomique**. Nous avons d'abord défini l'anatomie hodologique du PPN et du CuN chez le singe et chez l'homme en fonction des trois grands territoires anatomo-fonctionnels des ganglions de la base. Nos résultats ont montré que le PPN intègre des informations très diverses (sensori-motrices, associatives et limbiques), le CuN étant quant à lui plutôt impliqué dans un réseau limbique. Par la suite, l'innervation cholinergique du PPN sur le NST a été caractérisée en microscopie optique et électronique chez le singe et chez l'homme, comparant les innervations cholinergique et dopaminergique que reçoit le NST, afin de préciser leur implication dans les effets cliniques et comportementaux de la stimulation du NST.

**Mots clefs :** Maladie de Parkinson, Région locomotrice mésencéphalique, Noyau pédonculopontin, primate, noyau subthalamique.

# ABSTRACT

Parkinsonian patients suffer from disabling sleep disorders, resistant to dopaminergic treatment. Moreover, at an advanced stage of the disease, gait disorders become resistant to dopaminergic conventional treatment and lead to falls and severe handicap. Much evidence from experimental and clinical studies lead to consider the mesencephalic locomotor region (MLR), which associates the pedunculopontine nucleus (PPN) and the cuneiform nucleus (CuN), as highly implicated in the pathophysiology. Deep brain stimulation in this region has thus been proposed to treat doparesistant gait disorders in parkinsonian patients, and was shown to improve sleep parameters as well. Overall clinical results are still heterogeneous and questions relating to precise anatomy and function of this region and its relationship with the basal ganglia remain. In order to have an anatomo-functional study of the PPN and the CuN at normal and parkinsonian state, this project has associated a behavioral axis in monkeys and an anatomic axis in monkeys and humans. **Behavioral study.** Sleep disorders have been analyzed in an advanced Parkinson disease primate model. These symptoms were improved with dopaminergic treatment and melatonin administration. After a stereotactic cholinergic PPN lesion, there was an acute worsening of the symptoms, particularly the sleep architecture and quality. However these tended to improve three weeks after the lesion. **Anatomic study**. First, we analyzed the connections between the PPN and the CuN relating to the three anatomo-functional territories of the basal ganglia (BG) in monkeys and humans. Our results showed that the PPN integrated various information from the three territories (sensori-motor, associative and limbic), compared to the CuN which preferentially connected to limbic territories of the BG. We then studied the subthalamic cholinergic innervation arising from the PPN at optic and ultra-structural level in monkeys and humans, comparing its characteristics with the dopaminergic innervation. Our results showed a homogeneous cholinergic innervation of the subthalamic nucleus (STN) compared to the heterogeneous dopaminergic innervation. These data could account for the clinical and behavioral effects observed with high frequency stimulation of the STN.

**Key words**: Parkinson Disease, Mesencephalic locomotor region, Pedunculopontine nucleus, Primate, Subthalamic nucleus